NASA SP-190

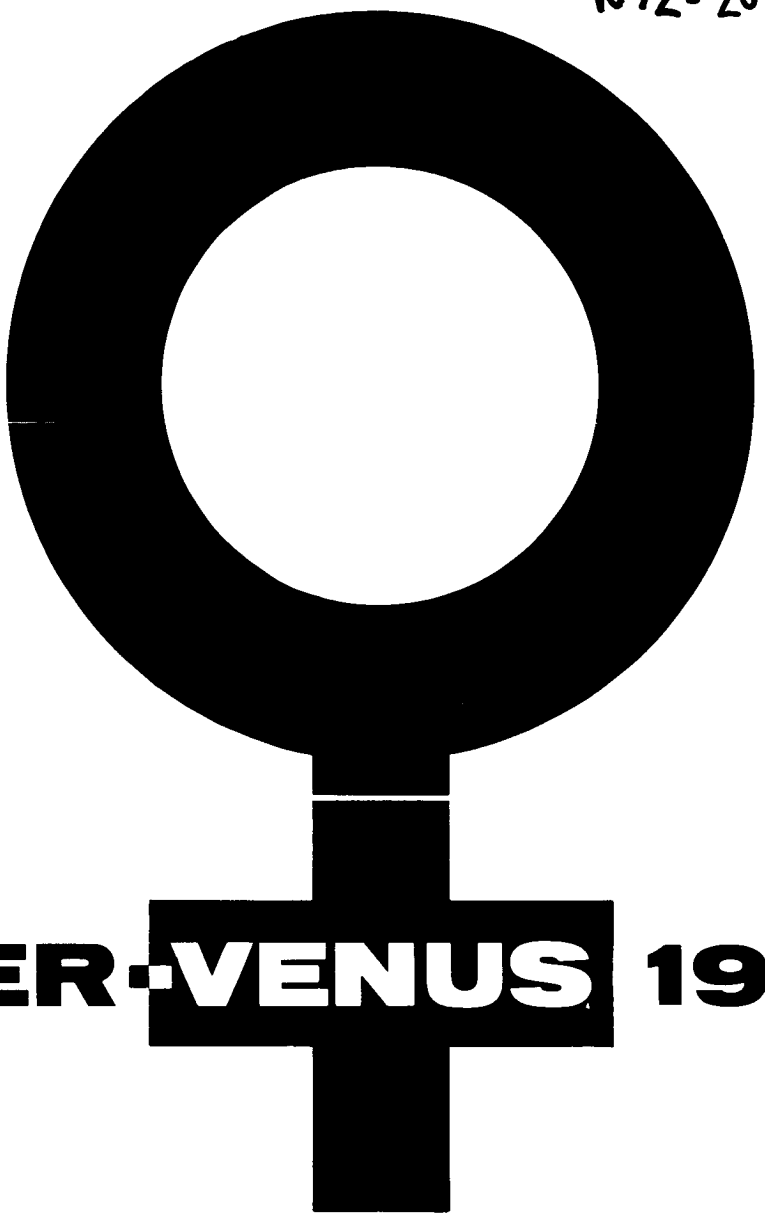

MARINER-VENUS 1967

Final Project Report

NATIONAL AERONAUTICS AND SPACE ADMINISTRATION

NASA SP-190

MARINER-VENUS 1967

Final Project Report

Scientific and Technical Information Office 1971
NATIONAL AERONAUTICS AND SPACE ADMINISTRATION
Washington, D.C.

Foreword

Thanks to Mariner-Venus 1962 (Mariner 2) and Mariner-Venus 1967 (Mariner 5), as well as the efforts of the Soviet Union, the world has learned enough in less than one decade to dispel several centuries accumulation of romantic notions about the planet Venus. In broad detail we know, for example, that the opaque clouds of Venus hide a surface less rugged than that of our Moon, but not uniformly smooth; that the atmosphere is almost entirely carbon dioxide; that the atmosphere pressure at the surface is up to 100 times the Earth's normal sea-level pressure; that the surface temperature is about 600 K; and that any possibility of Earth-type life existing on Venus is unalterably remote.

Nevertheless, while Venus is not what some people hoped it would be, and is indeed somewhat like others feared it might be, the veiled planet is still an object of tremendous and undiminishing scientific interest.

This book contains the record of the Mariner-Venus 1967 project. Mariner-Venus 1967 was, like its predecessor five years earlier, a flyby mission—gathering interplanetary data as it made the journey, and measuring and probing Venus with seven scientific experiments from its closest approach of slightly more than 4000 kilometers. The results, as we have seen, verified and extended the growing fund of Venusian data.

But apart from the contributions to knowledge of deep space, which were significant but by then not startling, Mariner-Venus 1967 stands as a unique achievement in two other respects: A secondary objective of the mission was to gain engineering experience by converting a spare Mariner-Mars 1964 spacecraft into one that could be flown to Venus. This we did with limited modifications and the addition of only enough new equipment to support the primary mission of extending and verifying the Mariner-Venus 1962 results. The savings were substantial not only because of the availability of the already purchased hardware but also because budgetary constraints in general were as strict as the technical requirements. The results showed the actual cost of the mission to be 10 percent less than anticipated.

These engineering and budgetary successes were by themselves worthy accomplishments to set alongside the mission's scientific achievements and are a tribute to the several hundreds of dedicated people who worked on the project.

GLENN A. REIFF
Mariner-Venus 1967 Program Manager

Contents

CHAPTER 1

Introduction

Mariner-Venus 1967 was authorized by NASA as a project in December 1965. Responsibility for management of the project, spacecraft system, mission operations system, and tracking and data system was assigned to the Jet Propulsion Laboratory (JPL). Responsibility for management of the launch vehicle system was assigned to the Lewis Research Center (LeRC). The assignment included administration and technical cognizance and control over launch vehicle system procurement and booster launch and flight operations, and analysis of flight performance and tracking information up to the time of spacecraft injection.

In accordance with interagency agreements, the Unmanned Launch Operations (ULO) Director at NASA's Kennedy Space Center (KSC) was delegated the responsibility for conduct of launch preparations and countdown at the Air Force Eastern Test Range (AFETR), under the technical direction and in support of LeRC launch vehicle system responsibilities. Flight performance data were routed through ULO to LeRC for final evaluation.

Mission requirements of the AFETR were levied through the NASA Test Support Office at Patrick Air Force Base. Local, as well as worldwide, coverage was obtained in this way. The Goddard Space Flight Center (GFSC) served as a relay point in the worldwide data-transmission links. The allocation of responsibilities for the agencies and the organizational relationships of the system managers are shown in figure 1–1.

Unique aspects of the Mariner-Venus 1967 project involved the use of existing hardware, the conversion of existing designs, and a single launch attempt. Equipment built to support Mariner-Mars 1964 (Mariner 4) as flight spares was used; modifications were limited to those necessary to meet the primary objective. Some new equipment was added as necessary to support the mission. Budgetary constraints were regarded as strict and as immutable as any of the technical requirements for the mission.

The primary objective of the Mariner-Venus 1967 project was to conduct a flyby mission to Venus to obtain scientific information that would complement and extend the results obtained by Mariner 2, relevant to determining the origin

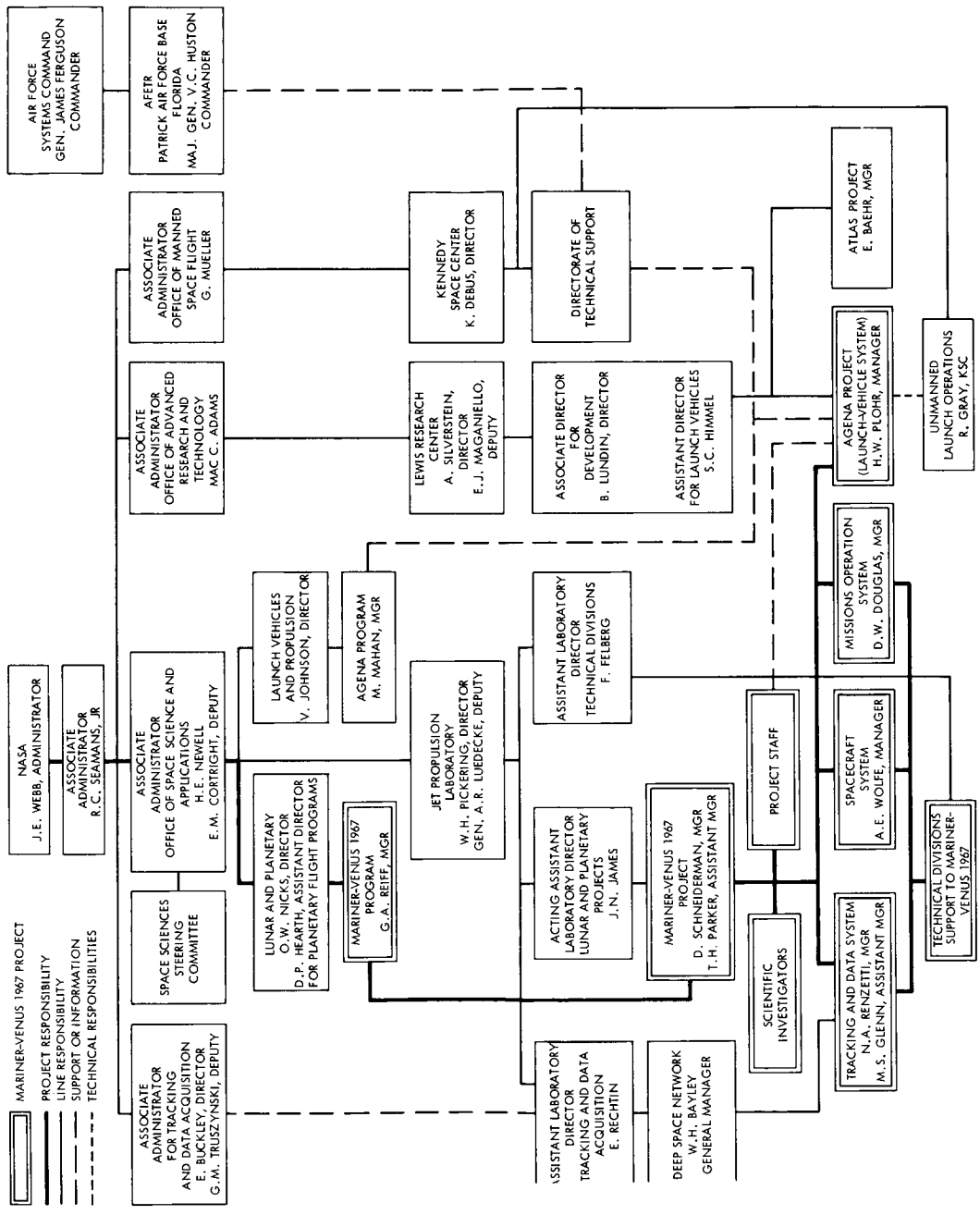

FIGURE 1–1.—Organizational relationships on the Mariner-Venus 1967 project.

and nature of Venus and its environment. Secondary objectives were to acquire engineering experience by converting (and operating) a spacecraft designed for a flight to Mars into one to be flown to Venus and to obtain information on the interplanetary environment during a period of increasing solar activity.

The single spacecraft, prepared by converting the spare Mariner 4 spacecraft, carried seven scientific experiments:

(1) Ultraviolet photometer
(2) Solar-plasma probe
(3) Helium magnetometer
(4) Trapped-radiation detector
(5) *S*-band radio occultation
(6) Dual-frequency radio propagation
(7) Celestial mechanics

The objective of the ultraviolet photometer experiment was to measure the properties of the uppermost layers of the atmosphere. The solar-plasma probe, helium magnetometer, and trapped-radiation detector experiments were designed to measure interrelated phenomena concerned with the interaction between the planet and the interplanetary medium (the environment of Venus). The *S*-band radio occultation and dual-frequency radio propagation experiments utilized communication radio waves to probe the properties of the Venusian atmosphere. The celestial mechanics experiment was designed to measure precisely the mass of Venus and the shape of its gravitational field. All experiments except *S*-band radio occultation acquired interplanetary data as well as near-Venus data.

The *S*-band radio occultation and celestial mechanics experiments used tracking and telecommunications facilities, but no special flight instruments; the dual-frequency radio propagation experiment required a new instrument package. The ultraviolet photometer, helium magnetometer, solar-plasma probe, and trapped-radiation detector experiments were modified only slightly from those of Mariner 4.

The needs for supporting a satisfactory scientific payload, meeting design constraints imposed by the *S*-band radio occultation experiment, and achieving the required electrical power at the encounter range within weight and funding constraints necessitated some spacecraft modifications. Other modifications were made to increase performance capability and operational flexibility (see table 1–I).

Mariner 5 was a fully attitude-stabilized spacecraft, using the Sun and Canopus as reference points. A two-way *S*-band communications system provided telemetry information, command capability, and tracking and ranging data.

Table 1–I.—Spacecraft changes

Unit affected	Modification	Reason
Command subsystem	Decoders replaced because of corroded transformers.	To replace inferior parts or those degraded by long-term storage.
Radio subsystem	Capacitors replaced because of poor quality, aggravated by long-term storage.	
Radio subsystem	Modified to permit ranging; exciters modified to eliminate spurious output mode.	
Tape recorder	Playback analog circuitry replaced because of inadequate potting; faulty logic eliminated potential source of relay malfunction.	To correct known deficiencies.
Canopus sensor	Removed high-brightness gate to eliminate potential tracking of dust.	
Helium magnetometer	Changed sweep-vector resistors; scale factor reduced 44 percent.	
Solar-plasma probe	Logic altered for increased energy-level sampling rate at encounter.	
Trapped-radiation detector	Changed from 2-level to 4-level solid-state detector; relocated detector A to point toward Sun; increased integration time constant to improve signal-to-noise ratio.	To improve spacecraft performance or flight operations.
Ultraviolet photometer	Operated throughout cruise	
Battery charger	Toggling controlled by one command	
Temperature-control reference	Replaced by new instrument	
Solar-plasma probe	Relocated sensor	
Helium magnetometer	Added heater to sensor assembly; added thermal "diaper" around ball part of sensor.	To accommodate Venus mission.
Data automation subsystem	Completely redesigned the logic and power converter; changed from pellet-type construction to integrated circuits.	

The central computer and sequencer (CC&S) supplied timing, sequencing, and computational services for other spacecraft subsystems. All spacecraft events were implemented in three distinct sequences: launch, midcourse, and encounter.

On June 14, 1967, at 06:01:00 GMT, Mariner 5 (fig. 1–2) was launched from Cape Kennedy, Fla. The Atlas/Agena launch vehicle successfully placed Mariner on a direct-ascent trajectory to Venus. The spacecraft entered a low-altitude, circular parking orbit, coasted for a predetermined time, then was injected into an escape trajectory by application of a final impulse. (The sequence of events from launch to Canopus acquisition is depicted in fig. 1–3.)

The nominal aiming point was designed to place the spacecraft 8165 km

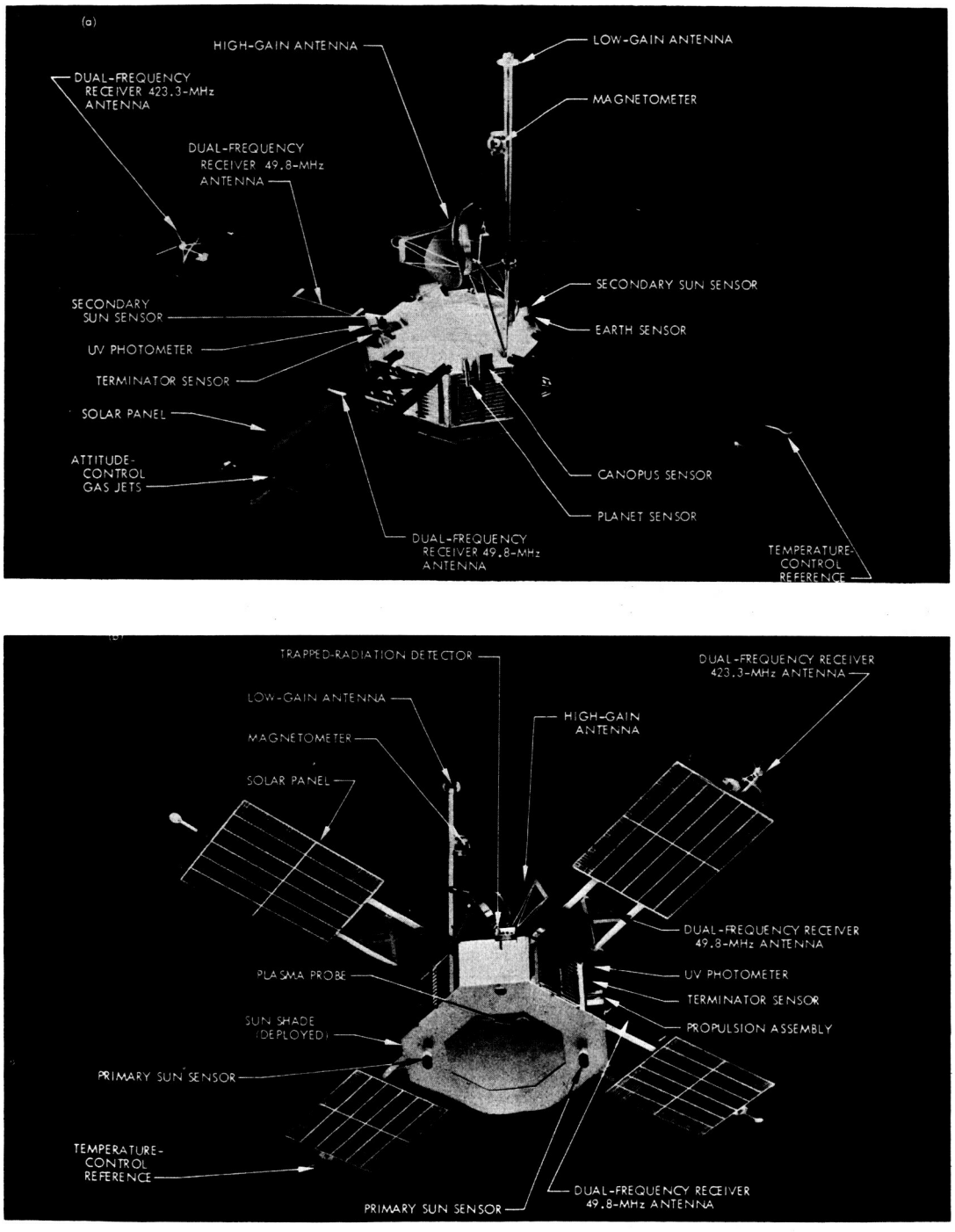

FIGURE 1–2.—Mariner 5 spacecraft configuration. *(a)* Top view. *(b)* Bottom view.

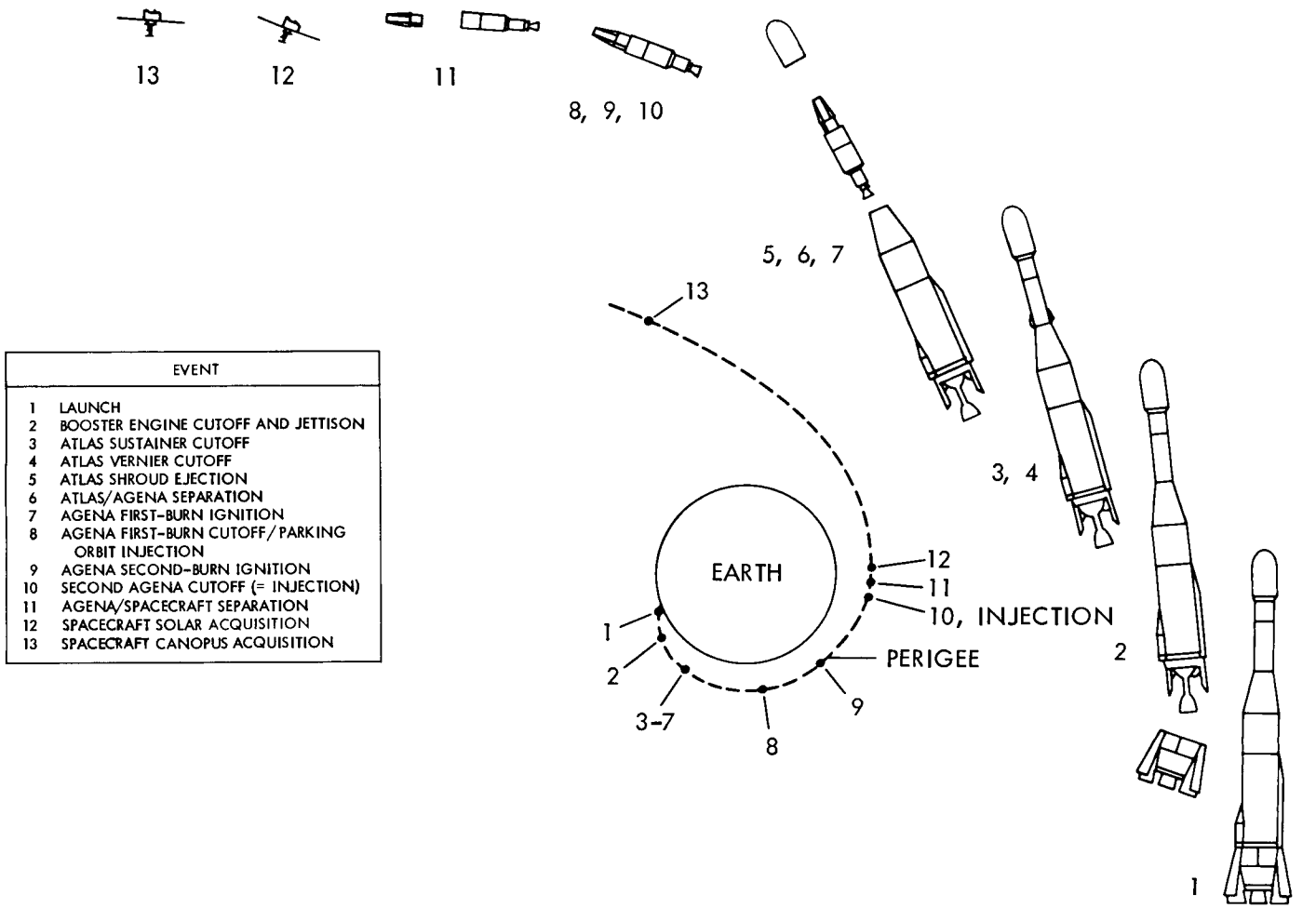

EVENT	
1	LAUNCH
2	BOOSTER ENGINE CUTOFF AND JETTISON
3	ATLAS SUSTAINER CUTOFF
4	ATLAS VERNIER CUTOFF
5	ATLAS SHROUD EJECTION
6	ATLAS/AGENA SEPARATION
7	AGENA FIRST-BURN IGNITION
8	AGENA FIRST-BURN CUTOFF/PARKING ORBIT INJECTION
9	AGENA SECOND-BURN IGNITION
10	SECOND AGENA CUTOFF (= INJECTION)
11	AGENA/SPACECRAFT SEPARATION
12	SPACECRAFT SOLAR ACQUISITION
13	SPACECRAFT CANOPUS ACQUISITION

FIGURE 1–3.—Mariner 5 sequence of events from launch to Canopus acquisition.

from the center of Venus on October 19, 1967. At injection, however, this aiming point was deliberately biased to 75 000 km to avoid any chance of the spacecraft and Agena impacting the planet. As a result, a midcourse maneuver was planned to achieve the nominal aiming point. Although the spacecraft had the capability of two maneuvers, the second maneuver capability was not exercised during the mission.

At 23:08:28 GMT on June 19, the midcourse maneuver was executed, placing the spacecraft at a closest approach distance of about 10 000 km from the planet's center. Canopus acquisition was maintained until the inertial-control mode was established.

After cruise-mode operations were reestablished following the trajectory correction, the spacecraft entered the interplanetary-cruise phase of the mission. This phase continued until the start of planetary encounter on October 19, 1967.

The encounter sequence was initiated from Deep-Space Station (DSS) 41 (Woomera) at 02:49:00 GMT. The closest approach to Venus occurred at 17:34:56 GMT (at the spacecraft). The altitude above the surface of the planet was 4094 km. All spacecraft data indicated a normal encounter.

From launch until the end of the mission, the spacecraft performance was excellent, and a large amount of useful scientific data was obtained. All mission objectives were successfully met.

Because of spacecraft capability, and because all objectives had been fulfilled, plans were made for an extension of the Mariner-Venus 1967 project. The technical plan was to acquire the Mariner 5 telemetry signal about July 22, 1968, and to maintain data and command capability necessary to attain the project objectives through about January 22, 1969.

The primary objectives of the Mariner-Venus 1967 extension project were to map uncharted regions of the celestial sphere at short wavelengths, acquire data on the interplanetary environment close to the Sun during a period of high solar activity, and continue refinement of celestial mechanics constants. A secondary objective was to obtain additional engineering knowledge of the effects of close perihelion passage on spacecraft equipment. No special tests were planned to exercise the capability of the spacecraft to increase spacecraft engineering design knowledge.

Acquisition attempts for a nominal spacecraft were started on April 26, 1968; five such attempts were made with negative results. Operations continued, assuming a nonstandard spacecraft condition until a successful reacquisition was accomplished on October 14, 1968. However, the spacecraft exhibited an anomalous behavior in both signal strength and stability. Two-way lockup with the

spacecraft receiver and transmitter could be obtained, but there was no evidence of telemetry in the received signals, nor was there any response to ground commands. This condition prevailed throughout all subsequent tracking activities. Accordingly, the Mariner-Venus 1967 project was considered complete and was terminated on November 5, 1968, without accomplishing the extension project objectives.

The subsequent chapters of this book contain detailed information on the spacecraft performance, mission operations, and tracking and data acquisition for the Mariner-Venus 1967 and Mariner-Venus 1967 extension projects. Scientific and engineering results and conclusions for each experiment on the Mariner-Venus 1967 project are discussed in chapter 2.

CHAPTER 2

Scientific and Engineering Results and Conclusions

The primary scientific objective of the Mariner 5 mission was to investigate the atmosphere, the ionosphere, and the magnetosphere of Venus. Despite its close proximity to the Earth and its similarity in size, Venus presented more problems than any other member of the solar system. Its thick cloud cover appeared, from Earth, to cover the planet at all times and no holes in the cover had been observed by the Mariner 2 infrared photometer in its three scans across the disk from a distance of less than 7 planet radii. Telescopic measurements of the radius of the visible disk had yielded the value 6120±7 km (ref. 2–1); analysis of the planetary radar measurements of the radius of the solid planet showed a value of 6056 km (ref. 2–2). The difference in these two measurements indicated that the depth of the atmosphere below the cloud tops was about 64 km. (The accuracy of this value had not been determined because radar radius measurements, although of high precision, could be subject to unknown systematic errors.)

The mass of Venus had been calculated from the gravitational perturbation of the orbits of asteroids, but a far more accurate value had been deduced from the tracking data of Mariner 2 (ref. 2–3), which had passed much closer than any observed asteroid. Relative to the mass of Earth, the mass of Venus was 0.815 027 ±0.000 012. Combining this with the 6056-km value for the density gave the mean density of Venus as 94.9 percent that of Earth.

Information regarding the nature of the planet's surface was limited to what could be deduced from measurements with radio waves of centimeter wavelengths, which are capable of traversing the dense clouds. Analysis of radar echoes from the surface indicated that the surface is generally smoother and more compact than that of the Moon (ref. 2–4).

Radar observations showed that the surface is not uniformly smooth, and hence not completely covered by ocean. The existence of localized regions of more than average roughness was detected first during the Venus conjunction of 1962, and additional detail was added in succeeding conjunctions. The map of Venus, as determined by analysis of data from the Goldstone tracking station, is given in figure 2–1 (ref. 2–5).

Observations of these rough regions in successive conjunctions provided

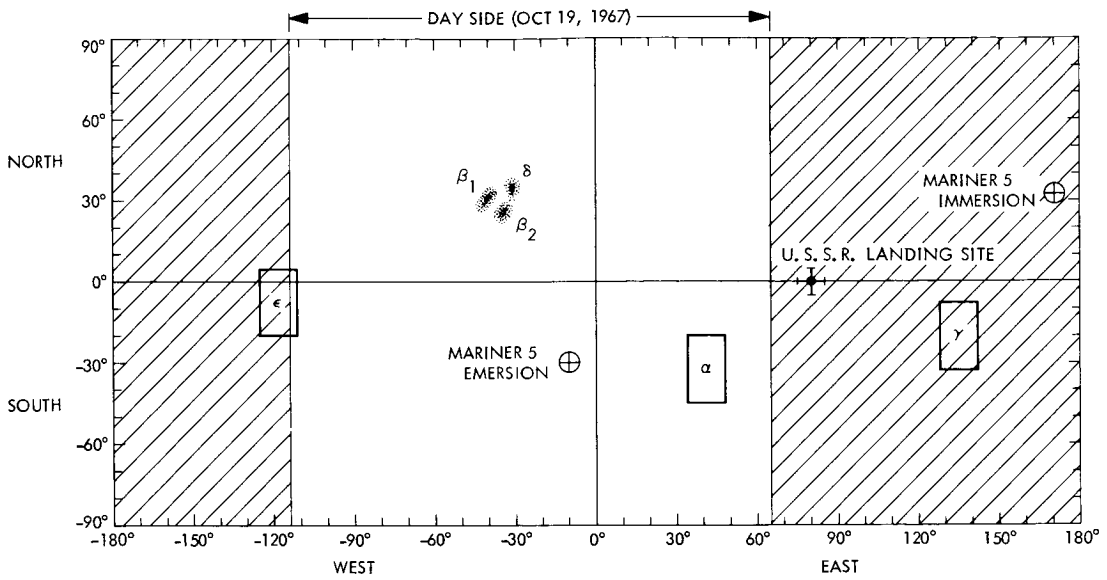

FIGURE 2–1.—Map of Venus showing regions probed by Venera 4 and the Mariner 5 occultation experiments and the radar-identified rough regions. Size and shape of regions β and δ are as shown, but the rectangles depicting α, γ, and ϵ indicate only the uncertainty in their locations.

answers to a longstanding controversy concerning the rotation of the planet. It was found that the retrograde rotation of Venus is slow (ref. 2–6); relative to the stars, it rotates once in 143.1 Earth-days. Relative to Venus, the Sun moves from west to east, and the time from noon to noon is 116.77 Earth-days. Relative to the Earth, a puzzling "resonance" appears, as the mean time between conjunctions is 583.91 Earth-days, which is equal to precisely 5.0 Venus-days with an accuracy of 0.01 percent.

Microwave radiation from the planet had been observed repeatedly over a decade; and it was uniformly found that for wavelengths between 3 and 20 cm, its intensity corresponded to that from a blackbody radiator at a temperature somewhat over 600 K. If the observed radiation were actually thermal radiation from the surface, then the surface temperature must approach 700 K, considering the correction for less than unity emissivity. It was suggested, however, that part of the microwave energy could come from nonthermal processes (ionospheric effects, lightning strokes, etc.), so that the surface would be much cooler. Close observations by Mariner 2 (ref. 2–7) revealed limb darkening (i.e., less intense radiation from the edges of the planet than from the center), as would be expected

if radiation from the hot surface were partially absorbed in a thick atmosphere. Also, the polarization measurements of Clark and Kuz'min (ref. 2–8) were consistent with the hypothesis of a high-temperature surface. Some advocates of low-temperature surface, however, remained unconvinced.

If the temperature of the bottom of the atmosphere was uncertain, the situation regarding the atmospheric pressure and composition was even worse. Before 1965, the only atmospheric component spectroscopically identified unequivocally and in abundance was CO_2 (ref. 2–9). Because of the uncertainty regarding the physical processes of interaction between the sunlight and the clouds (ref. 2–10), however, it was not certain whether this gas was a major or a minor constituent; fractions from 5 to 100 percent were quoted in the literature. Spectroscopic evidence for water vapor had been observed by several investigators, but there was no agreement regarding the quantity, except that it was small. In 1966, spectroscopic observations of unprecedented resolution and detail, obtained with an interferometer, showed traces of CO, HCl, and HF. These observations gave strong support to the presence of a large CO_2 abundance, but this conclusion had generally escaped attention (ref. 2–11).

The amount and depth of the atmosphere were also unknown. Surface pressures ranging from 5 to 300 bars were quoted in the literature. (The mean atmospheric pressure at sea level on Earth is 1.013 bars.) Because the nature of the physical processes in the atmosphere would be quite different at these extreme pressures, and there appeared to be no means available for determining the surface pressure from Earth-based measurements, this quantity was probably the most crucial unknown factor about the atmosphere of Venus.

Almost nothing was known about the upper atmosphere. No clear evidence for an ionosphere had been observed. The nature of the interaction of the solar wind with the planet was entirely unknown. Although it was expected that something similar to the Earth's magnetosphere (formed by the interaction of the solar wind with the geomagnetic field) would exist around Venus, but on a smaller scale, Mariner 2, which passed by the planet at a distance of 41 000 km on the sunlit side, apparently was too far away to observe it.

SCIENTIFIC MISSION

The primary objective of the Mariner-Venus 1967 project was to learn as much as possible about the planet within the stipulated mission constraints, which included a compressed schedule from mission inception to launch date and a tight budget allotment. Both constraints necessitated that the project use a Mariner 4 spare flight spacecraft and as much of its instrumentation as feasible.

The constraints on money and manpower dictated that no more instruments be carried than necessary to fulfill the most important objectives.

Intensive consideration of scientific payload alternatives began at the Jet Propulsion Laboratory and at NASA Headquarters in December 1965. In February 1966, seven experiments were selected: three to investigate the atmosphere of Venus, three to investigate the environment of Venus, and one to investigate the ephemeris and the gravitational field of Venus.

S-Band Radio Occultation Experiment

This experiment was, at least in concept, identical with that conducted by the Mariner 4 mission to Mars. The experiment used the spacecraft radio subsystem and special instrumentation at the Goldstone tracking station to record the changes in frequency and phase of the telemetry carrier wave as it passed through the atmosphere of Venus upon entrance into and exit from occultation. From these data, it was hoped that the altitude profiles of pressure, density, and temperature in the lower atmosphere would be derived. The experimenters were Dr. A. J. Kliore (Principal Investigator), JPL; D. L. Cain, JPL; Dr. G. Fjeldbo, Stanford University; G. S. Levy, JPL; and Dr. S. I. Rasool, Goddard Institute of Space Studies.

Ultraviolet Photometer Experiment

This experiment was chosen to investigate the uppermost layers of the atmosphere. The instrument was scheduled to be flown on Mariner 4, but difficulties experienced in late systems tests caused its deletion from the flight. The instrument was designed to point directly toward the planet at encounter, thus scanning through the atmosphere in a search for ultraviolet light from the Rayleigh scattering of sunlight in atomic hydrogen and oxygen. From the altitude profiles of intensity, it was hoped to determine the abundance, distribution, and temperature of these two atmospheric components in the exosphere. The experimenters were Dr. C. A. Barth (Principal Investigator), University of Colorado; W. G. Fastie, Johns Hopkins University; K. K. Kelly, University of Colorado; E. F. Mackey, Packard Bell Electronics; J. B. Pearce, University of Colorado; and Dr. L. Wallace, Kitt Peak National Observatory.

Dual-Frequency Radio Propagation Experiment

This experiment was added to supplement the other two atmospheric experiments by providing a very sensitive measurement of the electrically charged components of the atmosphere. It also would provide information regarding the neutral atmosphere and the electron density in the interplanetary plasma.

It utilized a dual-frequency receiver (DFR) on the spacecraft to process the two carrier waves transmitted from the 150-ft parabolic antenna at Stanford University. The experimenters were Dr. V. R. Eshleman (Principal Investigator), Stanford University; Dr. G. Fjeldbo, Stanford University; Dr. H. T. Howard, Stanford University; R. L. Leadabrand, Stanford Research Institute; T. A. Long, Stanford Research Institute; B. B. Lusignan, Stanford University; and Dr. A. M. Peterson, Stanford University.

Solar-Plasma Probe

The Faraday-cup plasma probe was essentially identical with that flown on Mariner 4, with the exception of its measurement sequence. The purpose of the Mariner 5 plasma probe was to measure the flux, density, bulk velocity, flow direction, and temperature of the solar plasma and to determine whether and how the plasma properties were altered in the vicinity of Venus. The experimenters were Dr. H. S. Bridge (Principal Investigator), MIT; Dr. A. J. Lazarus, MIT; and Dr. C. W. Snyder, JPL.

Helium Magnetometer

The Mariner 5 helium magnetometer was a modified Mariner 4 instrument designed to measure the three vector components of the interplanetary magnetic field and to determine whether and how the field was altered in the vicinity of Venus. The experimenters were Dr. E. J. Smith (Principal Investigator), JPL; Dr. P. J. Coleman, Jr., UCLA; Dr. L. Davis, Jr., Caltech; and Dr. D. E. Jones, Brigham Young University.

Trapped-Radiation Detector

This instrument consisted of a group of four charged-particle detectors, essentially identical to those on Mariner 4, designed to measure the fluxes of protons, alpha particles, electrons, and X-rays in space (particularly those coming from the Sun), and to search for trapped particles that could exist in "radiation belts" near Venus. The experimenters were Dr. J. A. Van Allen (Principal Investigator), University of Iowa; Dr. L. A. Frank, University of Iowa; and Dr. S. M. Krimigis, University of Iowa.

Celestial Mechanics

Sophisticated computer calculation techniques of celestial mechanics would be used to analyze the spacecraft tracking data to provide more accurate determinations of a variety of astronomical quantities such as the mass of Venus and other planets, the ephemerides of Venus and Earth, the astronomical unit (AU),

and the symmetry of the gravitational field of Venus. Similar calculations had been made on the doppler tracking data from earlier Mariners; these would be supplemented for the first time by direct ranging measurements (from round-trip signal flight times) of high precision at planetary distances. Although the special spacecraft receiver required to provide ranging had been aboard Mariner 4, it was not used because of interference problems with the command subsystem. The Mariner 5 experimenters were Dr. J. D. Anderson (Principal Investigator), JPL; Dr. L. Efron, JPL; G. E. Pease, JPL; and Dr. R. C. Tausworthe, JPL.

ENCOUNTER WITH VENUS

The spacecraft trajectory at encounter was planned primarily to satisfy the requirements of the *S*-band radio occultation experiment because they were the most stringent. Fortunately, this trajectory was also close to optimum for all other experiments. The requirements were (1) that the trajectory pass as close to Venus as consistent with the guidance accuracy and planetary quarantine specifications and (2) that it pass behind Venus, as seen from the Earth, and as close as possible to the extended center-to-center line of the two planets. The encounter orbit is shown in figures 2–2 through 2–5. Figures 2–2 and 2–3 show the actual shape of the orbit; figures 2–4 and 2–5 are projections of the orbit, viewed from the Sun and the Earth, respectively. In each figure, the numbers on the curve give the time from encounter, in minutes; the letters represent specific events. (See table 2–I for code explanations.) Encounter occurred at a planetocentric range of 10 151 km, corresponding to about 4100-km altitude; the trajectory, as viewed from Earth, missed the center of the disk by only 270 km (ref. 2–12).

The velocity of Mariner's approach to Venus was relatively slow, only 3.05 km/s, neglecting the velocity picked up in the planet's gravitational field. This fact, combined with the close approach, caused a large deflection of the trajectory, about 101.5° in the Venus coordinate system. This large gravitational perturbation was significant because it permitted accurate determinations of the planet's mass and of the spacecraft's trajectory relative to Venus. The accurate trajectory, in turn, permitted an accurate determination of the planet's radius. Analysis of spacecraft tracking data is a complex and lengthy process, which is not completed for Mariner 5. The latest available results are summarized as follows.

From tracking data acquired near encounter, the mass of Venus is derived. The directly determined quantity is the gravitational constant of Venus, for which the value derived by Mariner 5 is $324\,859.61 \pm 0.5$ km^3 s^{-2} (ref. 2–13); this is

FIGURE 2.2—Isometric projection of the Venus encounter orbit. Time (in minutes) from encounter is indicated. Code identifications for figures 2–2 through 2–5 are given in table 2–I.

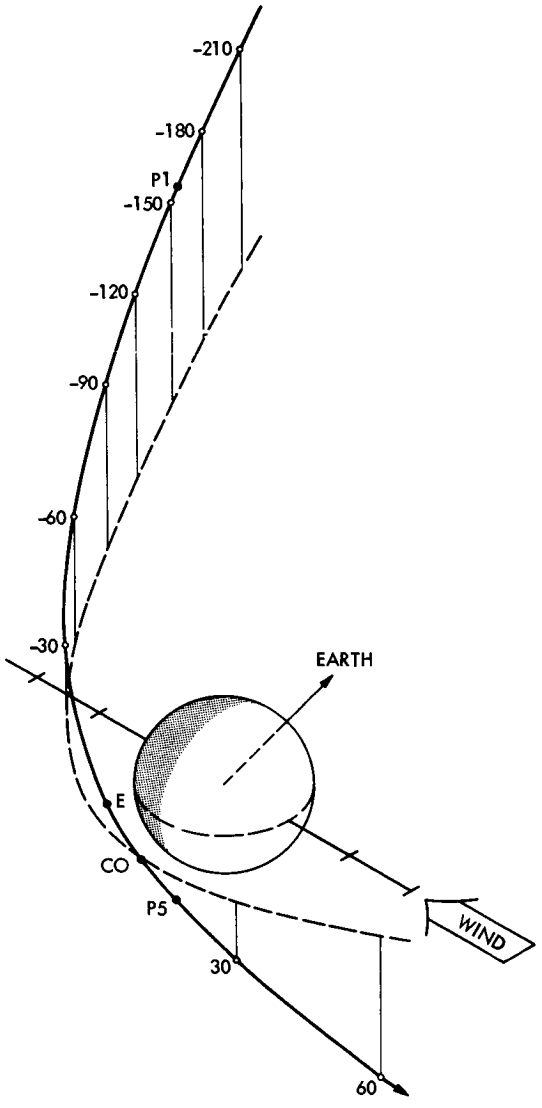

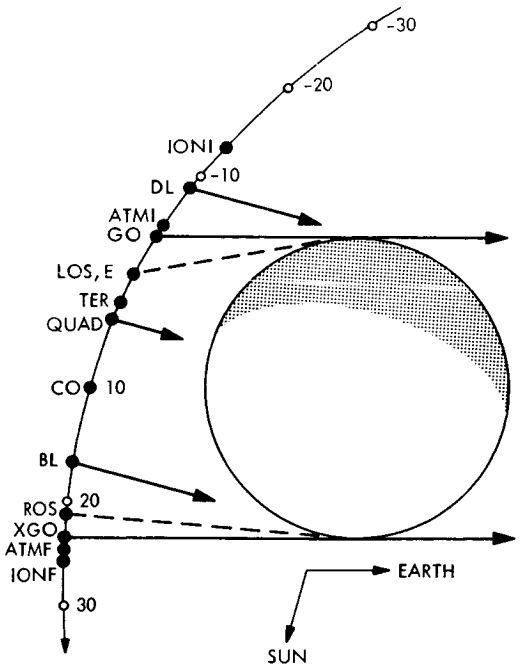

FIGURE 2–3.—Venus encounter orbit shown in the orbit plane. Short arrows show line of sight of ultraviolet photometer as it observed the crossings of the dark limb, terminator, and bright limb. Long arrows indicate paths of radio signal, at boundaries of occultation period, which would have been observed with very little atmosphere. Dashed lines indicate (schematically only) the actual radio rays at loss and reacquisition of the telemetry signal. Sun was 31.7° above the orbit plane in the direction shown.

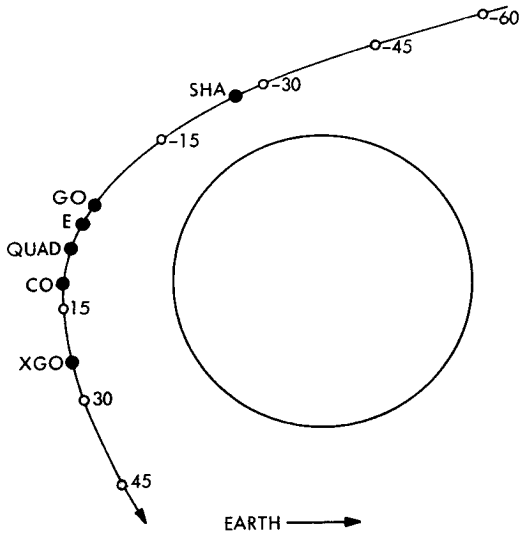

FIGURE 2–4.—Venus encounter orbit, as viewed from the Sun, projected onto the terminator plane.

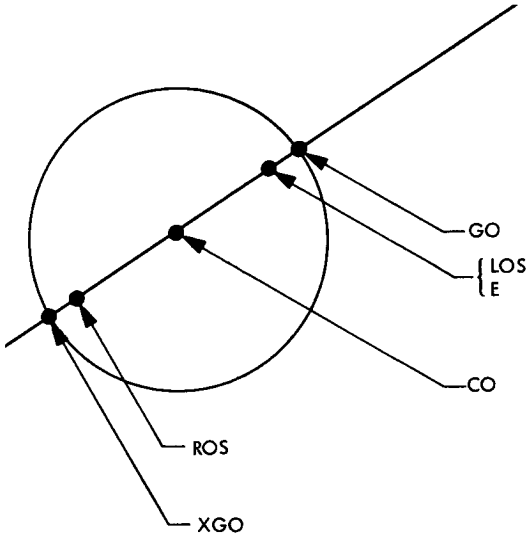

FIGURE 2–5.—Venus encounter orbit, as viewed from the Earth, projected onto the terminator plane.

Table 2–I.—Chronology of significant events during Venus encounter

Code	Time from encounter, E, min	Event
P1	−156	Initial passage through a boundary in solar plasma.
SHA	−22	Closest approach to shadow of Venus.
IONI	−13.1	Initial detection of ionosphere by dual-frequency receiver.
DL	−7.9	Dark limb of planet observed by ultraviolet photometer.
ATMI	−3.18	Initial detection of atmosphere by S-band radio-occultation experiment.
GO	−2.0	"Geometrical occultation"—Earth-to-spacecraft line of sight intersects dark limb of planet.
LOS	−0.23	Loss of signal (telemetry) resulting from occultation.
E	0	Encounter (periapsis).
	+2.73	Loss of spacecraft radio carrier wave.
TER	+3.4	Terminator crossing observed by ultraviolet photometer.
QUAD	+3.55	Quadrature; Sun-Venus-Mariner 5 angle: 90°.
CO	+10.0	Center of geometrical occultation.
BL	+16.7	Bright-limb crossing observed by ultraviolet photometer.
P5	+18	Final passage through a boundary in the solar plasma.
ROS	+20.6	Reacquisition of signal by Goldstone tracking station.
XGO	+22.8	Exit from geometrical occultation at bright limb.
ATMF	+23.0	Final observation of atmospheric effect on S-band signal.
IONF	+24.0	Final detection of ionosphere by dual-frequency receiver.

comparable to the value of $324\,859.95 \pm 1.8$ km^3 s^{-2} derived by Mariner 2 (ref. 2–14). Utilizing other astronomical constants, other quantities of more general interest can be calculated. Thus, assuming a value of 149 597 896 for the astronomical unit, the Sun/Venus mass ratio is $408\,522.62 \pm 0.63$; and assuming 398 601.33 for the gravitational constant of Earth, the Venus/Earth mass ratio is 0.814 998 8. The oblateness of the gravitational field of Venus, which is very small compared to that of the Earth, is measured by the second-order zonal harmonic coefficient J_2, which was calculated to be $(8.4 \pm 3.9) \times 10^{-6}$ (ref. 2–15) compared with the Earth value of 1.08×10^{-3}. The gravitational oblateness results from the oblateness of the body of the planet itself, which for the Earth amounts of 21 km out of 6371 km, and for Venus appears to be about 100 times less, as may be expected from the very low rotation rate. No evidence appears in the data for a gravitational bulge that has been postulated to account for the "resonance" in the rotation.

Throughout the mission, radar-bounce measurements on Venus were made at frequent intervals. The near simultaneousness of these radar-range measurements on Venus and the radio tracking data on Mariner enabled the planet's radius to be determined by a more direct method than the determination by radar alone, and is virtually independent of errors in the ephemerides of Venus and Earth. The position and velocity of the gravitational center of Venus were derived with high accuracy from the Mariner tracking data during encounter. The resulting geocentric range of the center of the planet at encounter was compared with the interpolated geocentric range at this epoch from the radar time-delay measurements. Because the radar data refer to the sub-Earth point on the surface of Venus, the radius is given directly by the difference between the two types of measurements.

As obtained by this technique, the value for the radius, when corrected for the time delay of the radar signal through the dense Venusian atmosphere as now understood, is 6054 ± 2 km (ref. 2–16). All radar-only determinations made using data from Goldstone, from MIT, and from the Arecibo Ionospheric Observatory are in the range of 6048 and 6056 km (ref. 2–5). The directness of the radar and Mariner determination, together with the good agreement of all determinations, has resolved the controversy over the Venus radius raised by the Venera 4 results, as discussed later in this chapter.

Lower Atmosphere

To determine the atmospheric density and pressure at the surface, a measurement of the highest priority, only two feasible techniques were known: (1) to

set a pressure sensor down on the surface and (2) to send a radio wave through the atmosphere and past the surface at grazing incidence. In 1967 the U.S.S.R. chose the former technique and the United States chose the latter. Neither experiment was completely successful, but a combination of the two has resulted in a reasonably accurate estimate.

In passing through the atmosphere of a planet, a light wave or a radio wave follows a slightly curved path because the density (and hence the refractive index) of the gas decreases with altitude. The refractive index is different for different gases; but for a given gas mixture, the "refractivity" (refractive index minus 1) is strictly proportional to density. The amount of deflection experienced by a radio wave in passing in and out of the atmosphere depends upon the profile of refractivity encountered along its path. In simple cases (e.g., spherical symmetry and fixed composition), it is possible to infer unambiguously the profile of refractivity with height from a continuous measurement of the amount of deflection of a grazing ray as it passes deeper and deeper into the atmosphere. It is also true, but less intuitively apparent, that the profile can be deduced from the change in doppler frequency of the radio signal as the spacecraft radio transmitter is "occulted" by the atmosphere; thus, the time history of the doppler frequency was the principal measurement sought by the *S*-band occultation experiment (ref. 2–17).

In addition to refraction by the neutral atmosphere, other physical processes occur as the wave crosses the atmosphere. The received signal intensity falls rapidly as the wave goes deeper because of absorption and because of the defocusing produced by the continuous variation of refractivity with altitude. Particles or small-scale turbulence can scatter the waves, and free electrons can cause both refraction and dispersion.

Because the Venusian atmosphere was known to be much denser than Earth's, the spacecraft and the mission were designed to maximize the signal received during occultation. It was recognized from the beginning that, even with unlimited energy in the radio signal, the phenomenon of super-refractivity could preclude probing the atmosphere to the bottom (ref. 2–18). The level at which the refractive index becomes so high that the radius of curvature of a horizontal ray is equal to the distance from that point to the planet center is called the level of critical refraction. Below that level, the atmosphere is super-refractive and a horizontal ray cannot escape, but spirals inward and strikes the surface. The refractivity of CO_2 is especially high (about 495×10^{-6} at normal temperature and pressure (NTP), and calculations of a variety of Venus model atmospheres showed that super-refractivity could be expected unless either the

surface pressure was low or the effect of the CO_2 was compensated by a large abundance of less-refractive gases (e.g., argon, about 278×10^{-6} at NTP).

As the spacecraft approached Venus, the doppler frequency of the signal received at Goldstone began to deviate from its calculated value, indicating the initial detection of the atmosphere at 3.18 min before encounter ($E - 3.18$ min), when the Goldstone-to-Mariner line of sight was passing Venus at a range of about 6140 km, corresponding to an altitude of about 90 km, well above the clouds. As shown in figure 2–6, the deviation (the residual) increased approximately linearly with time and had reached about 8.2 kHz at $E - 14$ sec when the closed-loop receiver was no longer able to maintain lock on the signal, resulting in loss of telemetry. The open-loop receiver continued to record the carrier-wave signal until the residual increased to about 16 kHz and the signal faded into the noise at $E + 2.73$ min. At this time, the signal path was about 6085 km from the planet's center (about 32-km altitude); the deflection of the signal was about 17°. The signal level obtained by processing the open-loop tape is shown in figure 2–7. The abrupt drop at the beginning is primarily the result of the defocusing effect; the complex structure at later times is not yet understood in detail.

Data obtained upon exit from occultation were similar to data recorded at

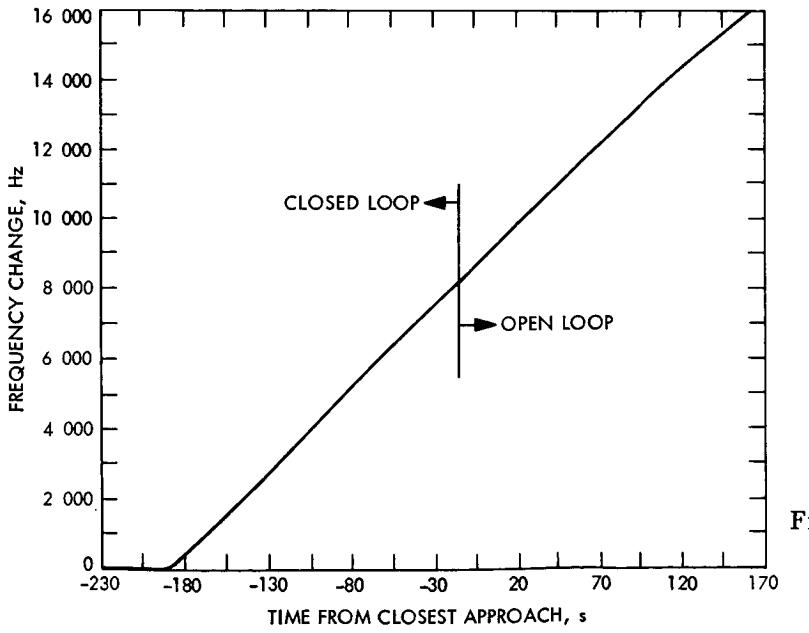

FIGURE 2–6.—Frequency residuals from data taken during entry into occultation.

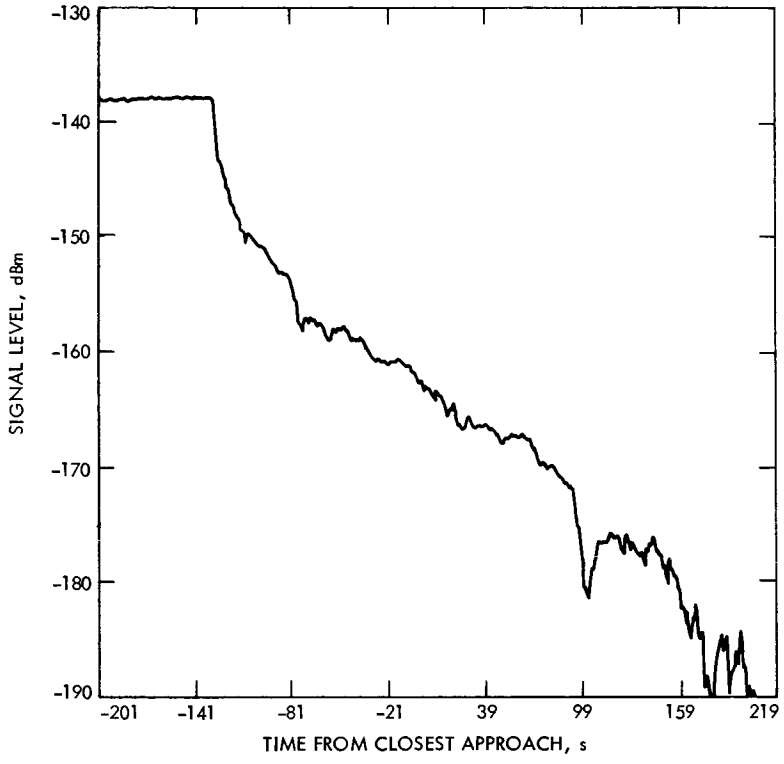

FIGURE 2–7.—Strength of received signal level during entry into occultation.

entrance, but did not extend as far into the atmosphere. The final analysis showed that the profiles of refractivity agreed within 1 km in altitude, even though the immersion data were taken on the night side of the planet and the emersion data came from the sunlit side (see fig. 2–1). The major difference between the two sets of data is shown by comparing figures 2–8 and 2–9. No effect of electrons in the upper atmosphere is apparent in the approach data, while the dense daytime ionosphere is clearly recorded in the postoccultation data. The dashed curves in figures 2–8 and 2–9 are calculated profiles for various assumed scale heights. (The scale height H, a measure of the rate of change of density with altitude, is given by $H = -\rho dz/d\rho = RT/gM$, were ρ is density, R is the universal gas constant, T is temperature, g is the local gravitational acceleration, and M is molecular weight.) It seems that H is approximately constant at 5.4 ± 0.2 km from about 6140 km down to about 6015 km, so that this region is approximately isothermal. If the composition is assumed to be 90 percent CO_2 and 10 percent N_2, consistent with Venera 4 results, the calculated temperature is 242 K, in good agreement with spectroscopic measurements of cloud-top temperature (ref. 2–19).

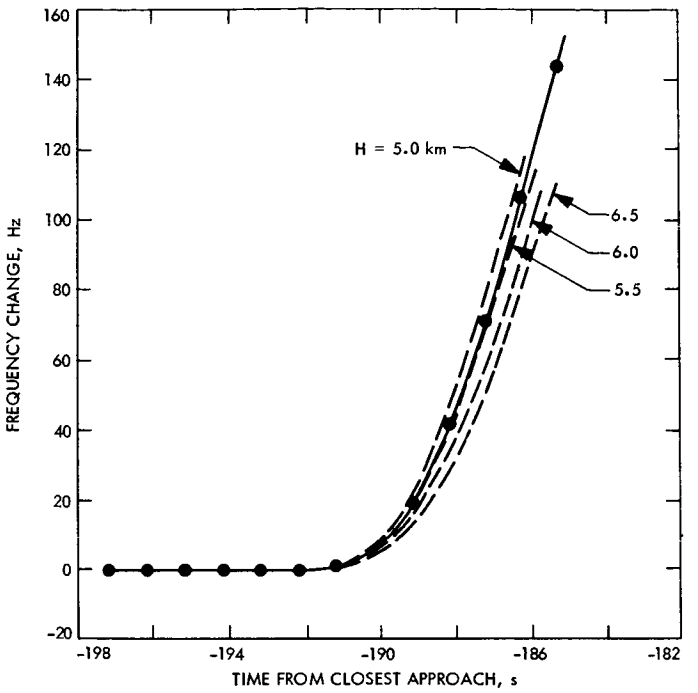

FIGURE 2–8.—Entry residuals with ← theoretical models.

FIGURE 2–9.—Exit residuals with ↓ theoretical models.

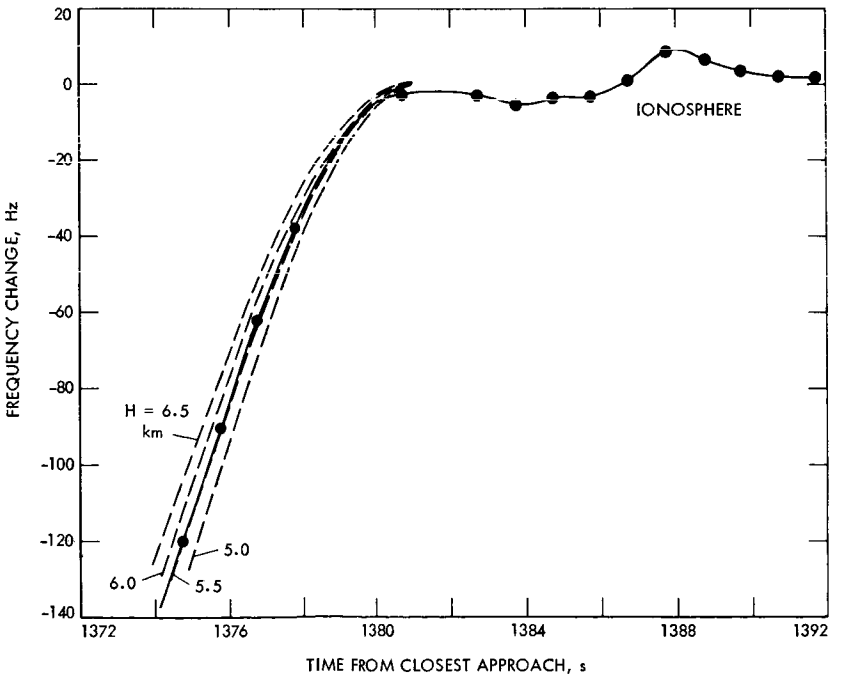

Figure 2–10 shows the refractivity profile on the night side (an N unit is 1 ppm). The solid part of the curve represents values directly computed from the data; the dashed portions are extrapolations. The upper part is a constant-temperature extrapolation to a range of 6140 km, where the first effects were observed. The lower part is an extrapolation at constant lapse rate to the 6085-km range, where the open-loop signal was lost.

Based on this refractivity profile, profiles of pressure, density, and temperature can be calculated if the composition is assumed (ref. 2–20). These are shown in figures 2–11 through 2–13 for two CO_2–N_2 atmospheres; in figure 2–11, the difference between the two profiles is no more than the line width on the graph.

On the day before the Mariner 5 encounter with Venus, the Soviet probe, Venera 4, dropped through the atmosphere on its parachute. It made frequent measurements of temperature for 94 min and of pressure for the first 50 min of this interval until the readings went off scale. Rough measurements of atmospheric composition were made near the beginning of the descent; these measure-

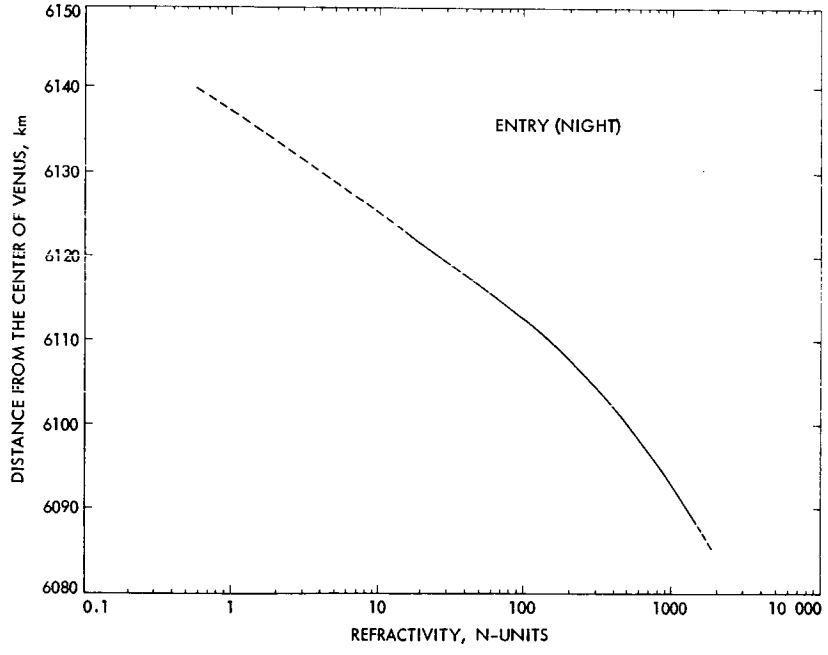

FIGURE 2–10.—Altitude profile of refractivity of the atmosphere on the night side of Venus. Solid part of the curve represents values computed directly from the data; the dashed parts are extrapolations.

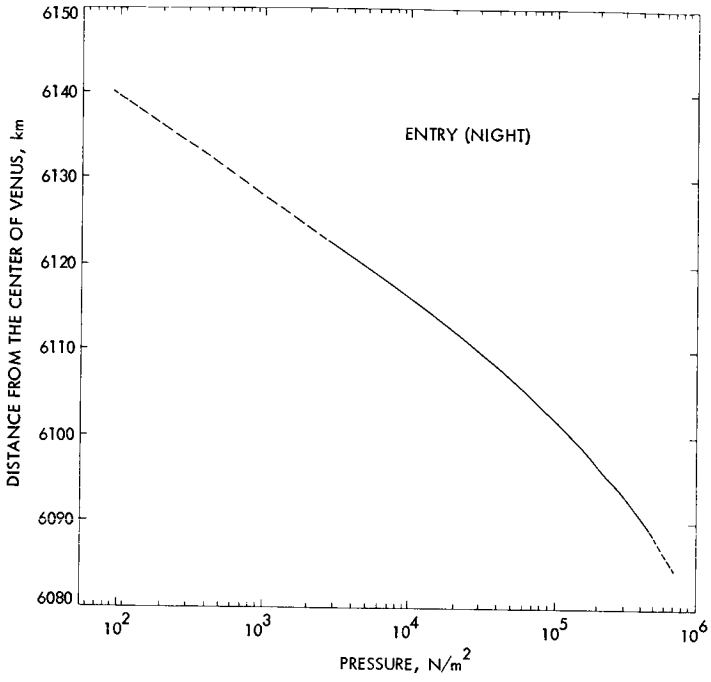

FIGURE 2–11.—Altitude profile of pressure on the night side.

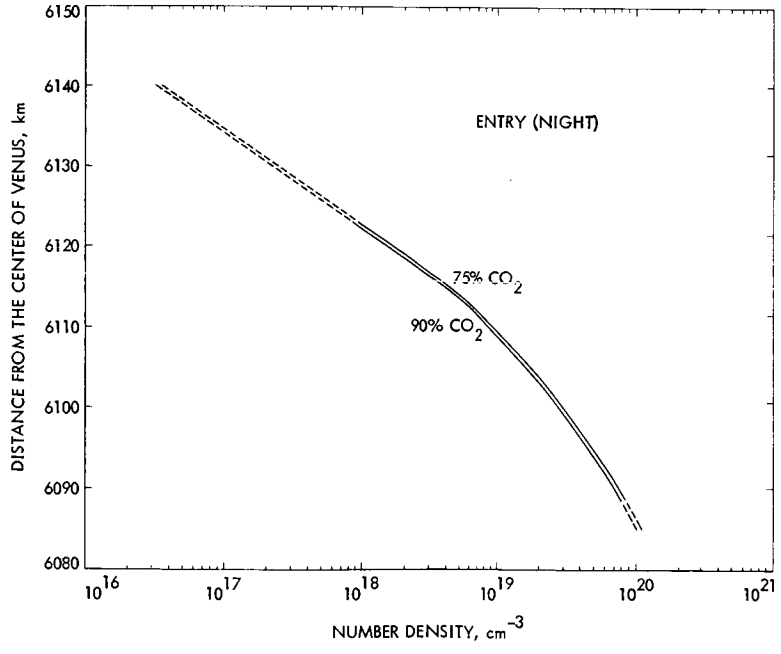

FIGURE 2–12.—Altitude profiles of density for two assumed CO_2/N_2 atmospheres.

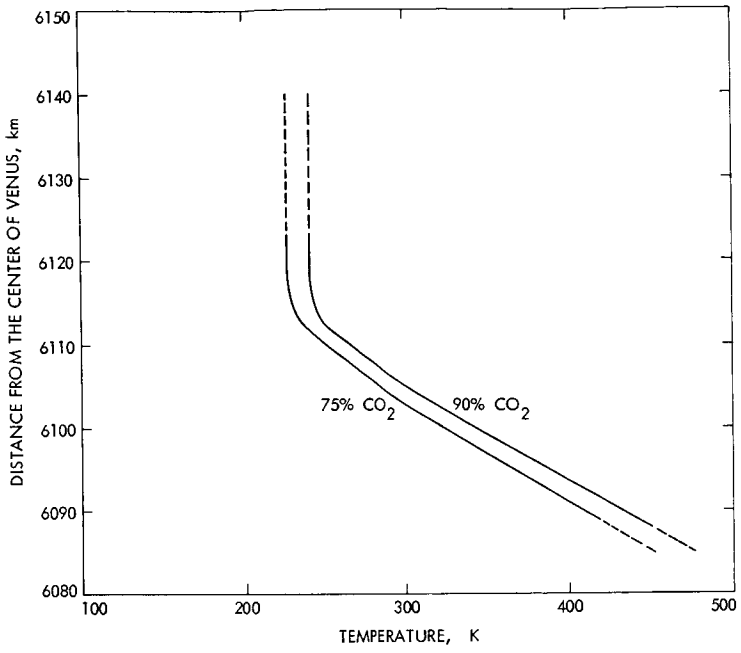

FIGURE 2–13.—Altitude profiles of temperature for two assumed CO_2/N_2 atmospheres.

ments indicated a composition of primarily CO_2 (90 ± 10 percent). No other major component was detected. From these measurements, the Soviet scientists constructed an atmospheric model for a region in the atmosphere that they assumed (on the basis of a single radioaltimeter measurement) to correspond to altitudes from 0 to 26 km. This model is compared with the Mariner 5 results in figure 2–14, which shows that the pressure and temperature profiles are in excellent agreement and that a CO_2 abundance near 85 percent may be the correct value. Mariner data showed that the region probed by Venera 4 was between 6078 and 6105 km from the planet's center. This corresponds to altitudes from about 25 to 52 km, based on the best estimate of the planet's radius (ref. 2–21).

Considering all information available, including the radar and radiometer results in the microwave region, the only tenable assumption appears to be that the Venera 4 radioaltimeter either malfunctioned or was misinterpreted (e.g., its signal at twice 26 km was taken as meaning a 26-km altitude), and that the Venera 4 telemetry did not extend to the surface (ref. 2–22). Thus, the conditions at the surface can be approximated by extrapolation. (See figs. 2–15 and 2–16.) The accuracy of the values obtained by these extrapolations depends on the

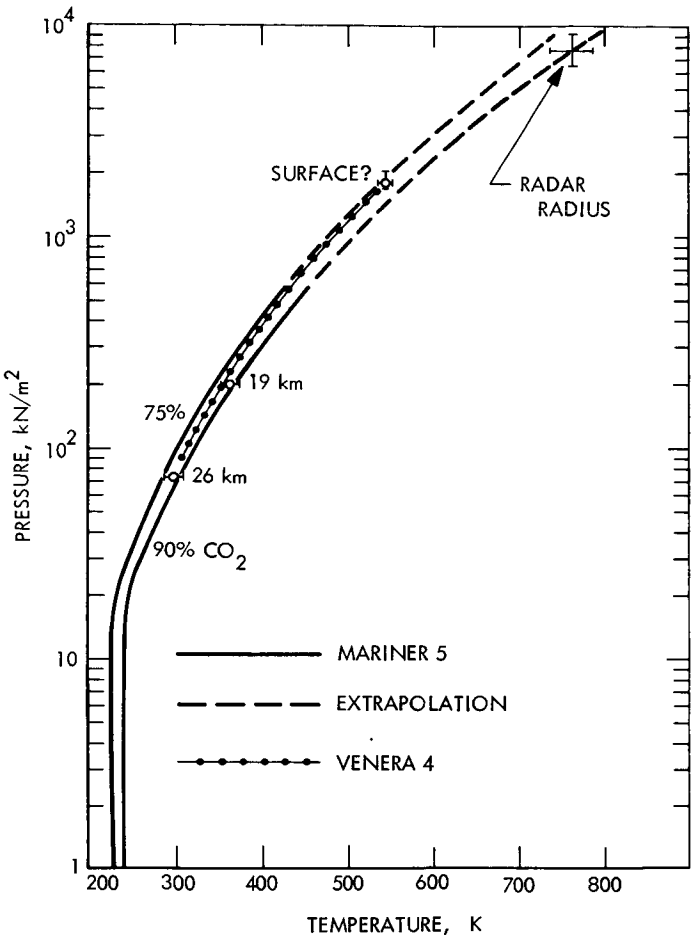

FIGURE 2–14.—Pressure versus temperature from Mariner 5 and Venera 4.

method by which they are performed and the depth to which they are extended. Pressures between 60 and 120 bars and temperatures between 650 and 800 K have been suggested by various authors.

As an explanation of the Venera 4 data, it also has been suggested that the probe landed on a high mountain. It can be seen, however, from figure 2–1, that the probe landed in a region where the radar mapping shows nothing unusual, and a mountain of the required size could hardly be missed. Nor do the radar results appear to permit an ellipticity of the equator of Venus of sufficient magnitude to reconcile the Mariner and Venera results, assuming that Venera's telemetry terminated at the surface.

Because critical refraction actually does occur at about 32-km altitude, the

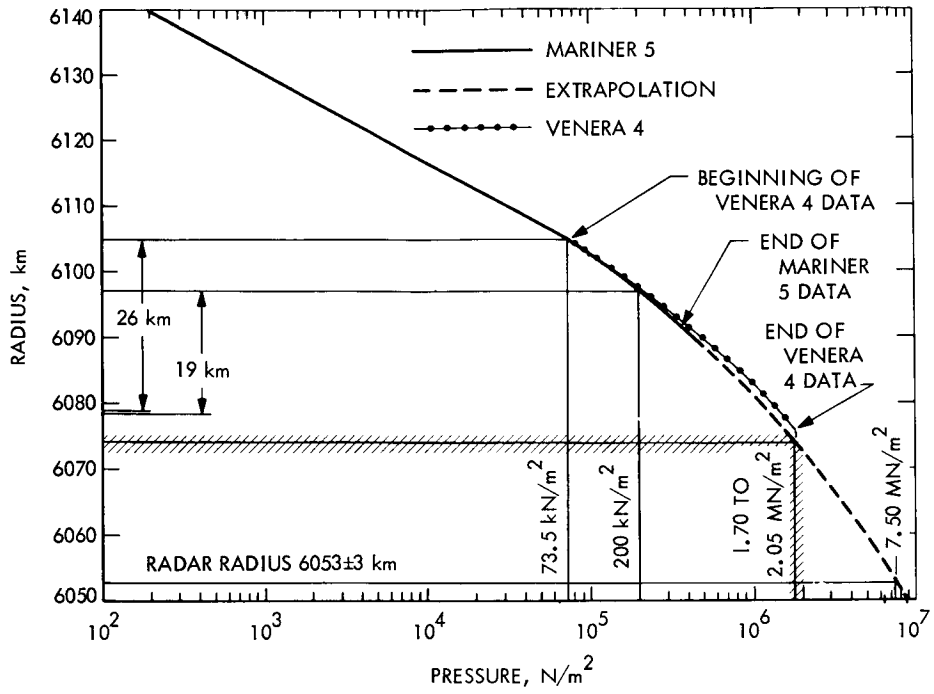

FIGURE 2–15.—Pressure profiles from Mariner 5 and Venera 4.

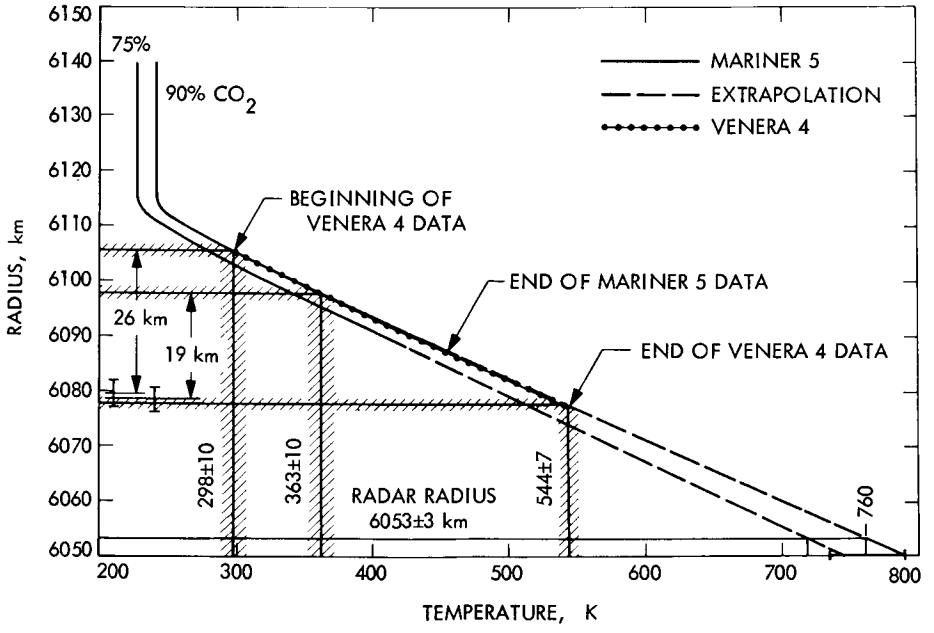

FIGURE 2–16.—Temperature profiles from Mariner 5 and Venera 4.

radio-occultation technique is incapable of probing the lower atmosphere. Nevertheless, in the absence of the Venera measurements, the Mariner results, which are firmly associated with a range scale, could have been extrapolated to give the surface conditions almost as accurately as they are now known. If Mariner 5 had not been flown, the original erroneous interpretation of the Venera data would not have been suspected, and the resulting theories regarding the bottom of the atmosphere obviously would be wrong.

Ionosphere and Upper Atmosphere

It was noted in figure 2–9 that the peak of the daytime ionosphere was detected by the *S*-band occultation experiment. The frequency shift observed was opposite to that produced by the neutral atmosphere, because the refractivity of an ionized medium is negative (given by the relation $N = -40.3\ n/f^2$, where n is the electron density and f is the frequency of the wave). Reduction of the *S*-band residual data gave the profile of electron density shown in figure 2–17, with a density peak of 5.5×10^5 cm^{-3} at a range of 6195 km (about 140-km altitude).

The inverse-square relationship between refractivity and frequency implies that much greater sensitivity in probing electron density can be obtained by using radio waves of lower frequency, and that is what the dual-frequency radio propagation experiment was designed to do (ref. 2–23). The dual-frequency receiver on the spacecraft received the signals transmitted from Stanford Uni-

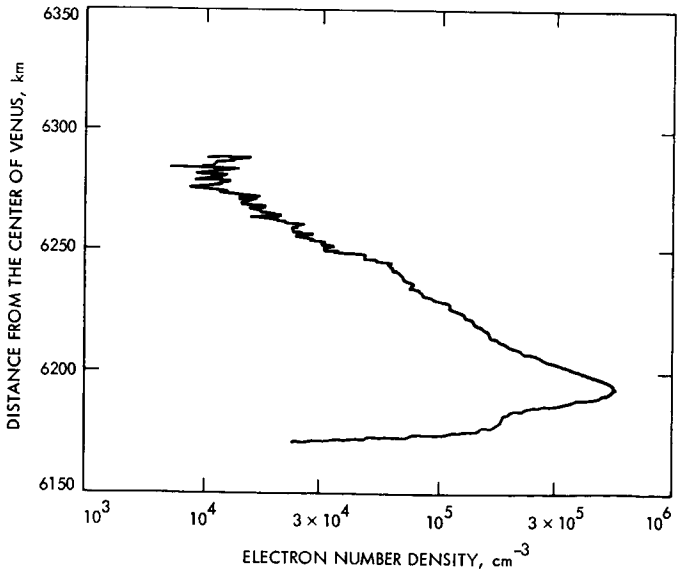

FIGURE 2–17.—Altitude profile of electron density, in daytime ionosphere of Venus.

versity (coherent continuous waves at harmonically related frequencies of 49.8 and 423.3 MHz) and processed them so as to measure and store, in the onboard tape recorder, the following quantities:

(1) A count of the beat frequency between the low-frequency carrier and the 2/17 subharmonic of the high-frequency carrier, which provided a dispersive doppler measurement of the change (in a 0.6-s sampling period) in the quantity of electrons in the wave path with a precision of about 2×10^{14} electrons/m^2
(2) Amplitudes of the two carrier waves
(3) Frequencies of the two signals
(4) Certain measurements on the modulation of the carriers (not relevant to this discussion)

Throughout the cruise to Venus (when Mariner was above the Stanford horizon), measurements were made of the electron content between the transmitter and the receiver; variations in the Earth's ionosphere and in the interplanetary medium were observed. These variations were relatively small, and their contribution to the total variations observed can be corrected for with reasonable certainty.

Results of the amplitude measurements at encounter are shown in figure 2–18.

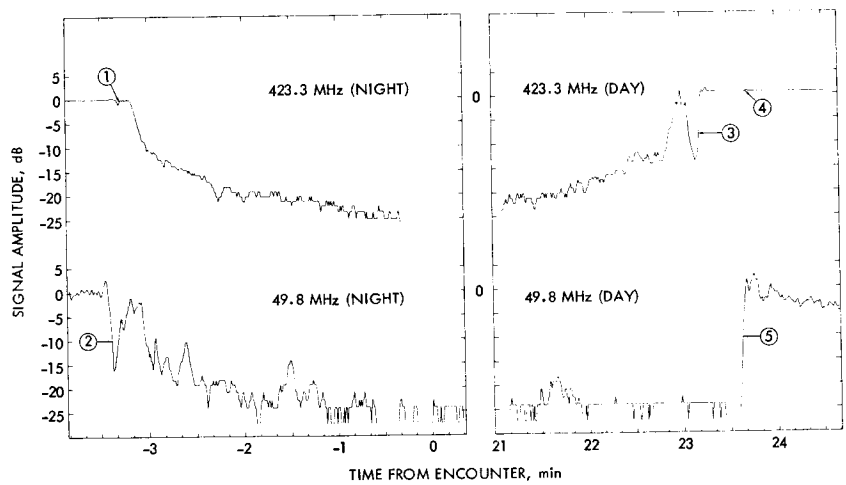

FIGURE 2–18.—Signal amplitudes at two frequencies during entry (night-side) and exit (day-side) occultation. Ionospheric effects are labeled ① to ⑤; the dense neutral atmosphere caused the general slow decay at entry and the rise at exit.

The large drop in amplitude between $E - 3.3$ min and $E + 23$ min resulted from the defocusing effect of the neutral atmosphere. The ionosphere produced the effects indicated by numbers ① to ⑤. The focusing and defocusing effect of the peak of the nighttime ionosphere appears at ① and much more strongly at ② because of the lower frequency. The peak of the daytime ionosphere shows up at ③; the effect on the low frequency was so strong that little or no radio energy reached the receiver before feature ⑤.

The initial calculation of the electron profiles from the dispersive doppler data is shown in figure 2–19. The broken parts of the daytime profile represent regions in which the doppler data were not interpretable and where the amplitude data were used to derive an approximate profile. Amplitude data are also required to verify the calculation of concentration in the nighttime peak below 6220 km. It is apparent from this figure, as well as from the amplitude data, that the

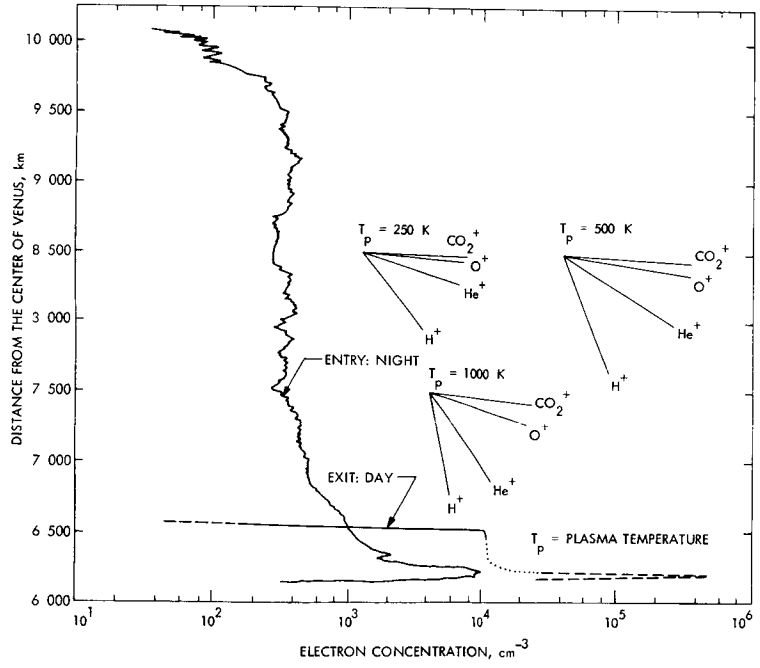

FIGURE 2–19.—Profiles of electron concentrations in the night and day ionospheres of Venus. The night profile and the solid part of the day profile are from integral inversion of the phase data. The dashed day peak is from preliminary model fitting to amplitude data. The dotted line is an area in which no direct measurements were made because of the formation of caustics.

ionospheric structure around Venus is too complex to be completely deciphered by a single pass through it. The current interpretation of the data is given in the subsequent paragraphs.

At present, the origin of the nighttime peak is not clear. Because it occurs at the same altitude as the daytime peak, it may be produced by horizontal transport of plasma from the day side. Above the peak, the atmosphere should be in diffusive equilibrium in the gravitational field, and the diagrams indicate the slopes that should be observed at three different temperatures for four ionized constituents. Just above the peak, any of several heavy ions may be present. Between 6300 and 6800 km, He^+ at temperatures from 620 to 970 K seems most likely, with H^+ between 625 and 1100 K filling in between 6800 and 7500 km. Between 7500 and 9500 km, the predominant ion is almost certainly hydrogen, but the curve is too flat to correspond to any reasonable temperature. It may be that the difficulty is that the data were reduced on the assumption of spherical symmetry, whereas the observed ionization actually may be confined by the solar wind to a cylindrical volume behind the planet. The persistence of such large electron densities to such high altitudes is a surprising discovery.

The most interesting feature of the daytime data is the abrupt drop in electron density between ranges of 6520 and 6570 km and the complete, or nearly complete, absence of any planetary plasma higher up. This boundary (called a "plasmapause" by the dual-frequency-receiver experimenters and an "anemopause" by the solar-plasma and magnetic field experimenters) appears to be produced by the interaction of the solar wind with the planet. (This point is discussed further in connection with the magnetic field and solar-plasma measurements.)

Among the most interesting results from Mariner 5 is the construction of theoretical model atmospheres based on the data of the two occultation experiments, the Venera 4 data, and other available information. (See refs. 2–24 through 2–26.)

Exosphere

Analysis of a planet's emissions in the ultraviolet wavelengths is the best tool available for studying the composition, structure, and properties of the highest region of the planet's atmosphere. Because of constraints on the Mariner 5 mission, an ultraviolet spectrometer to analyze these radiations in detail was not flown; however, a much simpler ultraviolet photometer was carried to search for atomic hydrogen and atomic oxygen, which (along with helium) were expected to be the most abundant constituents of the top of the atmosphere.

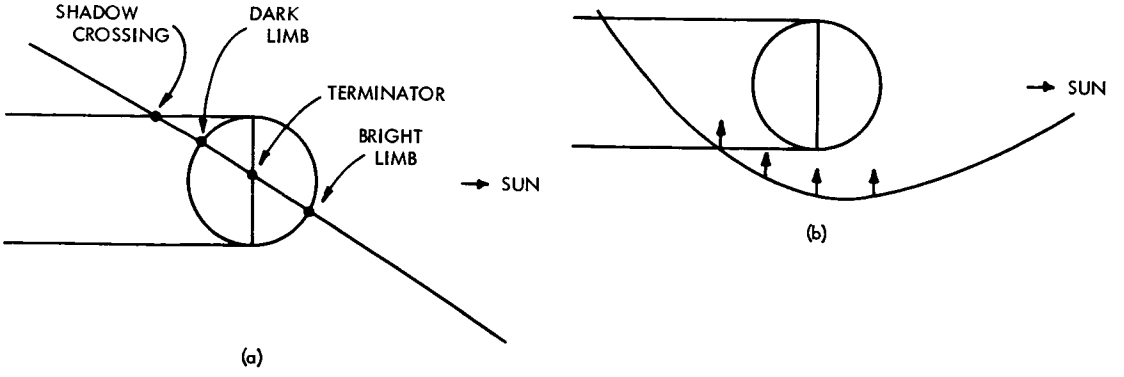

FIGURE 2–20.—Critical points in the ultraviolet photometer observations, as shown by the orbit and the planet viewed (a) along the line of sight from aft of the photometer and (b) at right angles to the line of sight of the photometer.

The brightest line in the atomic hydrogen spectrum is the Lyman-alpha line at 121.6-nm wavelength;[1] the corresponding transition in oxygen produces three lines at 130.2, 130.5, and 130.6 nm.

The ultraviolet photometer was mounted on the spacecraft with its line of sight at right angles to the Sun in the plane of the encounter trajectory so that it scanned across the planet, as shown in figure 2–20. From the profile of light intensity recorded, it was hoped to infer the altitude profile of the abundance of atomic hydrogen and oxygen, also obtaining the scale height and temperature of each species. It also was hoped that this information could be related by direct physical reasoning to otherwise unobservable processes in the lower atmosphere. (See ref. 2–27.)

Three photomultiplier tubes, identical except for the apertures of their collimators and the material of their filter windows, were used on the photometer. Because of the high work function of the photocathodes, these tubes were insensitive to light of wavelengths longer than about 220 nm. Their short-wavelength cutoffs were determined by the filters (e.g., LiF, 105 nm; CaF_2, 125 nm; BaF_2, 135 nm). Thus, by taking differences between the outputs of pairs of tubes, two spectral regions could be defined: 105 to 125 nm, containing the Lyman-alpha line; and 125 to 135 nm, containing the oxygen lines.

Figures 2–21 through 2–23 summarize data taken at encounter. Figure 2–21 is a plot of the emission intensity rate versus time for the LiF photometer. Be-

[1] 1 nm (or 1 nanometer) = 10 Å.

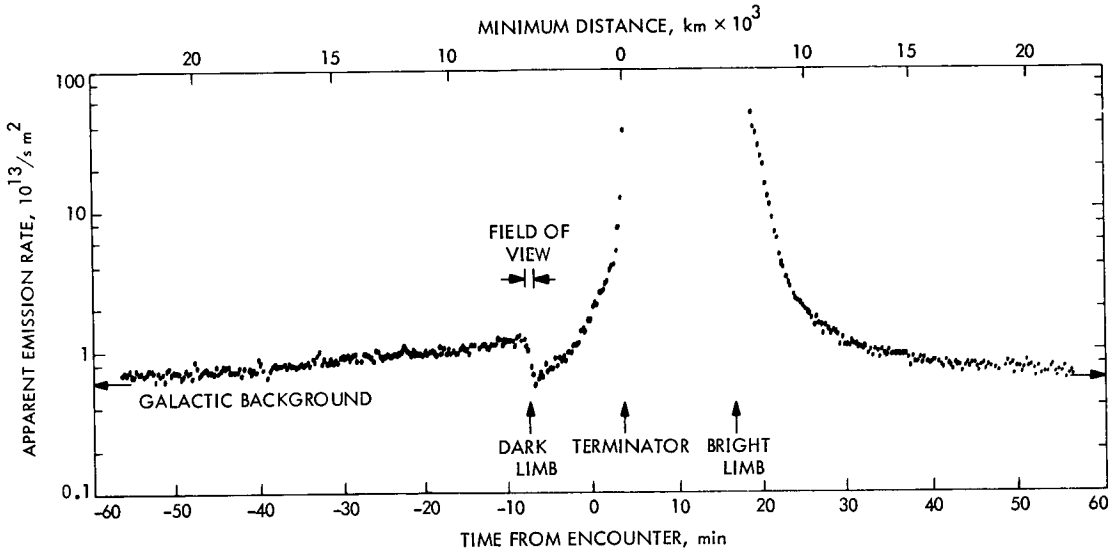

FIGURE 2–21.—Signal obtained from the lithium fluoride/Lyman-alpha channel during encounter. Times when the photometer observed the dark limb, terminator, and bright limb are indicated. The minimum-distance scale gives the perpendicular distance from the photometer line of sight to the center of the planet.

ginning at a background level of 0.58 kilorayleigh, produced by hydrogen dispersed in the galaxy, this sensor detected gradually increasing intensity from Venus-associated hydrogen for more than an hour before it crossed the dark limb of the planet. Then its signal dropped by about 0.58 kilorayleigh because of the exclusion of the galactic radiation. The maximum intensity up to this time was no more than 1.2 kilorayleigh because most of the hydrogen in the field of view was in the planet's shadow. As it scanned across the dark side of the planet, the signal increased rapidly because of the decreasing altitude of the shadow. The sensor was saturated (as expected) by the intense flux of long-wavelength light on the sunlit side of the planet, and scattered light made unreliable the last four points before saturation and the first one after it. The decrease in intensity after $E+17$ min corresponds to the decrease in hydrogen concentration with altitude in the sunlight; a break in the slope of this curve at 9000-km range (shown more clearly in fig. 2–23) is perhaps the most significant single feature of the data.

In figure 2–23, the curves for the CaF_2 and BaF_2 sensors show the difficulty in deriving a quantitative measure of oxygen radiation by taking the difference

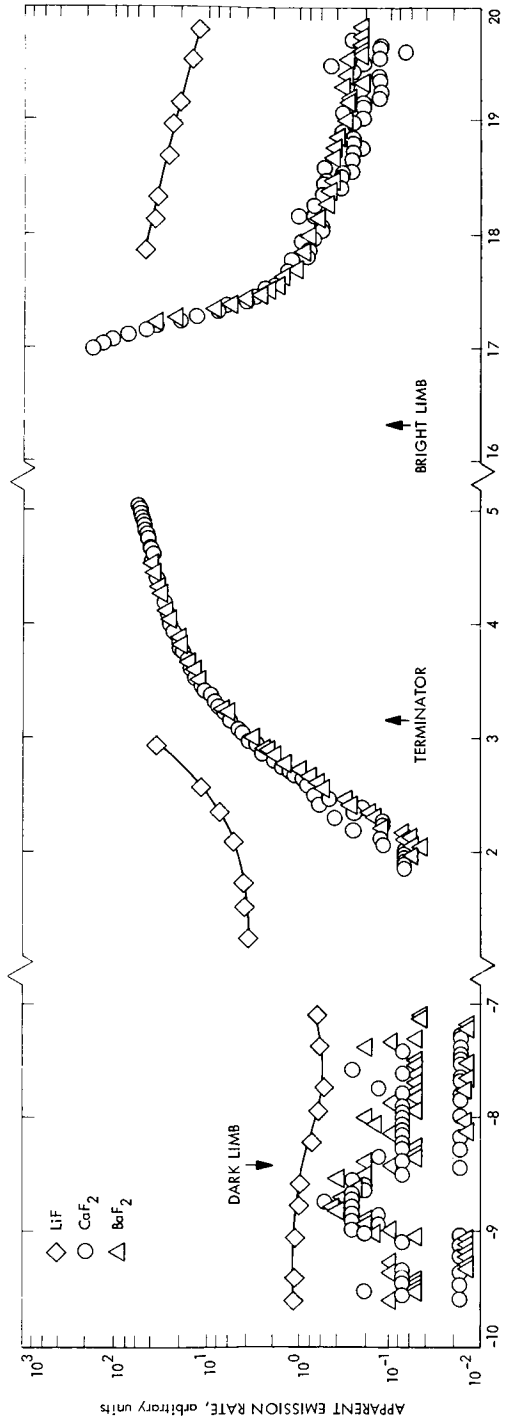

FIGURE 2–22.—Signals obtained from the ultraviolet photometer during critical periods of the Venus encounter. Three expanded time intervals are shown: dark limb, terminator, and bright limb.

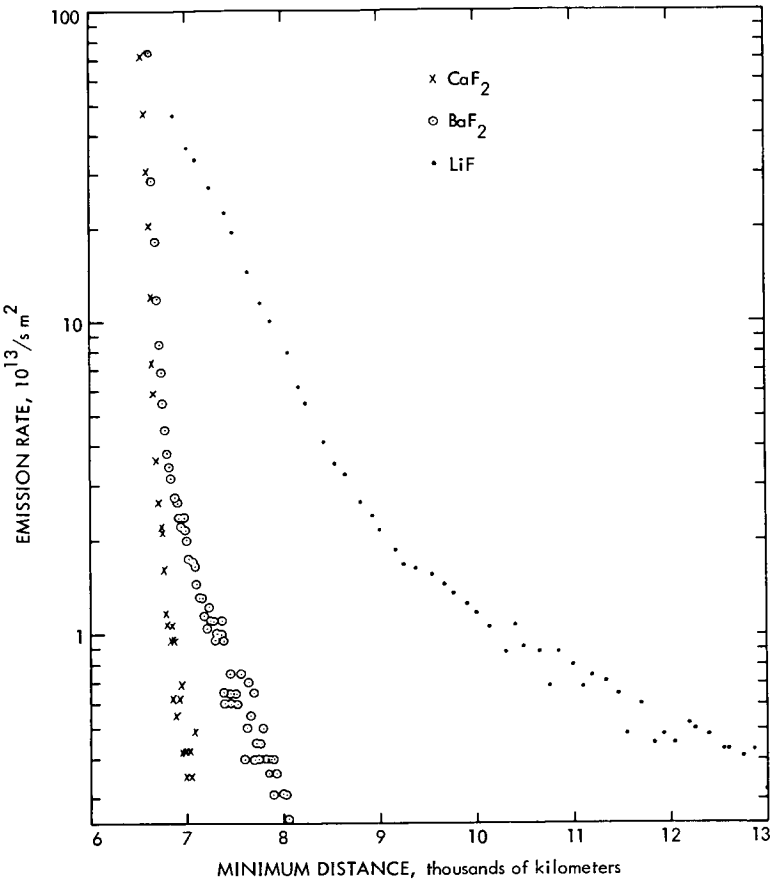

FIGURE 2–23.—Signals in the three channels of the ultraviolet photometer from the atmosphere, immediately after passing the bright limb.

between the two. The problem is compounded because the two sensors were not boresighted precisely parallel. No oxygen appears to have been detected.

The most intensive study of, and controversy about, the encounter data from the ultraviolet photometers centered on the Lyman-alpha emission from the sunlit hydrogen observed after encounter. The range covered was from 7000 to 39 000 km from the planet's center, all of which lies in the so-called "exosphere," where collisions between atoms are so rare as to be insignificant. As is the case with the ionospheric data from the dual-frequency receiver, the actual physical situation is complex and the data must be analyzed by comparison with atmospheric models that are simplified enough to be computationally tractable. A theory of planetary exospheres developed by Chamberlain (ref. 2–28) was used as the basis of the studies. Because of the break in slope at 9000 km, it was

impossible to fit the postencounter data with a single model, and two separate emission components must be postulated. The dominant component at large distances undoubtedly is atomic hydrogen, and the exospheric theory gives a temperature of 650±50 K. The dominant component at small distances has a scale height almost exactly two times smaller; therefore, it appears to be (1)

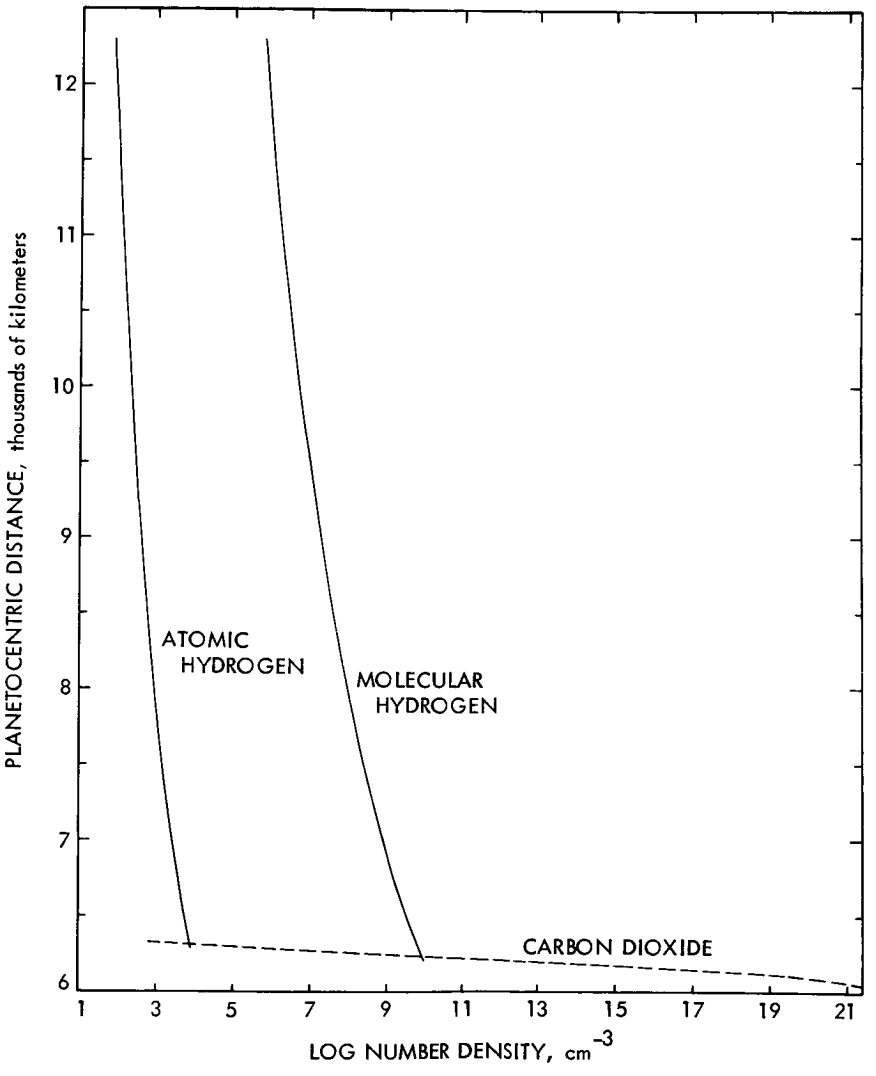

FIGURE 2–24.—Altitude profile of density in Venusian exosphere in the molecular hydrogen model.

atomic hydrogen at 325 K, (2) molecular hydrogen at 650 K, or (3) deuterium at 650 K (ref. 2–29). None of these hypotheses is without difficulties. The two-temperature model requires two distinct sources of hydrogen, which have not been identified; if they exist, it is surprising that they should supply hydrogen at two distinct temperatures with no intermediate values. The molecular hydrogen model (see fig. 2–24) is startling—it requires that molecular hydrogen be overwhelmingly more abundant than atomic hydrogen (even though it is almost nonexistent in the Earth's atmosphere) (ref. 2–30). It appears that the production rate of atomic hydrogen from molecular at the top of the atmosphere grossly exceeds the rate at which the atomic hydrogen will diffuse to lower levels where it can recombine. The deuterium model (see fig. 2–25) is even more startling, because rather remarkable phenomena must be postulated to explain how the deuterium/hydrogen ratio can be 10 in the exosphere of Venus and 0.0001 in the oceans of Earth.

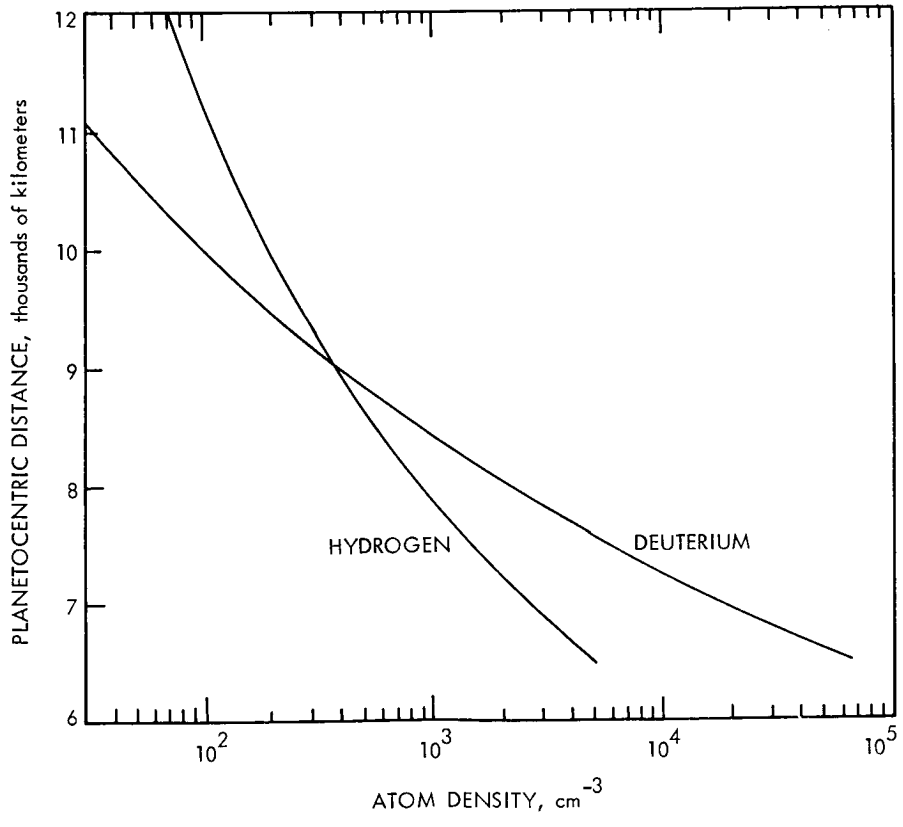

FIGURE 2–25.—Altitude profile of density in the Venusian exosphere in the deuterium model.

Further study may resolve some of the present confusion regarding which of these models is more probable; more data from future missions to Venus will be required. A fourth possible explanation undoubtedly exists, because during the encounter sequence, when 100 percent of the spacecraft telemetry was devoted to the scientific measurements, no data were received on the precise orientation of the spacecraft; it is possible, therefore, that the shape of the Lyman-alpha emission curve could have been distorted by small changes in the pointing direction of the photometers.

Wallace (ref. 2–31) has shown that if one attempts to incorporate the preencounter and postencounter data into the same model, a spherically symmetrical exosphere model will not suffice; asymmetric models must be used corresponding to lower densities and higher temperatures at low levels on the dark side of Venus than on the sunlit side.

Venus and the Solar Wind

Beyond the ionosphere and the exosphere of Earth lies a large and complex region known as the magnetosphere, which results from the interaction of the expanding solar plasma with the geomagnetic field. It is contained within a boundary called the magnetopause, which separates the magnetic field that originates in the Earth from the one that originates in the Sun. Several groups of charged particles exist within it; some are relatively permanent (the Van Allen belts) and others appear sporadically. The solar wind does not penetrate the magnetopause (except to a very small extent and in devious ways) so that the magnetosphere presents a barrier to its flow and sets up a collisionless plasma "bow shock" upstream. Additional groups of charged particles sometimes are accelerated to high energies by interactions that occur in the shock. Some of these features are shown in the data obtained by Mariner 5 on launch day, as discussed later in this chapter

It was learned from the Mariner 2 mission (ref. 2–32) and expected on theoretical grounds (because of the very slow rotation of Venus) that the "magnetosphere" of Venus would be smaller than that of Earth, but the planned encounter trajectory, approaching from the dark side and coming close to the planet, was almost ideal for detecting even the smallest one. Therefore, on Mariner 5, a complementary set of experiments was carried to investigate the interaction of the solar wind with the planet. The helium magnetometer measured three orthogonal components of the ambient magnetic field; the "Faraday cup" plasma probe directly measured the flux and energy spectrum (and, thus, indirectly the density, velocity, and temperature) of the solar plasma; the trapped-

radiation detector was capable of counting the high-energy protons and electrons that could be produced in the interaction region. All three instruments were slight modifications of those flown to Mars on Mariner 4.

Figure 2–26 is a polar plot showing the planet/spacecraft separation and the Sun/planet/spacecraft angles as coordinates. It is equivalent to tracing the path of the spacecraft in a plane that rotates about the Venus/Sun line with the spacecraft. To the extent that the phenomena have cylindrical symmetry about this line, these are the pertinent parameters.

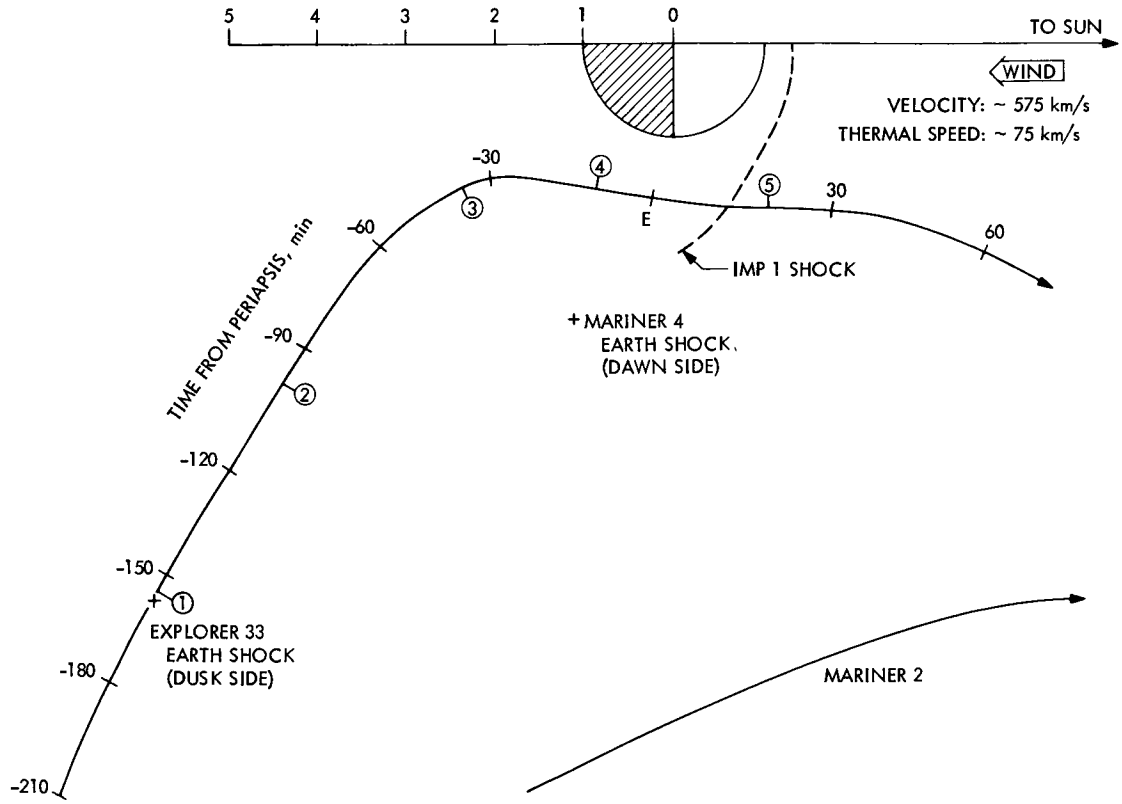

FIGURE 2–26.—Mariner orbits relative to Sun-Venus axis. Trajectories of Mariner 5 and Mariner 2 near Venus, rotated into a plane that contains the Venus-Sun line, are shown. Times in minutes relative to encounter (E) are indicated on the Mariner 5 trajectory. Circled numbers (here and in the following figures) refer to events described in the text. The dashed line and the two crosses represent the shape of the Earth's bow shock as observed by IMP 1, Mariner 4, and Explorer 33, scaled down so that the magnetopause passes through the observed boundary of the Venus ionosphere.

The plasma and magnetic field data are shown in figure 2–27 (ref. 2–33). The two uppermost curves (the positive ion number density n and the bulk velocity V) are plasma parameters computed from the observed flux-versus-energy measurements. The middle trace is the ambient-field magnitude $|B|$ computed from the three measured components after subtracting the spacecraft field. The two bottom curves give the field direction in spherical coordinates. The angle α is the longitude or azimuth measured in the **R**,**T**-plane, where **R** is a unit vector in the antisolar direction, and **T** is an orthogonal vector that lies parallel to the Sun's equatorial plane and points in the direction of the planet's orbital motion. The angle β is the latitude measured northward from the **R**,**T**-

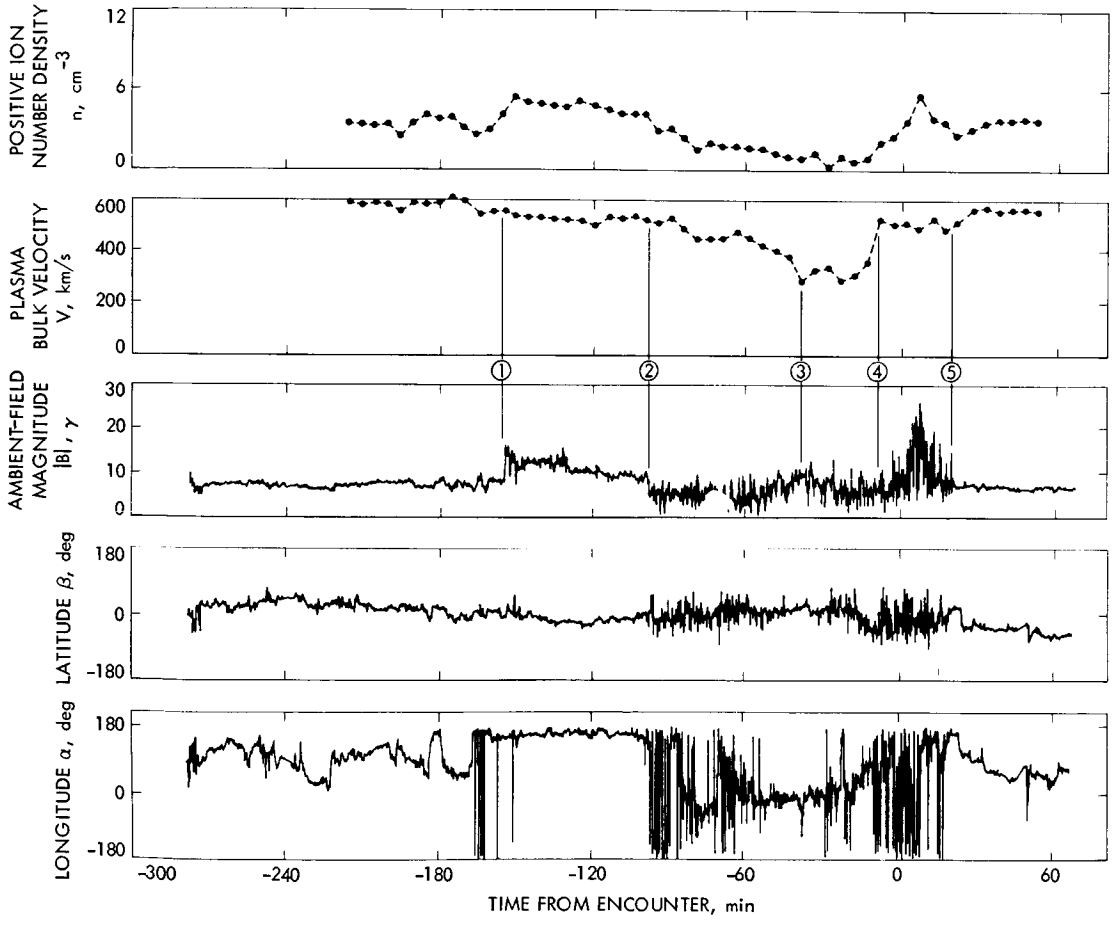

FIGURE 2–27.—Plasma and magnetic field data near Venus. Vertical lines and circled numbers denote the features of special significance discussed in the text.

plane. The direction toward the Sun corresponds to $\alpha = \pm 180°$; the ideal spiral field direction near the Venus orbit is $\alpha = 145°$ when the sense of **B** is toward the Sun, as it was on this day.

Phenomena not normally encountered in interplanetary space were observed between $E - 156$ min and $E + 18$ min; it is presumed that they resulted from the effect of the planet. Five features in the data, which seem interpretable with reasonable certainty, are identified in figure 2–27 by circled numbers. With only a single pass past the planet, however, the possibility cannot be excluded that certain of these or other features resulted from changes in interplanetary conditions that happened to coincide with encounter.

Interplanetary conditions before and after encounter were moderately disturbed. Plasma properties were steady, but the velocity (about 590 km/sec) and the temperature (about 3×10^5 K) were unusually high. The direction of the magnetic field showed substantial fluctuations, but its magnitude was nearly constant near 8γ, close to the expected value. The influence of Venus on the solar-wind flow first became apparent at point ①, with an abrupt increase in magnetic field intensity from 8γ to 15γ—a marked increase in fluctuation, but essentially no change in direction. The plasma velocity dropped slightly (about 10 percent), and the density increased markedly (about 40 percent). Such changes are frequently observed across a shock; together with the subsequent observations, they make the identification of point ① as a bow shock almost inescapable.

One sudden magnetic field change about halfway between ① and ② has no apparent planet-related explanation; along with several other later field changes, it must be interpreted as response to a change in the interplanetary medium. A more profound change occurred at ②, with a drop in field from 9γ to 6γ (less than the average magnitude in interplanetary space), a marked increase in fluctuation, and little change in direction. After event ②, the plasma density and velocity began steady decreases, reaching minima near event ③ and returning to high values near event ④. A magnetopause, if present, would have been apparent in this region, but none of its characteristic features were observed.

Phenomena between ④ and ⑤ cannot be explained in detail, but they are comparable with those observed behind the bow shock of Earth at about the same local time. Because of the abrupt decrease in the magnetic fluctuations and the return of the plasma velocity to its interplanetary value, event ⑤ is identified as the passage out through the bow shock, even though the absence of marked changes in field intensity and plasma density is puzzling.

Most of the features in the data are consistent with the model shown schemati-

cally in figure 2–28, although the detailed validity of the model can be demonstrated only by additional measurements. It appears that the electrically conducting ionosphere of Venus cannot be penetrated quickly by the magnetic field carried along by the solar wind, so that most of the plasma is prevented from reaching the atmosphere. A standing bow shock is formed, behind which the compressed plasma flows around the sides of the planet, becomes supersonic, and tends to leave a cavity behind the planet. The magnetic and gas-kinetic pressures should produce an expansion into the partially empty cavity. The edge of the expansion wave may approximate a cone running through point ②, near point ④, and about 500 km above the surface of Venus, where the data from the dual-frequency receiver indicate an abrupt decrease in the electron density from $10^4/cm^3$ to the interplanetary value.

Thus, it seems that if Venus has either a magnetosphere or an intrinsic magnetic dipole, it must be extremely small. From the absence of any observations attributable to either, the investigators conducting the helium magnetometer and plasma probe experiments concluded that an upper limit to the magnetic dipole moment is about 0.001 times that of Earth. (See ref. 2–33.) Approximately the same upper limit is inferred by the investigators of the trapped-radiation detector experiment, which showed no changes whatever in the flux of charged particles during the passage by the planet (ref. 2–34).

Summary of Results

Data returned from Venus by Venera 4 and Mariner 5 on consecutive days in October 1967 have dispelled the mystery that surrounded that planet.

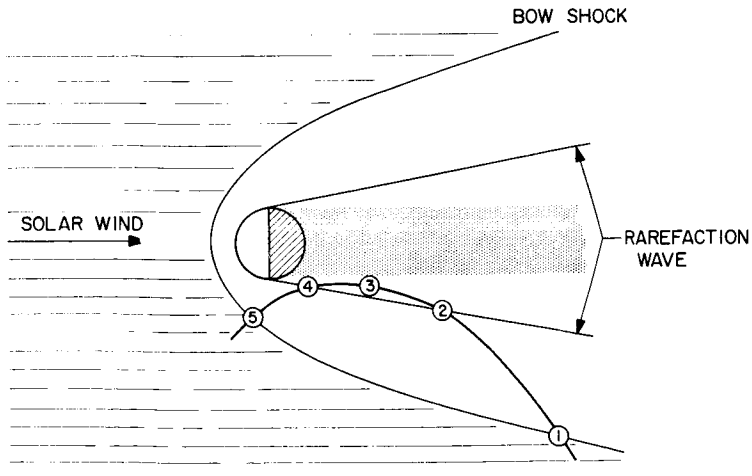

FIGURE 2–28.—Schematic representation of the solar-wind interaction with Venus. A rough approximation to the Mariner 5 trajectory containing the five features observed in the plasma and magnetic field data is shown.

Although many details remain unknown and some conclusions must be confirmed, the principal characteristics of the atmosphere and environment of the planet are no longer considered controversial by most scholars. These characteristics are discussed briefly in the following paragraphs.

(1) The equatorial radius is unlikely to differ by more than 3 or 4 km from 6053 km. This implies that the altitude of the cloud top is 67 ± 10 km.
(2) Carbon dioxide is the predominant constituent of the atmosphere, as demonstrated by both Venera 4 and Mariner 5. Its abundance cannot be less than 85 percent, and some more recent model studies suggest that it may approach 99 percent. The nitrogen abundance cannot exceed a few percent, and oxygen and water are even more scarce. It is doubted whether any other gas exceeds 1 percent.
(3) From the combined Venera 4 and Mariner 5 *S*-band occultation measurements, temperature and pressure profiles in the atmosphere are accurately known in the altitude range of about 25 to 90 km. Reasonably reliable extrapolations can be made upward and downward from this range.
(4) The temperature of the surface of Venus is very high, probably everywhere and at least near the equator. Until additional measurements are made that come from the surface, the bottom atmosphere numbers can be characterized by the values of about 700 K (800° F) temperature and 100 bars pressure.
(5) The puzzle of the high opacity of the atmosphere to infrared radiation, necessary to explain the high surface temperature, has been explained. The opacity is a result of the pressure broadening of the lines in the absorption spectrum of CO_2.
(6) Because of its high density, the lower part of the atmosphere is superrefractive. The level of critical refraction is at about 6088-km range or near 35-km altitude. This fact has many implications. The use of electromagnetic waves at grazing incidence, as in the *S*-band occultation experiment, cannot yield information about the lower atmosphere. It becomes possible, in theory, to communicate by radio with a Venus probe at any point on Venus; in practice, the defocusing effect would be extremely severe for signals to or from the opposite side of the planet. Also, in theory, from any given point on the surface, light rays exist along which one can "see" any other point on the surface, or any point above the surface such as the Sun. It is not likely, however, that any of the bizarre optical effects that can be imagined could be observed in visible

light, because all the rays with very long paths have a large fraction of their length at altitudes just below the critical refraction level, where the transparency to ordinary light rays is probably not high enough.

(7) The exosphere of Venus is very cold (~650 K, where that of Earth is ~1500 K), and it contains much less oxygen than that of Earth. On Earth, the exosphere temperature determines the rate of loss of the atmosphere; thus, the loss rate from Venus should be much smaller. However, protons and other ions in the solar wind strike the Venusian exosphere; this interaction provides another mechanism for atmospheric depletion, which may indeed be the dominant one.

(8) The ionosphere of Venus has a very complex structure, again because of the solar-wind interaction. In the sunlight, the charge density is high, and the ionosphere near the subsolar point is pushed down to low altitude by the impact of the solar wind. On the dark side, a moderate charge density extends almost up to 4000-km altitude, perhaps filling the void produced by the deflection of the solar wind around the planet.

(9) The interaction region between Venus and the solar wind is much smaller than Earth's magnetosphere because the magnetic moment of Venus is either nonexistent or too small to be significant. The solar wind interacts primarily with the ionosphere, setting up currents that deflect the solar plasma around the planet and force the ionosphere down close to the planet on the sunlit side. A bow shock apparently does exist. It is of particular interest that the three astronomical bodies for which the solar-wind interaction has been investigated differ qualitatively in the nature of this interaction. At Earth, it is the geomagnetic field that presents a barrier to the solar wind so that the plasma must flow around it. At Venus, the ionosphere serves a similar function. The Moon, on the other hand, having neither magnetic moment nor ionosphere, allows the plasma's magnetic field to pass essentially undisturbed through its body; the solar wind probably impacts the surface (or at least gets very close to it), and no bow shock forms.

Among the most significant questions about Venus are the following:

(1) What are the composition and depth of the clouds?
(2) What other major constituents of the atmosphere are there, if any?
(3) Do any cool places exist on the surface, and if so, where?
(4) Why are water and oxygen so scarce in the atmosphere?
(5) What is the nature of the general atmospheric circulation?

(6) Is there significant asymmetry, either in the shape of the planet itself or in its gravitational field?
(7) What is the nature of the surface, especially of the rough regions detected by radar?

More advanced missions to Venus will be needed to provide the answers to these questions.

OBSERVATIONS NEAR EARTH

The scientific instruments aboard Mariner 5 began to operate and to transmit data at the moment of Agena/spacecraft separation, 26 min after launch and just after injection into the interplanetary orbit. The first data came from a geocentric range of 6596 km. During the next half hour, the solar panels were deployed, solar orientation was acquired, and Mariner settled down to rolling about the spacecraft/Sun line at about 2 revolutions/hr. The rolling continued for 16 hr, until the Canopus sensor acquired the Earth at a range of 241 900 km. This long roll period was included in the mission for the primary purpose of determining the magnitude and direction of the spacecraft magnetic field at the magnetometer sensor. However, it also provided a directional scan for the ultraviolet photometer, and it did not degrade the data from the plasma probe or the trapped-radiation detector. Thus, all instruments except the dual-frequency receiver acquired significant Earth-related scientific data during the first hours of the mission.

Exosphere and Geocorona

During the time that the spacecraft was rolling, the ultraviolet photometer, oriented at right angles to the roll axis, looked back through the Earth's upper atmosphere once each revolution, and the LiF channel obtained the data shown in figure 2–29. The ordinates are uncorrected data numbers, which are roughly proportional to the logarithm of the Lyman-alpha intensity. Thus, the dashed curve through the peaks represents the altitude profile of the quantity of atomic hydrogen in the exosphere and the geocorona. This peak was much smaller, but still clearly distinguishable, in the last roll before the spacecraft was stabilized, and the geocoronal data were extended to a range of 98 000 km. This was the first extended observation of the geocorona from beyond the atmosphere.

Correcting for the galactic background of Lyman-alpha radiation, as measured during subsequent roll maneuvers, the data have been analyzed to give the hydrogen abundance at the top of the atmosphere. It has not proved possible to derive an accurate value of exosphere temperature because the data

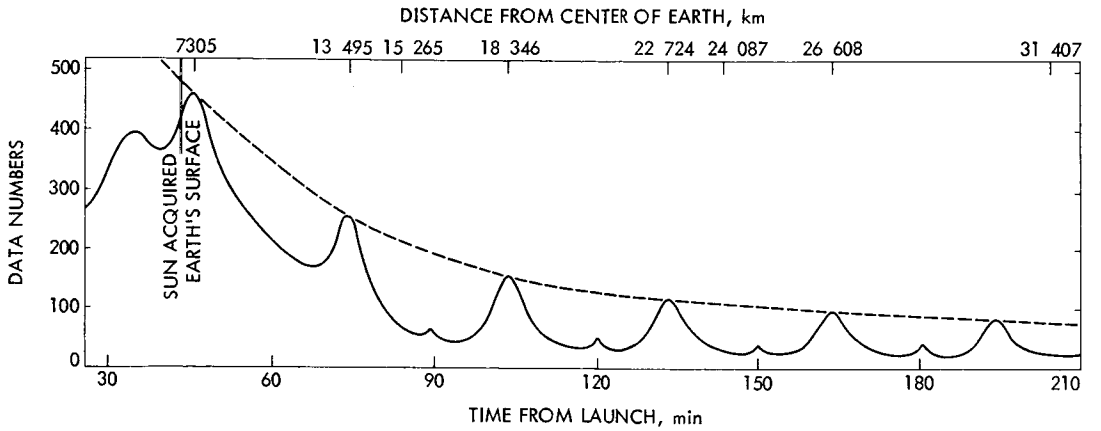

FIGURE 2–29.—Data obtained by the ultraviolet photometer through the Earth's upper atmosphere during the spacecraft roll.

from the first two rotations, which would be weighted heavily in the model calculation, were too contaminated by the effect of the radiation belt to be reliable. The problem was compounded by the uncertainty regarding the calibration at the high data rate, as discussed later in connection with the cruise data. One very significant result of the experiment was the demonstration of the absence of any appreciable change in atomic hydrogen density either at the plasmapause or at the magnetopause.

The second small peak in the ultraviolet data, about halfway between successive Earth peaks, had not been expected, and caused considerable excitement. As a result, three more spacecraft rolls were activated following the midcourse maneuver 5 days later. The little peak was again observed, and it was shown to originate in the galactic plane; i.e., the Milky Way.

The Magnetosphere

All three "magnetosphere" experiments obtained continuous data of excellent quality throughout the roll period, which took the spacecraft through the magnetosphere and the magnetosheath (between the magnetopause and the bow shock) and out into the undisturbed interplanetary medium. The spacecraft trajectory is shown in figure 2–30. Portions of the data obtained are shown in figures 2–31 and 2–32. These data are valuable for comparisons with those obtained near Venus by the same instruments and with those obtained by other instruments near Earth.

The peak counting rate from protons in the Van Allen radiation belt was

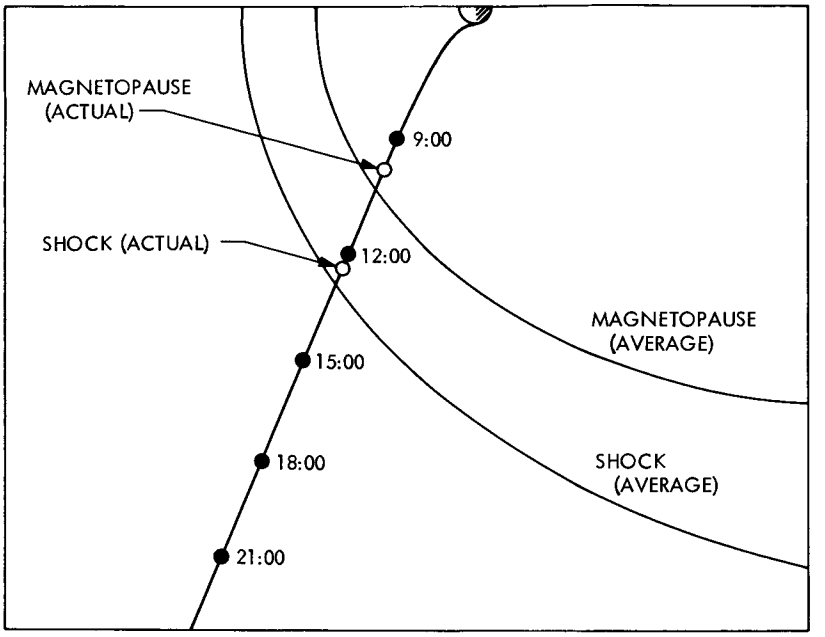

FIGURE 2–30.—Mariner 5 Sun/Earth probe angle and geocentric distance.

observed at 06:46 at a range of 1.9 Earth radii, associated with the geomagnetic field line that crosses the equator at 3.2 radii.[2] Passage through the magnetopause was first indicated by the magnetometer at 09:43 at a range of 10.4 radii; during the next 11 min, at least 12 additional crossings were detected, the final one at 10.8 radii (ref. 2–35). The multiple crossings are most clearly seen in the oscillations of the field direction. They result from the rapid pulsating or vibrating motion of the magnetosphere boundary and have been observed previously. Passage through the shock occurred only once, and was clearly marked in both the magnetometer and plasma data at 12:23, when the range was 16.5 radii. Both boundaries were located approximately 1 Earth radius inside their average positions.

The phenomena near the magnetopause are particularly interesting, as shown in figure 2–31. The plasma probe first saw appreciable fluxes at 09:44. (The values of velocity shown for earlier times are probably not meaningful because of the very low density.) The flux of high-energy electrons (detector C,

[2] J. A. Van Allen and S. M. Krimigis: Preliminary Report on Magnetospheric, Solar, and Interplanetary Observations with Mariner V. Unpublished University of Iowa report, Oct. 2, 1967.

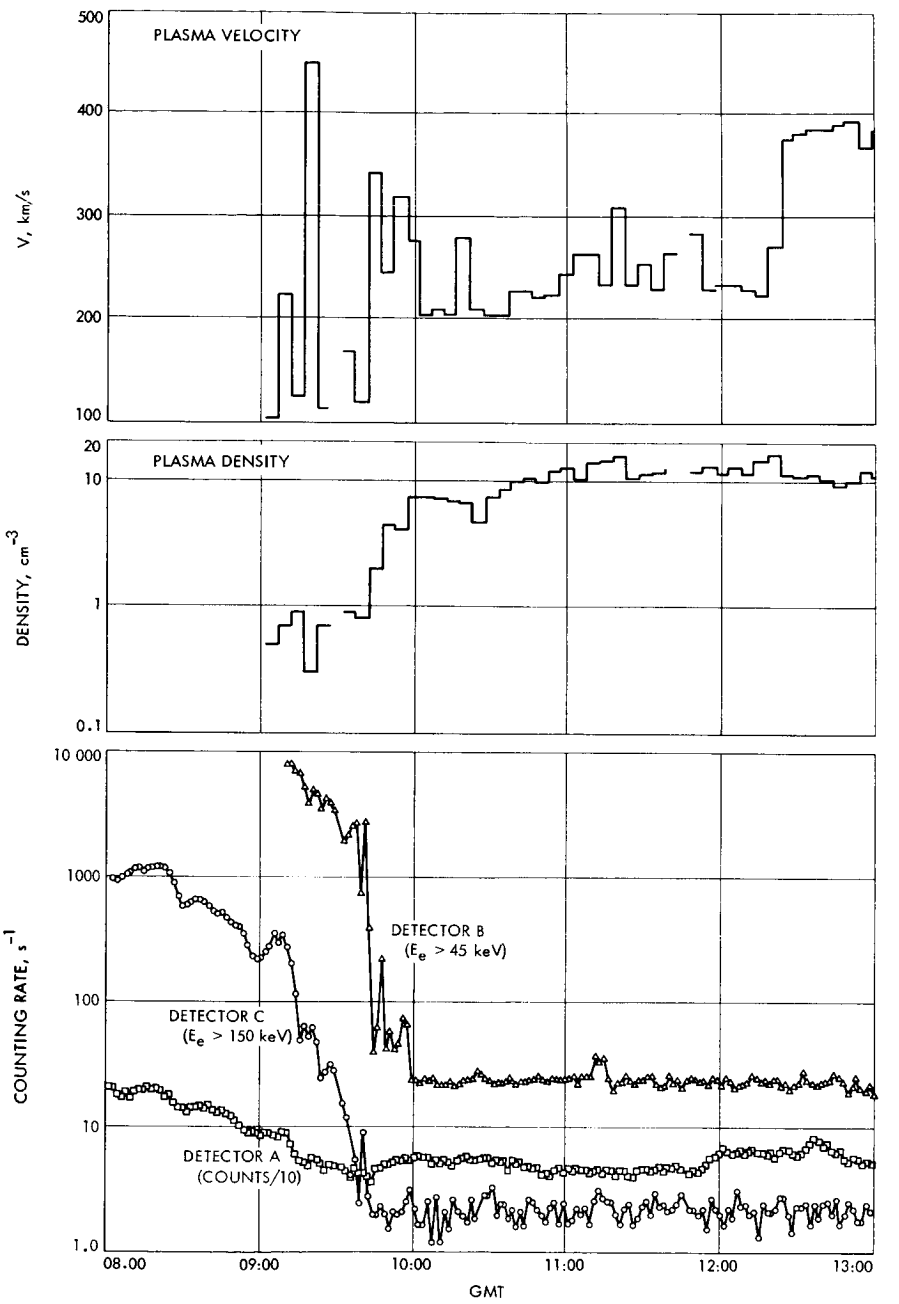

FIGURE 2–31.—Plot of part of data obtained through the magnetosphere. Phenomena near the magnetopause were especially interesting.

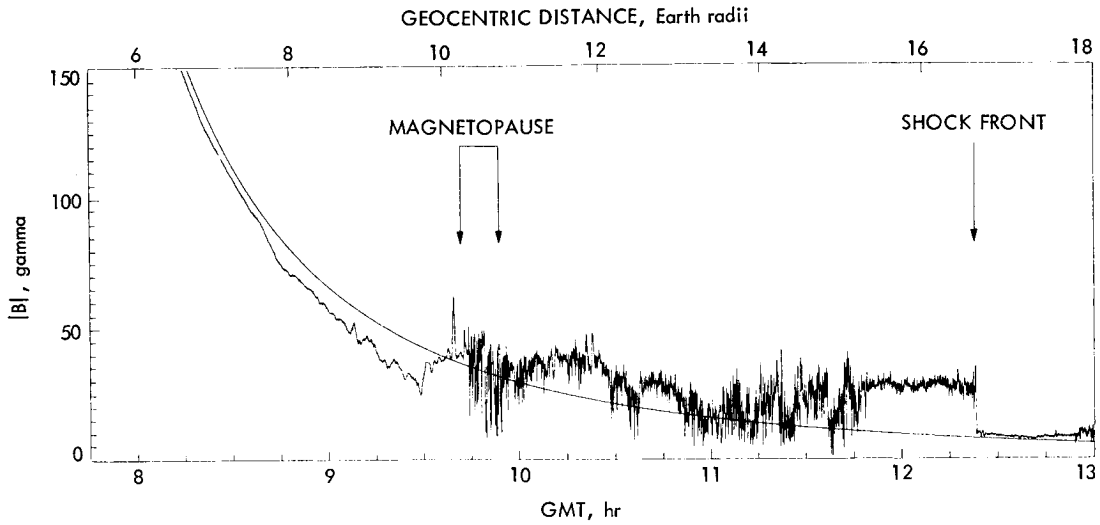

FIGURE 2–32.—Mariner 5 magnetic field data near Earth. Ambient-field magnitude is plotted as a function of time and geocentric distance. Three triaxial samples were telemetered every 12.6 s; the corresponding computed field magnitude is shown for all data without any averaging. The smooth curve is the magnitude of the extrapolated surface geomagnetic field. Multiple crossings of the magnetopause (caused by boundary motion) are indicated by the double arrow. The observations were made at about 15:00 local time and at a geomagnetic latitude of about −25°.

energy greater than 150 keV) decreased gradually and reached its steady value at this same time. Most of the low-energy electrons (detector B, energy down to 45 keV) disappeared at this time, but a significant flux remained until 09:58. At 09:58, a sudden change in magnetic field direction occurred.

The general features observed by Mariner 5 near Earth do not differ from those observed by other spacecraft. Study of the details of these features is not complete, however, but may yield some significant scientific results.

CRUISE PHASE OF THE MISSION

With the acquisition of Canopus, 19 hr after launch, the spacecraft settled into its normal stabilized cruise configuration. Except for a few brief perturbations or interruptions, it continued to monitor the interplanetary medium and the galactic Lyman-alpha radiation.

On June 19 the midcourse maneuver was performed, causing an interruption in the scientific data for a period of 109.6 min while the spacecraft was in data mode 1 (all engineering data). This minor loss was more than compensated

by the opportunity to acquire data with the spacecraft in a nonstandard orientation. To exploit this opportunity, especially for the benefit of the ultraviolet photometer, three 360° roll searches were commanded, following the normal automatic Sun reacquisition. Each roll required about 50 min.

On July 24 the telemetry data rate was reduced from 33⅓ bps to 8⅓ bps.

On October 1 the changeover of the transmitter from the omnidirectional antenna to the high-gain antenna was commanded from Earth. For a few days before the changeover, the signal received by the 85-ft antennas at the tracking stations had been weak, with a resulting degradation in the quality of the telemetry.

The cruise data were interrupted on October 9 for the encounter sequence, which occupied 15.7 hr. After 12.7 hr of cruise data, encounter data were played back, requiring 72.5 hr.

On October 25 the telemetry data rate was switched to high for about 4 hr and then returned to low to check the operation of the ultraviolet photometer against the results observed early in the mission.

Beginning on November 7, another special operation was conducted to permit the ultraviolet photometer to rescan the great circles observed after midcourse maneuver. Three complete spacecraft rolls were executed, with the data recorded on magnetic tape because the distance to Earth was too great to receive real-time data from the omnidirectional antenna. The exercise took slightly more than 6 hr. The playback of recorded data was resumed on the following day; about 47 hr were required to complete it.

Another maneuver was executed on November 19 to point the ultraviolet photometer in the same direction as at the beginning of the low-rate data on July 24. To accomplish this, it was required to make a 17° pitch turn followed by a roll, and to operate various spacecraft subsystems in modes that had never been contemplated during the design. The operation required that 19 commands be sent over a period of 29 hr. Again, the data had to be recorded on tape and played back.

Finally, on November 21, the transmitter was switched to the omnidirectional antenna, and the signal could no longer be heard. This ended the scientific history of Mariner 5, as the next time that the signal could be recorded at Goldstone, it was found that the carrier wave was unmodulated.

Ultraviolet Observations in the Cruise Phase

Of the three channels of the ultraviolet photometer (customarily designated by A, B, and C), it was expected that only the C channel with the LiF window

would provide interesting observations during the cruise phase of the mission. The other two channels had narrower fields of view (1° instead of 2.5°), and their spectral sensitivity did not extend to the wavelength of the most common ultraviolet radiation in space—the Lyman-alpha line from atomic hydrogen. The possibility was recognized that one of the rather rare stars that radiate strongly in the ultraviolet could enter the field of view; however, little significance was attached to it.

On launch day, after the spacecraft ceased to roll, all three channels settled down to constant data outputs; channels A and B read the noise level of the photomultiplier, and C read approximately data number (DN) 20, which was believed to correspond to an emission rate of 0.3 to 0.4 kilorayleigh. Some uncertainty was attached to the interpretation of this reading because, at the high bit rate, the length of time between the application of high voltage to the channel C photomultiplier and the measurement of the analog voltage output was not sufficient to insure that voltage transients in the circuits had completely died away. From the preflight calibration, which had been performed at very low sampling rates, a reading of DN = 6 was expected.

The lines of sight of the three channels were intended to be parallel and oriented at 90° (cone angle) to the Sun and at 95.5° (clock angle) to Canopus, which is 14° from the south ecliptic pole. Consequently, during cruise, the photometer looked back in the direction from which the spacecraft had come, always viewing a portion of the celestial sphere near the ecliptic. At the start of midcourse maneuver, it was pointed at 9.7° latitude, 177.6° longitude. During the maneuver, when no science data were being received at Earth, the lines of sight moved eastward and then northward, and stopped at 42° latitude, 118° longitude. After the motor burn, telemetry was restored to science data, and as Mariner turned toward the Sun, the photometer scan moved northward and then westward. In the rolls that followed Sun acquisition, it scanned southward at 177.6° and northward at 357.6° longitude. A portion of the raw data before and after the maneuver is depicted in figure 2–33. Several aspects of this and the remaining roll data have particular significance.

At least seven sharp "spikes" were observed, where two or three channels read large numbers for a single measurement. The spikes fell into two groups corresponding to angular separations from Canopus of about 46° and 70°, respectively. It was concluded that the odd-numbered spikes represent observations of the star Alkaid (η Ursae Majoris), which is the tip of the handle of the Big Dipper, at 54.4° latitude, 176.5° longitude, and that the other three come from

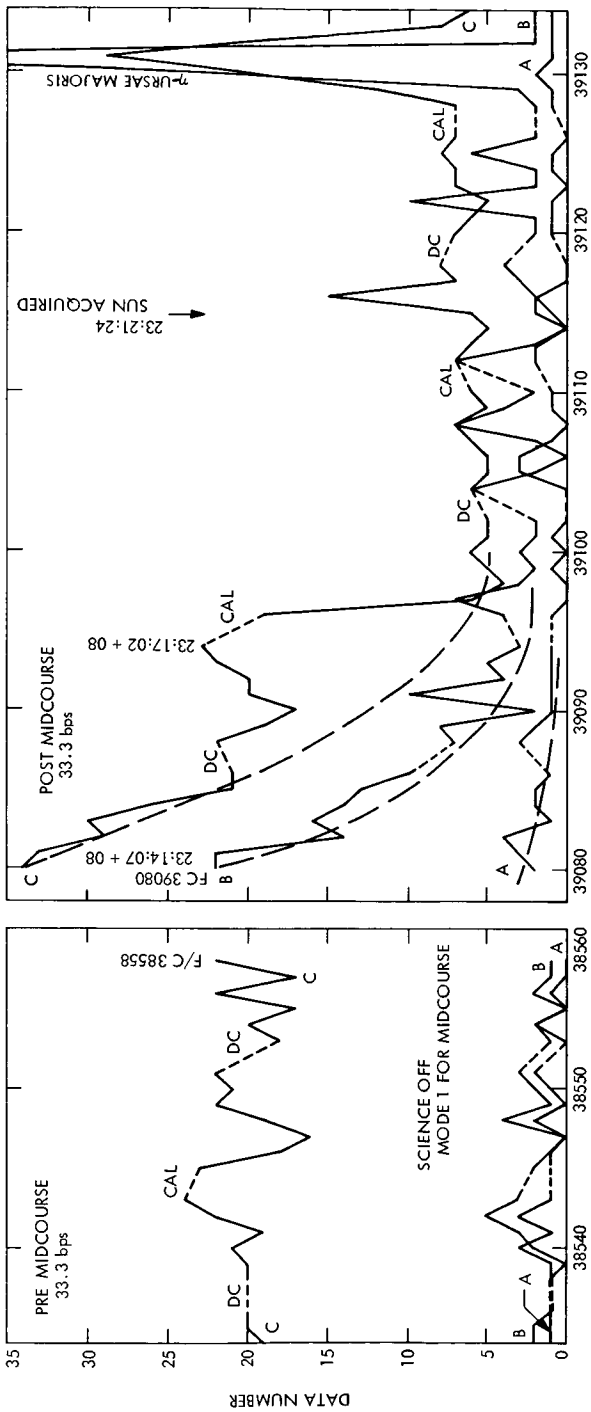

FIGURE 2–33.—Plot of ultraviolet photometer data in channels A, B, and C before and after midcourse maneuver on June 19, 1967. Breaks in the data occur at times of calibration (CAL) and d.c. level restoration (DC) of the photometers.

the star κ Velorum at −63.7° latitude, 178.4° longitude, in the southern part of the Milky Way.

The scan crossed the plane of the galaxy (Milky Way) twice; the southern crossing occurred in a region that is quite bright in Lyman-alpha radiation, but the northern crossing yielded hardly a noticeable increase in signal.

A lack of consistency in the relative outputs of the three channels in the various crossings of the same star indicated that the three collimators that defined the lines of sight were not alined as accurately parallel as had been intended.

The performance of channel C at the beginning of the telemetry was anomalous, and has not yet been satisfactorily explained. The first four data points show the output of all three channels dropping rapidly, probably because the photometer was observing the bright glow of the gas ejected from the maneuver motor. In the fifth to the tenth points, channel C seems to hover near the level DN = 20, which it read consistently before the maneuver; then it dropped suddenly to the mean level of DN = 6, which continued to be its background reading. This change corresponds to a decrease in the channel C sensitivity by the factor 4.5, if the photometer was operating correctly both before and after the shift.

It was possible to determine accurately the true lines of sight of the three channels. During the last week in August, the intended line of sight passed about 0.3° south of π-Scorpii and about 0.2° north of τ-Scorpii; both stars were known to have strong emissions in the ultraviolet. For periods of about 3 days, each star, in turn, appeared and disappeared repeatedly for each photometer channel as the spacecraft oscillated slowly within the deadbands of its attitude-control subsystem. By analyzing the engineering telemetry information from the attitude-control sensors, the precise orientation of the spacecraft could be calculated at any time so that maps of the star positions in clock- and cone-angle coordinates could be generated. The results showed that channels A and C were parallel within about 0.1° but 0.4° away from their intended position, while channel B was 0.9° away from them. The direction of this large separation was such that all three channels scanned across nearly the same region of Venus at encounter, but that channel B simply arrived a little late; thus, the effects of the misalinement could be corrected for.

The channel C sensitivity question, however, was not resolved so easily. At the time of the switch of telemetry data rate from 33⅓ to 8⅓ bps, its reading went from DN = 7 to DN = 36. Qualitatively similar changes, but of different magnitude, had been observed in the prelaunch testing at data-rate switching. During August and September, the reading gradually drifted from 36 to 24. In

an effort to determine whether this drift reflected a real change in Lyman-alpha intensity in different directions or merely an instrumental sensitivity change, a special pitch-and-roll maneuver was executed late in the mission (November 19) to point the photometer back at the region of space that it had been observing at the time of data-rate change. The results implied abroad band of intense Lyman-alpha radiation (DN readings of about 90) in this region and were not credible. The explanation for the high readings has not been determined with certainty, but it is probable that sunlight was scattered into the detector from some part of the spacecraft.

Another maneuver, three consecutive rolls, was carried out on November 7. At this time, Mariner was exactly 180° in ecliptic longitude from its position on the day of midcourse maneuver, so that the photometer scanned a circle that almost coincided with the one scanned earlier. The coincidence was not exact, however, because of the difference in spacecraft latitude, and the operation did little to clarify the performance of the channel.

These two maneuvers provided some interesting scientific information on the distribution of hydrogen in space. The regions scanned by the photometer during the November 7 rolls and part of the November 19 maneuvers are shown in figure 2–34 as a Mercator projection of galactic coordinates. Note that the same two stars detected on the day of the midcourse maneuver were observed

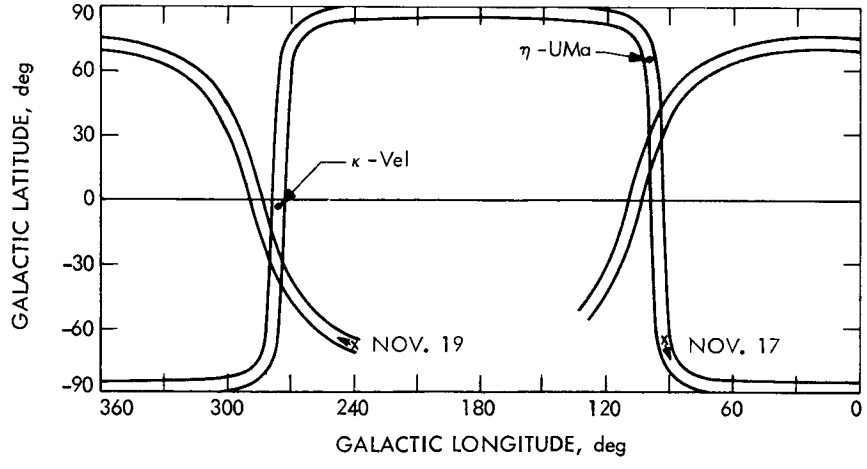

FIGURE 2–34.—Regions scanned by the photometer during the November 7 rolls and part of the November 19 maneuver shown as a mercator projection of galactic coordinates.

again, and that data were acquired both north and south of the galactic equator, defined by the plane of the Milky Way.

The November 7 data from channel C are shown in figure 2–35. The intensity scale is calculated in terms of extensive sources that fill the photometer field of view; thus, it is not correct for the two stars. The third object that stands out above the background is the large Magellanic cloud (LMC). The two significant features of the data are that the Lyman-alpha signal north of the galactic plane is about 1.4 times that to the south, and that an enhancement of the flux in the galactic plane in the region of Vela (280° longitude) was much greater than that in the region of Cygnus (100° longitude). The November 19 data showed a similar pattern. If the source of the diffuse Lyman-alpha glow were atomic hydrogen located in the solar system or at the outer boundary of the solar system, where the solar wind runs into the interstellar medium, the observed ultraviolet intensity would be isotropic or would have some asymmetry

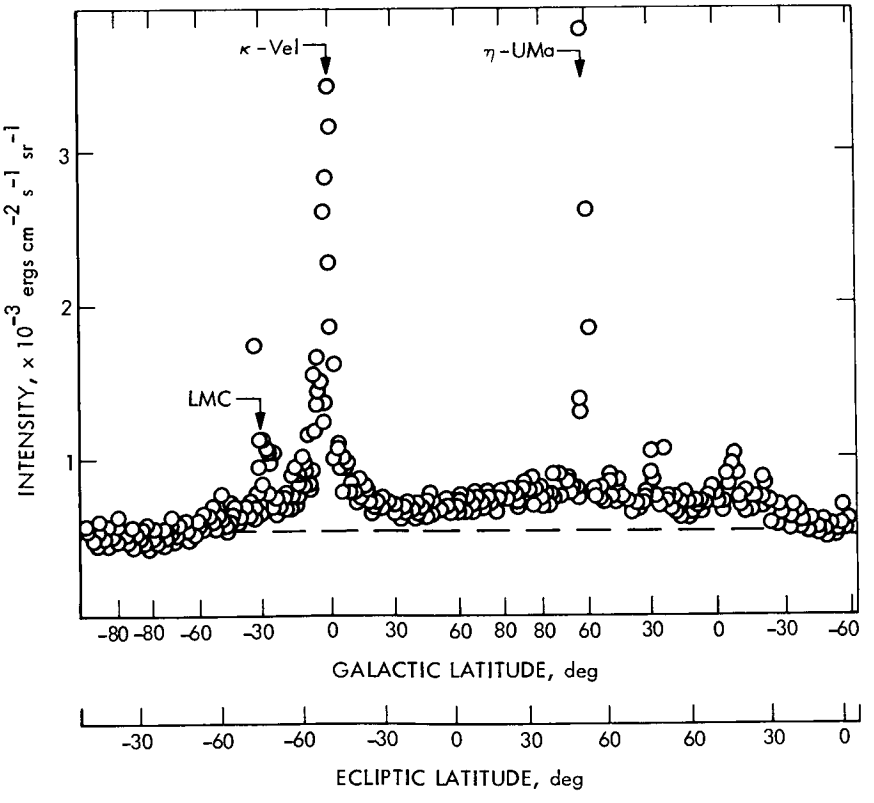

FIGURE 2–35.—Data from UV photometer channel C taken November 7.

related to the ecliptic plane or to the solar equator. The observed asymmetry relative to the galactic plane argues strongly for a galactic source. It may be that the relative abundance of interstellar hydrogen and dust is different in the northern and southern galactic hemispheres.

Observations of the Interplanetary Medium

The space between the planets contains photons, plasma, magnetic fields, and streams of charged particles, all coming from the Sun. A few photons and charged particles (cosmic rays) from other stars also intrude. The general pattern of interplanetary phenomena was first elucidated by the observations of Mariner 2 in 1962, and additional details have been added by more recent spacecraft. The expansion of the plasma in the solar corona produces the "solar wind," which flows radially out from the Sun. It carries with it the magnetic field lines attached to the solar surface; and the combination of radial flow and solar rotation produces a spiral field configuration on the average. Charged atomic particles, produced in particularly active regions in the atmosphere of the Sun, travel outward along the field lines and diffuse slowly across them. The symmetry of the situation is often disrupted by the intrusion of a cloud or a stream of fast-moving plasma from a particularly hot spot on the Sun.

Mariner 5 was well equipped to observe these complex interrelated phenomena. The plasma probe measured the particulate properties; the magnetometer measured the field properties of the solar plasma in which the spacecraft was immersed. The dual-frequency radio propagation experiment supplemented these data with a measure of the mean plasma density between Earth and Mariner. The charged particles of higher energy from the Sun were observed by the trapped-radiation instrument. One of the detectors gave a continuous monitoring of X-rays from the Sun; this monitoring provided information on the time and duration of occurrence of solar flares that could produce plasma clouds or high-energy particles subsequently detected at the spacecraft.

The primary interest in interplanetary observations by Mariner 5 lies in comparing them with observations from other spacecraft at other in the solar system. These studies are still in process; only the Mariner 5 data are summarized here.

Interplanetary plasma data are summarized statistically by the frequency distributions of density and velocity in figure 2–36. Similar data from IMP 1 are shown for comparison.[3] Differences among the various distributions probably are the results of accidental differences in the intensity and spatial distribution of active regions on the Sun at the times when the data were obtained.

[3] A. J. Lazarus, private communication.

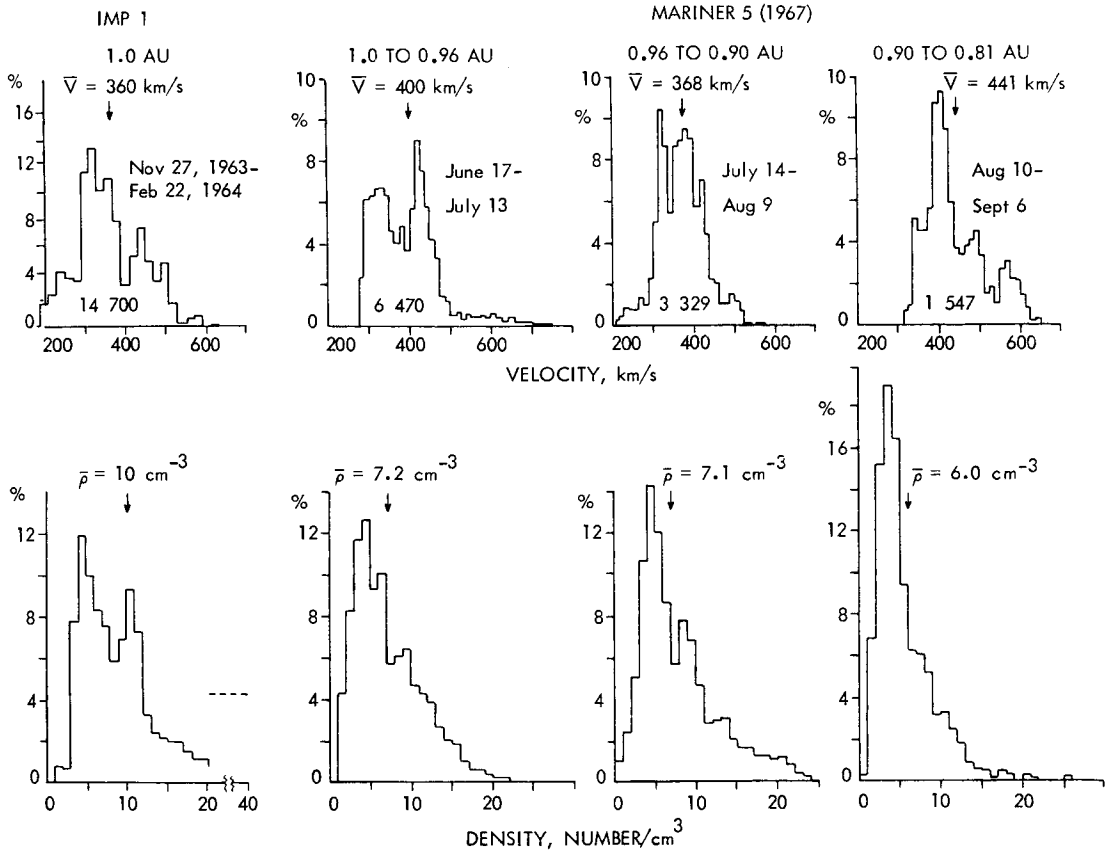

FIGURE 2–36.—Interplanetary plasma data summarized by the frequency distributions of density and velocity. Mariner 5 and IMP 1 data are presented.

Some of the data acquired by the three complementary instruments are shown in figure 2–37 (a) through (f). Each part covers the period of 1 solar rotation (27 days) with a 2-day overlap at each end; and 3-hr averages (eight per day) are plotted for each of the following parameters, reading from the bottom:

F = flux of protons between 0.3 and 12 MeV measured by the silicon diode detector in the trapped-radiation experiment, particles/cm² s sr.

N = solar-wind proton density, protons/cm³.

V_T = thermal velocity of solar-wind protons (most probable speed in distribution of thermal velocities), km/s.

V_W = radial component of bulk plasma velocity, km/s.

B = absolute value of magnetic field intensity, γ.

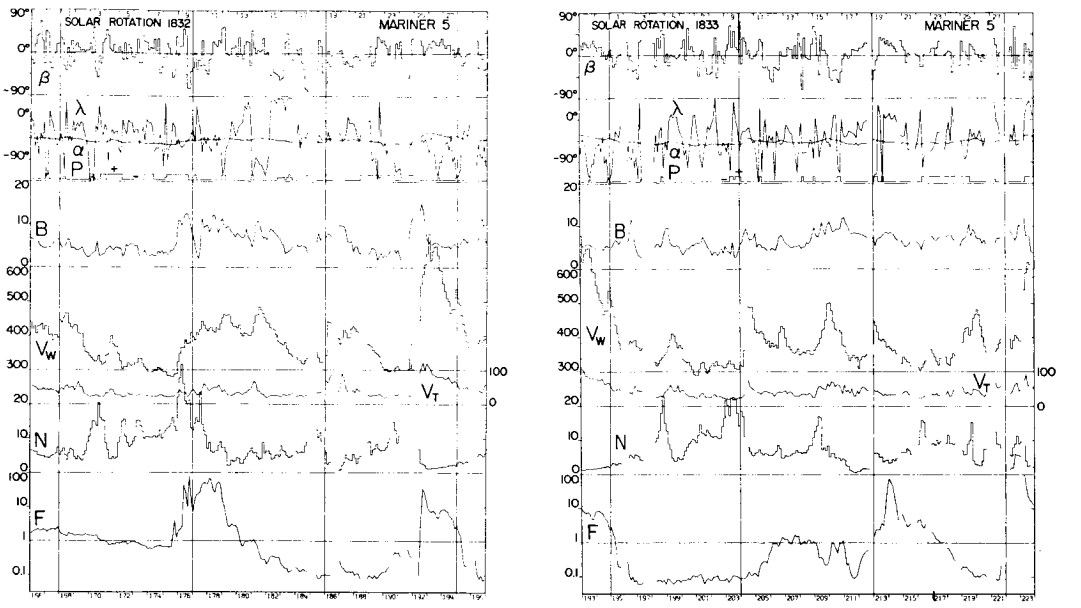

(a) June 15 to July 15, 1967.

(b) July 12 to August 11, 1967.

FIGURE 2–37.—Mariner 5 data obtained by the plasma probe, the magnetometer, and the trapped radiation detector, plotted as a function of the day of the year. Each part of the figure covers one solar rotation (27 days), with an overlap at each end.

P = polarity of magnetic field. *Up* indicates a field outward from the Sun; *down* indicates a field inward toward the Sun; and *in-between* means that the field was nearly normal to the ideal spiral direction, or that the polarity reversed near the middle of the averaging interval.

α = longitude of magnetic field vector in solar equatorial coordinates, measured from the meridian containing the spacecraft. Range of longitude is from —135° to +45°; sense of vector is given by P, as explained above.

γ = longitude angle of ideal magnetic spiral, calculated from observed plasma velocity. This angle is fairly close to —45° throughout the mission.

β = latitude of field vector, measured from the solar equator.

Detailed analyses of these data are still in progress. Some significant general features are discussed in the subsequent paragraphs.

Interplanetary conditions were relatively chaotic during the Mariner 5

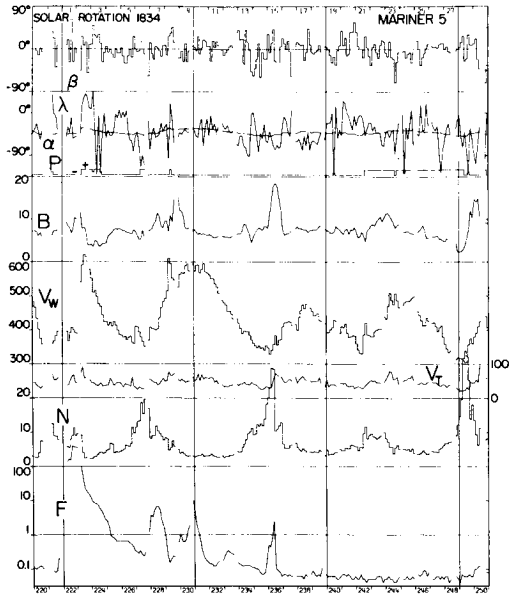

(c) August 8 to September 7, 1967.

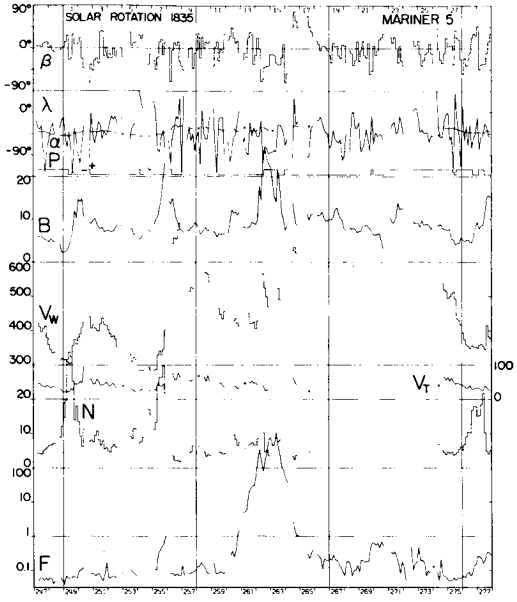

(d) September 4 to October 4, 1967.

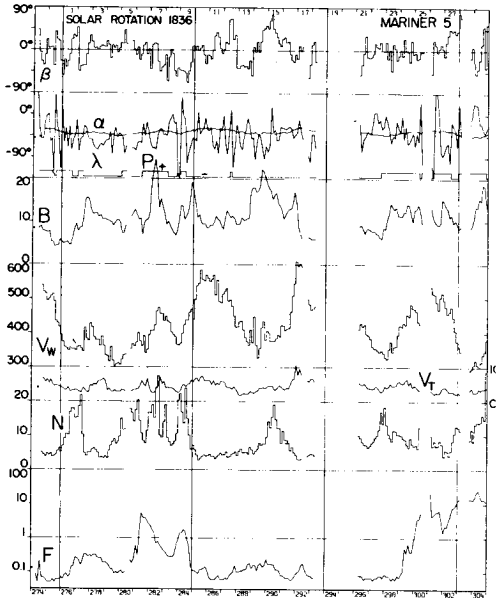

(e) October 1 to October 31, 1967.

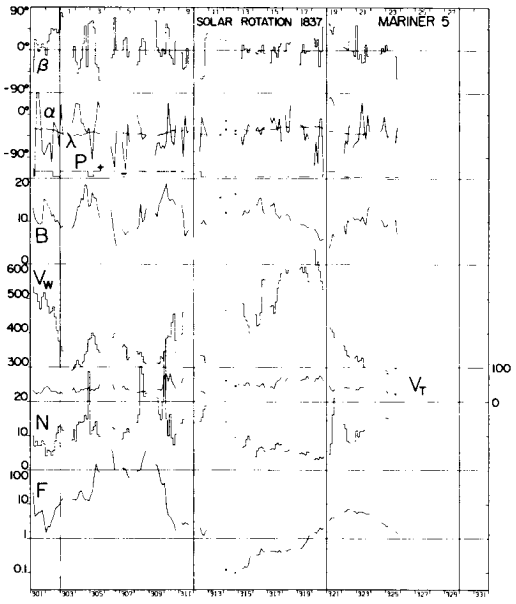

(f) October 28 to November 27, 1967.

FIGURE 2–37 (concluded).

mission and did not exhibit the stability and regularity that had been observed at earlier times. In the Mariner 2 data, four very stable streams of high-velocity plasma appeared in each revolution of the Sun; these streams so dominated the scene that the average plasma velocity observed during the mission was greater than 500 km/s. In the Mariner 5 data, there were only eight times when streams showed velocities appreciably above 500 km/s, and the profiles of successive solar rotations look quite different. In 1963, IMP 1 observed a stable structure of four sectors of alternating magnetic polarity. The only Mariner 5 feature similar to this structure is a slight tendency for the field to point outward during the last 7 days of a solar rotation and to point inward most of the rest of the time. The contrast probably reflects the fact that Mariner 5 flew when solar activity (as measured by the sunspot number) was high and rising rapidly toward its peak; during the other two missions, the activity was lower and decreased slowly.

Plasma density increases followed by velocity increases occur many times in the data. This phenomenon, first observed on Mariner 2, results from the "snowplow" effect of the fast-moving stream sweeping up plasma from the slower stream that it is overtaking.

An additional technique for studying these high-velocity plasma streams was provided by the dual-frequency radio propagation experiment, which measured the total electron content in the path between Earth and Mariner 5 for about 600 hr during July through November. Simultaneous observations of the Faraday rotation produced by the Earth's ionosphere on 136-MHz signals from a geostationary satellite were used to deduce the ionospheric electron content. These values were subtracted from the Mariner 5 data to produce a daily plot of interplanetary electron number density averaged over the propagation path in interplanetary space.

The time average density over the 5 months was about 5.5 electrons/cm^3; occasionally, however, large "pulses" of plasma crossed the path. (See fig. 2–38.) Before the pulse, the path had been disturbed for several days and had an average content of 10 electrons/cm^3. The plasma probe measured similar conditions during those days and observed a pulse of high-density plasma about 6 hr later than the dual-frequency receiver, and about half again as high. The current interpretation of the combined data is that the streaming solar plasma began to fill the Earth-to-spacecraft path and, therefore, was observed first by the radio experiment. Eventually, it filled about two-thirds of the path and enveloped the spacecraft.[4]

[4] H. T. Howard, private communication.

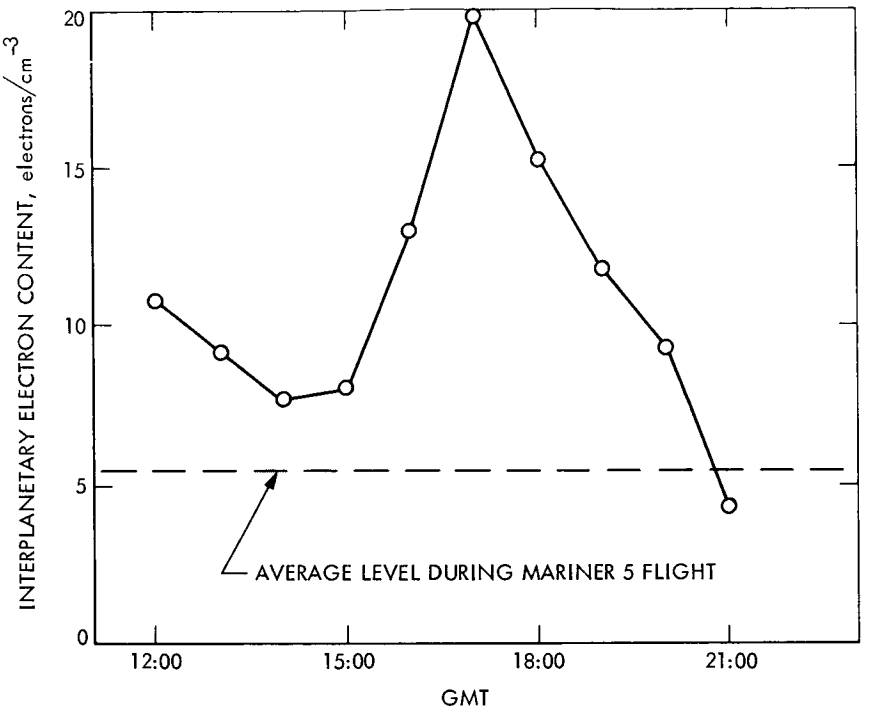

FIGURE 2–38.—Solar-plasma pulse, as measured by the dual-frequency receiver during the Mariner 5 flight.

By using the combined data, many such events are being studied. Comparison has shown the expected types: some types where the onboard plasma probe and the propagation experiment both observed a pulse, and others where only one or the other experiment observed it. Careful comparison of the two sets of data is expected to yield further understanding of the dimensions, velocity, and direction of the plasma streams ejected by disturbed regions in the Sun's corona.

Numerous cases of simultaneous sudden changes in plasma and magnetic field were observed, and are now being studied in detail. Also a close correlation between the radial components of the magnetic field and the plasma velocity often appears. Analysis of these two quantities in each of 444 six-hour intervals throughout the mission (ref. 2–36) shows that, in more than 30 percent of these intervals, the correlation coefficient between them was larger than 0.8. These intervals of high correlation are scattered sporadically throughout the mission, and there is no discernible pattern of association with large-scale structures such as the high-velocity streams or polarity patterns of the solar wind. This cor-

relation can be explained quantitatively in terms of Alfvén waves of large amplitude propagating outward along the magnetic field lines, as the ratio of the magnitudes of the fluctuations in field and in velocity agrees well with its theoretical value for such waves. The presence of Alfvén waves had been demonstrated statistically from the Mariner 2 data (refs. 2–37 and 2–38), but this is the first case in which they were clearly apparent without any statistical analysis. No examples of other modes of hydromagnetic waves have been identified in the Mariner 5 data, nor do inward propagating Alfvén waves appear to be present.

The seven data channels of the trapped-radiation detector instrument provided a wealth of information for comparison with other space missions and with solar observations from Earth. The Sun-oriented geiger counter (detector A), which monitored solar X-rays in the wavelength region 0.2 to 0.9 nm, observed several hundred X-ray flares. During the latter part of the mission many were on the back side of the Sun where they are inaccessible to observation either from Earth or from Earth satellites.

An example of the types of studies that such data make possible is one (ref. 2–39) in which X-ray flux data from Mariner and from four Earth satellites (Injuns 1 and 3 and Explorers 33 and 35) have been compared with Earth-based observations of solar radio flux at 2- and 10-cm wavelengths. The X-ray flux was found to correlate with the slowly varying component of the radio noise (see fig. 2–39) and with the noise bursts (believed to be of thermal origin) having time constants of tens to hundreds of minutes (see fig. 2–40), but not with the impulsive noise bursts having time constants of a few minutes or less. Assuming the high correlation with thermal noise burst to indicate a common origin for the X-ray and radio emissions, analysis yields information about the nature of the processes. It is indicated that the flare is optically thick in the microwave region, but optically thin to the X-rays. Typical flare diameters were found to be about 32 arcsec and typical peak flare temperatures about 4×10^6 K, with limiting values of diameter and peak temperature differing by about a factor of 2 from the typical values.

Coordinated Observations by Mariners 4 and 5

In the autumn of 1966, when the continued operation of Mariner 4 indicated that it could still be producing good scientific data during the mission of Mariner 5, it was recognized that the relative positions of the two Mariner spacecraft and the Earth would provide a unique opportunity for studying the motion of particles and waves in the interplanetary medium. The various Pioneer spacecraft provided the data for studying azimuthal variations, but observation plat-

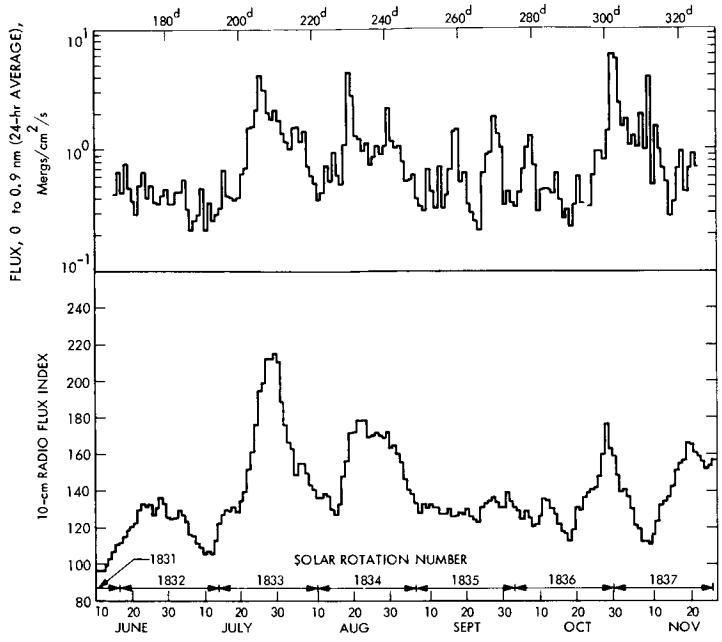

FIGURE 2–39.—History of Mariner 5 average daily X-ray flux measurements and the 10-cm radio flux index.

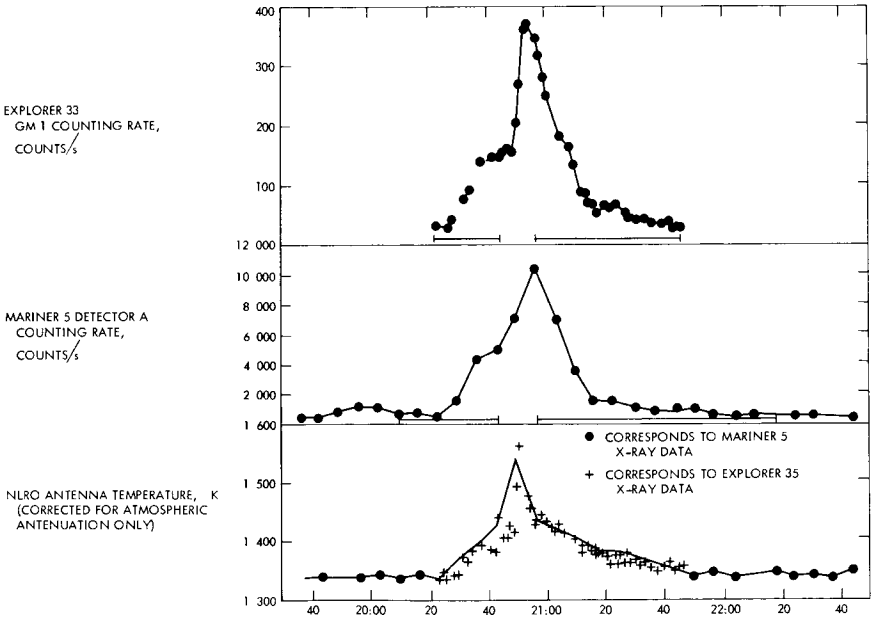

FIGURE 2–40.—Example of good correlation between solar X-rays and radio noise (July 24, 1967).

forms separated by large distances along the same radial line from the Sun are difficult to arrange. The configuration of Mariner 4, Earth, and Mariner 5 is shown in figure 2–41. It can be seen that in August the three "spacecraft" have nearly the same ecliptic longitude (although their latitudes differ by a few degrees), and in September and October all three lie close to the same spiral magnetic field line. (The three spirals drawn correspond approximately to minimum, mean, and maximum solar-wind velocities.) Accordingly, a plan was generated

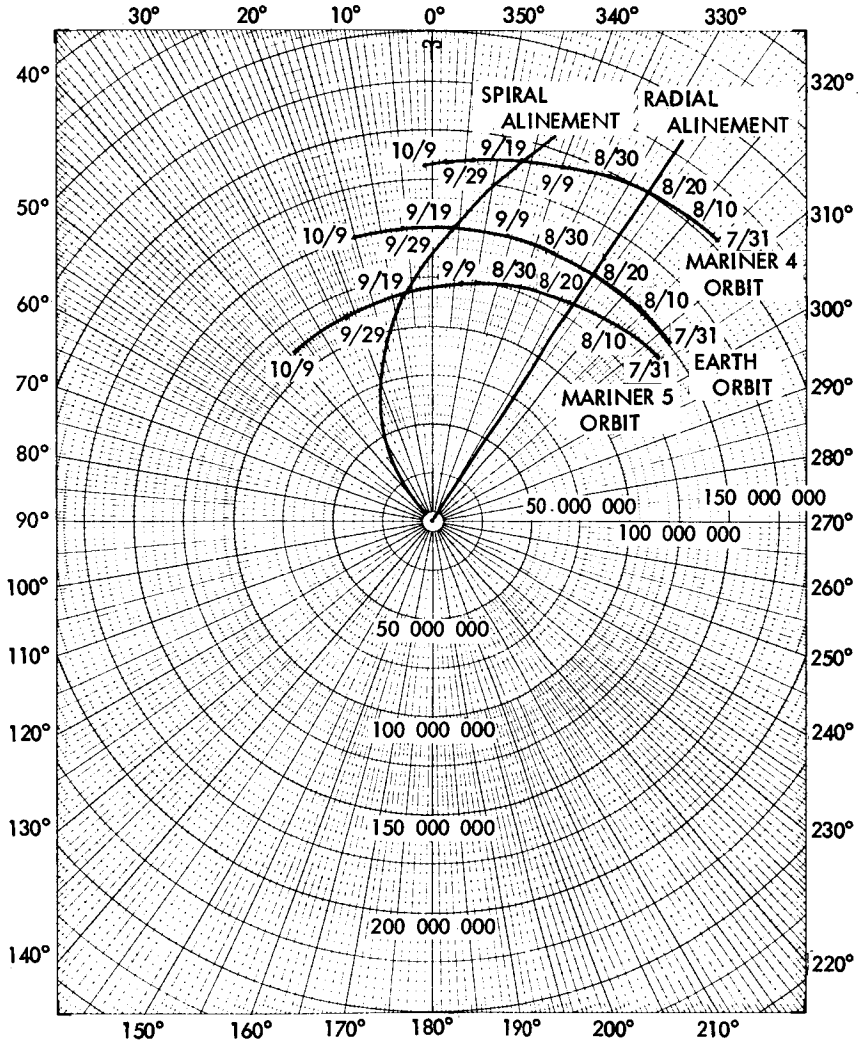

FIGURE 2–41.—Spiral and radial alinements for Mariners 4 and 5.

to provide, within the constraints of the requirements of other missions, the maximum feasible simultaneous reception of telemetry from the two Mariners during the "radial" and "spiral" phases of the mission.

At the time of the writing of this report, the detailed comparison of the magnetic field and plasma data from the two spacecraft has not been completed. The analysis of plasma data from Mariner 4 is especially difficult, as the instrument operated in a nonstandard mode after the failure of a resistor in the high-voltage power supply on the eighth day of the mission; the low instrument temperature resulting from the large distance from the Sun in 1967 further aggravated the problem.

Two studies based upon the charged-particle data from the two Mariners have been reported, and more are expected. Analysis by Krimigis et al. (ref. 2–40) of observations of solar particles by the two Mariners and Explorer 35 has led to the following conclusions.

(1) For flares on the eastern hemisphere of the Sun, particle propagation along the lines of the corotating spiral magnetic field occurs, with delays determined by the prevailing solar-wind velocity.
(2) For western-hemisphere flares, which have no field lines connecting to the vicinity of the spacecraft, particles are detected that have diffused across the magnetic field for large distances—more than 50° in heliocentric longitude in one instance.
(3) Protons and alpha particles with the same energy per nucleon appear to move in the same way.
(4) Absolute fluxes seem to be maintained over a radial distance of at least 1.4 AU on the assumption that the flux is, on the average, relatively isotropic.

The combined Mariner data also provided confirmation of the conclusion reached by Krimigis and Venkatesan (ref. 2–41), on the basis of other space-probe data, that the gradient of the intensity of protons above 50 MeV is inward toward the Sun instead of outward as expected. This surprising result is in contradiction to the conclusions of several earlier attempts to measure the cosmic ray gradient. Although the Mariner data are not as extensive as some of the others, they have the advantage of having been produced by precisely identical geiger counters, which maintained a nearly constant difference of 0.5 AU in heliocentric radial distance for 90 days. It was found that the mean count rate from mid-July to mid-October at Mariner 4 was 13.7 percent less than at Mariner 5. The resulting value of the gradient is 29 ± 4 percent/AU.

Meteoroids and Mariner 4

Among the alterations that transformed a Mariner 4 spacecraft into a Mariner 5 was the deletion of three of the scientific instruments—the vidicon imaging subsystem, the cosmic ray telescope, and the cosmic dust detector. Upon the return of Mariner 4 in 1966–67, no scientific information was obtained by the vidicon (although it was operated as a test) or by the cosmic ray telescope (which was no longer operating correctly). The dust detector, however, continued to produce useful data.

The dust detector consisted of an aluminum plate, 350 cm^2 in area, to the center of which was bonded a ceramic transducer that sensed the acoustical waves generated by the impact of a particle. The telemetry data consisted of two 8-bit words, one representing the magnitude of the latest pulse recorded and one providing a count of the hits. As the counter could register only seven hits before overflowing, nearly continuous telemetry was required to determine an accurate count of hits.

Reacquisition of telemetry began in March 1966, but the coverage was sparse for more than a year thereafter. Nevertheless, it was possible to deduce with high confidence that 66 hits were registered in the 151 days from May 21 to October 19 (ref. 2–42).

In 1967, from mid-July to mid-October, while Mariner 4 moved toward the Sun from 1.4 to 1.2 AU, telemetry coverage was fairly complete, and a similar rate of events was observed. During September, the background rate was about one-half event per day, corresponding to a flux rate of about 1.6×10^{-5} particles/m^2 s π sr; within about 45 min on September 15, however, at least 17 impact events were recorded. At the same time, the spacecraft experienced a slight, but readily detectable, torque, predominantly around the roll axis. It appears that the spacecraft actually encountered a stream of dust particles, and the number that struck the spacecraft was probably 2 or 3 orders of magnitude greater than the 17 that were recorded. Position of the spacecraft at the time was heliocentric range, 1.273 AU; ecliptic latitude, 2.25° N; ecliptic longitude, 343.6°. This spot does not appear to be close to the path of any known meteoroid stream or short-period comet that could provide the source of the particles. It does, however, lie very close to the plane of Encke's comet, and it is believed that debris from this comet, spiraling inward toward the Sun in response to nongravitational forces, may be responsible for the event.[5]

On December 5 the supply of attitude-control gas was exhausted, and

[5] W. M. Alexander, J. L. Bohn, and B. C. Connor: Mariner IV: Possible Encounter of Inspiraling Particles From Encke's Comet. Unpublished memo, 1968.

Mariner 4 went into a slow uncontrolled roll, still held pointing toward the Sun by the solar vanes. On December 10, when the daily tracking period began, it was found to be precessing approximately 30° about the sunline, while the dust detector was indicating an event rate of about 4 per hour. On December 12, the gyroscopes were used to remove the precession by coupling and uncoupling momentum into them at specific times. By the next tracking period on December 13, a precession of about 55° was found to have set in since the stabilization. The average dust count rate remained between 2 and 4 counts/hr from December 10 until the final loss of telemetry on December 14.

One suggested explanation for the observed count rate is that the precessional motion could cause alternating temperature changes in the dust-detecting plate and the spacecraft structure because of the varying incidence of solar radiation. Although it is known that temperature changes can cause spurious signals in such detectors, the principal investigator believes that the spacecraft actually encountered another meteoroid stream. The spacecraft coordinates were as follows: heliocentric range, 1.1 AU; ecliptic latitude, 0.2° S; and ecliptic longitude, 54°. This time there were at least three well-known meteoroid streams that came near this point—the Southern Taurids, the Northern Taurids, and the Leonids. The Southern Taurids[6] seem to be the most likely candidate because they are a "permanent stream" that crosses the ecliptic at about 53° longitude at 1.10 AU from the Sun. (The particles are spread more or less uniformly along the entire length of the orbit.) In addition, their orbit is inclined only about 5° to the ecliptic, and thus is near the ecliptic over a wide range of longitude.

ADDITIONAL SCIENTIFIC RESULTS FROM THE RADIO TRACKING DATA

The radio tracking of Mariner 5 has made available 6934 measurements of doppler velocity, 10 245 range measurements provided by the Mark I (lunar) ranging subsystem early in the mission, and 8493 range measurements from the Mark II (planetary) ranging subsystem at larger distances (out to 98 million km on November 5). These measurements, along with data from other Mariners and Pioneers and from Earth-based radar, are being used by the Mariner celestial mechanics experimenters and others to provide more refined planetary ephemerides and more precise values for astronomical constants.

An example of these results is provided by the determinations of the Earth/Moon mass ratio. This constant enters into the tracking data because the velocity of the Earth about the Earth/Moon barycenter projected onto the Earth/space-

[6] N. R. Haynes: Determination of the Meteor Stream Encountered by Mariner IV. JPL Interoffice memo 312.3–26, Jan. 24, 1968.

craft direction appears as a sinusoid with a period of about 29 days and an amplitude of about 12 m/s. The values determined from the tracking data of Mariners 2 and 4 (as of November 1967) were, respectively, 81.3001 ±0.0013 and 81.3015 ±0.0016. At present, even though the available computers and computer programs make it feasible to handle only about 4 percent of the tracking data points available from Mariner 5, the precision has been increased by an order of magnitude. The latest Mariner 5 figure is 81.300 71 ±0.000 21.

The precision of determination of tracking station location, which is crucial for the precision of spacecraft tracking required in future missions, has been similarly increased, and is now approaching 1 m. Mariner 5 contributed strongly to this determination not only because of its ranging data but also because its orbit crossed the Earth's equatorial plane twice. These zero-declination data are optimum for making the station-location calculations. A much more precise ephemeris of Venus will be available in the near future.

REFERENCES

2–1. De Vaucouleurs, G.: Geometric and Photometric Parameters of the Terrestrial Planets. Icarus, vol. 3, 1964, pp. 187–235.

2–2. Ash, M. E.; Shapiro, I. I.; and Smith, W. P.: Astronomical Constants and Planetary Ephemerides Deduced From Radar and Optical Observations. Astron. J., vol. 72, 1967, pp. 338–350.

2–3. Anderson, J. D.; Null, G. W.; and Thornton, T. T.: The Evaluation of Certain Astronomical Constants From the Radio Tracking of Mariner II. Prog. in Astronaut., vol. 14, 1964, pp. 131–155.

2–4. Carpenter, R. L.: Study of Venus by CW Radar—1964 Results. Astron. J., vol. 71, 1966, pp. 142–152.

2–5. Eshleman, V. R.; Fjeldbo, G.; Anderson, J. D.; Kliore, A.; and Dyce, R. B.: Venus: Lower Atmosphere Not Measured. Science, vol. 162, 1968, pp. 661–665.

2–6. Goldstein, R. M.: Radar Studies of Venus. Moon and Planets, 1967, North-Holland Pub. Co. (Amsterdam), pp. 126–131.

2–7. Barath, F. T.; Barrett, A. H.; Copeland, J.; Jones, D. E.; and Lilley, A. E.: Mariner II Microwave Radiometer Experiment and Results. Astron. J., vol. 69, 1964, pp. 49–58.

2–8. Clark, B. G.; and Kuz'min, A. D.: The Measurement of the Polarization and Brightness Distribution of Venus at 10.6-cm Wavelength. Astrophys. J., vol. 142, 1965, pp. 23–44.

2-9. ADAMS, W. S.; AND DUNHAM, T., JR.: Publ. Astron. Soc. Pac., vol. 44, 1932, pp. 243–245.

2-10. CHAMBERLAIN, J. W.: The Atmosphere of Venus Near Her Cloud Tops. Astrophys. J., vol. 141, 1965, pp. 1184–1205.

2-11. CONNES, P.; CONNES, J.; BENEDICT, W. S.; AND KAPLAN, L. D.: Traces of of HCl and HF in the Atmosphere of Venus. Astrophys. J., vol. 147, 1967, pp. 1230–1237.

2-12. SNYDER, C. W.: Mariner V Flight Past Venus. Science, vol. 158, 1967, pp. 1665–1669.

2-13. ANDERSON, J. D.; PEASE, G. E.; EFRON, L.; AND TAUSWORTHE, R. C.: Mariner V Celestial Mechanics Experiment. Science, vol. 158, 1967, pp. 1689–1690.

2-14. ANDERSON, J. D.; AND EFRON, L.: The Mass and Dynamic Oblateness of Venus. Paper presented at the 129th meeting of the AAS (Honolulu), Mar. 30 to Apr. 2, 1969.

2-15. ANDERSON, J. D.; EFRON, L.; AND PEASE, G. E.: The Mass, Dynamical Oblateness and Position of Venus as Determined by Mariner V Tracking Data. Paper presented at the 127th meeting of the AAS (Victoria, B.C.), Aug. 20–23, 1968.

2-16. ANDERSON, J. D.; CAIN, D. L.; EFRON, L.; GOLDSTEIN, R. M.; MELBOURNE, W. G.; O'HANDLEY, D. A.; PEASE, G. E.; AND TAUSWORTHE, R. C.: The Radius of Venus as Determined by Planetary Radar and Mariner V Radio Tracking Data. J. Atmos. Sci., vol. 25, 1968, pp. 1171–1173.

2-17. KLIORE, A.; LEVY, G. S.; CAIN, D. L.; FJELDBO, G.; AND RASOOL, S. I.: Atmosphere and Ionosphere of Venus From the Mariner V *S*-Band Radio Occultation Measurement. Science, vol. 158, 1968, pp. 1683–1688.

2-18. KLIORE, A.; TITO, D. A.; CAIN, D. L.; AND LEVY, G. S.: A Radio Occultation Experiment to Probe the Atmosphere of Venus. J. Spacecr. Rockets, vol. 4, 1967, pp. 1339–1346.

2-19. CONNES, P.; CONNES, J.; KAPLAN, L. D.; AND BENEDICT, W. S.: Carbon Monoxide in the Venus Atmosphere. Astrophys. J., vol. 152, 1968, pp. 731–743.

2-20. KLIORE, A.; CAIN, D. L.; LEVY, G. S.; FJELDBO, G.; AND RASOOL, S. I.: Structure of the Atmosphere of Venus Derived From Mariner V S-Band Measurements. Paper presented at the 11th meeting of COSPAR (Tokyo), May 9–11, 1968.

2–21. KLIORE, A.; AND CAIN, D. L.: Mariner V and the Radius of Venus. J. Atmos. Sci., vol. 25, 1968, pp. 549–554.

2–22. ASH, M. E.; CAMPBELL, D. B.; DYCE, R. B.; INGALLS, R. P.; JURGENS, R.; PETTENGILL, G. H.; SHAPIRO, I. I.; SLADE, M. A.; AND THOMPSON, T. W.: The Case for the Radar Radius of Venus. Science, vol. 160, 1968, pp. 985–987.

2–23. MARINER STANFORD GROUP: Venus: Ionosphere and Atmosphere as Measured by Dual-Frequency Radio Occultation of Mariner V. Science, vol. 158, 1967, pp. 1678–1683.

2–24. MCELROY, M. B.: The Upper Atmosphere of Venus. J. Geophys. Res., vol. 73, 1968, pp. 1513–1521.

2–25. MCELROY, M. B.: Structure of the Venus and Mars Atmospheres. J. Geophys. Res., vol. 74, 1969, pp. 29–42.

2–26. HUNTEN, D. M.: The Structure of the Lower Atmosphere of Venus. J. Geophys. Res., vol. 73, 1968, pp. 1093–1094.

2–27. BARTH, C. A.; PEARCE, J. B.; KELLY, K.; WALLACE, L.; AND FASTIE, W. G.: Ultraviolet Observed Near Venus From Mariner V. Science, vol. 158, 1967, pp. 1675–1678.

2–28. CHAMBERLAIN, J. W.: Planetary Coronae and Atmospheric Evaporation. Planet. Space Sci., vol. 11, 1963, pp. 901–960.

2–29. BARTH, C. A.: Interpretation of the Mariner V Lyman-Alpha Measurements. J. Atmos. Sci., vol. 25, 1968, pp. 564–567.

2–30. BARTH, C. A.; WALLACE, L.; AND PEARCE, J. B.: Mariner V Measurement of Lyman-Alpha Radiation Near Venus. J. Geophys. Res., vol. 73, 1968, pp. 2541–2545.

2–31. WALLACE, L.: Analysis of the Lyman-Alpha Observations of Venus Made From Mariner V. J. Geophys. Res., vol. 74, 1969, pp. 115–131.

2–32. NEUGEBAUER, M.; AND SNYDER, C. W.: Solar-Wind Measurements Near Venus. J. Geophys. Res., vol. 70, 1965, pp. 1587–1591.

2–33. BRIDGE, H. S.; LAZARUS, A. J.; SNYDER, C. W.; SMITH, E. J.; DAVIS, L., JR.; COLEMAN, P. J., JR.; AND JONES, D. E.: Mariner V: Plasma and Magnetic Fields Observed Near Venus. Science, vol. 158, 1967, pp. 1669–1673.

2–34. VAN ALLEN, J. A.; KRIMIGIS, S. M.; FRANK, L. A.; AND ARMSTRONG, T. P.: Venus: An Upper Limit on Intrinsic Magnetic Dipole Moment Based on Absence of a Radiation Belt. Science, vol. 158, 1967, pp. 1673–1675.

2-35. SMITH, E. J.; AND DAVIS, L., JR.: Magnetic Measurements in the Earth's Magnetosphere and Magnetosheath: Mariner 5. J. Geophys. Res., vol. 75, 1970, pp. 1233–1245.

2-36. BELCHER, J.; DAVIS, L., JR.; AND SMITH, E. J.: Large Amplitude Alfvén Waves in the Interplanetary Medium: Mariner V. J. Geophys. Res., vol. 74, 1969, pp. 2302–2308.

2-37. UNTI, T. W. J.; AND NEUGEBAUER, M.: Alfvén Waves in the Solar Wind. Phys. Fluids, vol. 11, 1968, pp. 563–568.

2-38. COLEMAN, P. J., JR.: Wave-like Phenomena in the Interplanetary Plasma: Mariner 2. Planet. Space Sci., vol. 15, 1967, pp. 953–973.

2-39. WENDE, C. D.: The Correlation of Solar Microwave and Soft X-Ray Radiation. Thesis, Univ. of Iowa, 1968.

2-40. KRIMIGIS, S. M.; ROELOF, E. C.; ARMSTRONG, T. P.; AND VAN ALLEN, J. A.: Low Energy ($\geqslant$0.3 MeV) Solar Particle Observations at Widely Separated Points ($>$ 0.1 AU) During 1967. J. Geophys. Res., to be published.

2-41. KRIMIGIS, S. M.; AND VENKATESAN, D.: The Radial Gradient of Interplanetary Radiation Measured by Mariners 4 and 5. J. Geophys. Res., vol. 74, 1969, pp. 4129–4145.

2-42. ALEXANDER, W. M.; AND BOHN, J. L.: Zodiacal Dust Measurements in Cis-Lunar and Interplanetary Space From OGO III and Mariner IV Experiments Between June and December 1966. Space Research VIII. Proc. 10th Plenary Meeting COSPAR (London), 1967, pp. 489–495.

CHAPTER 3

Flightpath Analysis and Mission Planning

During encounter with Venus, the Mariner 5 trajectory was perturbed so that the spacecraft would attain a perihelion of 0.58 AU. This trajectory comes close enough to the Earth each 14 months to allow measurements to be made during those periods.

TRAJECTORY DESIGN

Desirable characteristics were chosen from all possible trajectories spanning a large number of launch and arrival dates. Conic approximations were used in the early analysis because of the great number of cases examined. Trajectory characteristics were evaluated by examining three conics (refs. 3–1 and 3–2): the heliocentric ellipse, geocentric hyperbola, and planetocentric hyperbola.

(1) *Heliocentric ellipse.* This ellipse is defined as the ellipse that passes through the center of a massless Earth at time of launch L and passes through the center of a massless target planet at time of encounter E. This ellipse, a unique function of L and E, is an adequate approximation for initial design purposes.

(2) *Geocentric hyperbola.* The geocentric hyperbola is defined as one with a hyperbolic velocity equal to the vector difference between the velocity of the heliocentric ellipse at launch and the velocity of the Earth at launch. The hyperbola is determined by assuming a perigee equal to the radius of the parking orbit used (nominally 185-km altitude). The plane of the parking orbit then determines the launch azimuth as a function of time for a given launch site (nominally Cape Kennedy). These approximations have proved to be accurate.

(3) *Planetocentric hyperbola.* This hyperbola is defined as one with a hyperbolic velocity equal to the vector difference between the velocity of the heliocentric ellipse at encounter and the velocity of the target planet at encounter.

The following criteria were used to choose the Mariner 5 trajectories:

(1) A specific arrival date that insures identical relative positions for the Earth, Sun, and Canopus. This simplifies spacecraft design features

because the encounter geometry is then known and invariant, except for the approach orbit (which depends on launch date).

(2) Encounter geometry that satisfies experimental requirements.

(3) Near-minimum transit time.

(4) Near-minimum communication distance.

(5) Long launch period to allow for any delay that could occur if problems arise at the first launch attempt.

(6) Required injection energy within booster-vehicle capability. This bounds the launch period ranges mentioned in (5).

To satisfy these criteria, a class of minimum-energy trajectories was examined. Characteristics exhibited were

(1) The best geometry for the *S*-band radio occultation experiment occurred for arrival dates toward the end of October.

(2) If an earlier arrival date were chosen, transit time decreases (desirable), communication distance decreases (desirable), hyperbolic approach ve-

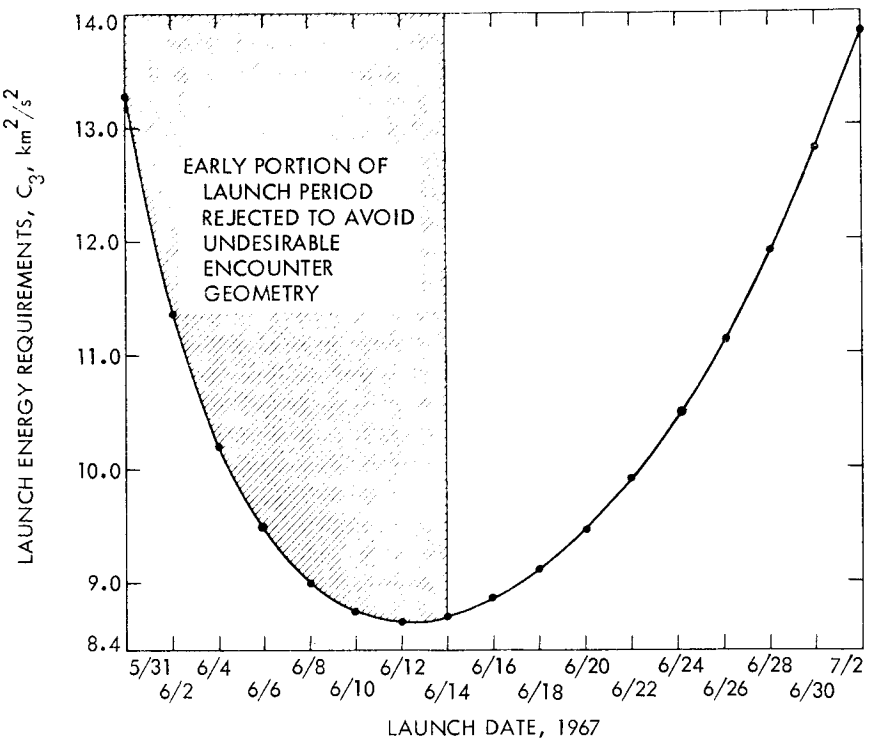

FIGURE 3–1.—Launch energy versus launch date.

locity increases (undesirable), and launch period decreases (undesirable) would occur.

October 19, 1967, was chosen as the optimum arrival date, with an arrival time of 18:00 GMT, approximately the middle of the view period of the Goldstone tracking station. With the arrival date chosen, the launch period was determined by examining the booster-vehicle capability. Required injection energy as a function of launch date is shown in figure 3–1. The first half of the launch period (shaded area) was rejected because of the poor approach geometry that would result for those dates.

After choosing the desired launch and arrival dates, based on conic approximations, integrated trajectories were sought by an iterative process. These integrated trajectories considered perturbative forces caused by other planets in the solar system and solar pressure, based on the effective area and reflectivity of the spacecraft. The desired aiming point was considered for these integrations to examine the actual expected approach geometry, even though biased aiming points would be used.

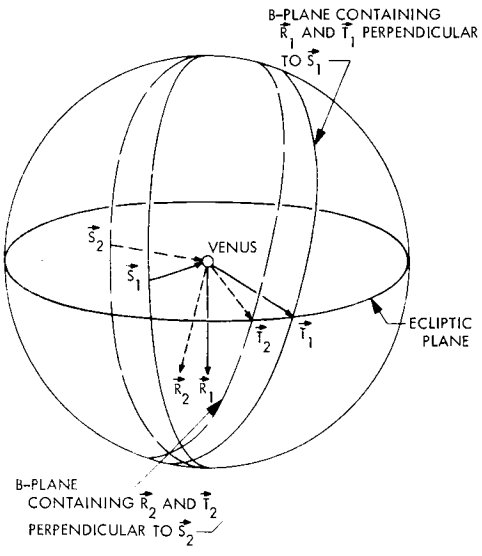

FIGURE 3–2.—Linearized **R, S, T** coordinates. Subscripts 1 and 2 indicate different launch dates.

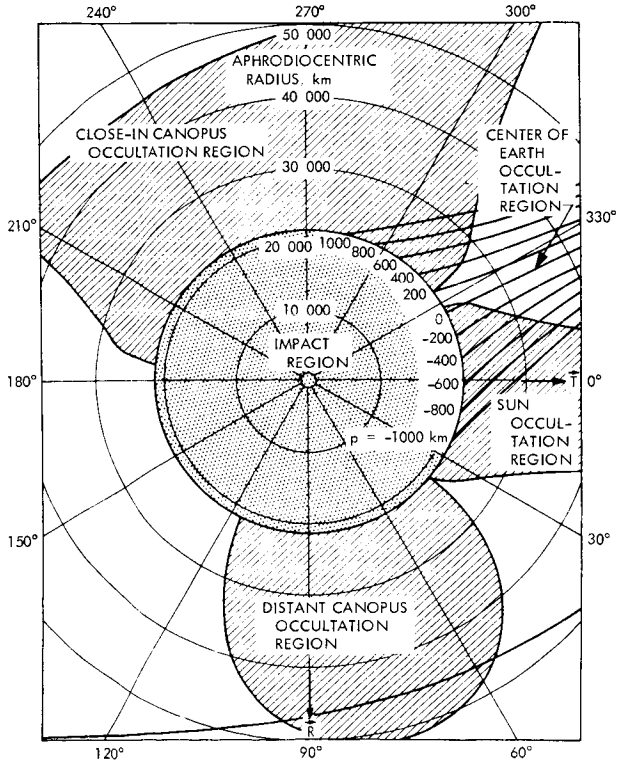

FIGURE 3–3.—Aiming zone and constraint regions for launch on June 14, 1967.

Approach trajectories vary as a function of launch date. (See fig. 3–2, which shows a convenient coordinate system that was used.) The base vectors are **S**, along the incoming asymptote; **T**, perpendicular to **S** and in the plane of the ecliptic; and **R**, which completes a right-handed coordinate system. Figure 3–3 shows the **R**,**T**-plane (also called the *B*-plane) with constraint regions for the June 14 launch date. Figure 3–4 shows the time variation in these regions and indicates how the launch period was chosen.

One ground rule used in the mission design was that the probability of placing a single viable organism on the surface or in the atmosphere of Venus had to be less than 3×10^{-5}. This rule was a NASA policy consistent with recommendations adopted by the Committee on Space Research, International Council of Scientific Unions (COSPAR). In accordance with this policy, the target aiming point was biased so that the **B**-vector was about 100 000 km at a polar angle θ of about 320°. This bias would correspond to a closest approach altitude of about 69 000 km; the exact aiming point was a function of the launch date. The Agena was programed to execute a yaw maneuver and to ignite a small, solid-propellant motor shortly after spacecraft separation. The completion of this program would cause the Agena stage to pass the planet at a closest approach altitude of 226 000 km.

LAUNCH CONSTRAINTS AND OPERATIONS

For each day in the launch period, the launch azimuth varies as a function of the time of day as the Earth rotates, and the required hyperbolic velocity vector stays fixed in space (ref. 3–3). Dependent on the declination of this vector, only a certain range of launch azimuths can be efficiently utilized. Considerations of range safety result in an allowable range of launch azimuths that avoid flying over populated land areas. The intersection of these two ranges determines the possible launch azimuths.

The requirement that telemetry coverage observe key critical events imposes additional restrictions by eliminating the launch azimuths that result in poor coverage geometry. Similarly, tracking stations must be able to track the powered-flight portion of the trajectory, as well as the separated spacecraft, as soon as possible after injection into orbit. If there are no conflicts with the requirements of other missions in progress, the existing worldwide tracking networks and appropriately located tracking ships normally can cover all allowable launch azimuths. When the existing resources must be shared, a reduction occurs. Data received during early portions of the flight give the first indications of mission status and allow rapid reaction to any nonstandard situation.

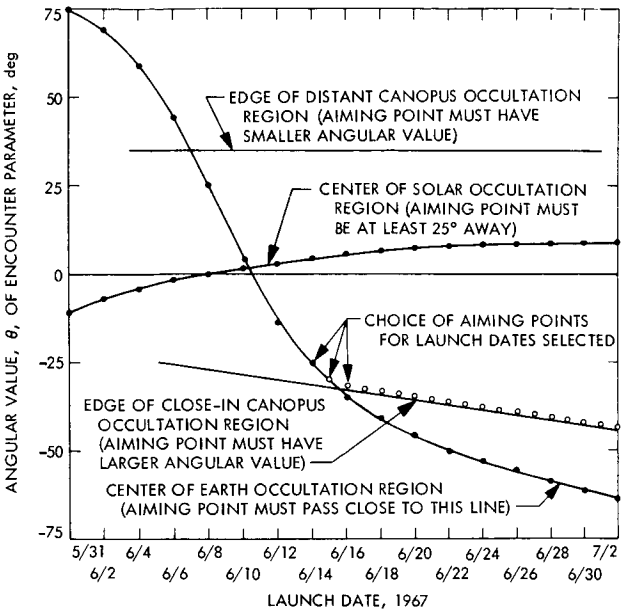

FIGURE 3–4.—Encounter geometry variation versus launch date.

Mariner 5 launch occurred at 06:01:00 GMT on June 14, 1967, with a launch azimuth of 101°. All details of the powered flight appeared normal. Parking orbit injection and transfer orbit injection were satisfactory. Spacecraft telemetry coverage, as it assumed its cruise configuration, showed that all events were occurring as scheduled.

ORBIT DETERMINATION

The ability to determine accurately the orbit of a spacecraft after it has been launched is essential to a space mission. Data types used in orbit determinations tend to differentiate between two tracking regions: (1) near-Earth tracking, when the altitude is less than 1852 km, and (2) deep-space tracking, when the altitude is greater than 1852 km. There is no sharp dividing line between these two regions because the altitude quoted is only a guideline.

Near-Earth tracking is characterized by rapidly changing relative positions and velocities. Position measurements, consisting of point angles and range obtained by skin reflection of a pulsed radar beam, provide good data sensitive to small changes in the position of the spacecraft. Doppler-shift measurements are not obtained easily because of the rapidly changing range rates and the typical narrow-bandwidth equipment used.

Deep-space tracking is characterized by almost insignificant angular rates

and ranges too great to allow skin reflection with existing equipment. Doppler-shift measurements then become the predominant source of tracking data. The calculated orbit is then adjusted to reproduce the range-rate profile that was measured. The accuracy of these measurements is on the order of a few millimeters per second. Ranging is still desirable, but a ranging transponder on the spacecraft is necessary to reradiate a coded range signal with sufficient signal strength so that the signal can be received at the tracking stations. This type of ranging measurement has an associated accuracy of about 30 m. When computations are performed using single precision (eight or more significant decimal digits), the computer truncation errors begin to dominate as a noise source as the range exceeds 10 000 km, a situation that occurs on all planetary missions. The data taken on Mariner 5 were recorded to be processed later by double-precision computer programs.

Techniques used for orbit determination have been described in references 3–4 and 3–5. Several methods may be used, but the basic concept may be described as follows:

A set of observable quantities $y_i(t_j)$ is measured as a function of time. This notation indicates a measurement of type i taken at time t_j. (For example, $i=1$, 2, 3, and 4 could indicate antenna azimuth, antenna elevation, range, and doppler shift, respectively. These quantities do not constitute a complete list of all possible data types.) Some or all of the data types are sampled at a discrete set of times, $j=1, 2, \ldots, N$.

Based upon some initial estimate X of the parameters to be estimated (for example, position and velocity components at some reference time; tracking station location parameters; mass of Earth, Moon, and Venus; magnitude of the astronomical unit), the expected value of the measured quantity is calculated to be $z_i(t_j,X)$. The difference between the observed and calculated value is called the residual, defined by

$$r_i(t_j) = y_i(t_j) - z_i(t_j, \mathbf{X}) \tag{1}$$

Partial derivatives are computed to form the A-matrix with elements:

$$A_{mn} = \frac{\partial z_m}{\partial X_n} \tag{2}$$

A diagonal weighting matrix W then allows weight assignment to be made to the different data types, so that a weighted least-squares procedure (ref. 3–5) yields differential corrections:

$$\mathbf{X} = (A^T W A)^{-1} A^T W \mathbf{r} \tag{3}$$

where $\mathbf{r}$ has components $r_i(t_j)$, as defined in equation (1). The process just described is then repeated, based on updated values of the estimated parameters, until the residuals display zero-mean and random-noise characteristics. This use of linear perturbation theory in an iterative mode results in very good fits. If the residuals display nonrandom behavior, a model error would be suspected; the model would then be changed until random behavior was displayed. For example, during the cruise phase of the Mariner 4 mission to Mars, orbit determination residuals showed an apparent sinusoidal behavior with an 88-day period. After the operations had been examined, it was realized that Mercury had been ignored in the planetary ephemeris used. When the ephemeris tapes were reconstructed to include Mercury, the residuals looked random.

Because the spacecraft position and velocity are measured from Earth, the predicted position and velocity with respect to Venus depend on an accurate Venus ephemeris. Using the information provided by recent radar bounces, an updated Earth/Venus ephemeris was produced to have the best possible estimate of the actual Venus encounter geometry before performing a midcourse maneuver and to plan time-critical sequences during the Venus encounter. By comparing the new ephemeris with the old one, a change of about 500 km was noted in the position of Venus at the predicted encounter time. The new ephemeris was correct, as the close-approach flyby proved.

Table 3–I lists the orbits calculated at various phases of the mission, as well as the desired values on which the midcourse maneuver was based. Also shown are the results achieved by the maneuver, which exhibited a 4.5-percent low proportional error, but which resulted in a satisfactory encounter geometry, obviating the need for a second maneuver. The close agreement between the last two columns is an indication of the quality of the new ephemeris.

Near encounter, when the spacecraft acceleration is high and the velocity profile is a strong function of position with respect to Venus, the orbit is determined accurately relative to Venus. This orbit, combined with the accurate orbit relative to Earth, based on the previous data, allows the orbit of Venus to be estimated. The range measurement capability is particularly significant and, when combined with the double-precision orbit determination program, allows the astronomical unit to be estimated with an accuracy of 1 to 2 km.

MIDCOURSE GUIDANCE

Although launch-vehicle guidance accuracy has increased significantly in

Table 3–I.—Orbit determination at different mission times

Terminal parameters	Premidcourse (L+5 days)	Desired values (midcourse aim point)	Midcourse +21 days	E+3 hr
B•R, km	−65 343	−12 761	−14 855	−14 708
B•T, km	81 483	21 738	24 278	24 362
B, km	104 477	25 212	28 462	28 458
θ, deg	−38.7	−30.4	−31.4	−31.2
t_{CA}[a]	03:53:15	18:00:00	17:34:22	17:34:56
σ_{max},[b] km	250	—	1200	12.5
σ_{min},[b] km	250	—	200	0.2
σ_T, s	300	—	150	0.1

[a]GMT of closest approach on Oct. 19, 1967.

[b]σ_{max} and σ_{min} are the semimajor and semiminor axes, respectively, of dispersion ellipse associated with estimate of B.

the last few years, midcourse maneuver capability is necessary to correct for intolerance injection errors and to allow for mission design flexibility (i.e., the use of a biased aiming point to satisfy planetary quarantine constraints). Future missions will demand even more stringent accuracy requirements that will necessitate a series of midcourse and approach maneuvers in the standard sequence of mission events.

Calculating the required velocity to change a set of trajectory characteristics is almost the inverse process of calculating differential corrections in the estimated velocity components to fit the observed tracking data (refs. 3–6 and 3–7). (The parameters that are actually estimated must be carefully chosen. If one attempts to estimate parameters for which the data type is not sensitive, the solution may diverge. The examples listed are typical of those considered during the Mariner 5 mission.) Basically, partial derivatives of terminal parameters m_i (taken to be $\mathbf{B} \cdot \mathbf{R}$, $\mathbf{B} \cdot \mathbf{T}$, t_{CA} for $i=1, 2, 3$), with respect to velocity components, are computed to form the K-matrix with elements

$$K_{ij}(t) = \frac{\partial m_i}{\partial v_j(t)} \tag{4}$$

where these elements depend on the time t at which the maneuver is to be made. If the difference between actual and desired terminal components is taken to form the miss vector $\Delta\mathbf{m}$, the required velocity change will be

$$\Delta\mathbf{v} = -K^{-1}\,\Delta\mathbf{m}$$

By integrating the short powered flight to attain this velocity and the subsequent cruise phase to encounter time, the resulting terminal parameters are computed. Any difference between these and the desired values forms a new miss, which is corrected in this iterative manner to find the required velocity that exactly nulls the miss. So that the best values are used at each step, variational equations are also integrated to update the partial derivatives.

Before a maneuver can be made, spacecraft constraints must be examined (i.e., a sensitive instrument is not pointed at the Sun; the spacecraft is not oriented so that the Earth is located in an antenna null; etc.). If such a constraint were violated, the maneuver would be modified (or possibly performed at a different time) to satisfy all other requirements and avoid that constraint.

Aiming-point constraint regions considered at the time of the maneuver selection are shown in figure 3–3. Because the Earth-Venus direction is approximately parallel to the direction of the spacecraft velocity relative to Venus, the Earth occultation region almost covers the entire *B*-plane. The ideal geometry for the *S*-band radio-occultation experiment would find the plane of the approach orbit that contains the Earth/Venus vector. Under those conditions, the spacecraft would pass directly behind the center of the planet, as seen from Earth. Depending on the orientation of this orbital plane, the spacecraft trajectory would carry it an apparent distance p from the center of the planet. The most desirable value would have been $p = 0$, but values as high as $p = 1000$ km would have given significant results; contours for this range of values are shown in figure 3–3. The spacecraft's high-gain antenna was oriented so that, as the atmospheric attenuation increased, the Earth appeared ever closer to the antenna boresight, achieving maximum signal strength to counteract maximum attenuation. When behind the planet, the antenna would change its angle to achieve a similar geometry for the ray passing through the atmosphere on the opposite side of the planet (fig. 3–5). The other aiming-point constraint was to approach as close as possible to the planet (to measure the magnetic field and detect possible trapped radiation), while avoiding regions that would result in impact or loss of optical reference.

The direction normal to the *B*-plane (figs. 3–3 and 3–6) represents flight time (i.e., the spacecraft is approaching the *B*-plane perpendicularly; if it is farther away at a given instant, it will arrive there later). It was determined that a closest approach between 15:25 and 20:35 GMT would result in the best use of the tracking configuration. The midpoint of that interval, 18:00 GMT, was chosen for the desired arrival time.

The postencounter orbit for Mariner 5 and associated parameters of interest are listed in tables 3–II and 3–III.

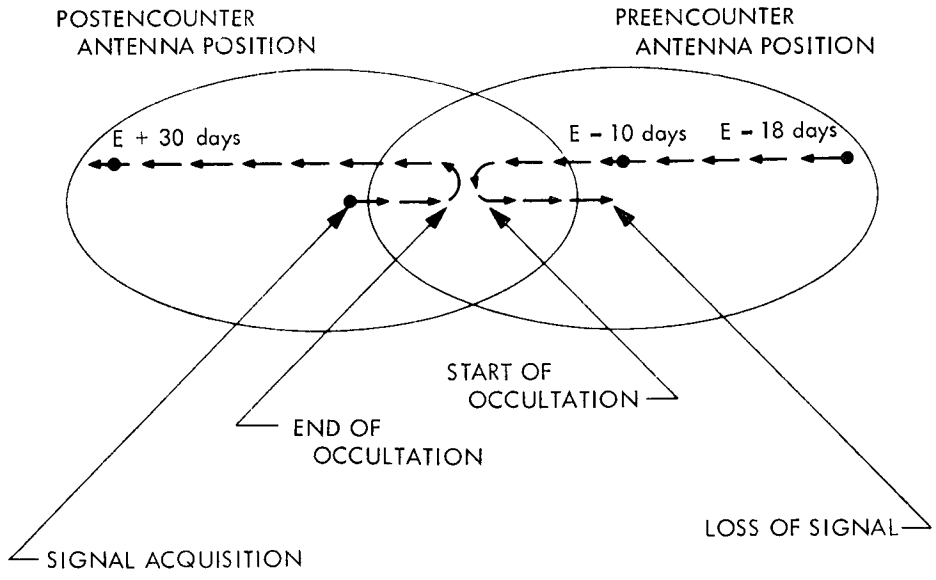

FIGURE 3–5.—Apparent Earth position relative to high-gain antenna pattern.

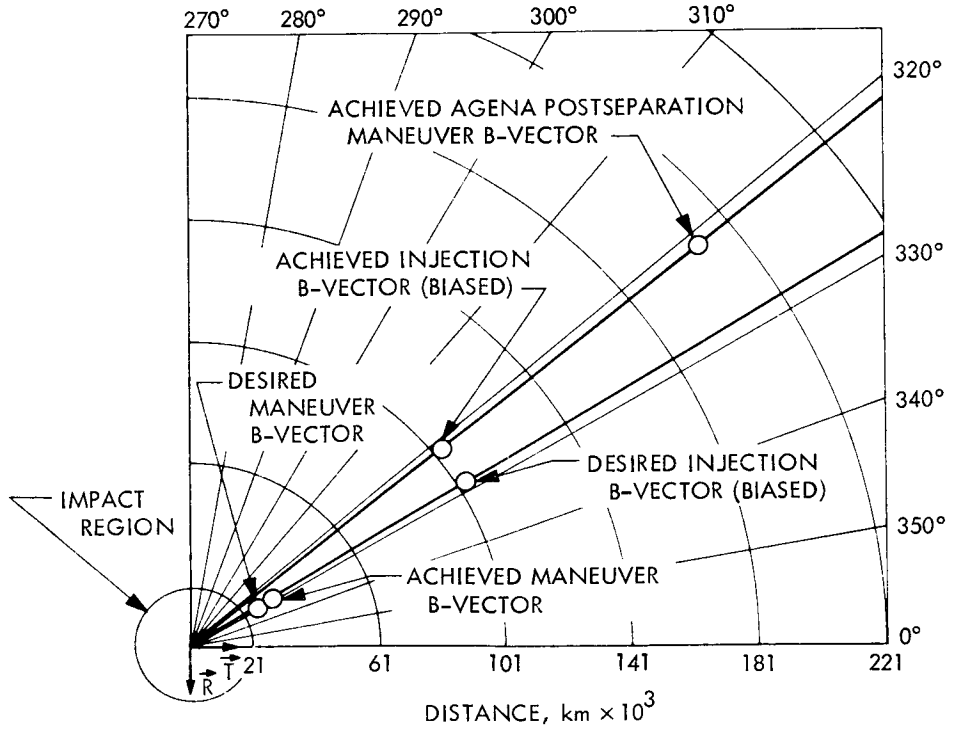

FIGURE 3–6.—Injection and maneuver aiming points and results.

Table 3–II.—Mariner 5 orbital parameters and associated quantities

Osculating conic fit in November 1967	
Eccentricity	0.11760
Period, days	194.61
Perihelion distance, km	86 758 000
Semimajor axis, km	98 320 000
Epoch of perihelion	11:19 GMT on Jan. 4, 1968
Aphelion distance, km	109 883 000

Closest approach to Earth[a]

Date	Distance, km
Oct. 27, 1968	39 000 000
Dec. 27, 1969	46 100 000
Feb. 17, 1971	56 600 000
Apr. 4, 1972	62 900 000
May 18, 1973	63 700 000
July 2, 1974	58 300 000

Next closest approach to Venus

Date	Distance, km
Oct. 27, 1975	4 300 000

[a] These are the centers of approximately 4-month periods, during which time the spacecraft can be interrogated from Earth.

MARINER 4 OPERATIONS SUMMARY (AFTER OCTOBER 1, 1965)

The Mariner-Mars 1964 project was officially concluded on October 1, 1965, with all mission objectives successfully completed. At that time, the Mariner 4 spacecraft was receding from the Earth and communications capability was rapidly diminishing. Periodic telecommunications and tracking activities of a largely experimental nature were conducted in the next 17 months. An analysis of the solar corona was performed near the end of March 1966, when the spacecraft passed within 1.0° from the center of the Sun, as viewed from Earth. On March 1, 1967, after the spacecraft had completed approximately 1¾ revolutions around the Sun, during which time Earth had completed 2¼ revolutions, the

Table 3–III.—Physical parameters estimated

Parameter	Value	Comment
AU	149 597 904±44 km	Radar measurement had yielded 149 597 900±100 km.
Venus ephemeris elements (corrections to DE 24 position at 17:35:33 GMT on Oct. 19, 1967)	$\Delta x = -0.76 \pm 23$ km $\Delta y = -29.23 \pm 12$ km $\Delta z = 11.95 \pm 34$ km	These very small corrections, as well as the AU measurement, are possible primarily because of the planetary ranging data capability.
Tracking station locations	Distance from spin axis r_s and longitude λ were estimated. The encounter solutions exhibited a mean spread in r_s of about 4 m and in λ of about 12 m on the Earth's surface.	A systematic change in λ, up to about 25 m on the Earth's surface, was observed between cruise and encounter solutions. This is believed to reflect an Earth/Sun ephemeris error of about 300 km.
Sun/Venus mass ratio	408 522.66±3	The Mariner 2 solution was 408 505±6.

relative geometry was such that the communications margin was increasing to an acceptable level. Figure 3–7 shows an ecliptic projection of these orbits plotted in an inertial reference frame; the same information, plotted in a rotating coordinate system with the Earth/Sun line fixed, is shown in figure 3–8, which illustrates the spacecraft motion as observed from the Earth (i.e., as actually observed).

Good data were accumulated from Mariner 4 during the summer of 1967 so that the orbit could be accurately established. To evaluate the capability of utilizing the midcourse motor after extended space storage, a second maneuver (motor ignition at the spacecraft) was performed 1062 days after launch, on October 26, 1967, at 06:03:05.8 GMT. This was observed at the Earth 189.2 s later, at 06:06:15.0 GMT. The spacecraft had been oriented with the Earth near the center of the high-gain antenna pattern so that a strong telemetry signal would be received; the motor orientation was determined in this manner. The motor was timed to burn for 70 s; engineering telemetry and tracking data indicated that this was achieved within the accuracy of the measurement. This burn should have imparted a velocity change of 59.2 m/s, and postmaneuver orbit determination indicated a velocity change of 62.06±0.8 m/s. The 4.8-percent overperformance is similar to the one that occurred during the first maneuver, performed on December 5, 1964. Table 3–IV shows the effect of this maneuver on the orbital parameters, as well as the behavior of these orbital parameters during the cruise phase. The first column represents the osculating ellipse as of October 1, 1965; the second column represents the osculating ellipse

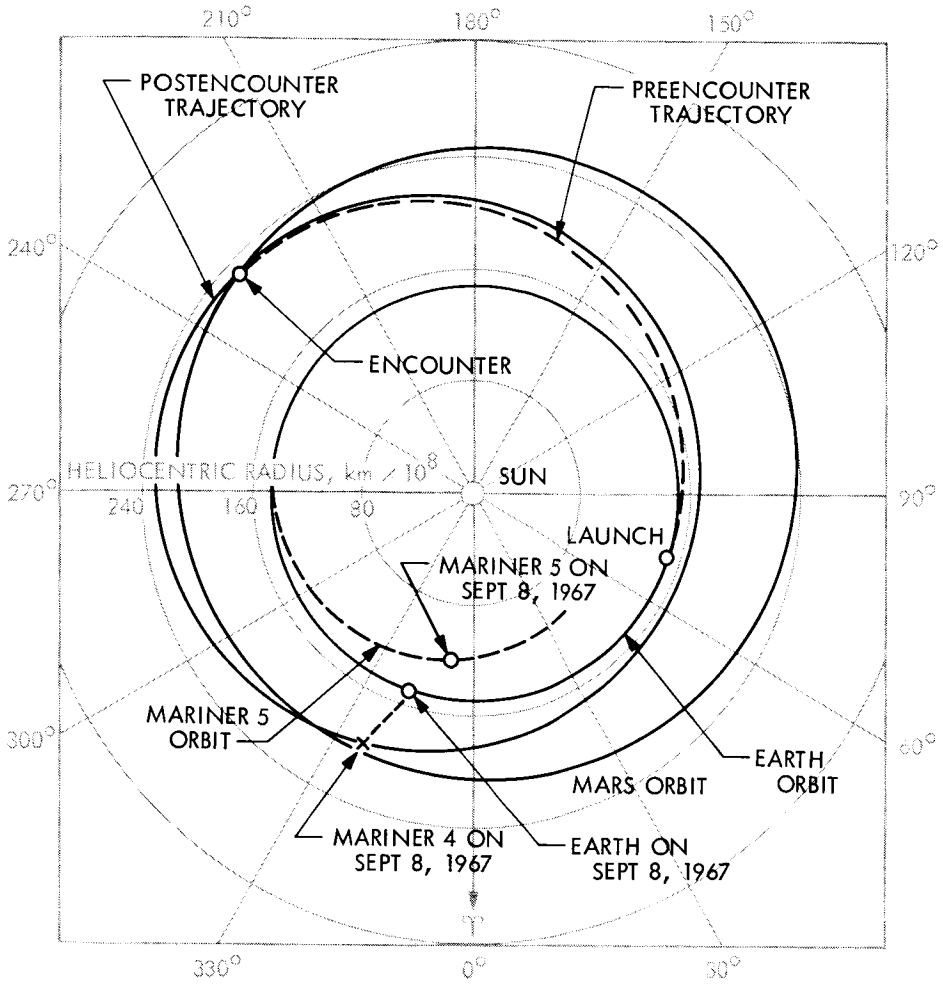

FIGURE 3–7.—Ecliptic view of preencounter and postencounter Mariner 4 trajectory, showing the Mariner 5 trajectory during the period of correlated solar measurements.

just before the maneuver. The changes are due to the perturbing effects of other planets in the solar system, principally the Earth/Moon system. The third column represents the osculating ellipse immediately after the maneuver; changes are due to the motor burn. The fourth column shows the osculating ellipse as of April 1968.

The first six rows in table 3–IV describe the orbit; the last three rows are derived quantities included to show the changes produced. Note that the ma-

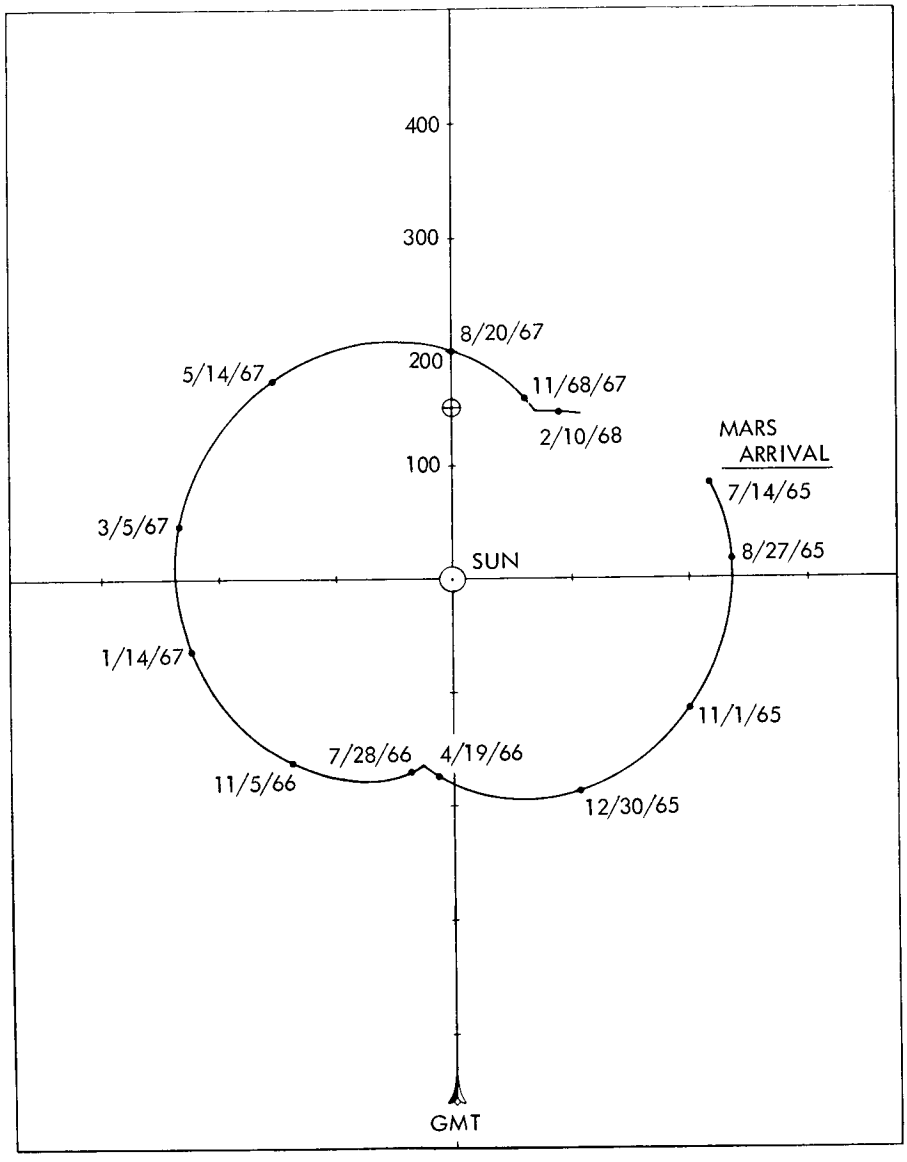

FIGURE 3–8.—Mariner 4 rotating coordinate system.

neuver was performed reasonably near perihelion (actually at a true anomaly of 306°) and in a manner that would reduce the heliocentric velocity. This decreased the orbital energy and resulted in only slight changes in perihelion distance and epoch of perihelion but in a large decrease in aphelion distance and in the orbital period.

Table 3–IV.—Mariner 4 orbital parameters

Parameter	End of primary mission (10/1/65)	Before second maneuver (10/26/67)	After second maneuver (10/26/67)	Present time (4/1/68)
Semimajor axis, km	200 589 970	200 606 710	199 574 900	199 591 220
Eccentricity	0.173 192 05	0.173 035 11	0.170 158 73	0.170 247 54
Inclination, deg	2.543 095 6	2.540 082 5	2.511 954 7	2.511 906 0
Longitude of ascending node, deg	226.753 47	226.759 81	227.143 98	227.147 41
Argument of perihelion, deg	200.632 94	200.647 98	201.439 72	201.435 10
Epoch of perihelion, GMT	11:56:55 (12/25/67)	14:21:13 (12/25/67)	22:15:25 (12/26/67)	22:08:34 (12/26/67)
Perihelion distance, km	165 849 380	165 894 710	165 615 490	165 611 300
Aphelion distance, km	235 330 550	235 318 710	233 534 310	233 571 130
Orbital period, days	567.115 34	567.186 33	562.819 49	562.888 50

Spacecraft attitude stabilization was accomplished by optical sensors that used the Sun and a bright star (nominally Canopus) as references. Cold-gas control jets were used to maintain the required orientation. Two independent cold-gas subsystems supplied redundancy; because they were very finely balanced, they were able to supply torques with negligible translational forces. Near the end of October 1967, one of the cold-gas subsystems was depleted. (The exact time can be only estimated because of the resolution in the telemetry subsystem.) To hasten the cold-gas depletion so that spacecraft stability could be observed while communications capability still existed, 54 commands, stepping the spacecraft back and forth 2° in roll, were sent within a 52-min period on November 14, 1967. Tracking data showed a doppler shift of −0.28 Hz, indicating a decrease in geocentric radial velocity of 1.83 cm/s. (Radial velocity measurement accuracy is about ±1.5 cm/s.) Calculations showed that this could be explained by the operation of only one of the cold-gas subsystems, indicating a point in time at which depletion was known to have occurred in the other cold-gas subsystem.

The second cold-gas subsystem was depleted on December 7, 1967, leaving the spacecraft rolling slowly in a counterclockwise direction. Roll torque, caused by solar pressure on the asymmetric Sun side of the spacecraft, was such that the roll rate was gradually decreased. On December 9, 1967, a series of micrometeorite impacts was observed and imparted a perturbing torque to the spacecraft. A high rate of impacts and disturbing torques continued through December 20, 1967. At this time, the spacecraft roll axis was nutating at a large angle (about 54°) from the sunline so that only 2 min of telemetry were recovered during the final tracking pass. The mission was officially terminated on that date, 1117 days after launch. It is speculated that the spacecraft began to tumble

shortly after, as additional disturbing torques were introduced by impacts. A survey of all known meteor streams indicated that the spacecraft position was extremely close to the intersection of two of them; the southern Taurids and the Leonids. Cosmic dust associated with one or both of these is regarded as responsible for the disturbing torques experienced.

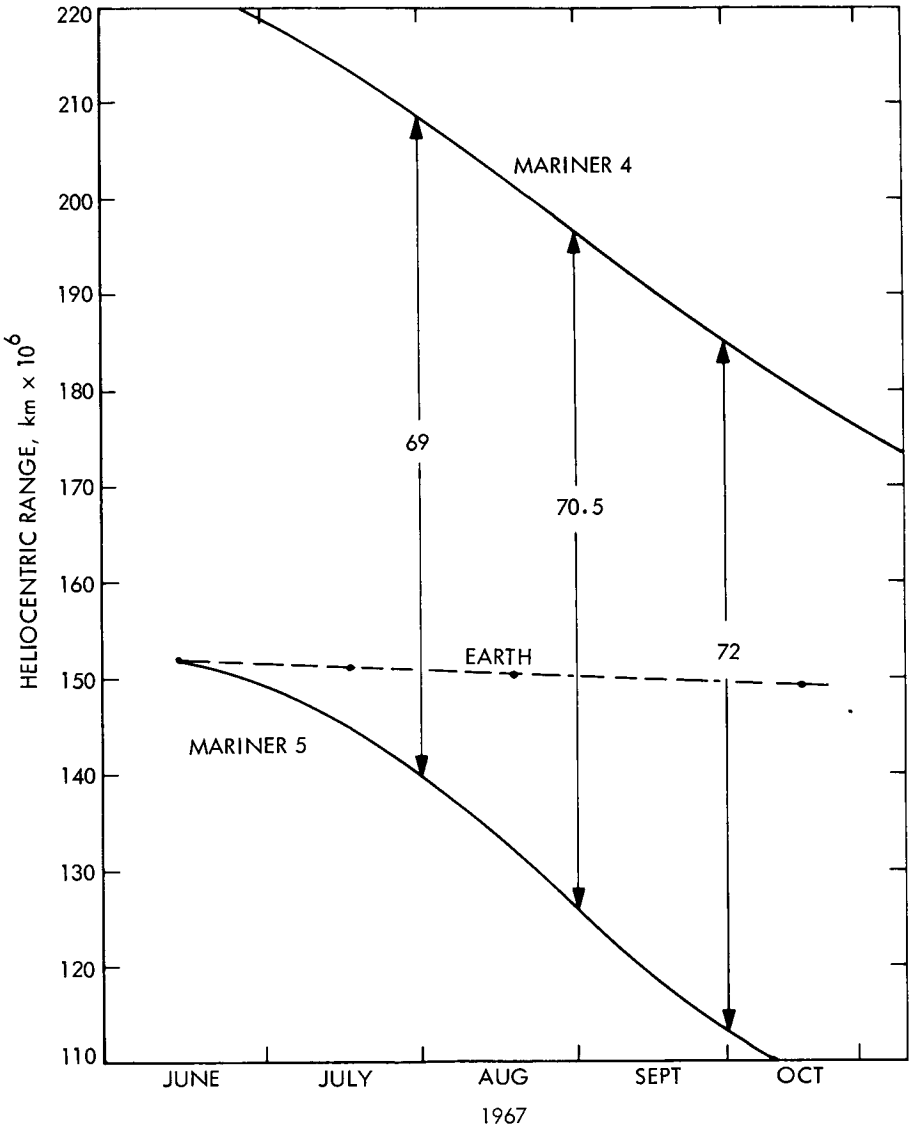

FIGURE 3–9.—Heliocentric ranges of Mariners 4 and 5 and the Earth from the Sun.

COMBINED OPERATIONS FOR MARINERS 4 AND 5

During the month of August 1967, a line from the Sun through Mariner 5, the Earth, and Mariner 4 was essentially radial. During the month of September 1967, this line appeared to lie along a spiral, close to the solar magnetic field lines. (These alinements are shown in fig. 2–41.) During this period, the two spacecraft maintained a separation of about 71 000 000 km. This relationship is shown in figure 3–9, which illustrates the distance of the Earth and the two spacecraft from the Sun. Figure 3–10 shows the angular separation between the two spacecraft as seen from the Earth; it may be seen that they were separated by nearly 180° during the period of interest. In August, during the radial configuration, nearly continuous coverage of both spacecraft was desired to correlate the effects of the relatively slow-moving solar wind. During this month, both spacecraft were above communications threshold for any of the standard 85-ft antennas at the tracking stations. In September, during the spiral-line period, the Mariner 5 antenna pattern was such that the 210-ft antenna at the Goldstone tracking station was required. As shown in figure 3–11, the Johannesburg station

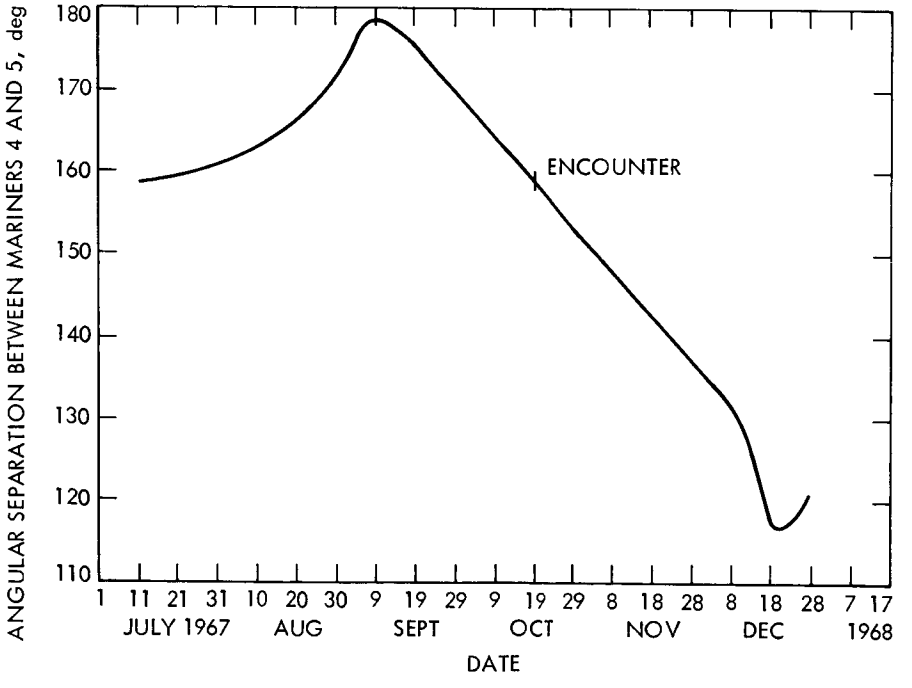

FIGURE 3–10.—Angular separation between Mariners 4 and 5 as seen from Earth.

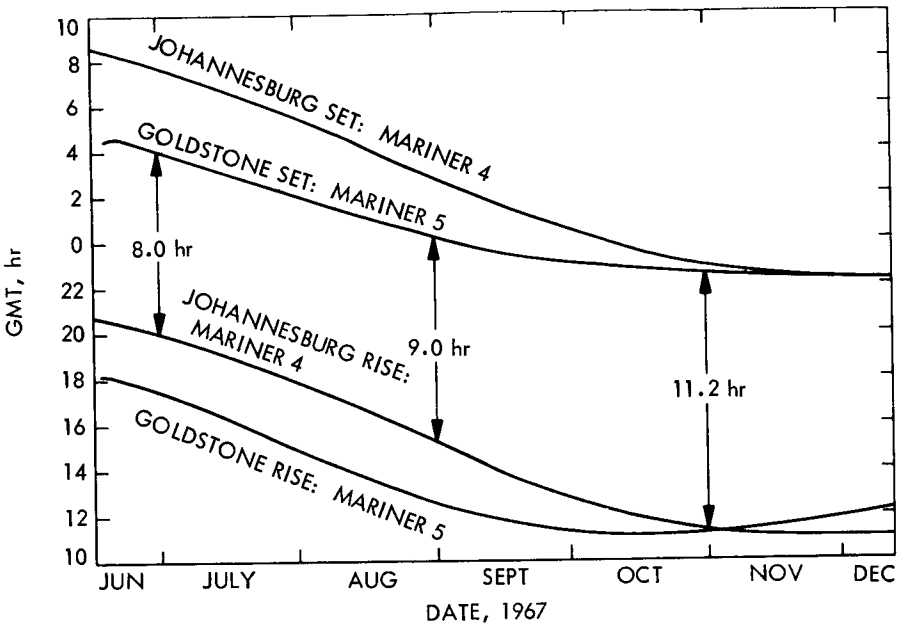

FIGURE 3–11.—View periods for Mariners 4 and 5.

view period for Mariner 4 was such that these two stations could provide simultaneous coverage of the two spacecraft for a minimum of 9 hr/day. Simultaneous observation was required to correlate the events associated with rapidly moving charged particles following the magnetic field lines. No major solar events were observed during these periods; however, there was a general increase in solar activity.

For about 3 months, the Earth, Mariner 4, and Mariner 5 permitted unique measurement patterns. Simultaneously, Pioneers 6 and 7 were accumulating data at approximately $\pm 90°$ from the Earth/Sun line, thus allowing local and widespread phenomena to be distinguished.

REFERENCES

3–1. CLARKE, V. C., JR.: Design of Lunar and Interplanetary Ascent Trajectories. Tech. Rept. 32–30, JPL, Pasadena, Calif., July 1960.

3–2. CLARKE, V. C., JR.; ROTH, R. Y.; BOLLMAN, W. E.; HAMILTON, T. W.; AND PFEIFFER, C. G.: Earth-Venus Trajectories, 1967. Tech. Memo 33–99, vol. 3, pt. B, JPL, Pasadena, Calif., July 1963.

3–3. KOHLHASE, C. E.: Launch-on-Time Analysis for Space Missions. Tech. Rept. 32–29, JPL, Pasadena, Calif., Aug. 1960.

3–4. ANDERSON, J. D.: Trajectory Determination From Observational Data. Sci. Technol. Ser., vol. 9, 1966, pp. 133–158.

3–5. WARNER, M. R.; AND NEAD, M. W.: SPODP–Single Precision Orbit Determination Program. Tech. Memo 33–204, JPL, Pasadena, Calif., Feb. 1965.

3–6. NOTON, A. R. M.; CUTTING, E.; AND BARNES, F. L.: Analysis of Radio-Command Midcourse Guidance. Tech. Rept. 32–28, JPL, Pasadena, Calif., Sept. 1960.

3–7. GORDON, H. J.: Functional Design of the Mariner Midcourse Maneuver Operations Program. Tech. Rept. 32–1139, JPL, Pasadena, Calif., July 1967.

CHAPTER 4

Spacecraft System

Mariner 5 was launched by an Atlas SLV–3/Agena D. To meet mission requirements for a flight to Venus, the Agena D second stage was modified to include a protective shroud and adaptor structure that encapsulated the spacecraft. Some changes were made in order to use the Agena D instrumentation for the output signal of the spacecraft data encoder and other diagnostic measurements of the flight environment.

MECHANICAL CONFIGURATION

Mariner 5 had the same basic configuration as that of Mariner 4 and retained many of the Mariner 4 hardware elements. (See fig. 4–1.) The areas that required modifications are summarized in the following paragraphs.

Antennas

To satisfy Earth-pointing requirements, the low- and high-gain antennas were oriented in the anti-Sun direction. The size of these antennas dictated that the under-shroud orientation could not differ appreciably from that of Mariner 4 without imposing serious design changes in the spacecraft and launch vehicle. These restrictions, plus the desirability of not articulating the antennas, made it necessary to locate the antennas physically by orienting the Mariner 5 in-flight attitude upside down compared with Mariner 4. Sun-oriented equipment such as Sun sensors, certain science experiments, and solar panels were then reoriented as required.

For improved coverage during occultation and after Venus encounter, the high-gain antenna support structure was redesigned to provide the correct pointing direction and mechanization to step change the pointing direction.

Solar Panels

Reversed sunline attitude of the spacecraft required that the solar panels be mounted on the same hinges with the celled surfaces reversed on the supporting spars. Maintaining the original length and locating the celled area away from the bus allowed the use of the remaining Mariner 4 attitude-control gas subsystem and much of the existing panel structure tooling and fixtures, and served

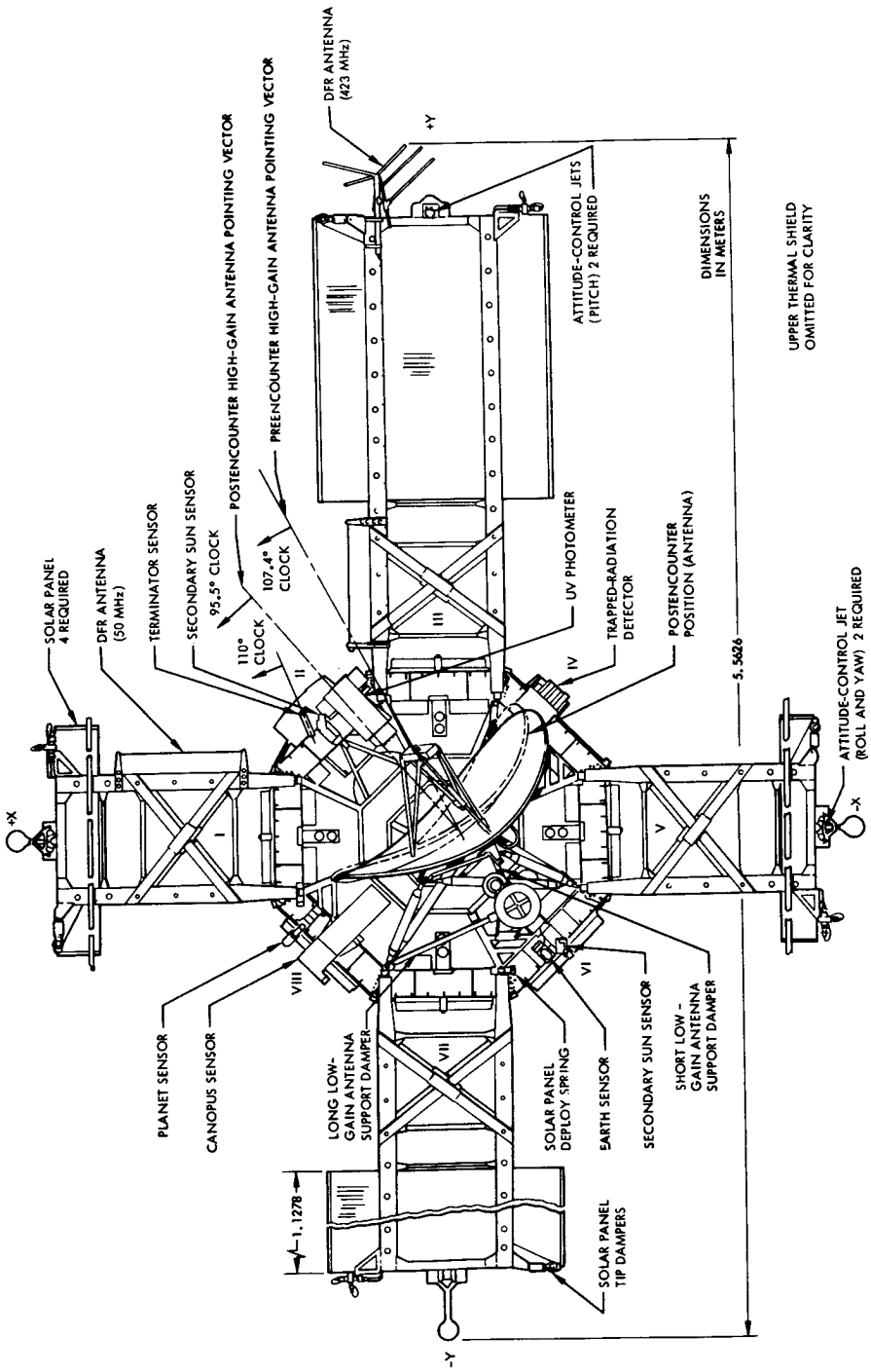

FIGURE 4–1.—Spacecraft mechanical configuration showing solar panels extended.

to provide needed thermal decoupling of the panels from the faces of the electronic bays. Temperature-control references were mounted on the gas-jet manifolds in bays I, V, and VII and attached at the interface previously occupied by the Mariner 4 solar vanes. Panel deployment springs and cruise dampers were unchanged. The boost latching and dampers were replaced with orthogonal pairs of dampers that tied the panels together at the tips. Four pinpullers, instead of the eight used on Mariner 4, were used to release the panels.

Attitude-Control Sensors

The reversed Sun attitude required that the primary and secondary Sun sensors be interchanged. Secondary sensors were mounted on the existing primary sensor pedestals, and the primary sensors were mounted on pedestals of sufficient height above the Sun-side thermal shield to obtain an unobstructed view. To provide an improved field of view, the Canopus tracker was also relocated from the bottom ring of bay VIII to a centerline location on the top ring of the same bay.

A modified Mariner 4 Earth sensor and planet terminator sensor were adapted with suitable bracketry to mount on the bay VI and bay II secondary Sun sensor pedestals, respectively. A new planet sensor was located on the upper ring in bay VIII.

Octagon Electronics Compartment

Mariner 5 used the same general equipment arrangement within the octagon as Mariner 4. The attitude-control (AC) gas bottles were the same as on Mariner 4; the postinjection propulsion subsystem was located in bay II. With the exception of bay III, the scientific equipment bay, the cabling and electronics arrangement in the other seven bays were the same as on Mariner 4.

Scientific Instrument Sensors and Antennas

The scientific instrument sensors were mounted on the spacecraft to satisfy their look-direction requirements. The helium magnetometer was mounted on the low-gain antenna, as on Mariner 4. The trapped-radiation detector was mounted in the same location as in Mariner 4, with the instrument reversed to provide the same orientation. The ultraviolet photometer was rigidly mounted on the top ring over bay II at a cone angle of 90° to allow a field of view compatible with the planet encounter geometry.

The dual-frequency receiver had two 49.8–MHz antennas mounted to the bay I and III solar panels and a 423.3–MHz antenna mounted at the outboard end of the bay III panel. Orientation and phasing provided peak gain in the direction of Earth at encounter. The solar-plasma probe was mounted on an

auxiliary support structure inboard of the lower ring on the Sun side of the spacecraft.

Temperature-Control Hardware

Shield philosophy and temperature-control louver hardware remained unchanged with the exception of the Sun-side thermal blanket. Concern over heat leaks at Venus intensities dictated a shield design with a minimum of penetrations for equipment mounted on the Sun side. The mechanization selected to satisfy these thermal requirements consisted of a deployable shade erected after launch-vehicle separation. All hardware that interfaced with the launch-vehicle adaptor was shielded from the solar input by this shade.

Weight Control

A weight-control program was initiated to provide all rigid-body mass parameters and consistent weight data from one official source. A mass goal of 250 kg was established; this included a 4.5-kg contingency allowance to cover expected discrepancies between the sum of the weights of the individual spacecraft subsystems and the total weight of the assembled spacecraft.

Flight-support spacecraft (M67–1) was weighed at JPL. The calculated mass proved to be 0.567 kg less than the measured value of 244.890 kg. The calculated mass was therefore adjusted to agree with the measured value to produce the most realistic values of calculated moments and products of inertia, because no actual measured values of moments and products of inertia were obtained.

Flight spacecraft (M67–2) was weighed at JPL. The final calculated mass of 245.080 kg was reduced by 0.517 kg to agree with the measured value, as explained in the previous paragraph. The spacecraft was weighed again at Cape Kennedy just before launch. In the interval between weighings, several modules were replaced with similar modules that weighed somewhat more. This exchange resulted in an increase of 0.259 kg in spacecraft mass for a total of 244.822 kg. The calculated mass was not readjusted to account for this small increase. A subsystem breakdown of the final calculated mass for the flight spacecraft is given in table 4–I.

Redundancy Techniques

Several methods of redundancy for increasing the probability of success at the system level were employed in the design of the Mariner 5 spacecraft; most of the redundancy was present in the Mariner 4 design. The new elements of redundancy are noted in table 4–II, which lists the command functions initiated by redundant signals. The following three redundancy techniques were used:

Table 4–I.—Final subsystem masses for flight spacecraft (M67–2)

Subsystem	Mass, kg	Subsystem	Mass, kg
Structure	30.999	Thermal control	7.824
Radio	21.550	Mechanical devices	2.477
Electronics	17.772	Tape recorder	8.777
Antennas	3.778	Science	22.394
Command	4.704	DFR antennas	.426
Power	59.366	Data automation subsystem (DAS)	6.622
Electronics	31.647	Trapped-radiation detector	1.193
Solar panels	27.719	Ion chamber	[a].109
CC&S	5.547	Plasma probe	3.121
Data encoder	10.614	Magnetometer	3.647
AC	25.846	Ultraviolet photometer	4.178
Pyrotechnics	3.869	DFR	3.098
Wiring	19.790		
Propulsion	20.806	Total	244.563

[a]This is the weight of a bracket on the low-gain antenna mast that could not be removed in converting the Mariner 4 design.

(1) *Block:* paralleling two identical units to achieve the desired function. This technique protects against a loss of function as a result of component or piece part failure. It is not effective if the failure is casual, e.g., a design failure or an overstress of all components due to an external environment.

(2) *Functional:* paralleling functionally identical units with different physical characteristics to achieve the desired function. This technique protects against causal failures, frequently at low cost in terms of weight, power, volume, and complexity. A prime objective of this redundancy form is to provide at least two separate and independent paths by which a critical function can be performed.

(3) *Alternate mode:* use of a nonprimary mode of operation to achieve the same or nearly the same level of performance as the primary mode. This technique frequently exploits equipment in the system for another purpose in order to keep the spacecraft operating in the event of some failure. Some increase in operational complexity or mission risk must be acceptable to use this technique.

SCIENCE SUBSYSTEM

The Mariner 5 science subsystem (see fig. 4–2) consisted of five scientific instruments and the DAS. All instruments were capable of making measure-

Table 4–II.—Command functions initiated by redundant signals

Command function	Redundancy type	Redundant command signals
Radiofrequency power up	Alternate mode	Removal of separation connector releases holding circuit. Turnoff of gyros releases holding circuit. Power up/down cycles with gyros.
Tape-recorder subsystem launch mode off	Alternate mode	Removal of separation connector activates count one end of tape (EOT) and stop logic. Gyro turnoff removes tape drive power.
CC&S relay hold off	Alternate mode	Removal of separation connector interrupts holding current. Gyros-off turns off holding current. Relays reset if gyros are turned on again.
AC on	Functional	Pyrotechnic arming switch. CC&S L–2 event. DC-V13, which also turns on Canopus sensor and sets maneuver inhibit logic.
Science on	Functional/ alternate mode	Power switched on at separation when holding current removed from power subsystem relay. DC–V2, which also switches encoder to data mode 2. DC–V25,[a] which also turns on terminator sensor and overrides science inhibit logic. Gyro turnoff before separation.
Solar-panel deployment	Functional	Separation-initiated timer. CC&S L–1 event.
Canopus sensor on	Functional	CC&S L–3. DC–V13, which also turns on AC and sets maneuver inhibit logic.
Switch data modes	Functional	To mode 1: AC signal at start of midcourse maneuver. DC–V1. To mode 2: AC signal at end of midcourse maneuver. DC–V2, which also turns on science. DAS signal at EOT recording phase. To mode 3:[a] DAS signal at receipt of MT–8 or DC–V24. To mode 4: CC&S MT–9. DC–V4.
Switch power amplifiers	Functional	DC–V7. Internal logic signal at receipt of CC&S CY–1 when power output is too low.
Battery charge off	Functional	DC–V28,[a] which toggles battery charger state, also turns off tape-recorder subsystem 2.4-kHz electronics. DC–V25, which also turns on the terminator sensor and tape-recorder electronics and overrides science inhibit logic.

Table 4–II.—Concluded

Command function	Redundancy type	Redundant command signals
		CC&S MT–7, which also turns on the terminator sensor and tape-recorder electronics.
		DC–V26, which also turns off science.
Switch data rates	Functional	CC&S MT–6 switches to 8⅓ bps.
		DC–V5 switch bit rates (toggle).
Canopus cone-angle update	Functional	CC&S MT–1, MT–2, MT–3, MT–4.
		DC–V17.
Antenna selection	Functional/ alternate mode	CC&S MT–5 switches to transmit via high-gain antenna and enables CY–1 logic.
		DC–V10 switches to transmit via high-gain antenna and to receive via low-gain antenna.
		DC–V11 switches to transmit and receive via high-gain antenna.
		DC–V12 switches to transmit and receive via low-gain antenna.
		Gyros-on switches to receive via low-gain antenna.
		2 consecutive CC&S CY–1 signals with the receiver continuously out of lock switches receiver to other antenna. Each subsequent consecutive CY–1 with receiver remaining out of lock switches receiver to other antenna.
Ranging off	Functional	CC&S CY–1.[a]
		DC–V9, which toggles ranging on/off.
Terminator sensor on/tape recorder on[a]	Functional	CC&S MT–7, which also turns off battery charger if on, and turns on science if off.
		DC–V25, which also overrides science inhibit logic and turns off battery charger if on.
Planet sensor on/establish DAS encounter mode.[a]	Functional	CC&S MT–8.
		DC–V24, which also enables or disables clock B on alternate commands.
Record sequence initiation	Functional	Planet sensor output.[a]
		DAS clock A signal.[a]
Antenna-pointing-angle change (APAC)[a]	Functional	Terminator sensor output.
		DAS clock A signal.
		DC–V22.
Record sequence stop	Functional	EOT signal interval to tape-recorder subsystem.
		Stop record signals from DAS initiated by clock A or clock B signal.[a]
Initiate playback	Functional	CC&S MT–9.
		DC–V4.
Switch tracks	Functional	EOT signal internal to tape-recorder subsystem.
		DC–V3.[a]
Switch exciters	Functional	Internal logic signal at receipt of CC&S CY–1 when exciter power output is too low.
		DC–V8.

[a] New elements of redundancy.

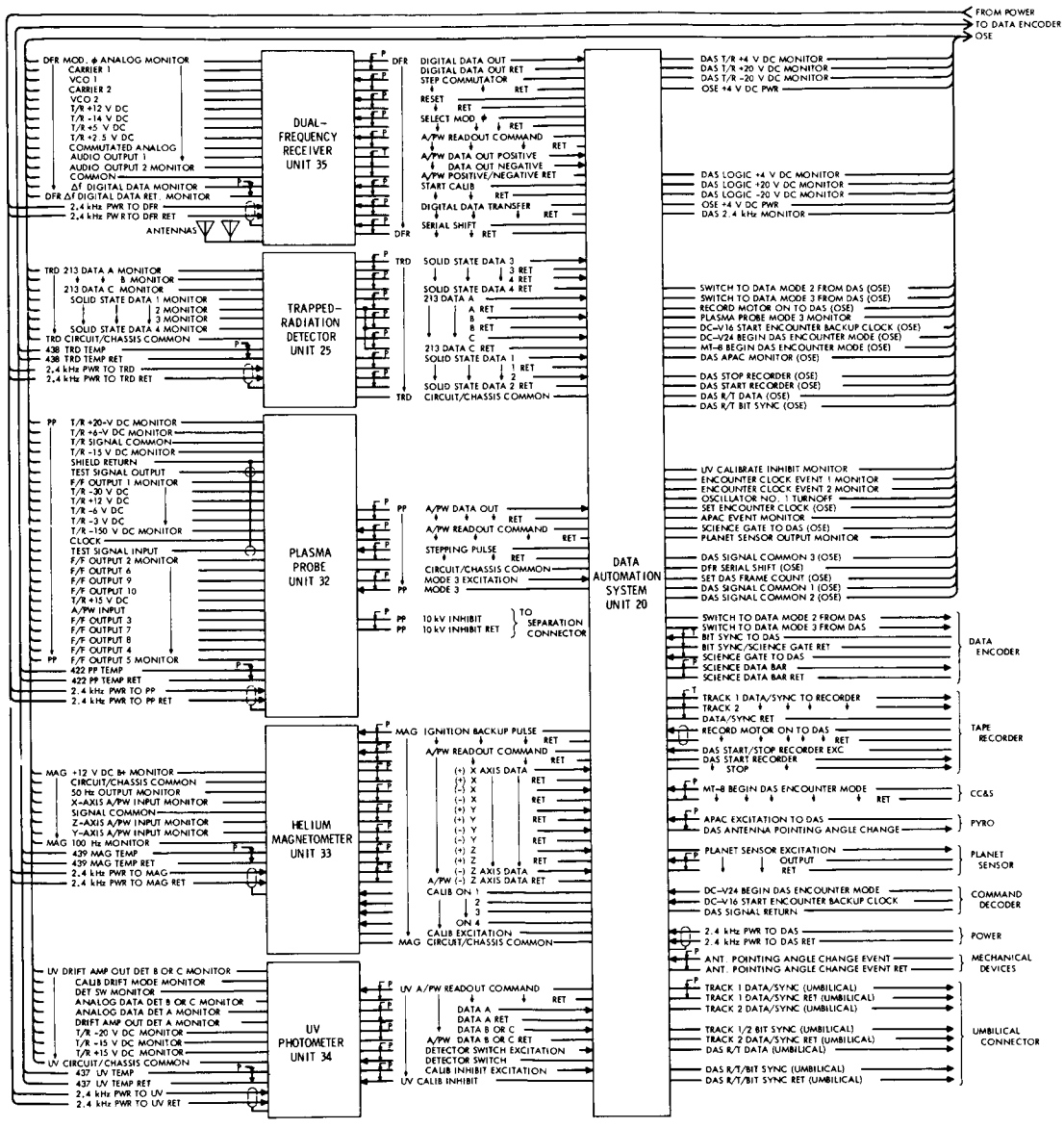

FIGURE 4–2.—Science subsystem block diagram.

ments during the cruise portion of the flight as well as during encounter. Three instruments carried on the Mariner 5 spacecraft were identical to those on Mariner 4, with the exception of the necessary modifications and design improvements required to meet the different environmental conditions.

Ultraviolet Photometer

The Mariner 5 ultraviolet photometer (fig. 4–3) was designed to measure atomic hydrogen resonance radiation at 121.6 nm and atomic oxygen resonance radiation at 130.4 nm in the upper atmosphere of Venus and in interplanetary space. The photometer was originally designed to measure a part of the hydrogen and oxygen density distribution in the vicinity of Mars (Mariner 4). One set of data readings, synchronized with the DAS, was telemetered during each frame at the rate of $8\frac{1}{3}$ bps. Once each eighth frame, ultraviolet photometer data were substituted by an alternately presented internal midscale calibration or a data zero-reference level.

The three ultraviolet sensors were identical 18-stage photomultiplier tubes with cesium iodide photocathodes and lithium fluoride windows. The photocathode material determined the wavelength-response rejection characteristics toward visible light; the window material determined the shorter wavelength-response cutoff point. Each solar blind phototube had a relatively flat spectral response from 105.0 to 190.0 nm. At the mercury line (253.7 nm), the output of

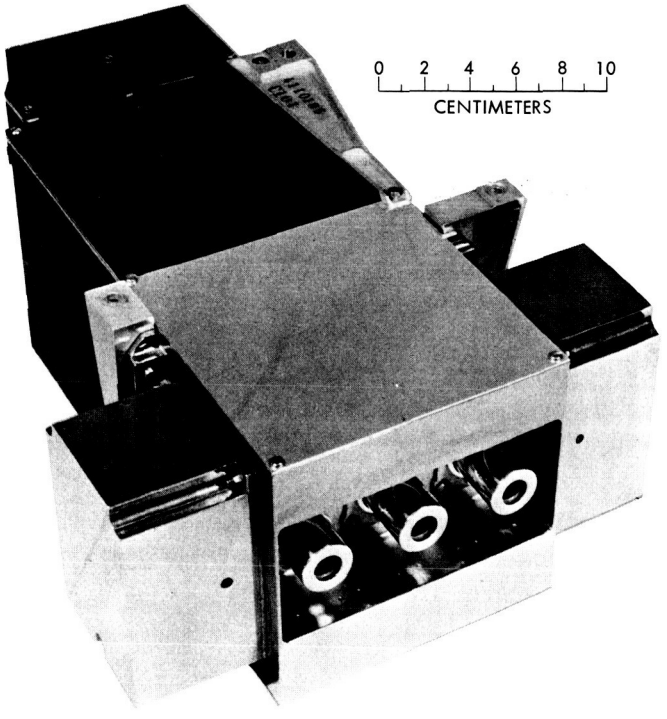

FIGURE 4–3.—Ultraviolet photometer.

each tube with equal source intensities was less than 1×10^{-3}, which is lower than the output at Lyman-alpha wavelength (121.6 nm).

Optical filters were used to modify the windows of detector tubes A and B, increasing the wavelength-response cutoff point. Tube C had no external filter. Tube A viewed through a cleaved calcium fluoride filter, resulting in a sensor bandpass of 125.0 to 190.0 nm. Tube B viewed through a cleaved barium fluoride filter, resulting in a sensor bandpass of 135.0 to 190.0 nm. The atomic hydrogen density measurement is proportional to the intensity difference between tubes A and C. The atomic oxygen density measurement is proportional to the intensity difference between tubes A and B.

A collimating aperture, in front of each phototube and filter, was used to restrict the field of view. Detectors A and B had a field of view of a cone with a half angle of 0.5° at an aperture output of half amplitude. Detector C had a field of view of a cone with a half angle of 1.25° at an aperture output of half amplitude; this view cone was measured with collimated light to have a half angle of 15° at an aperture output of 1×10^{-5}.

Apertures for detectors A and B were alternately stacked disks of 0.02- and 0.10-mm thickness and had chemically etched patterns of hexagonal holes, 0.51 mm between opposite edges and 0.71 mm between hole centers. The aperture for detector C consisted of alternately stacked disks of 0.08- and 0.30-mm thickness, which had a chemically etched pattern of hexagonal holes, 1.27 mm between opposite edges and 1.78 mm between hole centers. Each stack of aperture disks had a total length of 3 mm and had a light transmission of 60 percent.

Dynamic range of the ultraviolet photometer was such that it could measure a source brightness in the range from about 5×10^{12} to 10^{15} s^{-1} m^{-2}. Voltage across the phototube without optical excitation was about 3250 V (phototube output of about 10^{-13} nm), decreasing to about 2600 V with 10^3 times equivalent dark current excitation on the photocathodes.

Solar-Plasma Probe

The solar-plasma probe consisted of a sensor (fig. 4–4) facing the Sun mounted outside the spacecraft and a set of electronics located in three modules within the spacecraft. The sensor was a cuplike structure with an aperture through which the solar wind entered, a series of grids, and a segmented collector plate. All grids, with the exception of the modulation grid, were used to establish desired dc field conditions within the sensor. The modulator grid was the second grid from the input and, being always positive, caused incoming positive particles to experience a repelling field, because the first grid was maintained at instrument

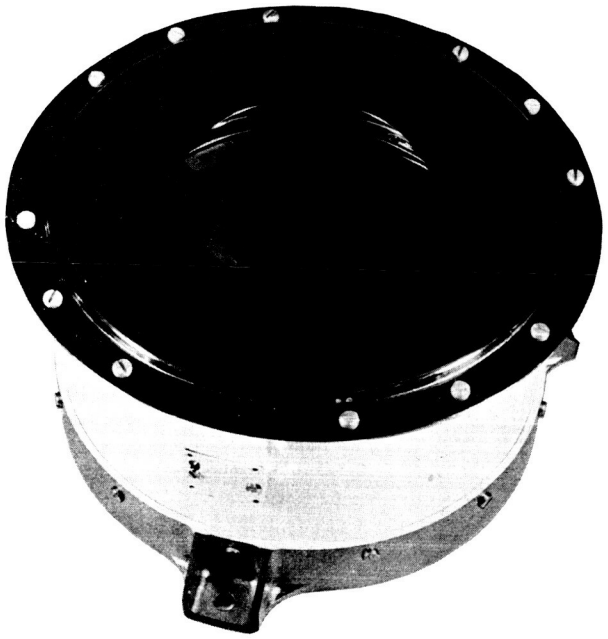

FIGURE 4–4.—Solar-plasma probe sensor.

ground potential. Only those positive particles with sufficient initial velocity to pass the modulator grid reached the collector plate, which allowed the sorting of particles, according to velocity, by the adjustment of modulator grid voltage.

The instrument measured particle concentration in 32 overlapping velocity ranges (otherwise known as energy windows). This was accomplished by driving the modulator grid with a 2-kHz square wave (added to a dc voltage), whose upper value was a voltage sufficient to repel all particles of velocities within the desired window and whose lower value passed all particles within the window. At the collector plate there was a modulated beam of those particles within the selected energy window. This was sensed as an ac current and processed by the electronics to result finally in an output related to the density of particles within the particular energy window. Nominal modulating voltage ranged from a square wave between 30 and 40 V to one between 7700 and 10000 V.

The instrument sequenced through the energy windows under the control of the DAS, which provided one stepping pulse each 2.1 s at the high data rate and each 8.4 s at the low data rate. At each step, the DAS provided an interrogate pulse, which read the density at that step.

Because the Mariner 5 spacecraft was essentially inverted with respect to Sun direction from the Mariner 4 spacecraft, it was necessary to relocate the

sensor with respect to the spacecraft. This made it necessary to relocate the plasma electronics within the spacecraft so that proximity to the sensor could be maintained. For scientific reasons, the plasma sensor look direction was directly along the sunline, rather than tilted at a 10° angle as on Mariner 4.

As the solar intensity for a Venus mission is much greater than for a Mars mission, thermal-control considerations were important to the plasma sensor. Analysis and testing showed that the plasma sensor could tolerate much higher temperatures than those to which it had previously been exposed and that the temperatures could be held within this range through the use of gold plating and thermal-control paint.

The manner in which the instrument sequenced through the energy windows was modified for Mariner 5. Two different sequencing modes were used: one for the cruise portion of the flight and the other only during encounter. The cruise-mode sequencing was similar to that used for Mariner 4, except that it was rearranged slightly. On Mariner 4, half of the energy windows were examined first with the collectors summed, then with independent collectors. The remaining half of the energy windows, interlacing the first, were examined in the same way. The Mariner 5 technique sampled all energy windows with the collectors summed, then all with separate collectors. In this way, there was less chance of solar-wind conditions changing appreciably between overlapping summed collector readings. The calibration part of the sequence, which consisted of two groups of eight readings on Mariner 4, consisted of one continuous set of 16 readings on Mariner 5. Because of this, a few of the steps in the calibration sequence were either redundant or unnecessary; e.g., the second noise measurement, the second temperature reading, the first reset zero, and both markers (retained in the measurement program to avoid modification of the calibration sequence logic).

Encounter-mode sequencing was designed to provide increased energy information at the expense of direction information by eliminating all separate collector sampling. A complete encounter-mode sequence consisted of two complete common collector samples, followed by an eight-step calibration sequence. This sequence was identical to the second half of the cruise-mode calibration sequence.

Some modifications were made to improve the basic performance and/or reliability of the instruments. With the exception of the failure of the high-voltage bleeder resistor, the Mariner 4 instrument operated well beyond its design lifetime. For Mariner 5, a series string of 15 resistors of a type known to be reliable replaced the high-voltage bleeder resistor.

Design of the grids and their supporting structure within the sensor was

changed to provide increased high-voltage safety margins. This design effort included both analytical and experimental work. A few minor changes, e.g., increasing the integration time constant to reduce the noise level, also were made to the electronics to obtain small improvements.

Helium Magnetometer

The helium magnetometer (fig. 4–5) was designed to measure the intensity and direction of magnetic fields that originate on the Sun and are convected out through the solar system by the solar wind. The magnetometer operated on the principle of detecting the amount of light absorption of the proper wavelength in a helium gas cell.

Modifications to the Mariner 4 unit changed the scale from ± 360 (0.7γ/DN) to ± 204.8 ($0.4\,\gamma$/DN) and increased the sweep vector to about 300γ. By increasing the sweep vector, the signal-to-noise ratio was significantly improved. (See table 4–III.)

Functionally, the operation of the Mariner 5 magnetometer was identical to

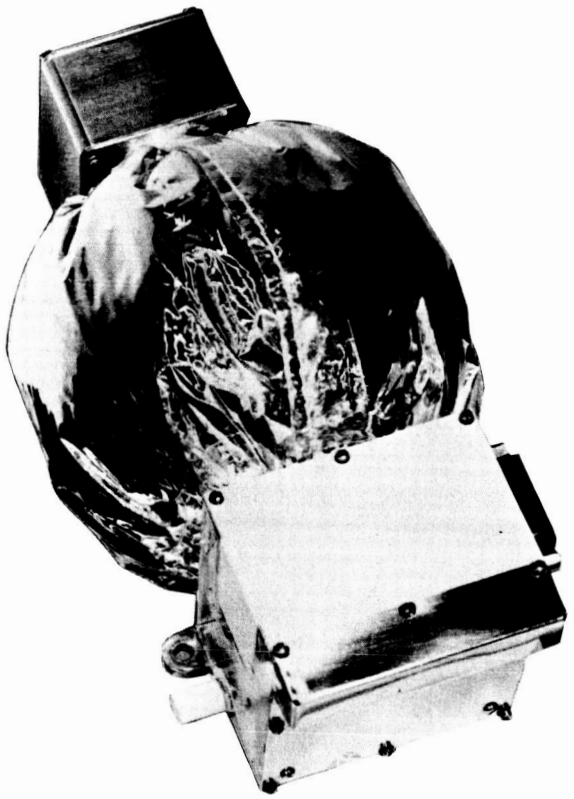

FIGURE 4–5.—Helium magnetometer.

Table 4–III.—Helium magnetometer noise and offset

Parameter	Axis		
	x	y	z
Noise (100 samples at about 1/s):			
Maximum deviation, γ	±0.15	±0.15	±0.12
Standard deviation, γ	±.090	±.100	±.074
Analog zero-offset:			
Instrument offset, γ	−0.4	−2.7	+0.8
Heater-current offset, γ	+.2	+.2	+.1
Total offset, γ	−.2	−2.5	+.9

that of Mariner 4. All parts, with the exception of the resistors needed to effect the scale and sweep vector changes, were identical. A sensor heater was required because of the inverted orientation of the spacecraft.

To provide better temperature control and stability, especially during the midcourse maneuver, a thermal "diaper" was added to the ball, and 21 cm^2 of JPL PV100 white paint was applied to the igniter end of the sensor.

Trapped-Radiation Detector

The volume of the chassis of the trapped-radiation detector on Mariner 5 was about 1350 cm^3, with a total weight of 1.211 kg. The power consumption was 450 MW or less, and the input voltage was 50 V, rms ±2 percent 2400 Hz (square wave). Turn-on and short-circuit current were limited to 200 percent of the normal operating current. Extra protection to the spacecraft power subsystem was provided by two 50-mA fuses in parallel (1/10 A) in the 2400-Hz input powerline. The input rise time requirements were 5±4 μs. Thermal requirements for the operating temperature limits of the entire unit were 253 to 323 K; nonoperating temperature limits were 240 to 333 K.

A four-channel, solid-state detector was substituted for the two-channel detector on Mariner 4. Electronic components for the additional two channels were packaged in modules and were mounted on the available space in the existing instrument. The look-angle axis of detector A was changed from 135° to 0° to the Sun-probe line of the spacecraft, and a beryllium foil was added. The full-aperture angle of the detector was decreased from 60° to 10° to prevent saturation during periods of high solar activity. Detector A was mounted on the instrument so that no part of the spacecraft would obscure its conical field of view.

Three Geiger-Mueller (GM) tubes were used for proton and electron detection. Detectors A, B, and C were EON-type 6213 GM end window counters, which measure the total number of charged particles passing through their sensitive volumes. The sensitive volume of each tube was shielded so that low-energy particles could enter only by passing through the window at the end of the tube. By allowing for omnidirectional flux of higher energy particles, a directional measurement of the low-energy particles could be made.

The window of detector A was covered by about 1.4 mg/cm^2 of mica. Detector A measured electrons greater than 95 keV and protons greater than 2.7 MeV. A beryllium (9.4-mg/cm^2) shield defined the energy threshold of the flux that entered the window. The window of detector B was covered by about 1.6 mg/cm^2 of mica. Detector B measured electrons greater than 45 keV and protons greater than 0.65 MeV. A sunshade was incorporated on the end of each tube housing to protect the detectors from exposure to direct sunlight during the cruise mode.

The window of detector C was covered with 1.6 mg/cm^2 of mica; an aluminum foil of about 20 mg/cm^2 was placed behind the aperture of the detector. This increased the threshold energy to 150 keV for electrons and 3.1 MeV for protons. The GM-counter outputs were shaped by means of saturating current amplifiers before being sent to the DAS.

The solid-state detector (detector D) was a totally depleted silicon surface-barrier diode with a thin (0.2 mg/cm^2 air equivalent for alpha particles) nickel foil for light shielding. The sensor was 31.7 μm thick, with a normal sensitive area of 12 mm^2. The detector, used as a four-channel (D1–D2–D3–D4) proton- and alpha-particle spectrometer, was capable of detecting protons and alpha particles in a high flux of electrons. Sensitivity to electrons was minimized by making the detector too thin to stop energetic electrons and by setting the discrimination level much higher than the expected electron energy loss. The aperture angle of detector D was increased from 60° to 80° to increase the total collecting area and thus raise the count for a given flux density. The configuration of all four detectors is shown in figure 4–6.

Dual-Frequency Receiver

The dual-frequency receiver was designed to measure radio propagation effects in the dual-frequency radio propagation experiment. The instrument measured the average interplanetary electron density and the characteristics of the atmosphere of Venus. Frequencies of 49.8 MHz and 423.3 MHz were transmitted from the 150-ft diameter antenna at Stanford University to the DFR on the spacecraft. The receiver measured the differential doppler frequency, differential group path, signal amplitudes, and frequencies.

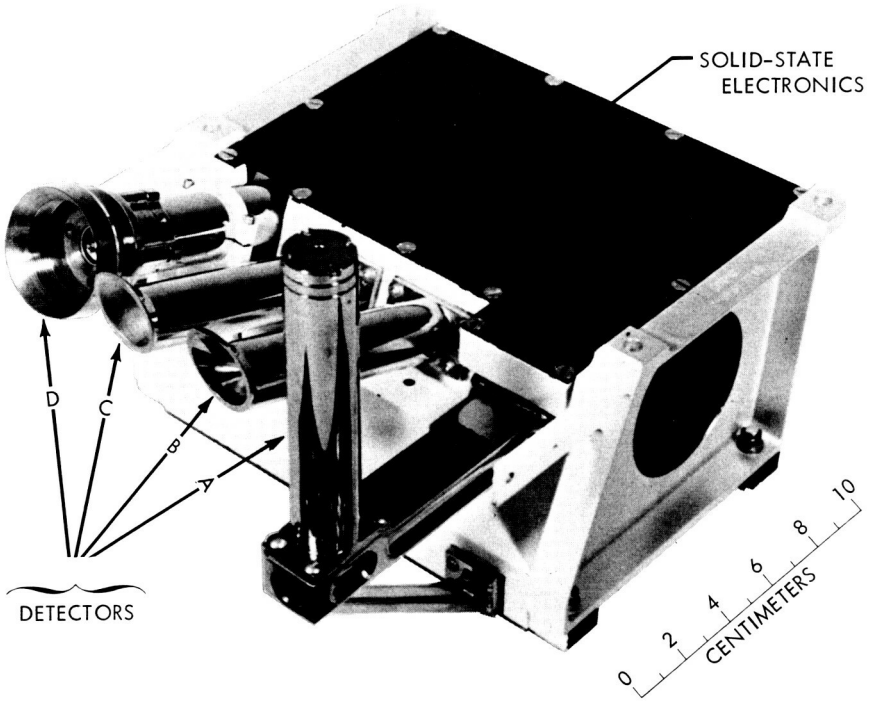

FIGURE 4–6.—Trapped-radiation instrument showing locations of the four detectors.

Two phase-locked loops with the same reference oscillator detected and tracked received frequencies. The phase of the radio waves passing through an ionized medium was advanced by an amount directly proportional to the integrated electron density and inversely proportional to the frequency. The 423.3 MHz was relatively unaffected by the amount of ionization in interplanetary space. Thus, the relative phase shift due to the propagation path was determined by comparing the output of the voltage-controlled oscillator (VCO) in each loop. The dispersive doppler frequency was determined by counting the VCO's beat cycles with the frequency-difference phase detector. The doppler frequency due to path-length change also was considered because it adds to this effect. The frequency was counted and read out as word 20 of the science data format.

The two rf carriers were phase modulated with an audiofrequency of either 8692 or 7692 Hz. The modulation envelope was delayed by the dispersive medium so that a measure of the differential group delay was obtained from the phase shift of the modulation. The modulation-phase detector contained two low-frequency, phase-locked loops. The low-frequency VCO outputs were phase

compared to obtain the modulation-phase analog voltage. This voltage was subcommutated with four other analog voltages and read out as word 21 in the science data format.

The VCO frequencies of the two carrier amplitudes were determined from the other subcommutated analog voltages. The analog voltage was changed to digital by an analog-to-pulsewidth converter in the DFR. Radio-propagation effects on the amplitude and VCO voltages during encounter were observed at a higher data rate, stored by the tape recorder, and played back after encounter.

The antenna was a quarter-wave stub with two reflector elements. The received signal was filtered by a low-pass filter that isolated the dual-frequency receiver from the *S*-band telemetry subsystem. The signal was amplified and converted to the intermediate frequency of 24.9 MHz. The intermediate-frequency amplifier had a crystal filter with a −3-dB bandwidth of 45 kHz and a −60-dB bandwidth of 500 kHz. The filter determined the bandwidth of the intermediate-frequency amplifier and was phase matched with an identical filter in the 49.8-MHz receiver to prevent introducing spurious phase shifts. A second mixer converted the signal to the second intermediate frequency of 7 MHz. This 7-MHz frequency was amplified, limited, and applied to the loop phase detectors. The audiofrequency component went to the modulation-phase comparator; the dc voltage was amplified in the loop amplifier and used to control the frequency of the local oscillator (i.e., the 31.9-MHz VCO).

The 49.8-MHz, phase-locked loop functioned in the same way as the 423.3-MHz loop. The 49.8-MHz antenna operated by shunt feeding the two adjacent spars of the bay I and III solar panels. This bandpass filter provided greater than −30-dB isolation from the *S*-band telemetry and intermediate amplifier frequencies. There was greater than −50-dB isolation from interfering signals at the image frequency. The 49.8-MHz signal was amplified and converted to the intermediate frequency of 24.9 MHz. The signal passed through the intermediate-frequency switch used to calibrate the receiver. When activated by a calibrated pulse from the DAS, the switch connected the 24.9-MHz intermediate-frequency signal from the 423.3-MHz first mixer to the input of the 49.8-MHz intermediate-frequency amplifier. Calibration occurred each 512 frames.

Data Automation Subsystem

Primary functions of the DAS were to control the operation of the scientific instruments, collect the data generated by the instrument, and format the data for transmission to Earth via the telemetry channel and/or storage on the spacecraft tape-recorder subsystem.

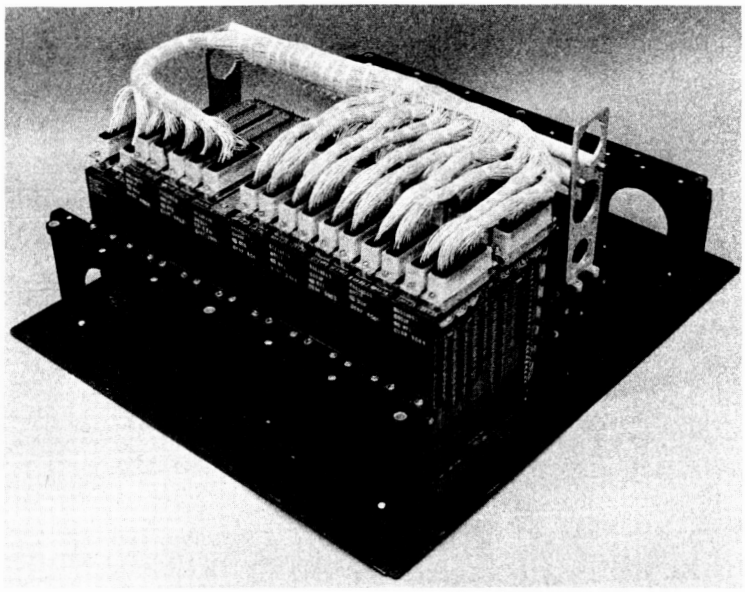

FIGURE 4–7.—Data automation subsystem.

Spacecraft requirements for the Mariner 5 DAS (fig. 4–7) were originally the same as those on Mariner 4. Data rates of $33\frac{1}{3}$ bps in the near-Earth environment and $8\frac{1}{3}$ bps in the near-Venus environment remained the same.

The Mariner 5 DAS consisted of five integrated circuit logic subassemblies (fig. 4–8), three discrete component subassemblies, one power converter subassembly, and 10 analog-to-pulsewidth converter modules located in the scientific instruments. A total of 1114 discrete components and 566 integrated circuits were packaged in a volume of 9260 cm^3 with a mass of 6.963 kg for a component density of 1.814×10^5 parts/m^3 and 2.413×10^2 parts/kg. Considering the specific discrete component equivalents for the integrated circuits used, the subsystem had 2.54×10^6 parts/m^3 and 3.37×10^3 parts/kg. The DAS internal harness, not included in these figures, contained 750 wires and had a mass of 2.041 kg.

Major outputs from the DAS consisted of data sampled from the various instruments and correctly formatted. The two destinations for the data from the DAS were the data encoder and the tape-recorder subsystem.

TELECOMMUNICATIONS

Dual-Frequency-Receiver Antenna Subsystem

The dual-frequency-receiver antenna subsystem on Mariner 5 was designed to receive 49.8- and 423.3-MHz signals transmitted from Earth to the spacecraft.

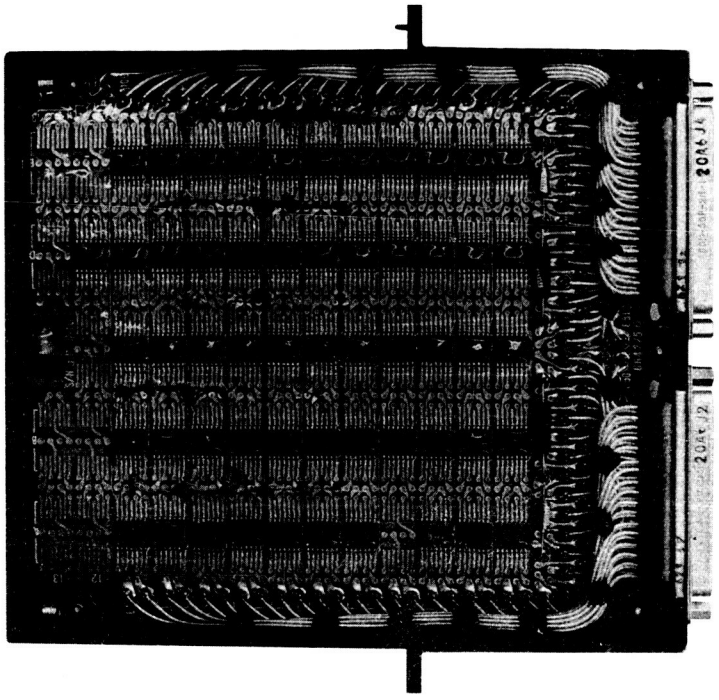

FIGURE 4–8.—Integrated-circuit logic subassembly.

The subsystem consisted of an antenna, transmission lines, and a filter for each frequency. Electrical parameters of the antennas are given in table 4–IV. The experiment was not included on Mariner 4.

Table 4–IV.—Dual-frequency-receiver antenna parameters

Parameter	49.8-MHz antenna	423.3-MHz antenna
Gain (in direction of Earth at encounter, relative to linear isotropic), dB	0.5	5.5
Voltage standing wave ratio (VSWR) (at center frequency)	1.15:1	1.13:1
Bandwidth (2:1 VSWR), MHz	0.95	21.0
Cabling insertion loss (from gain measurement point to receiver, including filters), dB	0.8	0.95
Polarization	(a)	(a)
Mutual coupling (minimum isolation between antenna terminals), dB:		
At 2297.6 MHz from high gain	57	62
At 2115.7 MHz from high gain	56	54
At 423.3 MHz from high gain	NA	79
At 49.8 MHz from high gain	70	NA

[a] Linear.

The 49.8-MHz antenna consisted of shunt feeding the two adjacent spars of the spacecraft bay I and III solar panels simultaneously through a power divider "tee" element. Unequal lengths of flexible coaxial cable connected the two arms of the "tee" element across the solar-panel hinges and along the adjacent spars to the feed units. Each feed unit was fixed relative to the respective solar panel; the antenna, therefore, was deployed with the panels. The 49.8-MHz antenna was connected to the DFR through two lengths of flexible coaxial cable and a bandpass filter.

Tuning of the antenna was determined by the relative coaxial line lengths connecting the "tee" to the feed units and by the adjustment of the series capacitor on the bay III solar-panel feed unit. The tuning was such that the maximum antenna gain at 49.8 MHz was most nearly in the direction of Earth at encounter. This direction was 1.040° and 102.5° in spacecraft cone and clock angle, respectively.

The 423.3-MHz antenna consisted of a stub radiator with two reflector elements over four ground-plane radials. The ground-plane radials were at 90° angles to each other and formed a 120° conic angle with the stub. A dielectric bar extended from the antenna mast to the two radials with reflector elements for mechanical support. The antenna was mounted on a mast at the tip of the bay III solar panel spar. The entire antenna assemblage remained in a fixed position relative to the solar panel and was deployed with the panel. The mast consisted of aluminum tubing with an inner conductor, which connected the coaxial cable center conductor to the antenna stub. The antenna was implemented so that the maximum gain at 423.3 MHz was most nearly in the direction of Earth at encounter. The received 423.3-MHz antenna signal was passed along the solar panel through a length of semirigid coaxial cable and across the panel hinge through a length of flexible coaxial cable. The received signal was then passed through a low-pass filter and another length of flexible cable to the DFR.

S-Band Antennas

The spacecraft antenna subsystem included a low-gain antenna, a high-gain antenna, and their transmission lines. The function of the low-gain antenna was to receive commands from Earth and to transmit telemetry to Earth during the first half of the mission and during midcourse maneuver. The Earth look angles were somewhat different than those for the Mariner 4 mission. Look angles for Venus continue away from the low-gain peak after encounter, while those at Mars reverse and retrace through the low-gain beam. The primary function of the high-gain antenna was to transmit telemetry to Earth during the last half of the transfer orbit and for a period after planetary encounter.

S-band antennas made for Mariner 4 were used for Mariner 5 with only minor changes. The low-gain antenna consisted of a right-hand circularly polarized mode launcher in the base of a 2.1-m-long, 0.10-m-diameter circular aluminum waveguide, with a crossed slot radiator and ground-plane system at the other end. The base of the antenna was mounted in a fixed position on the spacecraft structure with the waveguide extending parallel to the spacecraft $-Z$-axis.

The high-gain antenna consisted of a reflector and feed. The reflector was a sectoral paraboloid, with an elliptic aperture that had a major axis of 1.17 m and a minor axis of 0.53 m. The feed was an array of two turnstile elements driven in phase through a stripline power divider and matching network. The high-gain antenna was right-hand circularly polarized. Unlike Mariner 4, the Mariner 5 high-gain antenna had two separate positions.

Changes made to accommodate the two positions included the addition of a new mounting interface structure and revision of the coaxial cabling between the antenna and the electronic cases. A tuned mismatch was inserted in the low-gain antenna transmission line as a result of an interferometer problem on Mariner 4.

Command Subsystem

The Mariner 5 command subsystem was, with minor exceptions, identical in design to the Mariner 4 command subsystem, although some components differed from those used on Mariner 4. Some interface changes were required between the command subsystem and various users. The Mariner 5 command subsystem used a phase-shift-key modulation technique. Basically, this technique assigns the weight of a binary "one" or "zero" to a cosine wave. If a binary "one" is assigned to the cosine function, then a binary "zero" is represented by the negative cosine function (biphase modulation).

To distinguish a "one" from a "zero," the polarity of the received command data must be known. This was accomplished in the command detector, whose functions were to establish phase coherence between the ground command subsystem and the spacecraft command subsystem and, once coherence is established, to determine the phase of the transmitted data.

Once the phase of the incoming data channel was determined, the data were converted back to binary form. The detector transmitted the information to the decoder, whose primary purpose was to look at the data emanating from the detector and determine whether valid information was being transmitted. Once it was established that a valid command was being sent, the decoder de-

ciphered the incoming data and routed it to the subsystem requiring the command. All interfaces between the command subsystem and its users were isolated through either isolated pulse or isolated step switches.

Tape-Recorder Subsystem

The Mariner 5 tape-recorder subsystem was a modified Mariner 4 flight subsystem. The tape recorder on Mariner 4 was designed to record digital data from the DAS at a rate of 10700 bps and to play back synchronously through the data encoder at a rate of $8\frac{1}{3}$ bps. Operation of the tape-recorder subsystem consisted of 21 start/stop cycles to record the 21 video pictures.

Acceleration and deceleration of the tape recorder during the record stop/start periods were adjusted so that the amount of tape used in each stop/start cycle was 0.9 to 1.5 m. This amount of tape took from 1 hr to 1 hr and 40 min to play back, which was the amount of "dead" time required for engineering data between pictures during playback (telemetry mode 4).

The primary function of the Mariner 5 tape-recorder subsystem was to record science data in the vicinity of the planet Venus. The subsystem was required to record two data streams of digital data from the DAS, each at a rate of $66\frac{2}{3}$ bps, and to play back synchronously through the data encoder at a rate of $8\frac{1}{3}$ bps.

Flight Telemetry Subsystem

The flight telemetry subsystem was composed of the telemetry transducers (temperature and pressure) and the data encoder, whose functions were to accept spacecraft measurement data in the form of analog voltages and digital information; to convert the data into 7-bit non-return-to-zero words in serial form; to modulate a subcarrier with the binary data; and to add synchronization information, which forms a signal to be presented to the radio transmitter.

The Mariner 5 flight data encoder was essentially the same as the Mariner 4 flight data encoder; modifications were made in the following categories:

(1) *Mode 3 modification.* In operational mode 3, engineering words 105 and 106 were inserted into the data train instead of science data. These two words were inserted as words 46 and 47 after issuance of the science DAS.

(2) *Component part substitutions.* Part substitutions made for the Mariner 5 data encoder are given in table 4–V.

(3) *DAS interface modification.* The interface between the data encoder and the DAS was modified to provide bit synchronization with a rise time less than 5 μs. The rise time of the Mariner 4 data encoder bit synchro-

Table 4–V.—Component part substitutions

Mariner 4	Mariner 5 substitution
Kilvin 3 HR resistor	Ultronics 202 A resistor.
IRC MEA–T resistor	Angstrom J51 resistor.
2N2185 transistor	2N2946 transistor.
MM2N338 transistor	2N338 transistor.
VK 36/26 capacitors	VK 37/27 capacitors.

Table 4–VI.—Formats for 4 data modes

Mode	Format
1 (maneuvers)	Decks 100 and 110 are sampled sequentially.
2 (launch and cruise)	Decks 100 and 110 are sampled sequentially, with a 280-bit science DAS read-in occurring after deck 110.
3 (encounter)	Science DAS read-in with engineering words 105 and 106 inserted instead of science data as words 46 and 47 after issuance of the science gate pulse to the DAS.
4 (tape-recorder data playback)	Data storage read-in only, in presence of "data present" signal from recorder; otherwise, the data encoder reverts back to the mode 1 format.

nization pulse was about 400 μs, which was incompatible with the new integrated-circuit requirement of a rise time less than 10 μs.

The data encoder operated at two data rates ($8\frac{1}{3}$ and $33\frac{1}{3}$ bps) and four data modes; each data mode created a different data format. (See table 4–VI.)

Radio Subsystem

The Mariner 5 radio subsystem was basically the same as the Mariner 4 subsystem and provided for phase-coherent, two-way tracking; reception and demodulation of command signals; transmission of telemetry data; reception and transmission of a pseudorandom sequence for ranging information; and an rf signal for the occultation experiment.

Some modifications of the Mariner 4 subsystem were made to make it more compatible with Mariner-Venus 1967 project requirements. These changes involved the elimination of the probability of self-lock, thus providing ranging capability throughout the mission, and utilization of the interferometer effect to maintain two-way tracking and command capability at encounter without antenna design changes.

GUIDANCE AND CONTROL

Central Computer and Sequencer

Conversion of the Mariner 4 flight CC&S subsystem for use on Mariner 5 necessitated a basic redesign because of the differences in the spacecraft flight sequence between a mission to Mars and a mission to Venus.

Spacecraft Control

Spacecraft control for Mariner 5 consisted of the AC subsystem; the autopilot subsystem; and the planet, terminator, and Earth sensors. The concept and design of the AC and autopilot subsystems were unchanged from Mariner 4, but some modifications were necessary. The planet sensor was redesigned, and the terminator and Earth sensors were modifications of the Mariner 4 narrow-angle Mars gate and Earth detector, respectively.

The function of the Mariner 5 planet sensor was to detect the sunlit edge, or limb, of the planet Venus and to signal the DAS to begin the science encounter sequence. During planetary encounter, the terminator sensor detected the terminator of the planet and signaled the pyrotechnic subsystem to initiate the high-gain APAC. The Earth sensor served as a backup method of obtaining a reference in spacecraft roll coordinates for midcourse maneuver.

The function of the AC subsystem was to orient the spacecraft positionally to a preselected set of references and to maintain that orientation throughout the cruise and planetary encounter phases of the mission. The AC subsystem had the capability of repositioning the spacecraft to any given orientation in space during midcourse maneuver. This temporary spacecraft attitude was maintained during the firing of the postinjection propulsion subsystem by the autopilot subsystem. The AC subsystem then automatically could reorient the spacecraft to its references; the subsystem also had the capability of automatic reacquisition of these references if a loss of attitude control occurred.

The AC subsystem was functionally composed of the control electronics, the gyro-control assembly, the Canopus sensor, the cruise and acquisition Sun sensors, the Sun gate, and the gas subsystem. All units were used unchanged in form and modified only slightly from the Mariner 4 design.

The spacecraft attitude was controlled on three orthogonal axes: pitch, yaw, and roll. The spacecraft roll axis was (ideally) oriented along the spacecraft/Sun line, and AC pitch and yaw were referenced to the Sun. Deviation of the roll axis from the spacecraft/Sun line was sensed in pitch or yaw by a cruise Sun sensor; the error signal generated was fed to the control electronics. If the error signal exceeded a given level,[1] a device called a switching amplifier in the elec-

[1]Either positive or very active. The range, positive to negative, is termed the "deadband."

tronics activated a solenoid valve in the gas subsystem. Opening this valve permitted dry nitrogen gas at low pressure to flow through a small nozzle located at the end of a solar panel, thus applying torque to the spacecraft in a direction that tended to reduce the error signal. Sunline orientation was maintained in pitch and yaw within the deadband.

The spacecraft roll axis was referenced to the star Canopus. The Canopus sensor sensed angular deviation from the star and generated an error signal for roll control in the same way a Sun sensor does for pitch-and-yaw control. Spacecraft position was thus controlled by the Sun and Canopus sensors.

Spacecraft rate, in the cruise mode, was controlled by feeding back to the switching amplifier input a voltage proportional to the time a solenoid valve has been activated. This "derived rate" feedback permits the gyros in the gyro-control assembly to be turned off when all celestial references have been acquired. Before cruise-mode acquisition, these pitch, yaw, and roll rate gyros provided rate damping to the spacecraft, enabling rapid acquisition of the Sun and Canopus. If Sun or Canopus acquisition is lost, the gyros would be turned on to expedite the reacquisition process.

Acquisition Sun sensors augment the limited field of the cruise Sun sensors, providing a full 4π-sr field of view, enabling Sun acquisition regardless of the initial orientation of the spacecraft. When the roll axis of the spacecraft was within a cone of given half angle from the spacecraft/Sun line, the Sun gate disabled the acquisition Sun sensors and initiated (upon initial Sun acquisition only) the magnetometer-calibration constant spin rate about the roll axis or, subsequently, the Canopus-search constant spin rate about the roll axis.

Changes made to the Mariner 5 gas subsystem were removal of the solar vanes and internal modifications to the solenoid-operated gas valves for improved operation over an expanded temperature range.

The Mariner 5 planet sensor was designed to sense the illuminated limb of Venus and initiate the spacecraft encounter sequence. The planet sensor output (PSO), backed up by an onboard timer, provided a start signal about 1 hr before planet encounter.

The terminator sensor, an electrically modified, Mariner 4, narrow-angle Mars gate, was used as the primary signal source for activation of the high-gain APAC by providing a signal to the pyrotechnic subsystem when the Venus terminator entered its 1.5° by 2.5° field of view. The sensor was mounted on bay II of the spacecraft and had look angles of 110° clock and 110° cone. These angles were determined by the geometrical relationship between the spacecraft and the terminator at the desired time of APAC. These angles were analyzed

and adapted for the Mariner-Venus 1967 project to verify the dispersion of terminator sensor output times.

The Mariner 5 Earth sensor was used as a backup to the Canopus sensor. In the event of a Canopus sensor failure before the midcourse maneuver, the spacecraft would be placed in the roll inertial control mode and incrementally stepped until the Earth appeared in the field of view of the Earth sensor, or placed in the roll-search mode until the Earth appeared in the sensor's field of view. Spacecraft roll position would subsequently be controlled using the roll inertial control mode. The Earth, instead of Canopus, would then serve as the roll position reference, although the accuracy of the reference would be degraded to $\pm 1°$.

To convert the Mariner 4 Earth detector for the Mariner 5 Earth sensor, a set of baffles was designed to produce a field of view of 50° in cone angle and 3° in clock angle.

The four Mariner 5 solar panels were designed to meet the raw electrical power requirements and environmental extremes that would be experienced during the mission to Venus. Each solar panel had 1.01 m^2 of area available for solar-cell mounting. The cell layout on each solar panel consisted of a "folded" string that, after deployment, was maintained in a plane perpendicular to the z-axis of the spacecraft. Each panel was divided for improved reliability into three isolated electrical sections of two "folded" strings of 105 cells in series and 14 cells in parallel. The cells used in the design were 1- by 2-cm p-on-n (p-n) silicon solar cells interconnected into seven cell submodules with gold-plated kovar bus bars. The output of each electrical section of the array was shunt regulated by a string of six zener diodes to limit the voltage output to less than 50 V. Basically, the electrical design was the same as that used on Mariner 4. Similar materials, submodules, and techniques were incorporated wherever possible.

The following significant changes in the Mariner 5 power subsystem were made because of different power requirements:

(1) Maximum output power of the main 2.4-kHz inverter (4A15) was increased from 80 to 105 W.
(2) For Mariner 5, no 400-Hz, single-phase power was required.
(3) Raw power was required to keep the magnetometer warm.

The following changes were required to convert the Mariner 4 power-conditioning equipment:

(1) Addition of several small circuits to the power regulator (4A8).

(2) Extensive rework of the logic on the power distribution assembly (4A11).
(3) Addition of a sense lead to determine whether the battery charger (4A13) was on or off for the DC–V28 command toggling.
(4) Use of main 2.4-kHz inverters (4A15) for Mariner 4 as spares for the Mariner 5 maneuver 2.4-kHz inverters (4A16), and fabrication of new modules for the main inverter.
(5) Slight modification of maneuver 2.4-kHz inverter (4A16) so that no power could be applied to it if it were accidentally used as a main inverter.
(6) Removal of 400-Hz, single-phase inverter (4A17).

PROPULSION AND PYROTECHNICS

Propulsion Subsystem

The primary function of the propulsion subsystem was to remove or reduce launch-vehicle injection dispersion errors and to remove biased trajectories of the launch vehicle caused by contamination constraints. This function is fulfilled during the two possible spacecraft postinjection maneuvers during which the spacecraft is directed to turn to a prescribed position in space and impart a corrective impulse via the propulsion subsystem.

Design of the subsystem for Mariner 5 was identical to the Mariner 4 subsystem, except for a modification of the pyrotechnic cable harness. A liquid monopropellant, anhydrous hydrazine, was used as a propellant. Principal subsystem components consisted of a high-pressure gas reservoir, a pneumatic pressure regulator, a propellant tank and propellant bladder, an oxidizer ignition cartridge, and a rocket engine. The rocket engine contained a catalyst to accelerate the decomposition of hydrazine.

The design concept was predicated on the basis that it satisfy the long term space storage (maximum of 250 days) and multiple-start (maximum of two starts) requirements imposed by Mariner 4. The propulsion subsystem required no major changes to accomplish the mission to Venus.

To better fulfill the long term storage requirement, pressurization by nitrogen gas was used instead of gaseous helium, which was more prone to leakage. In a similar manner, welded and brazed tubing and fittings were used wherever possible to minimize the number of potential leak sources. Metal seals were used (where welding and brazing was impractical) in place of elastomeric seals to alleviate the effects of radiation, hard vacuum, and long term storage. Multiple-start capability was realized by the inclusion of "ganged" explosive valves with two parallel branches of normally closed (start) and normally open (shutoff)

valve groups in the nitrogen and fuel circuits and two normally closed valves in parallel in the oxidizer circuit. Individual oxidizer cartridges (13 cm^3 of nitrogen tetroxide, N_2O_4) were used for each of the two starts; both cartridges were pressurized by a common source.

Pyrotechnic Subsystem

Squib firing current was provided by the Mariner 5 pyrotechnic control assembly (PCA) for the following six spacecraft functions:

(1) Pin retraction of four solar-panel latches
(2) First start, postinjection propulsion subsystem (PIPS) motor
(3) First stop, PIPS motor
(4) Second start, PIPS motor
(5) Second stop, PIPS motor
(6) Pin retraction of one latch on the high-gain antenna

Firing units contained switching circuitry that, upon command, would inhibit firing of the propulsion subsystem, release the inhibit, and transfer the command to fire the propulsion subsystem to either of the two groups of on-off squibs.

The Mariner 4 PCA, in its original configuration, could have performed all required Mariner 5 pyrotechnic functions except for the added APAC. To accommodate that function, a circuit board was fabricated that included a solid-state switch that supplied excitation to the terminator sensor and DAS upon command. Because of the high-output impedance of the terminator sensor, an integrating circuit with unijunction transistor was provided to supply an adequate gate signal to trigger the antenna pinpuller squib firing circuit.

Redesigned solar-panel latches required that the pins in the pinpullers be lengthened. The surplus pinpullers were reworked.

To satisfy firing cable requirements for category A squibs, new cables with continuous no-gap circumferential shielding were made for the PIPS. It was necessary to provide new firing cables to pinpuller squibs because of the relocation of the solar-panel latches; these cables were fabricated with continuous circumferential shields.

ENGINEERING MECHANICS

Structure Subsystem

The basic spacecraft structure, which consisted of the primary octagon and internal secondary structure, was the same as the Mariner 4 structure. Modification of the Mariner 4 structure was limited to add-on bracketry for support of

relocated equipment. No structural resizing was required to accommodate packaging revisions.

The superstructure was developed from three of the Mariner 4 superstructure attach points on the octagon structure top ring and a triangular structure mounted on the back of the reflector on the high-gain antenna.

The existing Mariner 4 high-gain antenna reflector, feed-support truss, feed, and attached rf coaxial cable were used for Mariner 5. Trajectory geometry necessitated that the antenna be repositioned at planet encounter to maintain Earth communication. This required a new support structure on the rear of the reflector. The coaxial cable from the antenna feed to the rear of the dish remained unchanged from the Mariner 4 configuration; however, an additional section of hardline was formed along the back of the antenna to the vicinity of the deployment hinge. A new hardline cable was formed from the radio subsystem to the hinge area. The rf link was completed by a section (about 0.2 m long) of 6.4-mm-outside-diameter flexible coaxial cable across the hinge.

Design of the low-gain antenna was almost unchanged from the Mariner 4 configuration. Although the ion chamber was removed, the instrument mounting bracket, which was bonded to the mast, was not removed because of the possibility that bracket removal would distort the waveguide. The ion-chamber honeycomb shade was removed by peeling the foil face skin from the support bracket. The temperature-control paint was removed from the ground plane to minimize heat losses from the antenna.

The Mariner 5 solar panels were mounted to the same hinge points as the Mariner 4 panels, but were attached to each other at the tips during boost, rather than to the antenna-support structure as on Mariner 4. The panel's backbeam structure was the same as Mariner 4 except for two brackets that attach the tip dampers, and an added set of cross-braces about halfway up the backbeams. Retention of the Mariner 4 backbeam structure made possible the use of the Mariner 4 attitude-control gas subsystem, solar-panel cruise dampers, solar-panel deployment hardware, and solar-panel open switches without design modifications. The corrugated substrate aluminum foil thickness was increased to raise structural reliability and to reduce the possibility of handling damage. The corrugations were mounted on the side of the spars opposite that of the Mariner 4 panel because of the spacecraft's reversed solar orientation. This change resulted in some rerouting of panel power cabling and in moving the diode mounting surface to the side opposite that of the Mariner 4 panel's backbeam.

Universal and flexible characteristics of the Mariner 4 chassis and subchassis design demonstrated the soundness of the electronic packaging concept for Mari-

ner 5 applications. Minor modifications for Mariner 5 were made with little difficulty.

The propulsion subsystem support structure was the same basic design as Mariner 4. Existing flight spare frames were utilized and fitted with 1.5° tilt blocks to replace the 2° blocks optimum for thrust axis positioning on Mariner 4. Because the structure design originally allowed for tilt blocks from 0° to 4°, the slight change in angle did not constitute a design modification. No requalification testing was required.

Cabling Subsystem

General arrangement and design of the Mariner 5 cabling was essentially the same as that of Mariner 4. The subsystem included 12 subsystem harnesses, three ring harnesses, eight pyrotechnic cables, one midcourse motor harness, two AC gas subsystem cables, and four science signal cables. The following features differed from the Mariner 4 subsystem:

(1) Addition of a squib firing cable to each solar panel to accommodate the new tip latching. A connector interface, with the panel connector "hard mounted," was provided at the solar-panel hinge line.
(2) Deletion of pinpuller motion sensor harness; this function was performed by wiring in the gas subsystem harness.
(3) Removal of AC solar sail assemblies from the ends of the solar panels, allowing the use of identical gas subsystem harnesses and leaving unused wires for wiring of the motion sensors.
(4) Addition of temperature-control references (TCR's) to the ends of the panel. The TCR's were wired into the upper ring through circuitry, which was added to the solar-panel wiring for access to the telemetry channels formerly used by the absorptivity standard.
(5) Deletion of the scan platform and its cabling. The platform latch squib firing cable was rerouted to the top of the spacecraft to perform the APAC. The ultraviolet photometer was moved to the top of the spacecraft. Its functions were added to the upper science signal harness.
(6) Interchange of several items (Canopus sensor, Sun gate, and Sun sensors) from top to bottom on the spacecraft. The ring harness wiring was rerouted and lengthened accordingly.

A third major change was the addition of a 100-percent shield on all pyrotechnic firing lines to satisfy range safety requirements. Although most of the pyrotechnic firing cables were replaced because of new routing, the shield requirement added the task of developing a technique for incorporating this feature into

the design. A metal backshell, developed for this application during the Ranger project, was used. This backshell was used directly for the "singly" shielded cables at squib connectors and was modified for use at the larger connectors where several shields had to be connected.

Full-circle shielding of several individual shields was accomplished by distributing the shield strands around a single, large, crimped ferrule. This ferrule was then potted into the metal backshell; the shield strands were clamped to the shell with a locking nut.

Temperature-Control Subsystem

Major changes accommodated by the temperature-control subsystem were the reversal of the Sun-to-spacecraft orientation and the higher solar intensities encountered. Several thermal design changes were required; however, the basic approach and much of the hardware was unchanged.

The Mariner 5 temperature-control subsystem was functionally similar to that of Mariner 4. Some design changes were required, however, because of the nature of the mission and the upside-down configuration. The solar intensity for this mission was about 1.35 kW/m^2 at launch, 2.67 kW/m^2 at Venus encounter, and 4.16 kW/m^2 at perihelion. The Mariner 4 range was from 0.57 to 1.43 kW/m^2. This extreme variation in solar intensity made effective solar isolation an absolute requirement for spacecraft survival. Necessary improvements in isolation were provided by two design changes:

(1) Solar input to the bus by infrared radiation from the solar panels was reduced below Mariner 4 levels by eliminating 0.7 m of the inboard cell area of the panels.
(2) Efficiency of the solar shield was greatly improved by deploying the sunshade over known leaks.

The sunlight shield on Mariner 4 was covered with an outer layer of black Dacron cloth. The black cloth was replaced with a 25-μm Teflon blanket, aluminized on one side with the Teflon side out. The interior of the blanket was composed of multiple layers of aluminized Mylar. Shield area and seams were reduced by not covering the high-gain antenna superstructure. The blanket was secured to the spacecraft around the periphery by a nylon hook and pile closure strip. Mariner 4 used metal attach angles sewed to the blanket. The Mariner 5 attachment method reduced the installation time and the probability of damage during installation of the upper shield late in the spacecraft assembly sequence (after final systems test and solar-panel installation). The addition of the ultraviolet photometer and the relocation of the Canopus sensor and planet sensor to

the upper ring on the bus offset the simplification to the blanket by forcing the removal of the Mariner 4 cosmic dust detector and absorptivity standard and the relocation of the plasma probe.

Additional shields required for the Venus mission included four attitude-control jet shields, one trapped-radiation-detector helium shield, and one magnetometer shield. The polished aluminum side shields used were Mariner 4 spares with minor modifications.

The Mariner 5 sunshade was designed to reduce the solar input to the bus by shading the Agena/spacecraft interface hardware and spacecraft equipment outside the octagon periphery. Because of its configuration resulting from the necessary shadow pattern, the shade had to be retracted and stowed during the boost phase to clear the Agena adapter and separation hardware. When deployed by means of lanyards attached to the solar panels, the shade formed an octagonal-shaped awning about 0.25 m wide and 1.226 m^2 in total area on the periphery of the spacecraft on the sunlit side. A 0.10-m-diameter clearance hole was provided at bay IV to allow the X-ray tube of the trapped-radiation detector an unobstructed view of the Sun. Deployed, the shade extended about 0.08 m beyond the edge of the bus in bays I, III, V, and VII and 0.13 m for bays II, IV, VI, and VIII. Although not required by the equipment shadow pattern, the shade was symmetrical to balance solar pressure and to simplify construction.

The shade was constructed of a single sheet of 25-μm Teflon aluminized on one side. An octagonal tubular support ring was sewn to the shade at the inner perimeter; the outside edge of the shade was hemmed to contain the four support tubes and a Dacron cord around the outer perimeter. All shade edges were reinforced with glass-backed aluminum tape to prevent tearing. Eight pieces of nylon hook (15.9 by 25.4 mm) were sewn to the Teflon. When the shade was stowed, these eight pieces mated with nylon hook retainers that prevented the shade from slipping from its stowed position.

Deployment and support of the shade were provided by eight spiral-wound spring assemblies, located in pairs, that attached to shade-support tubes. Each spring assembly contained a nonmagnetic, high-strength steel spring mounted on an adjustable center arbor. Before installation on the spacecraft, the spring assemblies were preset to a torque of 0.112 ± 0.014 J. The torque increased to 0.224 J when the spring was rotated 150° to fix the shade in the stowed position. Each of the four shade-support tubes to which the shade was attached deployed independently by relaxation of a Dacron release lanyard attached through a series of eyelets to the solar panel in that bay. The sunshade was deployed at a rate limited by the solar-panel deployment. Full deployment of the shade occurred when the

solar panel was three-quarters deployed. The shirttail release occurred during the shade deployment, when the perimeter cord tightened between the two adjacent support tubes. Full deployment was achieved when the perimeter cord was taut.

Shields were required to shade each of the four attitude-control gas-jet assemblies mounted at the ends of the panels. Each shield consisted of a multilayer blanket that contained a clearance hole for the pitch or yaw jet exhausts, and a sheet-metal blanket support structure mounted by sandwiching it between the solar panel and the manifold.

The trapped-radiation detector shield, intended to shade the instrument detectors, was similar to the attitude-control jet shields. The shield-support structure was polished aluminum sheet metal with the multilayer thermal shield attached to the sunlit side. The support was attached directly to the instrument mounting brackets.

A multilayer shield with stable thermal properties was required to protect the coils of the helium magnetometer. The vacuum-deposited aluminum on the ball had degraded and exhibited variations in surface emittance that could not be tolerated in the temperature control of the instrument. The shield was constructed from nine layers of aluminized Mylar to cover the ball.

The same side shield used for Mariner 4, with thin-gage aluminum (0.41-mm) shield elements, was used on Mariner 5. These elements were bolted to the sides of the octagon as required. No new hardware was required because sufficient Mariner 4 side shields were available.

The only change to the louvers was the inclusion of sunshade lanyard guides. These guides were bonded to the upper and lower corners of the bimetal housing cover to prevent the lanyards from becoming entangled in the louvers. The Mariner 5 louvers were mounted in the same bays as those of Mariner 4.

The TCR's consisted of a 76-mm-diameter sensor area, a "tee" section fiberglass epoxy laminate support, and an aluminum bracket attached to the attitude-control gas-jet manifold at the tip of the solar panel. A standard flight transducer was mounted on the TCR bracket to measure the temperature of the attitude-control manifold.

TCR surfaces were coated to provide engineering information of significance to spacecraft thermal designers. Shaded sides of all assemblies were painted black for similar response to simulated background radiation and for handling and maintenance simplicity. The coatings selected for the sunlit surfaces were flat black epoxy, S–13 white (zinc oxide pigmented methyl silicone paint), and modified S–13 white (formulated with a treated zinc oxide for improved stability).

CHAPTER 5

Tracking and Data System

NASA's scientific investigations of space have been performed primarily by unmanned, automated spacecraft. Although these complex mechanisms are engineered to perform intricate tasks, they are dependent upon some amount of control from Earth to execute their missions, and the scientific information they collect must be received on Earth. A worldwide complex of facilities guides the spacecraft and gathers the data it provides. The ground-based command and communications system that provides this support is the Deep-Space Network (DSN).

One of several tracking facilities of the NASA Office of Tracking and Data Acquisition, the DSN is operated for NASA under the systems management and technical direction of JPL. It is composed of three main elements: the Deep-Space Instrumentation Facility (DSIF), a network of tracking stations encircling the globe; the Space Flight Operations Facility (SFOF), the JPL control center; and a ground communications system that connects all parts of the DSN by telephone, Teletype, and high-speed data lines.

The DSN performs four basic functions in support of each space-flight project:

(1) *Tracking:* includes locating the spacecraft; calculating its distance, velocity, and position; and following its course.

(2) *Data acquisition:* consists of recovering information from the spacecraft in the form of telemetry. This includes the recorded measurements of the condition of, and the scientific data obtained by, the spacecraft.

(3) *Command:* consists of transmitting signals to the spacecraft to guide it in its flight and to operate scientific and engineering equipment on board the spacecraft.

(4) *Control:* consists of making command decisions from a central facility and directing overall flight operations (including the tracking stations) during a mission.

Among DSN-supported missions were the Ranger photographic reconnaissance flights to the Moon, Surveyor, the previous Mariner missions to Venus and Mars, Mariners 6 and 8, Lunar Orbiter, Pioneer, and Apollo.

DEEP-SPACE INSTRUMENTATION FACILITY

The DSIF is a worldwide chain of tracking stations that provide radio contact with the spacecraft. To maintain continuous mission coverage, the stations are situated about 120° apart in longitude around the Earth, so that the spacecraft is always in the field of view of at least one of the stations.

The United States has made cooperative agreements with Australia, Spain, and the Republic of South Africa to establish and operate deep-space stations in those countries, and with the United Kingdom for a station at Ascension Island in the South Atlantic Ocean. Australia has two stations, one near Woomera village in South Australia and one in Tidbinbilla Valley near Canberra. Two other locations are at Robledo de Chavela and Cebreros, west of Madrid; the South African station is about 64 km north of the city of Johannesburg.

There are five deep-space stations in the United States, all operated by JPL. The Goldstone Deep-Space Communication Complex, situated in the high Mojave Desert of California, consists of four sites: Pioneer, Echo, Venus, and Mars. The fifth is located at NASA's Kennedy Space Center. All stations are located far enough from major population centers to minimize electrical and commercial radio and television interference.

Radio contact with the spacecraft begins on the launch pad at KSC, and is maintained throughout the mission as the spacecraft passes from within the range of one station into the field of view of another. KSC tracking facility monitors the spacecraft during and immediately after launch. Later in the launch trajectory, while the spacecraft is relatively low in altitude, the signal is picked up by the 9.1-m antenna at Ascension Island. Once the spacecraft is in orbit, the tracking stations' large antennas take over radio communications and follow the vehicle to its destination.

These antennas have highly concentrated signal power, highly sensitive receivers, and powerful transmitters that send a very strong signal. The stations operate at frequencies ranging from 2110 to 2120 MHz for transmitting commands from Earth to spacecraft, and from 2290 to 2300 MHz for receiving signals from the spacecraft.

The standard antenna used at the stations is a perforated-metal, paraboloidal (dish-shaped) reflector, 25.9 m in diameter. A diplexer allows both transmitter and receiver to be operated simultaneously at different frequencies on a single antenna.

A 210-ft-diameter antenna, located at the Mars site of the Goldstone station, stands as tall as a 21-story building and weighs about 7.3 million kg; it has more

than 6½ times the transmitting and receiving capacity of the standard 85-ft antenna.

All data collected at the stations during a mission are processed and recorded by ground instrumentation and data-handling equipment. Tracking data and portions of the spacecraft telemetry data are recorded on paper tape and transmitted by Teletype to SFOF in Pasadena, where spacecraft conditions are determined and orbit determinations and command decisions are made. Tracking and telemetry data received at the stations are recorded on magnetic tapes, which are airmailed to SFOF for data processing and analysis.

SPACE FLIGHT OPERATIONS FACILITY

It is essential that the great quantities of tracking, telemetry, and operational data produced during a single mission be processed quickly and reliably and made available to flight project personnel. The central control and data processing facility of DSN is SFOF, which contains some of the most advanced communications, data processing, and display systems available, with technical capabilities that meet the requirements of current space missions and anticipate those of future projects. JPL designed and supervised the construction of SFOF for NASA and is responsible for its management and operation.

From launch through mission completion, SFOF is the control center for tracking and data acquisition activities, as well as for spacecraft trajectory determinations, generation of commands transmitted to the spacecraft, and analysis and interpretation of the data received. Throughout the mission, the project manager, flight operations personnel, spacecraft engineers, and teams of scientists stationed at SFOF during the mission are kept constantly informed of the status of network operations and events and conditions aboard the spacecraft. Internal communications are maintained by means of telephones, voice intercom units, a public address system, closed-circuit television, and other types of visual displays.

SFOF, which accommodates a variety of missions, can be arranged to support and control activities for two concurrent flights, with monitoring capability over a third. SFOF is equipped for 24-hr/day operation, and provides maintenance labs and an emergency power supply to insure uninterrupted service.

Incoming spacecraft telemetry and tracking data from the stations are automatically routed to the SFOF data processing subsystem, where special telemetry-processing equipment and high-speed digital computers convert the data into readable form. Information from the data processing subsystem is distributed throughout SFOF by a network of electronic equipment that presents the information in printed or graphic form.

GROUND COMMUNICATIONS SYSTEM

The ground communications system provides voice and Teletype communications among the oversea tracking stations, Goldstone, Kennedy Space Center, and SFOF. A special microwave link is used between SFOF and Goldstone to transmit critical data during a mission. Oversea communications are transmitted by landlines, submarine cables, microwave relays, high-frequency radio circuits, and even communications satellites.

Although Teletype is the primary means of transmitting tracking and telemetry data from the stations to SFOF and for sending predictions and other data to the stations, voice circuits are used for transmission of other high-priority communications. Special communications-processing computer equipment at the stations formats all information sent to SFOF so that it is labeled and identified by date, time received, station, and spacecraft number.

REQUIREMENTS AND CONFIGURATIONS

Mariner 4 Support Requirements (Phase II)[1]

Project coverage

As a result of project requests, it was planned to use the advanced engineering facilities of DSN to track the Mariner 4 spacecraft to determine the presence or absence of the Mariner 4 signal. Reacquisition of the Mariner 4 signal began on a monthly basis starting November 1, 1965, initially from the Venus site (DSS 13) and later from the Mars site (DSS 14) at the Goldstone station. Spectrograms were made to provide measurements of total power received; power, rf carrier, and modulation sidebands; frequency separation between carrier and sidebands; and the received signal.

Internal coverage

A requirement existed for the measurement of two-way doppler data for the inherent accuracy project of the DSN. Two-way doppler data are useful in refining not only the elements of the Mariner 4 orbit, but also the astronomical unit and other astronomical constants. Measurements over a period of about 1 month were sufficient for these data. The accuracy of the measurement technique was limited by the extremely small signal-to-noise ratio, the residual errors in the

[1]The primary mission was the Mariner-Mars 1964 project and is thus referred to as phase I. During the period between the end of phase I and reacquisition, the spacecraft was released to DSN for tracking experiments. This period is defined as phase II. The Mariner 4 project covered and funded the operations performed after reacquisition on May 8, 1967, to the end of tracking on Dec. 20, 1967. This period is defined as phase III.

Mariner 4 ephemeris, and the tracking errors inherent in the closed-loop, ephemeris-tuned local oscillator.

Mariner 4 passed within 2° of the Sun at the end of March 1966. By measuring the additional frequency shift in the signal induced by the presence of electrons in the solar corona, an accurate two-way doppler measurement could be made, using the Mars site, to determine the electron-density profile of the solar corona. It also was possible, by spectrum measurements, to determine the inhomogeneity of the solar corona as a result of the broadening of the spectrolines transmitted from Mariner 4. The Mariner 4 *S*-band signal allowed significant advanced engineering work to be conducted at DSS 13 and 14 and also was used to verify the results from the 210-ft antenna at Goldstone.

Mariner 1967 Project[2] Requirements

The Mariner 1967 project indicated the degree of importance of support requirements by categorizing them as class I, II, or III. Class I requirements reflected the minimum essential needs to insure accomplishment of primary mission objectives; class II requirements defined the needs to accomplish all of the stated mission objectives; and class III requirements defined the ultimate in desired support and set an upper limit upon mission tracking and data acquisition requirements.

Requirements also were identified as occurring in either the near-Earth or deep-space phase. The near-Earth phase began with prelaunch activities and continued through launch to continuous DSIF view. At this point, the deep-space phase began and continued until the end of the mission. (The near-Earth phase applies only to Mariner 5; the deep-space phase applies to Mariners 4 and 5.)

Mariner 5: near-Earth phase

Originally, the project required that the tracking and data system (TDS) plan to support the launch period from June 12 to 27, 1967, with a launch window each day between 90° and 114°. This information generally defined the scope of operations within which other requirements would fall. When a long launch period and extensive launch windows are possible, TDS support of all tracking and data acquisition requirements becomes difficult because of the changing locations of events associated with class I requirements. To minimize TDS support difficulties, the project requested that TDS establish a configuration

[2]The Mariner 1967 project was the combination of the Mariner-Venus 1967 project and the Mariner 4 project (reacquisition). Tracking operations were conducted simultaneously for the two projects.

that would optimize support for the first 6 days rather than over the entire period, thereby avoiding degradation of support in the early days. June 12 and 13 were eliminated as possible launch dates. (To correlate class I requirements with the flight profile, see fig. 5–1.)

Metric requirements

Metric data (see tables 5–I and 5–II), obtained by tracking the Agena *C*-band beacon, were required for launch-vehicle performance evaluation, early spacecraft orbit determination, range safety, and acquisition information for the supporting AFETR, Manned Space Flight Network (MSFN), and DSIF stations.

Telemetry requirements

Launch-vehicle telemetry. (See table 5–III.) These data were required for overall launch-vehicle performance evaluation, monitoring and verification of important launch-vehicle events (mark events), and postflight analysis.

Spacecraft telemetry. (See table 5–IV.) Spacecraft telemetry provided an early indication of the status of the mission and, in the event of nonstandard spacecraft performance, would have been extremely vital. Spacecraft data were available via the spacecraft *S*-band link or via the Agena link until Agena/spacecraft separation.

Data-transmission requirements

Metric data. For range safety and acquisition information computation purposes, it was a class I requirement that metric data from the launch phase be transmitted in real time to user areas. Orbital metric data were desired in real time, but near-real time was acceptable.

Launch-vehicle telemetry data. The user required data from the launch phase to be transmitted and displayed in real time. Near-real-time playback and readouts were required of parts of the data received during the Earth-orbital phase.

Spacecraft telemetry data. The project required real or near-real-time transmission of spacecraft data received by the TDS stations during the four class I intervals.

Data processing requirements

Data processing tasks accommodated by the TDS during the near-Earth phase consisted primarily of trajectory computations and spacecraft engineering and science telemetry conversions. Data processing, in this sense, is defined as those requirements necessitating the use of central computer facilities. Because data processing is not an independent TDS function, the project stated a portion of the requirements in terms of equipment needs rather than data needs. For

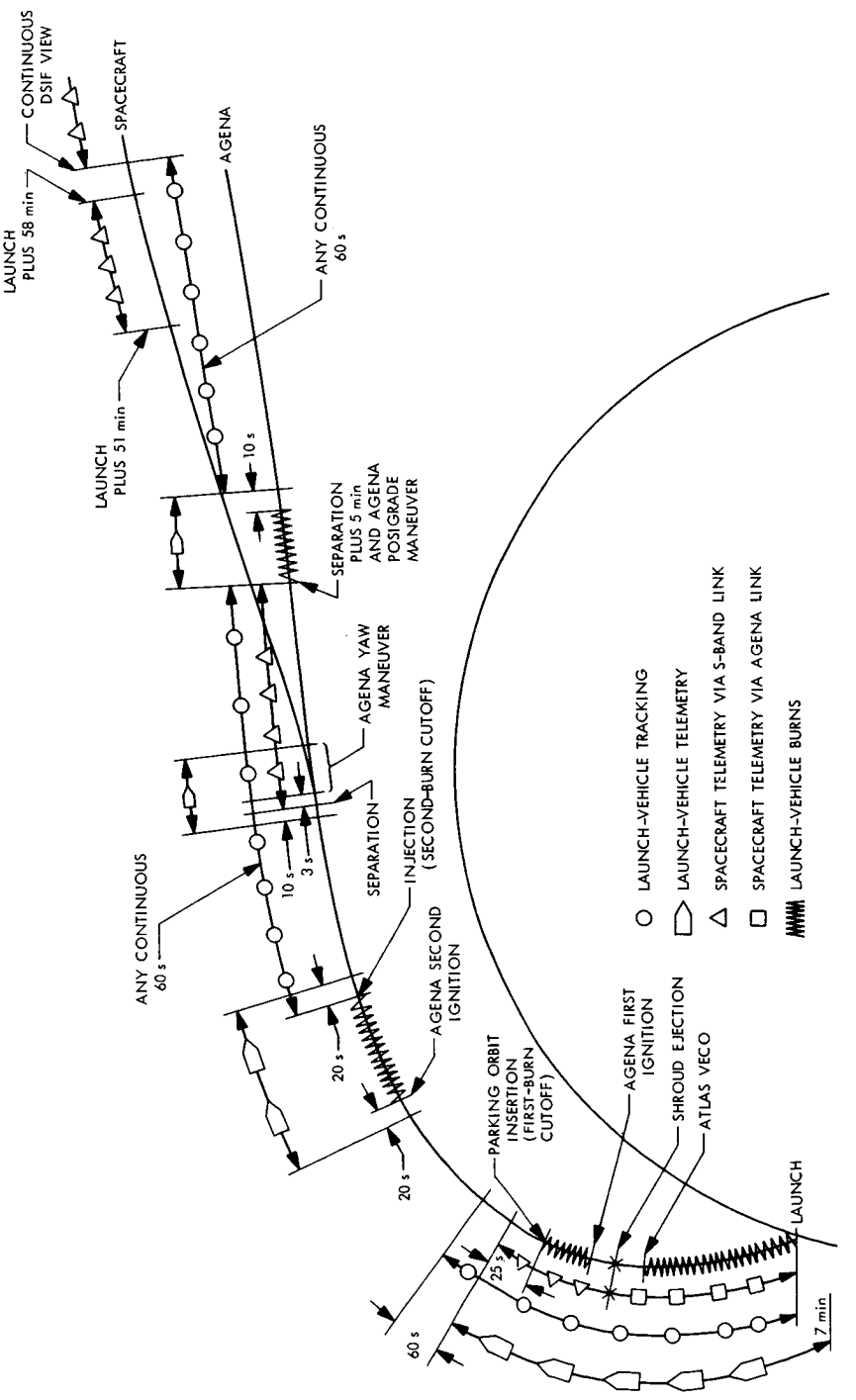

FIGURE 5–1.—Mariner 5 flight profile showing correlation with class I requirements.

Table 5–I.—Launch-vehicle metric requirements

Item	Data required[a]	Interval	Data points per second	Reduced data accuracy			Remarks
				Class I	Class II	Class III	
1	Position: X, Y, Z	0 to 1500 m	10	±7.6 m slant range	±7.6 cm or 0.25 percent slant range	±3.0 cm or 0.1 percent slant range	Items 1 through 6 needed to verify Agena position, altitude, and velocity at Atlas/Agena separation.
2	Velocity: V_x, V_y, V_z, and total **V**	0 to 1500 m	10	±1.5 m/s	±.3 m/s	.....	
3	Acceleration: Ax, Ay, Az, and total **A**	0 to 1500 m	10	±1.5 m/s^2	±.3 m/s^2	.....	
4	Position: X, Y, Z	1500 m to Atlas/Agena separation	10	±15 m	±3.0 m	±1.5 m	
5	Velocity: V_x, V_y, V_z, and total **V**	1500 m to Atlas/Agena separation	10	±6.1 m/s	±.9 m/s	±0.3 m/s	
6	Acceleration: A_x, A_y, A_z, and total **A**	1500 m to Atlas/Agena separation	10	±3.0 m/s^2	±0.9 m/s^2	±0.3 m/s^2	
7	Band 10 radar data: T, A, E, R	Launch to Atlas/Agena separation	10	±300 m	±150 m	.....	For postflight analysis of Atlas/Agena performance.
8	Position: X, Y, Z, H	Launch to Atlas/Agena separation	10	.....	±150 m	.....	
9	Velocity: V_x, V_y, V_z	Launch to Atlas/Agena separation	10	.....	Consistent with position data	.....	
10	Band 10 radar data: T, A, E, R	Atlas/Agena separation through first-burn cutoff plus 10 s	10	±300 m	±150 m	.....	For postflight analysis of Agena performance.

11	Position: X, Y, $\tilde{Z}$, H	Atlas/Agena separation through first-burn cutoff plus 10 s	10		±150 m		
12	Velocity: V_x, V_y, V_z	Atlas/Agena separation through first-burn cutoff plus 10 s	10		Consistent with position data		

T = time; A = azimuth; E = elevation; R = range.

[a] X = downrange; $Y = 90°$ counterclockwise from the positive x-axis; $\tilde{Z}$ = upward from the x, y-plane; and H = upward referenced to the Kaula NASA spheroid.

Table 5–II.—Near-Earth-orbital metric requirements

Class I	Class II	Class III
Liftoff to parking orbit insertion +50 s	Agena first-burn cutoff to first-burn cutoff +180 s	Same as class II plus Agena first-burn cutoff to Agena second-burn ignition, and during Agena second burn
Any continuous 60 s of coverage between Agena second-burn cutoff and Agena/spacecraft separation	Continuous tracking from transfer orbit injection to start of Agena retrothrust	
Any continuous 60 s of coverage after Agena retrothrust termination	Any continuous 120 s of coverage after Agena retrothrust termination and tracking to loss of signal	

Table 5–III.—Launch-vehicle telemetry data requirements

Class I	Class II	Class III
Atlas telemetry from L —120 s to Atlas/Agena separation Agena telemetry from L —120 s to parking orbit insertion +25 s Agena second ignition —20 s to Agena second cutoff +20 s Agena/spacecraft separation —10 s to Agena/spacecraft separation +10 s Start of Agena yaw maneuver to termination of posigrade thrust	From L —120 s to Agena/spacecraft separation and during Agena retrothrust	From launch through Agena retrothrust

Table 5–IV.—Telemetry data requirements during the Mariner 5 near-Earth phase

Link	Class I[a]	Class II	Class III
Agena	Prelaunch calibrations	Launch to Agena first-burn cutoff +25 s	From launch to Agena/spacecraft separation +5 s
	Launch to shroud ejection Shroud ejection to Agena first-burn cutoff +25 s[b]	Agena second-burn ignition —25 s to Agena/spacecraft separation +5 s	
Spacecraft	Prelaunch calibrations	Launch to Agena first-burn cutoff +25 s with real-time indication of increase in received S-band signal strength	From launch to continuous DSIF view +10 min[d]
	Shroud ejection to Agena first-burn cutoff plus 25 s[c]		
	Agena/spacecraft separation —10 s to separation +5 min	Second-burn ignition —25 s to continuous DSIF view +2 min[d]	
	From launch +51 min to launch +58 min		

[a] Class I requirements for data are contingent upon real- or near-real-time reception of these data at SFOF, as well as recording of the data. Near-real-time reception means, for Mariner 5, reception of the data as close to real time as feasible, and in any case, no later than 7 min after its occurrence.

[b] Receipt of these class I data via the S-band link is preferred.

[c] Detection of an increase in received S-band signal strength is the preferred method of confirming shroud ejection.

[d] Under the present ground rules, DSIF continuous view begins with DSS 42 (Tidbinbilla) rise.

the near-Earth phase, the project required dual 7044/7094 computers at SFOF for conversion of spacecraft data to engineering and science units and for processing tracking data to provide trajectory computations and predict information. Requirements for computations resulting from tracking data were as follows:

(1) *Parking orbit:* JPL elements, interrange vector (IRV), standard orbital parameter message (SOPM), *I*-matrix, and DSN predicts.
(2) *Preposigrade transfer orbit:* JPL elements, IRV, SOPM, *I*-matrix, DSN predicts, and planetary mapping.
(3) *Post-posigrade transfer orbit:* JPL elements, IRV, SOPM, *I*-matrix, DSN predicts, and planetary mapping.

These items were computed by the AFETR real-time computer subsystem and were required by the project at the SFOF and various supporting sites in near-real time.

Mariner 4 (phase II) and 5: deep-space phase

Project requirements on the TDS for tracking and data acquisition support during the deep-space phase were extensive, but not as complex as in the near-Earth phase, because fewer agencies (only the DSN and the supporting NASA communications system) were involved. Tracking and telemetry requirements are outlined in the following paragraphs.

Tracking requirements

Tracking data requirements existed whenever telemetry data were received. Special comments regarding these requirements are:

(1) Ranging data were required whenever two-way doppler data were received, on a best obtainable basis within present capability.
(2) Horizon-to-horizon coverage was required from all stations during the intervals from continuous DSIF view through first maneuver plus 2 days, from second maneuver through second maneuver plus 2 days, and from $E-12$ hr through $E+24$ hr.
(3) One short, two-way lockup once every 5 days was a mandatory requirement from $E-45$ days to the end of the mission. This requirement existed to inhibit the switch of the spacecraft receiver from the high- to the low-gain antenna on each second cyclic pulse ($66\frac{2}{3}$ hr between each cyclic pulse).

Telemetry requirements

Telemetry requirements for Mariners 4 and 5 are listed in table 5–V.

Table 5–V.—Instrumentation summary chart: near-Earth phase

Instrumentation	Location	Station ID	Agency	Use
Manual antenna, 4-ft diameter: receives at 2290 to 2300 MHz, transmits at 2110 to 2120 MHz.	DSIF: Cape Kennedy	DSS 71	DSN	DSN/spacecraft compatibility testing, spacecraft checkout, telemetry reception in early launch phase, and processing of AFETR telemetry in launch phase.
Telemetry antenna, 85-ft parbolic, auto track: receives at 130 to 2300 MHz; azimuth/elevation mount.	Tel 4: Cape Central TLM Site	TAA–2A	AFETR	AFETR/spacecraft compatibility.
	AFETR Station 3: GBI	TAA–2A	AFETR	Launch-vehicle and spacecraft telemetry.
Telemetry antenna, 30-ft parabolic, auto track: receives at 1000 to 2300 MHz; azimuth/elevation mount.	Cape Central telemetry site	TAA–3	AFETR	Spacecraft *S*-band telemetry coverage.
	AFETR Station 3: GBI	TAA–3	AFETR	
	AFETR Station 91: ANT	TAA–3	AFETR	
	AFETR Station 12: ASC	TAA–3	AFETR	
Telemetry antenna, 60-ft parabolic, auto track: receives at 130 to 1000 MHz; azimuth/elevation mount.	AFETR Station 1: CKAFS	TLM–18	AFETR	Launch-vehicle telemetry coverage.
	AFETR Station 91: ANT	TLM–18	AFETR	
	AFETR Station 12: ASC	TLM–18	AFETR	
Telemetry antenna, 60-ft parabolic reflector, auto track: receives at 130 to 420 MHz.	AFETR Station 13: PRE	AT–36	AFETR	Launch-vehicle telemetry coverage.
Telemetry antenna, log periodic, quad-conic array for very-high-frequency coverage, with 3-ft disk on array for *S*-band reception: receives at 130 to 2300 MHz.	AFETR Station 13: PRE (log periodic now serves as backup to larger *S*-band antenna at CKAFS, GBI, ANT, ASC, and on ships)	Log periodic (broad-band)	AFETR	Primarily *S*-band telemetry coverage, range limited.
Telemetry antenna, 12-ft parabolic, auto track: receives at 2200 to 2300 MHz.	AFETR range instrumentation ships (RIS): *Twin Falls* and *Coastal Crusader*	CTS	AFETR	*S*-band coverage in broad ocean areas.
Telemetry antenna, auto track, array of 16 dipoles on common ground plane: receives at 225 to 260 MHz.	AFETR range instrumentation ships (RIS): *Twin Falls* and *Coastal Crusader*	TAA–1	AFETR	Very-high-frequency telemetry coverage in broad ocean areas.
Antenna, 30-ft: operates at 2290 to 2300 MHz; azimuth/elevation mount.	DSIF: ASC	DSS 72	DSN	Spacecraft telemetry coverage.
Telemetry antenna, quad helix.	MSFN Stations: BDA and TAN	FPS–16	MSFN	Launch-vehicle telemetry coverage (very high frequency).
Telemetry antenna, tele-track, 18-dB gain: receives at 225 to 260 MHz.	MSFN Station: CRO	FPQ–6	MSFN	Launch-vehicle telemetry coverage.

Telemetry antenna, 30-ft parabolic: receives at 2275 to 2300 MHz (USB).	MSFN Station: CRO	USB-8	MSFN	Spacecraft telemetry coverage.
Tracking antenna, *C*-band monopulse radar, 29-ft Cassegrain reflector: transmits and receives at 5400 to 5900 MHz; peak power 2.5 MW.	Patrick Air Force Base	FPQ-6 (0.18)	AFETR	Radar tracking of launch-vehicle *C*-band beacon to provide for acquisition information and orbital calculations.
	Merritt Island	TPQ-18 (19.18)	AFETR	
	AFETR Station 3: GBI	TPQ-18 (3.18)	AFETR	
	AFETR Station 7: GTK	TPQ-18	AFETR	
	AFETR Station 91: ANT	FPQ-6 (91.18)	AFETR	
	AFETR Station 12: ASC	TPQ-18 (12.18)	AFETR	
	MSFN Station: BDA	FPQ-6	MSFN	
	MSFN Station: CRO	FPQ-6	MSFN	
Tracking antenna, *C*-band monopulse radar, 12-ft parabolic: transmits and receives at 5450 to 5825 MHz; peak power 1 MW.	Cape Kennedy	FPS-16 (1.16)	AFETR	Radar tracking of launch-vehicle *C*-band beacon to provide for acquisition information and orbital calculations.
	AFETR Station 3: GBI	FPS-16 (3.16)	AFETR	
	AFETR Station 12: ASC	FPS-16 (12.16)	AFETR	
	AFETR RIS: *Twin Falls*	FPS-16	AFETR	
	MSFN: BDA	FPS-16	MSFN	
	AFETR Station 13: PRE	FPS-16 (3.16)	AFETR	

TDS Configuration for Mariner 4 (Phase II)

DSS 13 and 14 were used, singly or in combination, depending upon the activity period, to track Mariner 4 during phase II.

The DSS 13 configuration was a direct result of the Mariner 4 planning effort. During midsummer of 1963, it was determined that if the spacecraft lost orientation during the mission, it would be necessary to have a transmitter power in excess of the 10-km power available at the operational stations. This led to the decision to provide a ground transmitter of 100-km continuous wave at DSS 13. A low-noise, narrow- and broad-band, flexible receiving capability was implemented for the Mariner 4 encounter, and was used again early in phase II. These characteristics were achieved by using planetary radar techniques and hardware, adapted to operational frequency and telemetry requirements. In addition to telemetry reception just before encounter and for some weeks after, it was planned to provide redundant recording of the received spectrum during the occultation period to be analyzed later in conjunction with a similar experiment conducted simultaneously at the Pioneer site. This spectrum-analysis capability also was used during phase II.

Construction of DSS 14 was completed during phase II. As capabilities became available, they were verified using the Mariner 4 spacecraft *S*-band telecommunications subsystem. The first operational use of DSS 14 was for the Mariner 4 solar occultation experiment in March 1966, for which the station receive capability, augmented with much R&D-type equipment, was used. In October 1966, the 20-kW transmitter was verified during Mariner 4 tracking.

Configuration for solar occultation experiment

Configurations used in phase II can be described best by explaining the solar occultation configuration, the most complex configuration, in detail and discussing the others as simplifications or modifications. A simplified block diagram of the solar occultation configuration is shown in figure 5–2.

The transmitter was located at DSS 13; the receiver was at DSS 14, over 23 km away. All reference frequencies of the system were derived from a primary rubidium frequency standard located at DSS 13. An output from this standard was transmitted to the other site via a microwave link, where it was used to phase-lock the remote site.

Also provided was a test link, which included a transponder similar to that on board Mariner 4 and which provided the same frequency multiplication of 240/221. With the necessary exception of certain parts of the ephemeris-tuned local oscillator, the test link was used to test the condition and stability of the

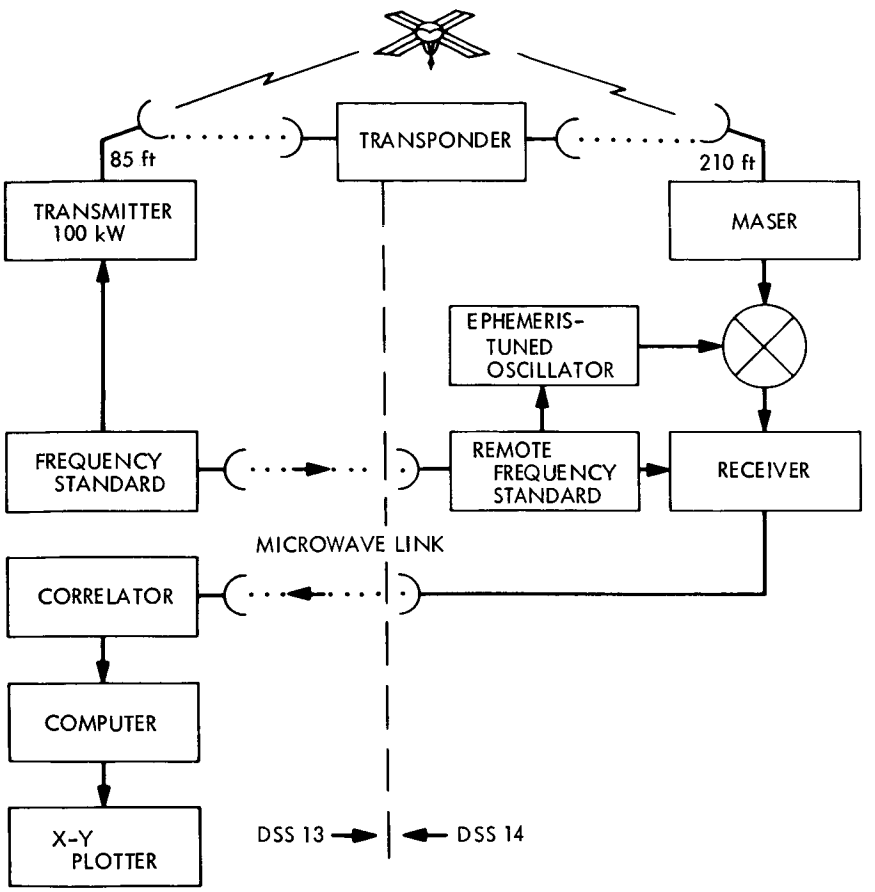

FIGURE 5–2.—Configuration for solar occultation experiment performed by Mariner 4 during phase II.

entire system. The transponder had no velocity; therefore, it produced no frequency shift. Because of this weak signal and the greatly increased noise, it was not possible to observe the signal in the normal manner. Instead, an adaptation of the techniques developed was used to study extremely weak planetary radar reflections. The basis of this technique was spectral analysis of the signal; i.e., the power spectrum of the received waveform was measured.

A signal, spectrally as pure as possible when transmitted to the spacecraft, arrived spectrally impure at the spacecraft receiver, because it passed through the solar corona. The Mariner 4 transponder maintained phase lock with the signal and retransmitted it toward Earth. The transponder interacted with the

signal and probably modified its spectrum. The return trip through the corona again increased the spectral width of the signal. Because the receiver was automatically tuned under ephemeris control, the returning signal was too weak to track with phase-lock methods. The ephemerides were calculated in advance from the known orbits of Mariner 4 and the Earth. Automatic tuning served to remove the doppler shift from the signal so that it was centered in the passband of the receiver.

The power spectrum of the signal was obtained by autocorrelation. The autocorrelation function of the signal was measured with a small special-purpose computer, and the Fourier transform was performed on a general-purpose machine, yielding the power spectrum. The spectrograms, which constitute all the data of this experiment, were displayed on an x–y plotter by the computer.

Configuration for DSS 13 carrier acquisition

In the period between the end of phase I and the solar occultation experiment, DSS 13 performed monthly one-way tracks and one two-way command track. The configuration for these tracks included the transmitter and spectrum-analysis equipment described, plus an existing R&D receiver used extensively in lunar and planetary radar research.

Configuration for DSS 14 after solar occultation

Because DSS 13 was down for maintenance and upgrading of equipment from April 15 to June 1, 1966, DSS 14 conducted one-way tracks during this period, continuing to use the spectrum-analysis equipment. Starting in June 1966, after the solar occultation experiment and followup work, DSS 14 was able to make recordings of Mariner 4 spacecraft telemetry data; therefore, an analog tape recorder was added to the solar occultation configuration. Between June and September, DSS 14 conducted three one-way tracks and four two-way tracks, using the DSS 14/13 solar occultation configuration. On October 4, 13, and 18, 1966, the DSS 14 20-kW transmitter was checked out, followed by DSS 14 one-way passes when telemetry recordings were made. Between March 10 and May 7, 1967, DSS 14 was down for antenna modifications. It returned to operation on May 8, 1967, using the Mariner 5 configuration through the end of phase II.

TDS Configuration for Mariner 5: Near-Earth Phase

For the Mariner 5 near-Earth-phase support, the TDS was composed of selected resources of DSN, AFETR, MSFN, and the NASA communications network (NASCOM). Within each agency, specific supporting stations were:

AFETR:

Station 1: Cape Kennedy/Patrick AFB, Florida (CKAFS)
Station 3: Grand Bahama Island (GBI)
Station 7: Grand Turk Island (GTK)
Station 91: Antigua Island (ANT)
Station 12: Ascension Island (ASC)
Station 13: Pretoria, South Africa (PRE)
Range instrumentation ship, Twin Falls (TF): South Atlantic
Range instrumentation ship, Coastal Crusader: South Atlantic

MSFN:

Bermuda Island Station (BDA)
MSFN/USB Site: Ascension Island
Tananarive site: Malagasy (TAN)
Carnarvon site: Australia (CRO)
Goddard Space Flight Center, Maryland

NASCOM:

Worldwide facilities of NASCOM provided communications between supporting agencies

JPL/ETR:

Building AO at Cape Kennedy, Fla.

DSIF:

DSS 71: Cape Kennedy, Fla.
DSS 72: Ascension Island
DSS 51: Johannesburg, South Africa
SFOF: Pasadena, Calif.

Based on trajectory data and on requirements, the TDS agencies selected the appropriate metric and telemetry data acquisition instrumentation from resources available at the supporting sites. Special attention was given to class I intervals to insure a high probability of providing the required coverage. Table 5-V briefly describes these instruments, their locations, common identifying nomenclature, agency, and general use.

Configuration for metric data

The AFETR was the primary agency responsible for meeting metric requirements during the launch and near-Earth orbital phases. The addition of MSFN radar instrumentation to that of the AFETR provided the required coverage with a reasonable degree of redundancy. AFETR and MSFN radars tracked the Agena *C*-band beacon in meeting both launch-vehicle and spacecraft metric

requirements. AFETR optical tracking instruments provided the most accurate source of metric data from liftoff to 1500-m altitude.

Figure 5–3 shows the configuration of the metric subsystem and data flow that supported the early launch phase. Optical instruments, as well as *C*-band radars, are shown. Figure 5-4 shows the metric configuration for supporting the near-Earth orbital phase. AFETR and MSFN *C*-band radars are shown, and the flow and format of the data are described.

Configuration for telemetry data

Launch-vehicle telemetry data, like metric data, required standard and well-exercised TDS configuration support. Some difficulty was encountered by the TDS in establishing a configuration that would meet the spacecraft telemetry coverage and transmission requirements.

Launch-vehicle telemetry data

AFETR, MSFN, and KSC/ULO instrumentation, as listed in table 5–V, was selected to provide the required coverage. The antennas at Cape Kennedy (AFETR Station 1), Grand Bahama Island (AFETR Station 3), Antigua Island (AFETR Station 91), and Bermuda provided for continuous reception of launch-vehicle telemetry from launch through injection and into the parking orbit, as required. Very-high-frequency antennas at Ascension Island (AFETR Station 12), Pretoria (AFETR Station 13), Tananarive (MSFN station), and on range instrumentation ships (RIS) provided coverage for most of the class I interval associated with Agena second burn. Depending upon the launch azimuth and day, plans specified that AFETR telemetry aircraft would be used to cover small gaps expected along the more northern launch azimuths. The same resources were applied to the class I intervals associated with Agena/spacecraft separation and Agena posigrade maneuver.

Launch-vehicle telemetry data received directly by personnel at Building AE, KSC, were displayed in the vehicle analysis area. Data received by AFETR Tel 4 antennas were also displayed, as well as remoted to Hangar E and Building AF. AFETR Station 91 transmitted launch-vehicle data to Cape user areas in real time via the submarine cable, subject to bandwidth limitations of the sub-cable (40 kHz). Data on channels with greater bandwidths were transmitted in near-real time via slow-speed tape playback techniques. Launch-vehicle data received by downrange sites were processed on site to display selected channels for mark event identification and reporting. Provision was made for selected intervals and channels of data (chamber pressure and velocity meter) to be returned from downrange sites in near-real time via high-frequency communica-

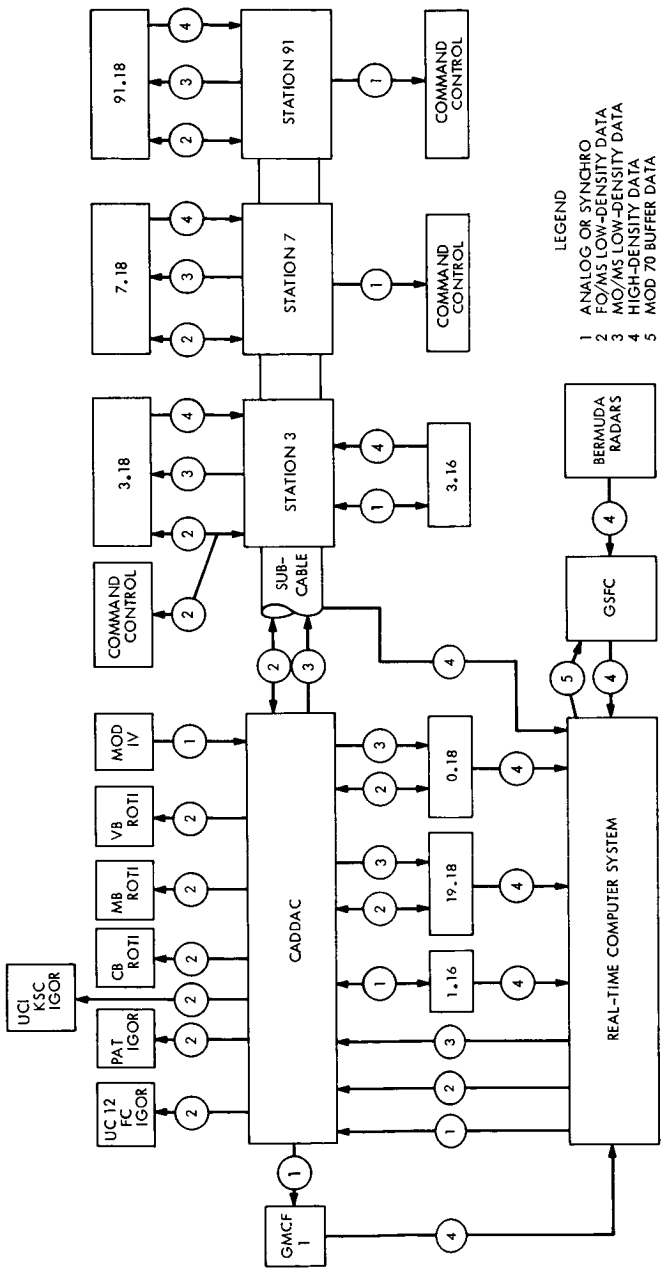

FIGURE 5–3.—Configuration for metric subsystem showing data flow: launch phase.

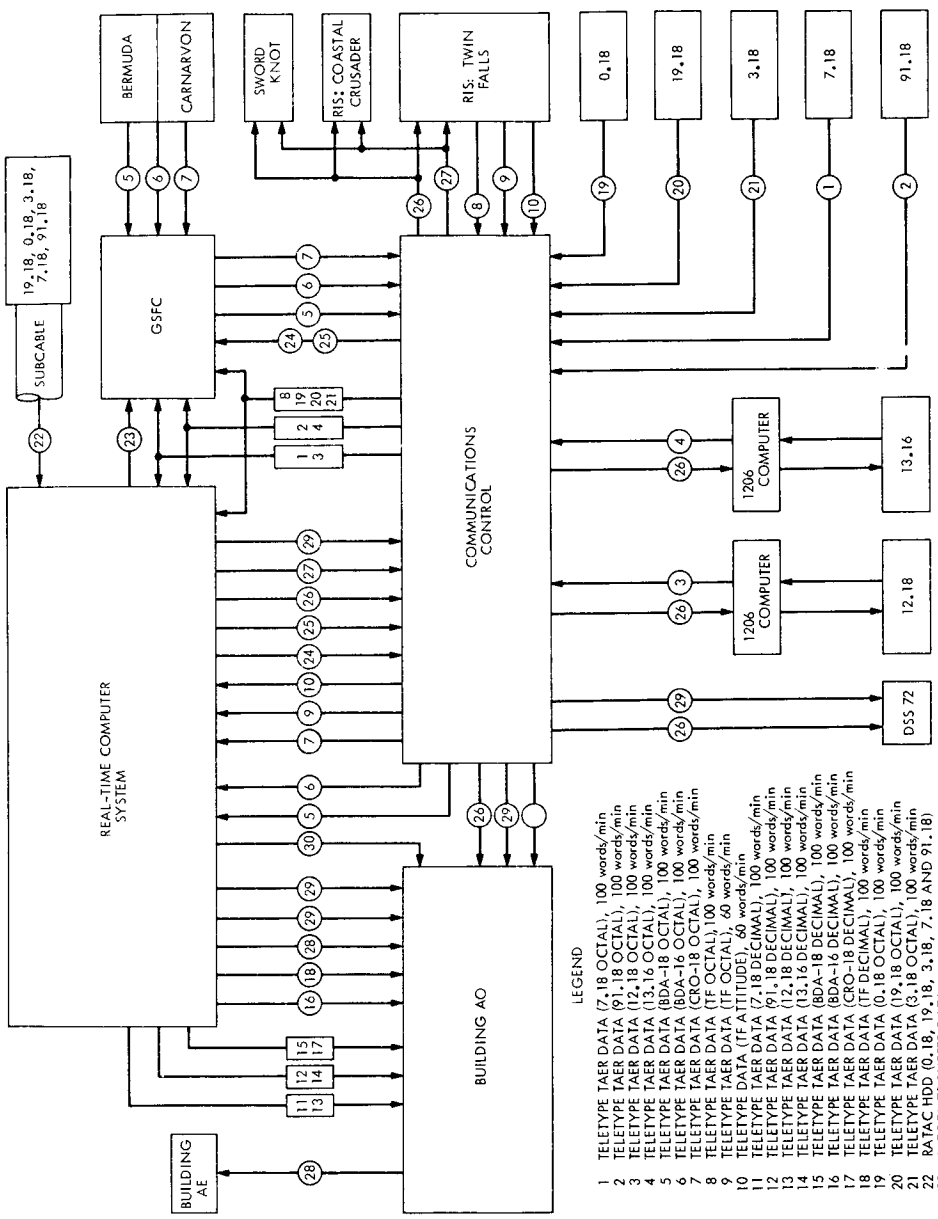

FIGURE 5–4.—Configuration for metric subsystem showing data flow: near-Earth phase.

tions. Launch-vehicle personnel at Kennedy Space Center were responsible for identifying and reporting mark events 1 through 10; mark events 11 through 16 were read by the appropriate downrange station.

Spacecraft telemetry data

There were two basic problems in establishing a TDS configuration for spacecraft telemetry support. These problems and their solutions are discussed in the subsequent paragraphs.

Receiving subsystem configuration. Because of the characteristics of the composite telemetry signal, the receiver loop bandwidth could not exceed 48 Hz. However, doppler rates expected shortly after launch and during Agena second burn indicated that a receiver loop bandwidth of 100 Hz would be required to track, and that use of the recommended 10-kHz intermediate frequency by AFETR would reduce the expected coverage by more than one-half. It was imperative that the TDS solve this problem before adequate support could be provided.

Special tests were scheduled and conducted between AFETR and DSS 71 (KSC) to determine the capability of the telemetry receiver to handle certain characteristics of the Mariner telemetry signal. Use of a 2500-Hz intermediate frequency, in conjunction with the 100-Hz loop bandwidth, provided satisfactory performance. As a result of tests and discussions, it was decided that the AFETR would use the 100-Hz receiver loop bandwidth and 2500-Hz intermediate frequency in the telemetry subsystem.

It was originally thought that *S*-band acquisition at Ascension Island (DSS 72) and Johannesburg (DSS 51) would be a problem. Results from a study of initial acquisition at these stations indicated that acquisition could be accomplished.

Also, to insure against failure of the TDS to acquire the most important class I interval, from spacecraft separation to separation plus 5 min, a minimum capability was established at the MSFN unified *S*-band (USB) station at Ascension Island. Data from the MSFN station were available to DSS 72 for transmission to user areas in real time in case of loss of signal by DSS 72. Mariner crystals were supplied for the MSFN receiver voltage-controlled oscillator, and the appropriate wideband cables were assigned. (See fig. 5–5.)

Data-transmission subsystem configuration. A basic cause of problems encountered in establishing a spacecraft data-transmission capability from AFETR stations was the fact that no Mariner telemetry demodulators were provided for installation. Without a demodulation capability, the entire composite signal had to be transmitted. In the Cape area, wideband circuits were used. From

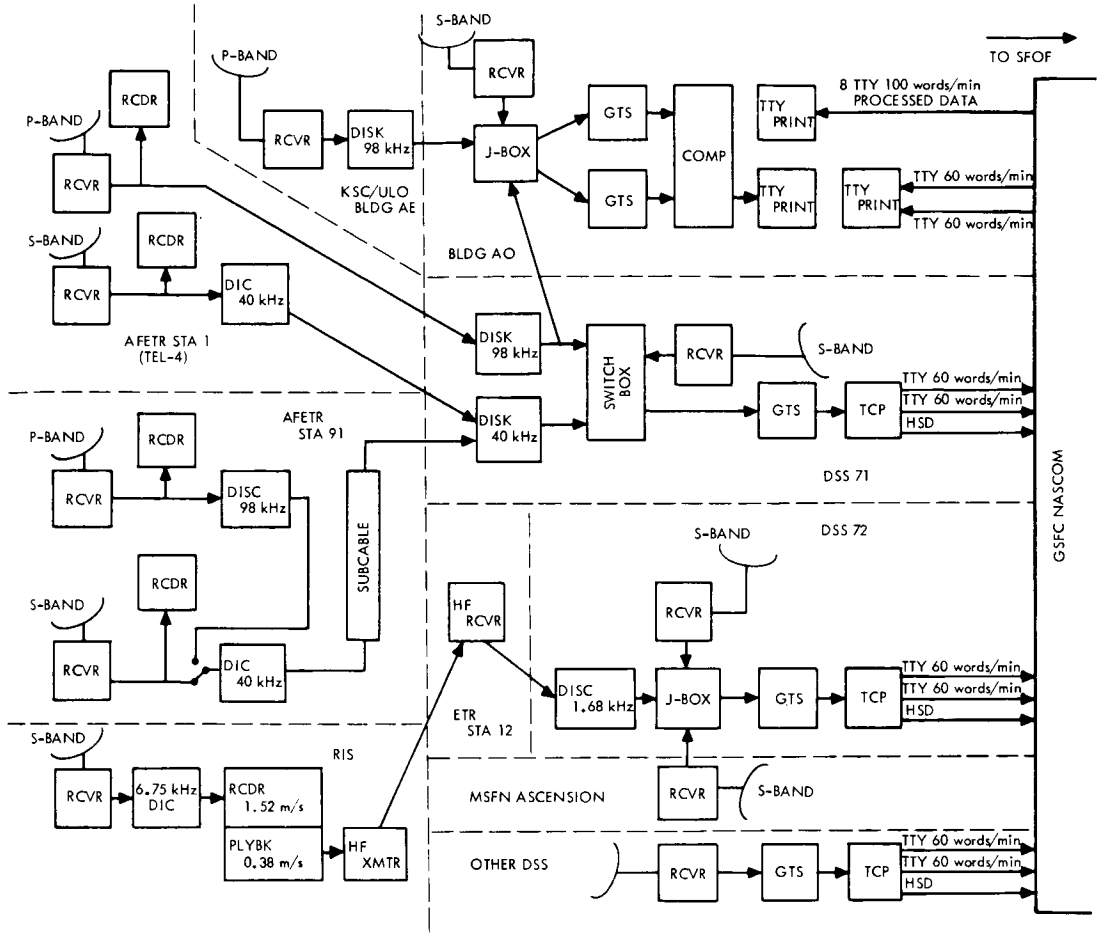

FIGURE 5–5.—Configuration for spacecraft telemetry: near-Earth phase.

Antigua, the 40-kHz subcable circuit was available; from downrange sites and ships, radio communications imposed a 3-kHz bandwidth limitation. Because demodulators were available in the ground telemetry subsystem (GTS) at DSS 71, 72, and 51, in addition to the other tracking stations, these stations were of primary importance in the design of a subsystem to meet spacecraft telemetry requirements in the near-Earth phase.

Special tests determined that Tel 4 could transmit the 98-kHz subcarrier of the Agena link containing spacecraft telemetry data to DSS 71 via wideband circuit. It also was determined that the combined output of the *S*-band link, by using a 40-kHz data insertion converter (DIC), could be transmitted to DSS

71 in real time. Similarly, AFETR Station 91 could feed the output of the *S*-band receiver to a 40-kHz DIC and transmit the DIC output to DSS 71 in real time via a 40-kHz submarine cable circuit. As an alternative, Station 91 found it feasible to discriminate the output of the 98-kHz channel of the Agena link and to transmit these data to DSS 71 in real time using the same 40-kHz DIC/subcable capability. (See fig. 5–5.)

To obtain this real-time capability in the uprange area, 40-kHz digital insertion converters were purchased and installed at Tel 4 and Station 91. Because data arrived at DSS 71 on 98- or 40-kHz carriers, discriminators were purchased and installed ahead of the GTS.

Because of the incompatibility between the composite signal and high-frequency communications subsystems, AFETR downrange sites and ships could not transmit spacecraft telemetry in real time. Many near real-time plans (receive/record/playback) were studied to solve this problem; the resulting plan was that the *S*-band receiver output would pass through a 6.75-kHz DIC to a recorder running at 152 cm/s. Playback would be made at 38 cm/s (1.69 kHz ±40 percent) via single-sideband circuit to DSS 72 by way of the AFETR Station 12 communications circuits. The 6.75-kHz digital insertion converters were purchased and installed at the appropriate AFETR downrange sites and ships. DSS 72 received the corresponding discriminator.

Operational plan. The configurations described above resulted in a TDS plan for supporting near-Earth-phase spacecraft telemetry requirements. (See fig. 5–5.) This plan is described in the following paragraphs.

In the launch phase, DSS 71 was the primary acquisition site for spacecraft data derived from the *S*-band link. Although shroud attenuation was expected to cause early loss of signal, the use of a recently installed parametric amplifier would extend DSS 71 coverage to the horizon. DSS 71 would transmit these data to Building AO and SFOF in real time via GSFC/NASCOM Teletype and high-speed data circuits.

In the launch phase, KSC/ULO, Building AE, was the primary acquisition site for spacecraft data derived from the Agena link. Data would be transmitted from Building AE to AO in real time, input to the GTS, and displayed for evaluations by data analysts.

AFETR's Tel 4 would serve as a backup source of spacecraft data derived from the *S*-band link and as a second prime source of data derived from the Agena link; Tel 4 would transmit both streams of data to DSS 71 in real time. After discrimination at DSS 71, both streams of data would be available to DSS 71 (GTS and telemetry and command processor) in case of loss of signal by the

S-band receiver at the station. The data stream derived from the Agena link also would be available at Building AO as an input to the second GTS.

AFETR Station 91 was the primary acquisition site during the interval from the station's loss of signal through spacecraft insertion into the parking orbit. Both the Agena and *S*-band links would be received, and one or the other (*S*-band preferred) would be transmitted to DSS 71 in real time via the submarine cable. After loss of signal, DSS 71 would switch to this source of spacecraft data and continue to process and transmit the data in real time to Building AO and to the SFOF.

DSS 72 was the primary acquisition site for spacecraft telemetry data in the Ascension Island area. Received data would be processed and transmitted in real time via high-frequency or communications-satellite circuits to Building AO and the SFOF. The MSFN USB site would act to serve as a backup source during this interval; the ground telemetry subsystem could be switched to this data stream in case of loss of signal at the DSS 72 receiver.

AFETR ships, positioned in the Ascension Island/South Africa broad ocean area, would be the primary acquisition sites for spacecraft telemetry in the event the particular flight azimuth did not provide for adequate coverage of requirements by DSS 72 and 51. Ships do not transmit data in real time. Using a $\frac{1}{4}$-speed tape-playback technique, ships would transmit data to DSS 72 in near-real time at $8\frac{1}{3}$ bps. DSS 72 would process and retransmit the data to the SFOF only. To minimize the time required to play back and recover the class I interval data, ships would be instructed to set up one recorder and to record only during the required interval.

DSS 51 was the primary acquisition site for spacecraft coverage in the South African and Indian Ocean area. The DSS 51 view period extended to continuous DSIF view. Data would be transmitted in real time to Building AO and to SFOF.

Configuration for communications

NASCOM furnishes worldwide voice, data, and Teletype facilities in support of NASA's space-flight projects and missions. The DSN ground communications facility (GCF) is a configuration of NASCOM.

It is important to note that Mariner-Venus 1967 was the first project to use operationally a GCF configuration containing the JPL communications processor (CP) as an integral part. The CP's constitute a real-time computer subsystem (RTCS) that is programed to switch Teletype messages from the sending location to the desired receiving location. Switching is controlled by certain elements of the message.

However, AFETR RTCS Teletype outputs to SFOF are not compatible with the CP, because Kennedy equipment is not programed to introduce automatically the NASCOM message header required. To overcome this incompatibility, a "torn-tape" operation was conducted at the JPL Communications Center in Building AO. In this operation, prepunched paper tapes containing the correct headers were inserted ahead of the RTCS Teletype data before retransmission to SFOF via Goddard Space Flight Center.

Figure 5–6 more specifically identifies the Teletype circuitry configuration that supported both the near-Earth and deep-space phases of the mission. Figure 5–7 further illustrates the communications configuration for the near-Earth phase by identifying specific Teletype, voice, and high-speed data circuits established to meet specific data transmission and operational control requirements. All circuits shown were scheduled from existing resources, except the eight 100-word/min Teletype lines from SFOF to Building AO. These circuits required special ordering and were used to transmit processed telemetry data from launch through first maneuver to data analysts located at Building AO.

TDS Configurations for Mariners 4 and 5: Deep-Space Phase

From the end of the near-Earth phase to the end of the mission, telemetry, tracking, and command requirements for Mariners 4 and 5 were met by various combinations of these deep-space stations:

DSS 11	Pioneer site, Goldstone station, California
DSS 12	Echo site, Goldstone station, California
DSS 14	Mars site, Goldstone station, California (during the 25.9-m antenna grayout period and at encounter for occultation)
DSS 41	Woomera, Australia
DSS 42	Tidbinbilla, Australia
DSS 51	Johannesburg, South Africa
DSS 61	Robledo station, Madrid, Spain
DSS 62	Cebreros station, Madrid, Spain

Capabilities and operating parameters of the stations that supported Mariners 4 and 5 are presented in table 5–VI.

DSS 11, 42, and 61 were considered prime stations through the first correction maneuver plus 2 days. Throughout the remainder of the mission, combinations of other deep-space stations were established, as required, to meet mission objectives. The TDS plans outlined here reflect the support required for Mariner 4 and 5 combined operations.

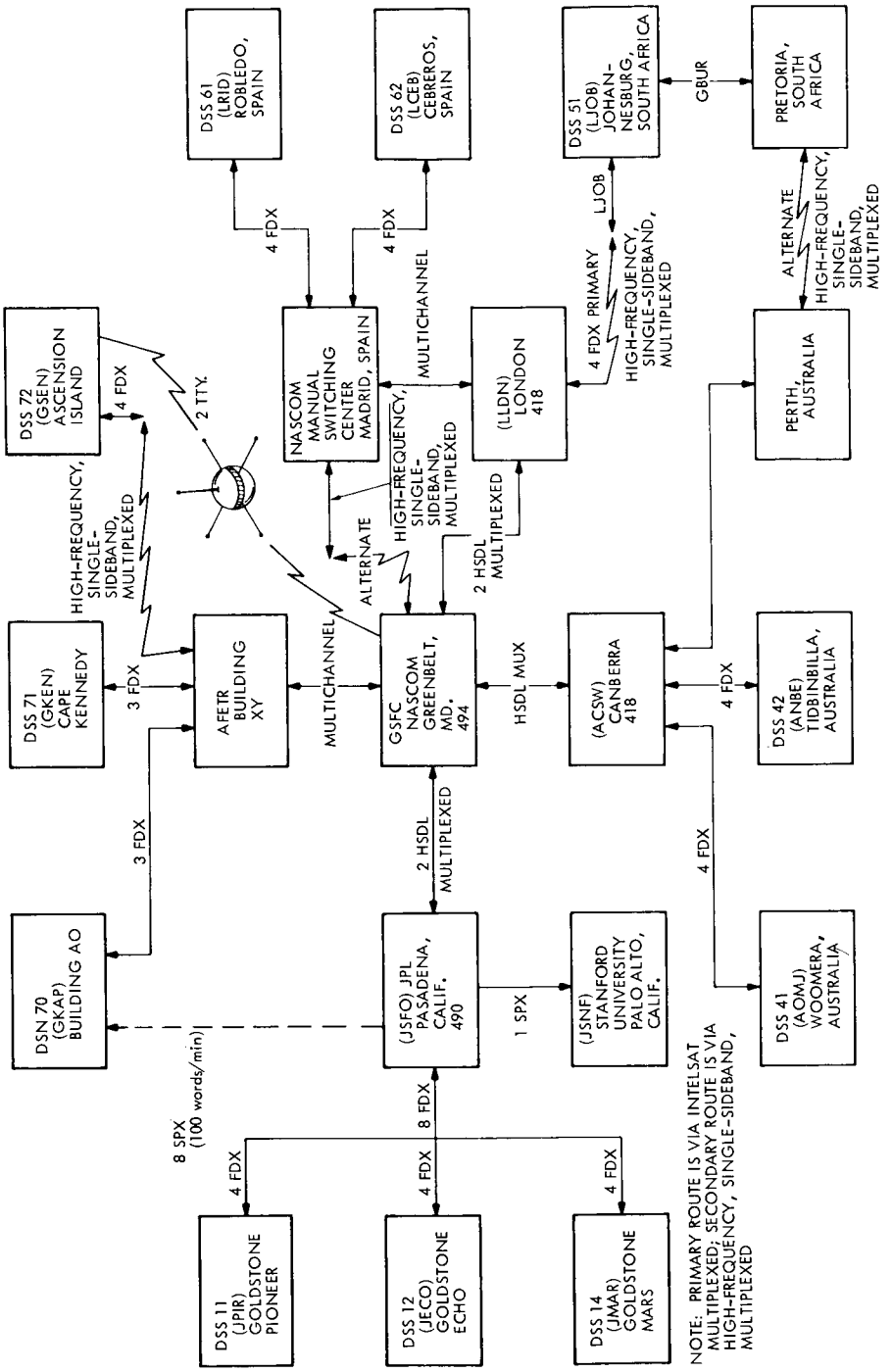

FIGURE 5–6.—Configuration for Teletype circuitry: near-Earth and deep-space phases.

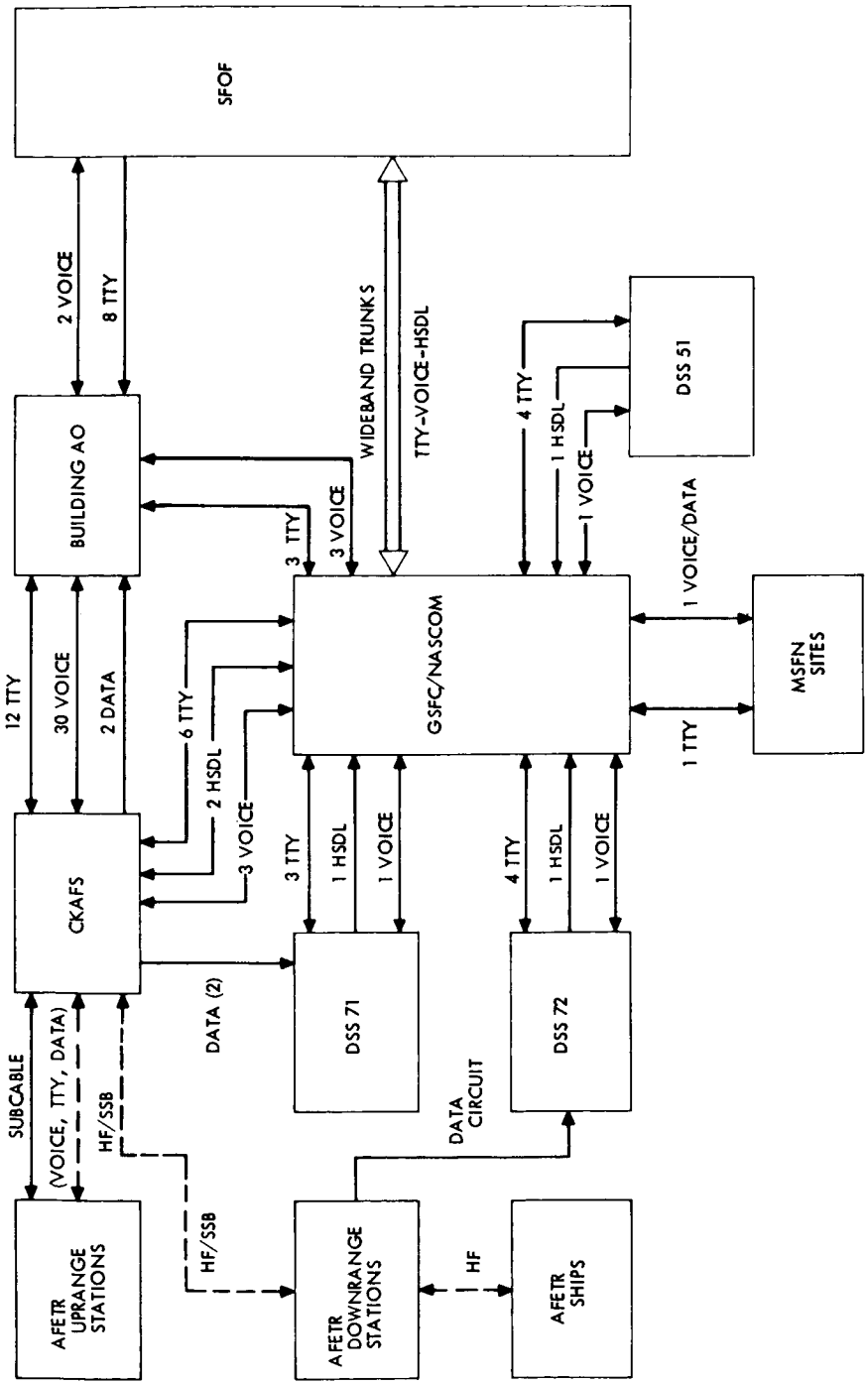

FIGURE 5–7.—Communications configuration showing Teletype, voice, and high-speed data circuits: near-Earth phase.

Table 5–VI.—Capabilities of supporting

Capability	Goldstone Pioneer[a] GSDS *S*-band	Goldstone Echo GSDS *S*-band	Goldstone Mars
Station identification	DSS 11	DSS 12	DSS 14
Receiver capability	2	2	2
Antenna	85-ft parabolic	85-ft parabolic	210-ft
Mount	Polar (HA, DEC)	Polar (HA, DEC)	Azimuth/elevation
Maximum angular rate (both axes), deg/s	0.7	0.7	0.5
Antenna gain, dB:			
Receiving	$53.0\ ^{+1}_{-0.5}$	$53.0\ ^{+1}_{-0.5}$	~61.0
Transmitting	51.0 ± 1	51.0 ± 1	~59.0
Antenna beamwidth, deg	~0.4	~0.4	0.1
Typical system temperature, K	55 ± 10	55 ± 10	—
Transmitter power, kW	10	10	20
Data transmission (Teletype):			
Angles	Real time	Real time	Real time
Doppler	Real time	Real time	Real time
Ranging (to 800 000 km)	Real time	Real time	Real time
Telemetry	Real and near-real time	Real and near-real time	Real and near-real time
Demodulated telemetry	Dual channel	Dual channel	Dual channel
Command capability	Yes	Yes	Yes
Data pack air shipment time to JPL	1 day	1 day	1 day

GSDS = Goldstone duplicate standard.

[a] This station has acquisition aid.

Configuration for telemetry subsystem

The telemetry subsystem configuration for Mariner 5 is shown in figure 5–8. The TDS acquired spacecraft data from the rf carrier; the composite signal was processed from the receiver to the demodulator, where data, bit synchronization, and word synchronization were generated from the spacecraft signal. Demodulator inputs and outputs were recorded.

The tracking stations assigned a ground-receipt time to the spacecraft data, recorded data in digital form, and formatted the data for transmission to SFOF via Teletype and high-speed data circuits. These operations were performed by the telemetry and command processor (TCP). A mission-dependent program, which resided in the TCP, performed manipulation of the data as prescribed by the project. The TCP also outputted receiver automatic gain control (AGC) and static phase error data.

Teletype and high-speed data were transmitted to the SFOF by the GCF.

stations for Mariners 4 and 5

Woomera[a] GSDS *S*-band	Tidbinbilla[a] GSDS *S*-band	Johannesburg[a] GSDS *S*-band	Robledo GSDS *S*-band	Cebreros GSDS *S*-band
DSS 41	DSS 42	DSS 51	DSS 61	DSS 62
2	2	1	2	
85-ft parabolic	85-ft parabolic	85-ft parabolic	85-ft parabolic	
Polar (HA, DEC)	Polar (HA, DEC)	Polar (HA, DEC)	Polar (HA, DEC)	
0.7	0.7	0.7	0.7	
$53.0\ ^{+1}_{-0.5}$	$53.0\ ^{+1}_{-0.5}$	$53.0\ ^{+1}_{-0.5}$	$53.0\ ^{+1}_{-0.5}$	
51.0 ± 1	51.0 ± 1	51.0 ± 1	51.0 ± 1	
~ 0.4	~ 0.4	~ 0.4	~ 0.4	
55 ± 10	55 ± 10	55 ± 10	55 ± 10	
10	10	10	10	
Real time	Real time	Real time	Real time	
Real time	Real time	Real time	Real time	
Real time	Real time	N/A	Real time	
Real and near-real time	Real and near-real time	Real and near-real time	Real and near-real time	
Dual channel	Dual channel	1	Dual channel	
Yes	Yes	Yes	Yes	
2 weeks	2 weeks	2 weeks	10 days	10 days

Teletype data arriving at SFOF were processed by the CP, which routed data to various devices in SFOF. High-speed data were received at the SFOF communications center and were forwarded to the telemetry-processing subsystem to be formatted for entry into the input/output processor (7044 computer).

Configuration for tracking data handling subsystem

The purpose of the tracking data handling (TDH) subsystem (see fig. 5–9) was to process, display, record, and encode for Teletype, DSIF tracking data and doppler information. Data provided were in digital form of angles representing antenna position, doppler frequency, transmitter voltage-controlled-oscillator frequency, ranging, data condition, time, and associated identification information. The representation was in the form of standard five-level Baudot code punched on paper tape. The prime function of the TDH was that of counting doppler; it also served as the assembly and formatting center for other tracking data at the station. One TDH subassembly was provided to each deep-space station.

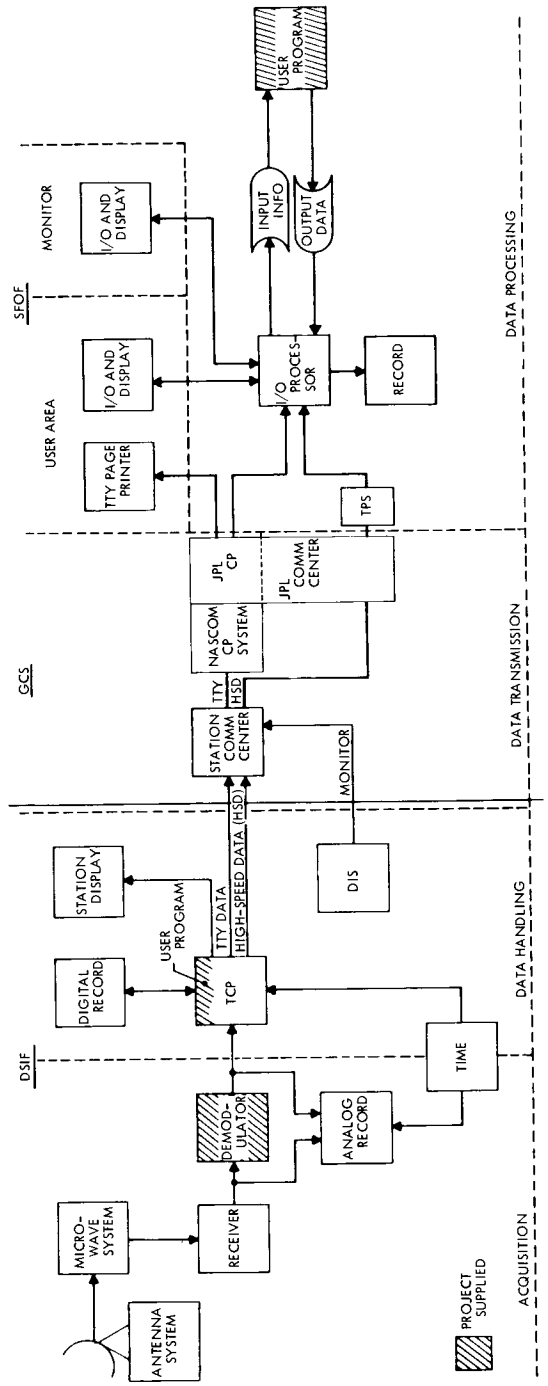

FIGURE 5–8.—Configuration for Mariner 5 telemetry subsystem.

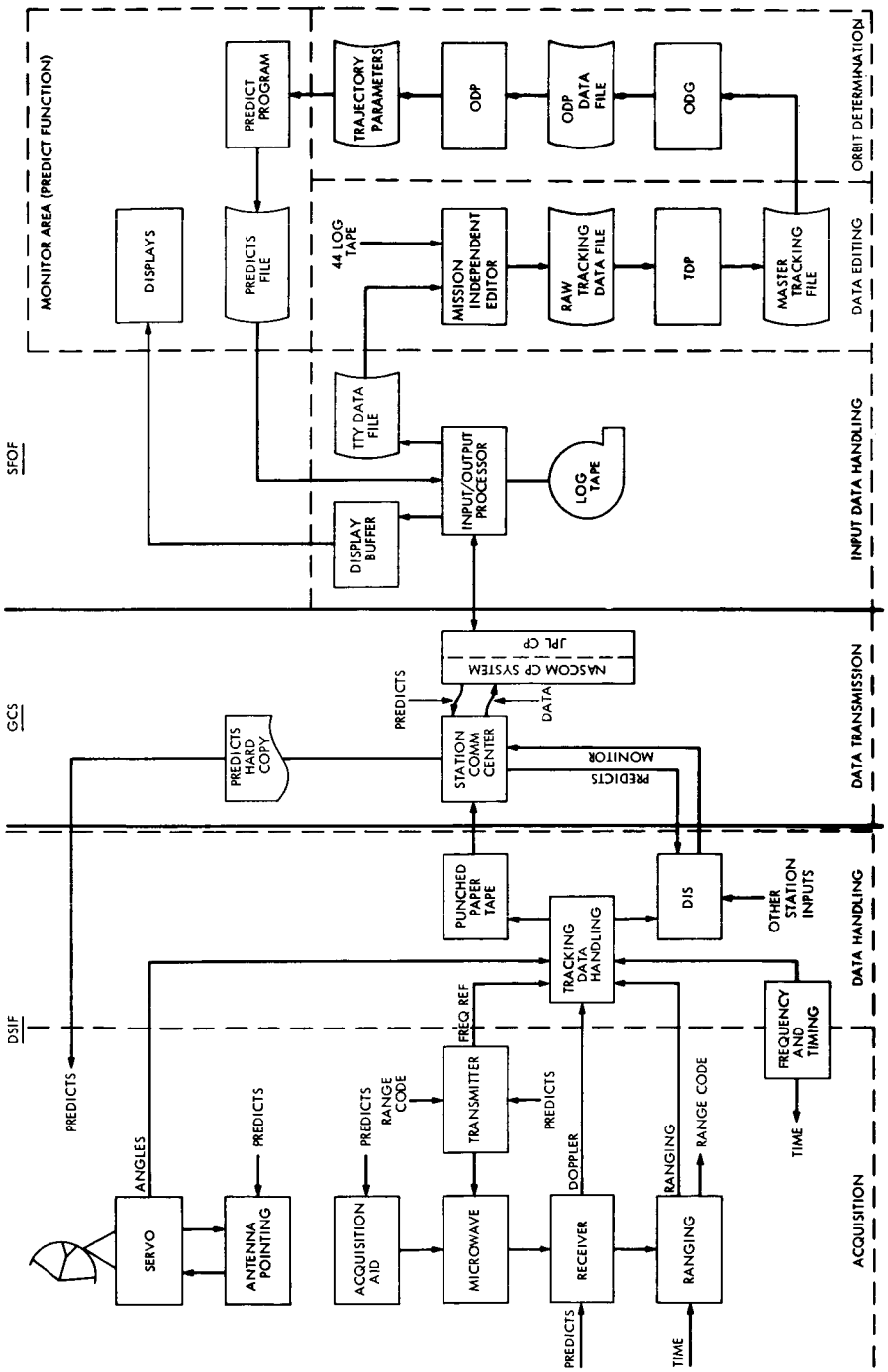

FIGURE 5–9.—Configuration for Mariner 5 tracking data subsystem.

Tracking data were transmitted from the stations to the JPL communications center by the GCF. The JPL CP routed incoming Teletype data to the 7044 computer, which was the input computer for the data processing subsystem, and to Teletype page printers.

Raw Teletype data from the CP were passed by the 7044 computer directly to the 7044/7094 shared disk and logged on tape. Data were tapped from the stream and processed for display purposes. The 7044 processor used the Teletype preambles to identify data types.

Configuration for command subsystem

Commands could be sent to the spacecraft during any phase of the mission. The spacecraft command subsystem consisted of a command detector and decoder and a set of switches to provide logical outputs to the spacecraft subsystems. Upon reception of a direct command in the spacecraft, a logical output was provided to the appropriate subsystem; upon reception of a quantitative command, timing information was provided to the CC&S.

Configuration for ranging subsystem

The standard DSIF configuration with Mark I ranging could be used at any station in the early part of the mission (out to a few million kilometers). The second part of the mission ranging was conducted only from Goldstone, using research and development (R&D) personnel and equipment to supplement the standard DSIF configuration. The planetary ranging (Mark II) experiment required the Mars site 210-ft antenna fitted with a 20-kW transmitter and a supplement to the existing receiver. Figure 5–10 shows the planetary ranging interface. The Mark II ranging subsystem had—

(1) A 920 computer, based with one digital rack and two intermediate-frequency racks in DSS 14 Alidade room.
(2) Two correlation channels that reduce acquisition time by one-half.
(3) Narrower code loop bandwidths (0.01 Hz); doppler-aided tracking results.
(4) Resolution of 0.15 m, compared with 1.0 m in the Mark I ranging subsystem.
(5) Range greater than 80 million km, compared with 0.08 million km in the Mark I ranging subsystem.

Configuration for encounter

Oversea station configuration

Oversea stations used for the encounter period were DSS 41 (with DSS 42

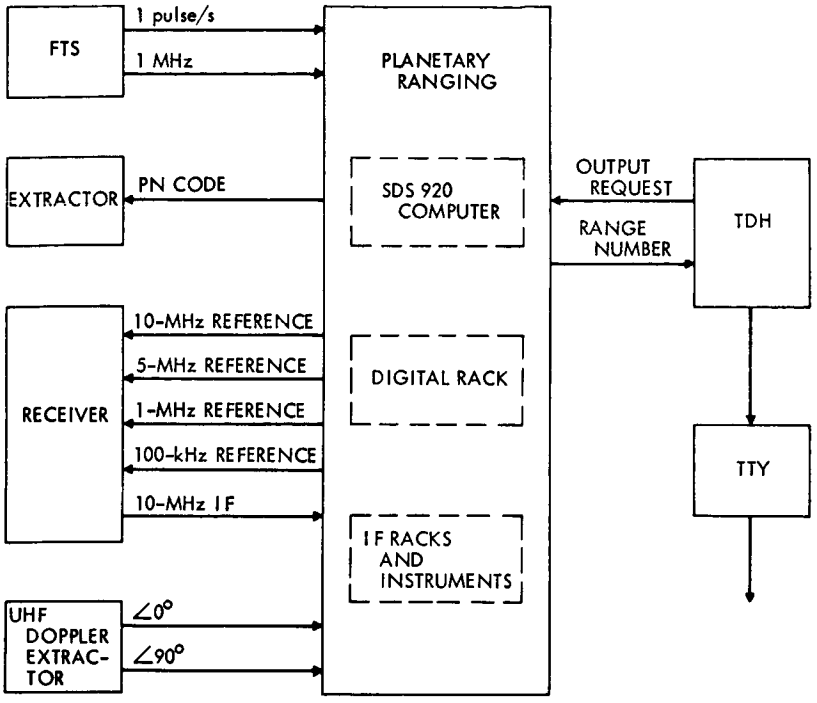

FIGURE 5–10.—Configuration for planetary ranging (Mark II) subsystem interface.

as backup) and DSS 62 (with DSS 61 as backup). These stations operated in a completely standard configuration.

Goldstone station configuration

The encounter of Mariner 5 took place in view of the Goldstone complex. All four Goldstone sites participated in the encounter sequence (see fig. 5–11). DSS 14 was the prime station for the occultation, bistatic radar astronomy, and R&D ranging experiments, as well as for the command function. DSS 12 was backup for the occultation experiment closed-loop receiver and also was backup for the command function. DSS 11 was the DSIF backup and processed DSS 14 telemetry data under the multimission concept. DSS 13 was backup for the occultation experiment open-loop receiver. At exit occultation, DSS 12 was the first station to acquire the spacecraft in two-way.

S-band occultation experiment configuration. It was expected that the high atmospheric density of Venus would cause doppler perturbations on the order of 30 kHz, compared to 3 Hz (one-way) for the Mariner 4 occultation of Mars, and that the atmosphere would act as a defocusing lens, which produces refractive attenua-

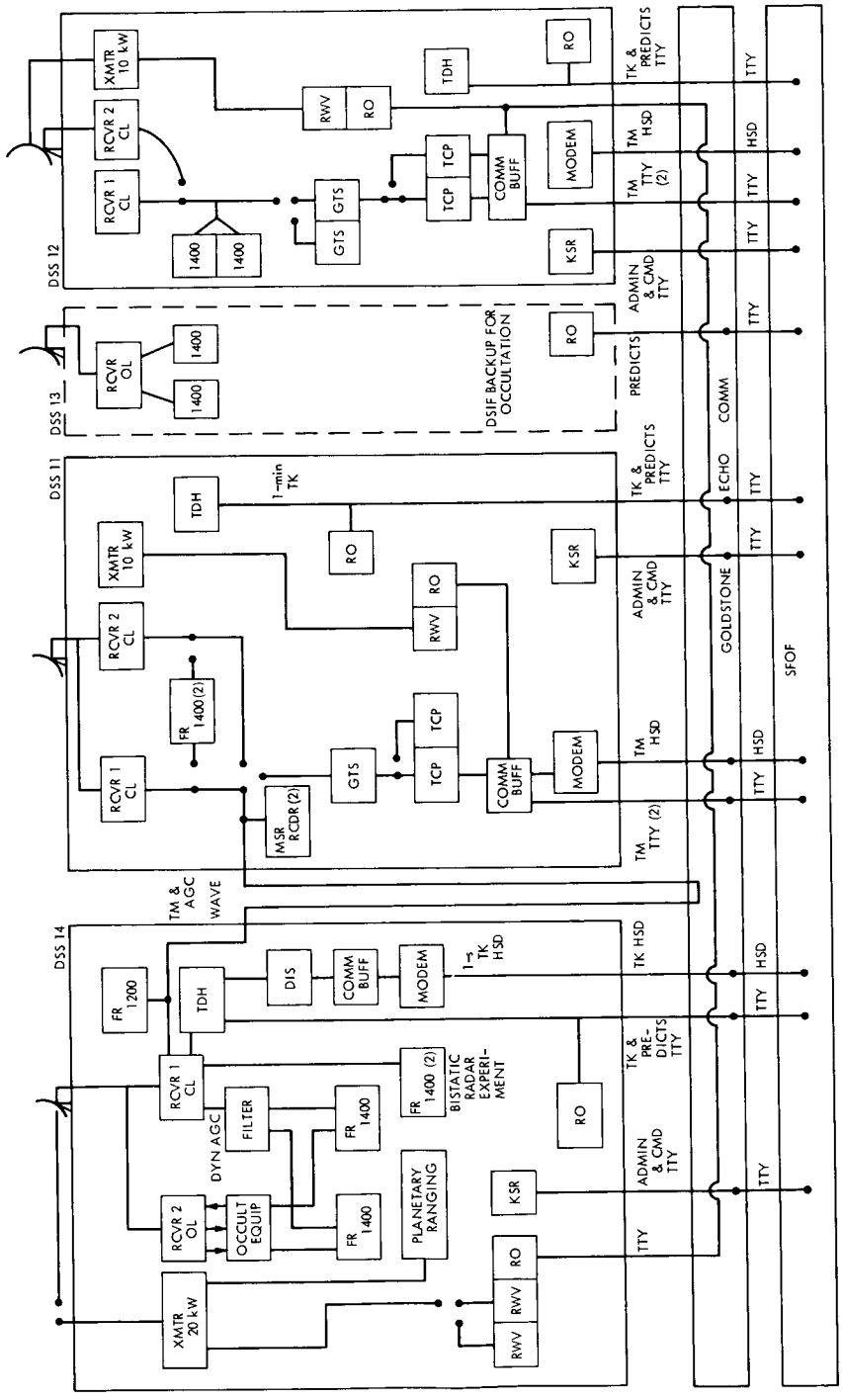

NOTE: DSS 62 (DSS 51 AS BACKUP) AND DSS 41 (DSS 42 AS BACKUP) ARE IN STANDARD CONFIGURATIONS.

FIGURE 5–11.—Configuration for the Goldstone tracking station at Mariner 5 encounter.

tion. These conditions required a large aperture antenna to insure the most favorable signal-to-noise ratio. To meet this requirement, a special configuration was established that involved all four sites at the Goldstone station. Two racks of special occultation experiment equipment were installed at DSS 14 in late March. One DSS 14 receiver operated in an open-loop configuration, and the other in a closed-loop configuration. The receiver at DSS 13 was operated as backup to the open-loop receiver at DSS 14. The "ultra cone," with a system noise temperature of 16.4 K, was installed at DSS 13 for the occultation experiment. DSS 11 and 12, backups to the DSS 14 closed loop, were in standard configuration, except that a special filter was inserted between the dynamic AGC output and the FR 1400 recorder where AGC was recorded.

To evaluate the occultation data, 1-s tracking data samples were sent to SFOF in real time. Because ordinary Teletype lines do not have the capacity for this 1-s data rate, a high-speed data line (HSDL) was planned for use. A special configuration was conceived and installed at DSS 14 to use the HSDL. The TDH tracking and resolver data were output to the data input subsystem (DIS). The TDH counter, which is normally used for measuring voltage-controlled-oscillator frequencies, was used in the resolver circuit because the standard resolver had insufficient power to drive the DIS. A special program was written for the DIS, which was to output the high-rate tracking data to a communications buffer, and then to a data modem. The data were then microwaved to the communications center at the Echo site, Goldstone, and then transmitted to SFOF.

Bistatic radar astronomy experiment configuration. A belated request to observe the Mariner 5 signal after it had been reflected off the surface of Venus resulted in the bistatic radar astronomy experiment. Because of the polarization change due to the reflection, a second maser was installed at DSS 14 to act as a backup, and the unused angle channels of the receiver were modified to receive and process the reflected signal. Figure 5–12 shows the configuration for this experiment. Two FR 1400 recorders were removed from the multimission support area at DSS 12 and installed at DSS 14 in support of this experiment. DSS 14 virtually ceased support of mission operations from September 21 through October 12 to make the installations and modifications mentioned, to conduct the testing required to check the experiment configuration, and to verify that these changes did not seriously compromise the unmodified performance capability of the station.

SFOF configuration

SFOF was configured for the Mariner 5 encounter with two 7044/7094

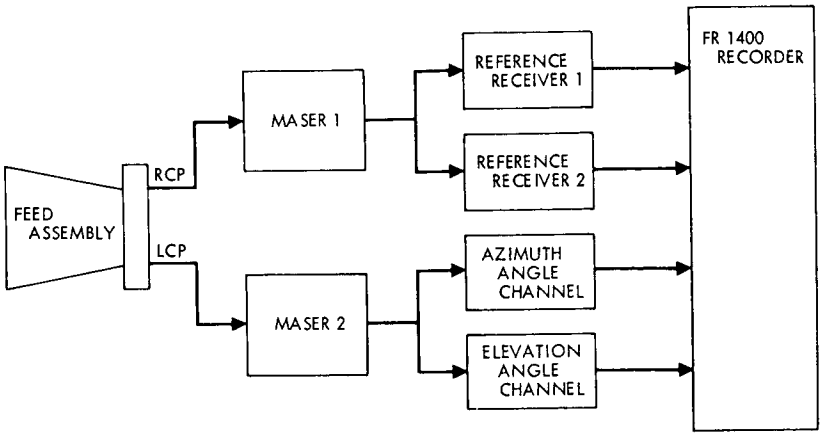

FIGURE 5–12.—Configuration for bistatic radar astronomy experiment performed by Mariner 5.

computer strings (fig. 5–13): one prime for tracking data (orbit determination) and pseudo residuals (1-s tracking data samples for occultation analysis) and the second prime for telemetry processing. However, either string was capable of performing both jobs. Three digital phone line formatters that fed three 7044 computer subchannels allowed for three high-speed data sources to be input simultaneously. For the encounter period, these were (1) 1-s tracking data samples from DSS 14, (2) telemetry from DSS 14 via the TCP at DSS 11, and (3) DSS 12 telemetry. In addition, selected Teletype tracking and telemetry data were routed by the TCP to the 7044 computers.

Configuration for digital demodulation technique

Received signal levels throughout the mission were close to nominal. The predicted signal level dropped below the telemetry threshold of the 85-ft antennas about September 15. To prevent the loss of telemetry data, a digital demodulation technique (DDT) was conceived and used. The DDT is a computer program that uses one-half of the TCP to perform the function of the GTS analog demodulator. The second half of the TCP performs the decommutation function as before. The two halves of the TCP were operated in series to extract usable data that would have been lost if the normal receiver/GTS/TCP configuration had been used during the 85-ft antenna grayout period from September 15 through October 1, 1967. Figure 5–14 shows the DDT configuration. The DDT improved telemetry threshold by about 5 dB, but was limited to the spacecraft mode 2 at $8\frac{1}{3}$ bps.

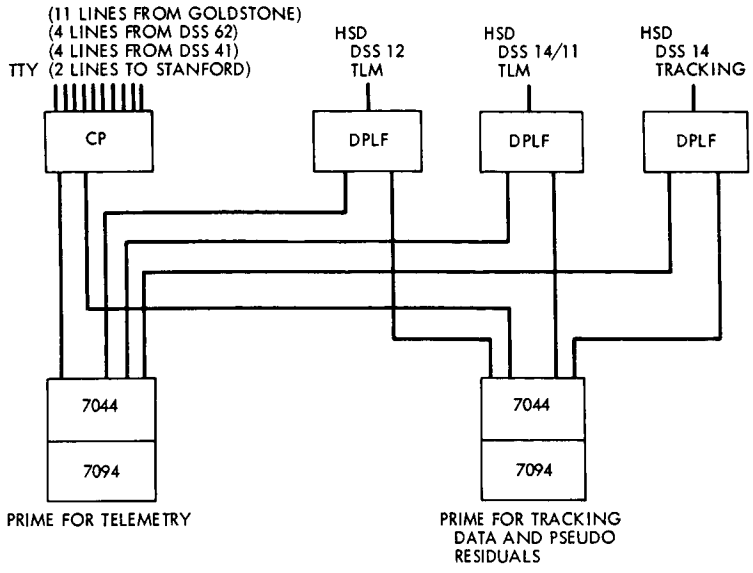

FIGURE 5–13.—Configuration for SFOF at Mariner 5 encounter.

Configuration for dual-frequency-receiver experiment

JPL facilities also supported Stanford University's dual-frequency experiment. During the flight, Stanford radiated the 423.3- and 49.8-MHz dual frequencies whenever the spacecraft was above the Stanford local horizon and the deep-space stations were tracking. The DFR telemetry data were received by the stations in real time during assigned tracking periods. The data were relayed to SFOF for real-time processing and subsequent transmission to Stanford, where the data were analyzed and evaluated.

Configuration for ground communications facility

The GCF was designed to provide those communications circuits, switching facilities, terminals, equipment, and personnel required to insure the effective transfer of information between the deep-space stations and SFOF (see figs. 5–6 and 5–15). Figure 5–16 further illustrates the communications configuration for the deep-space phase by identifying specific Teletype, voice, and high-speed data (HSD) circuits established to meet requirements. The GCF was divided into three subsystems:

Voice communications

The GCF provided full-period, leased, four-wire, engineered voice circuits

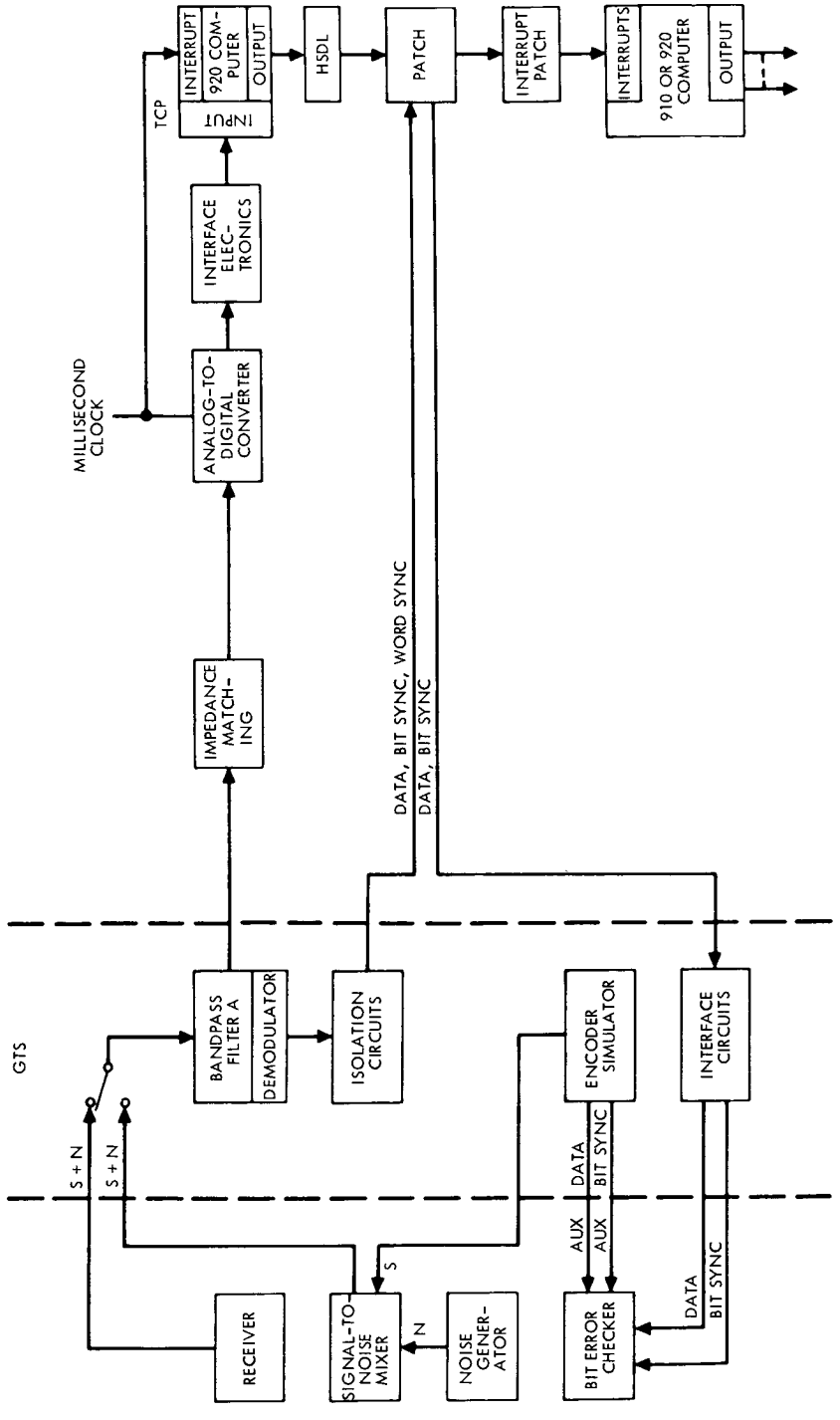

FIGURE 5–14.—Configuration for the DDT computer program.

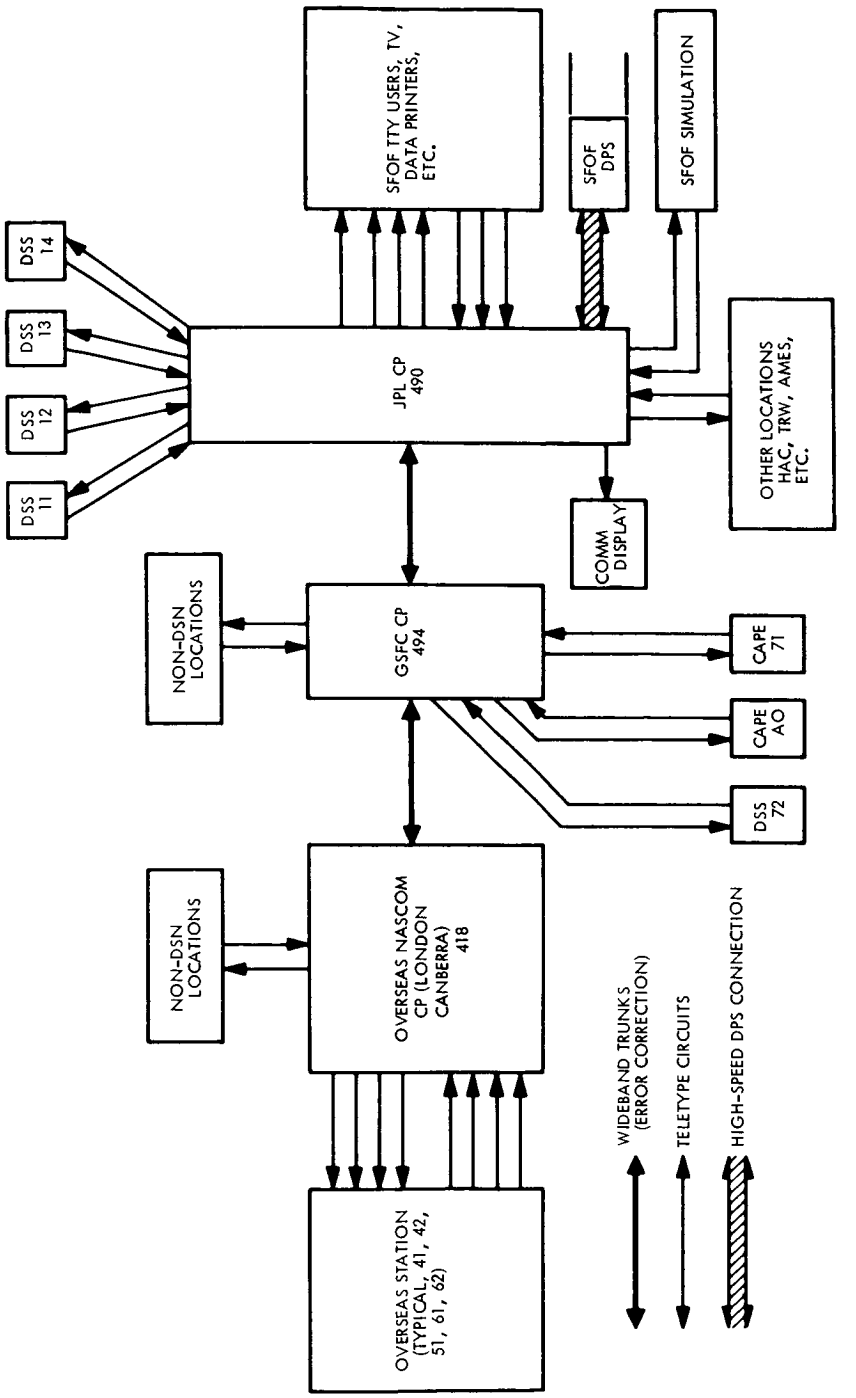

FIGURE 5–15.—Configuration for GCF, illustrating CP subsystem.

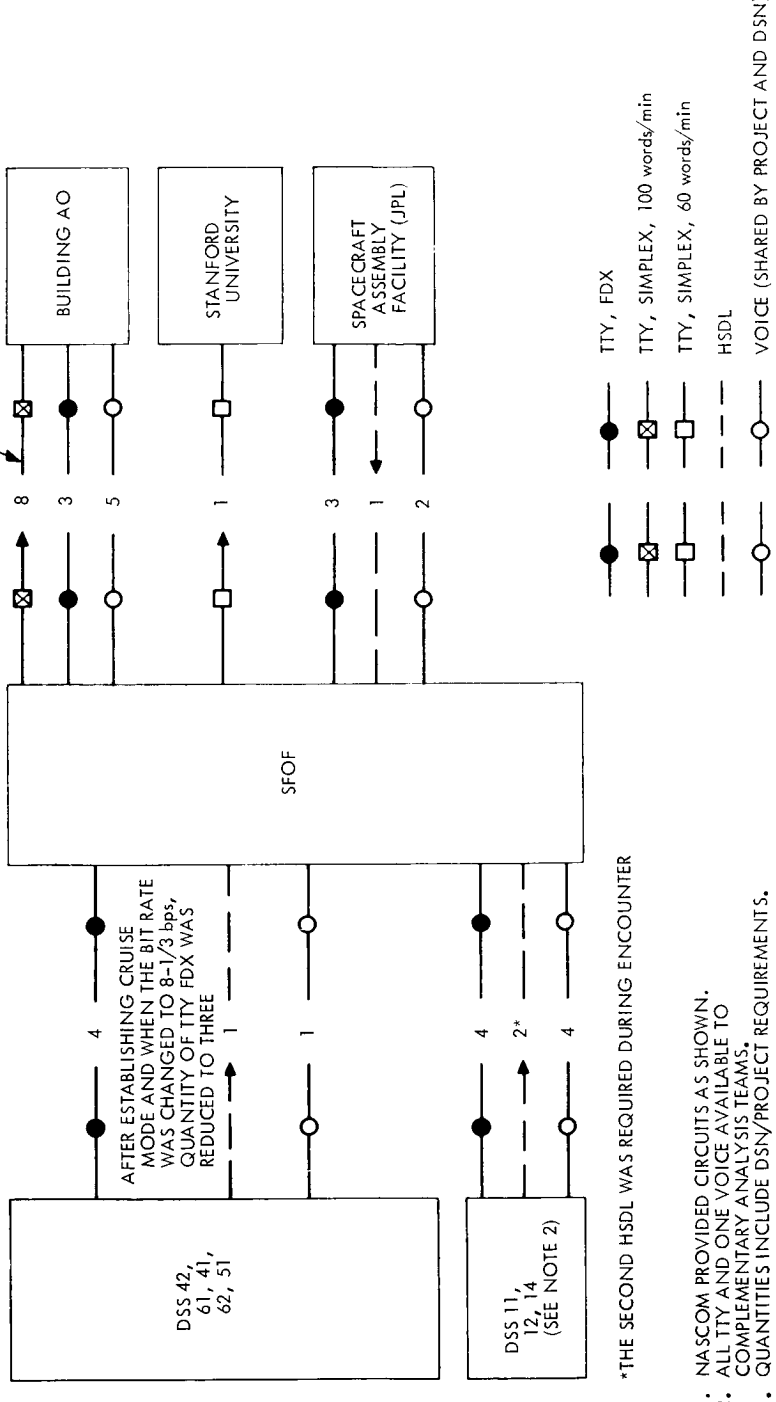

FIGURE 5-16.—Communications configuration showing specific Teletype, voice, and HSD circuits: deep-space phase.

to the majority of stations in the network. Most voice circuits were routed via the switching center at Goddard Space Flight Center and comprised the signaling, conferencing, and monitoring arrangement. Circuits were routed by hardwire and microwave, whenever possible, and extended to oversea points through transoceanic cables or by high-frequency radio links when cables were not available. They were used for both operational and nonoperational traffic. Both common user and private lines were provided.

High-speed data

The GCF provided full-period, leased, HSD circuits to transmit spacecraft telemetry that required a higher bit rate than that of Teletype. These circuits were assigned solely to operational traffic. At SFOF, all HSD were routed to the telemetry-processing station for preprocessing and then to the 7044 input/output processor.

Teletype

The GCF provided a Teletype subsystem of full-duplex links composed of leased and commercial facilities obtained from national, international, and foreign common carrier agencies. For reliability purposes, oversea circuits employed undersea cables wherever possible, but were necessarily routed via radio facilities to reach certain locations. Error detection and correction systems were, where required and available, provided on the oversea circuits by the common carriers to reduce error rates to the minimum possible within the state of the art. All Teletype circuits could be used for operational and nonoperational traffic. Both common user and private lines were provided.

In nonoperational modes, the circuits were used for the non-real-time transmission of nonoperational messages. In the operational mode, the circuits were used for the transmission of—

(1) Spacecraft tracking data
(2) Spacecraft telemetry data (low bit rates)
(3) Spacecraft commands, predictions, and reports
(4) Information for control and coordination of launch and station operations
(5) Information controlling and coordinating communications

Teletype data were switched on a message basis by the command processors of the NASCOM command processor subsystem (fig. 5–15). The command processors are:

(1) A 418 computer at London, serving DSS 51, 61, and 62

(2) A 418 computer at Canberra, serving DSS 41 and 42
(3) A 494 computer at GSFC, serving DSS 71, 72, Building AO at AFETR, London, and Canberra
(4) A 490 computer at JPL, serving DSS 11, 12, 14, and Stanford

All oversea Teletype data were routed from the oversea command processors to Goddard Space Flight Center, and then to JPL over wideband trunks with error-correction capability. The JPL command processor routed all data, based on preamble information, to the appropriate preplanned points in SFOF (data processing subsystem, Teletype page printers, and/or closed-circuit television).

DSIF data processing

The stations performed onsite data processing as described below:

Telemetry and command processor

(1) Formatting the telemetry data received from the Mariner mission-related hardware for transmission to SFOF in real time
(2) Providing selected station functions to SFOF (receiver in/out of lock, demodulator in/out of lock, and receiver AGC)
(3) Assigning DSIF time to the telemetry data

Tracking data handling equipment

(1) Formatting tracking (angle, doppler, ranging and/or transmitter frequency) for transmission to SFOF
(2) Assigning DSIF time to the tracking data

Recording subsystem

(1) Recording telemetry data (composite and mission-related hardware output
(2) Recording selected station functions
(3) Recording DSIF time

Figure 5–17 is a station configuration for performing TCP.

SFOF data processing configuration and plans

The major data-handling effort within SFOF consisted of the processing and display of incoming tracking and telemetry data. In meeting user requirements, the SFOF data processing subsystem provided the services listed below.

Input/output processor (7044R)

(1) Formatting, converting to engineering units, and outputting to display devices in real time the telemetry and tracking data received from the DSIF and spacecraft testing areas

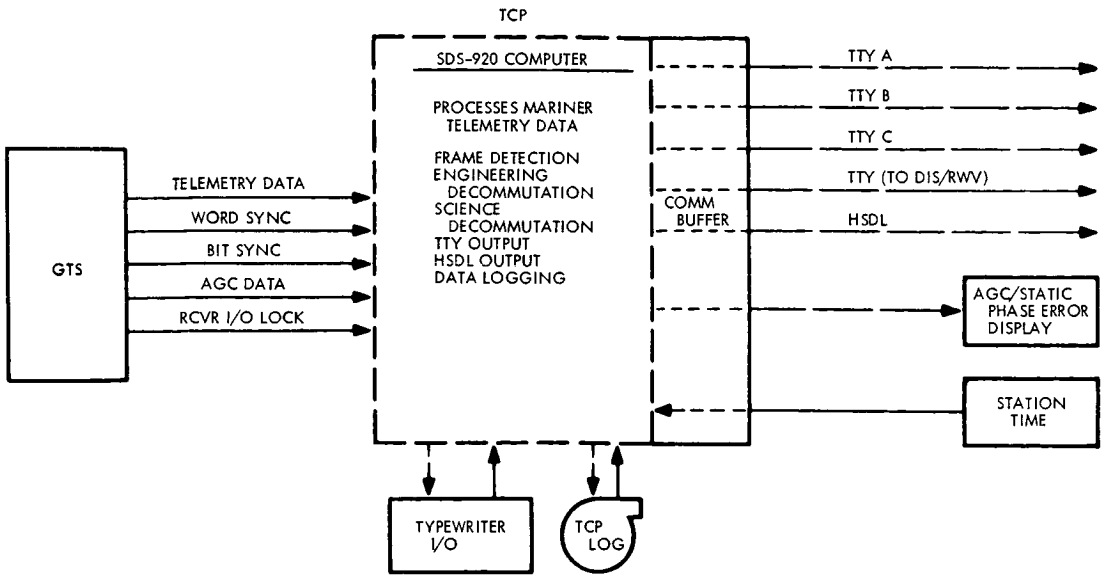

FIGURE 5–17.—Station configuration for performing TCP.

(2) Alarm-monitoring engineering and science telemetry data from the spacecraft
(3) Recording all incoming DSIF data on digital magnetic tape
(4) Transmitting tracking predictions and commands to the stations

Main processor (7094)

(1) Performing detailed analysis of spacecraft engineering and science data in non-real time when required by the sequence of events, or upon request from the Space Flight Operations Director
(2) Performing spacecraft positioning analyses
(3) Determining spacecraft orbit and generating tracking predictions
(4) Generating maneuver commands
(5) Generating a master data library consisting of all spacecraft data forwarded from the stations

TRACKING AND DATA SYSTEM PERFORMANCE

Mariner 4 (Phase II)

During the Mariner 4 mission (phase II), there were four significant DSN activity periods: (1) carrier acquisition, (2) solar occultation, (3) Mars site testing, and (4) operational experience for DSS 14.

Carrier acquisition

After the termination of phase I of the Mariner-Mars 1964 project, it was decided that the DSN would search for the Mariner 4 *S*-band signal, at times opportune to its own activities, at approximate 1-month intervals. Monthly tracks from DSS 13 were performed from November 1, 1965, to March 1, 1966.

During each of these tracks, measurements were made of the received signal spectrum. Examination of the spectrogram provided certain measurements:

(1) *Total power received.* This information, when combined with the gains of the ground and spacecraft antennas and the range to the spacecraft, provided a good indication of the power output of the spacecraft transmitter, and thus the general status of Mariner 4.

(2) *Power in the rf carrier and the modulation sidebands.* This information provided an indication of the modulation index and whether the transmitter was still being modulated.

(3) *Frequency separation between the carrier and the sidebands.* This provided a positive indication that the Mariner signal had been received by verifying that the separation coincided with the design value of 150 Hz.

(4) *Frequency of the received signal.* This information provided a good indication of the transmitter frequency (and frequency stability) when the doppler frequency component was removed.

The integration time to obtain a positive identification of the Mariner 4 signal was about 1 hr, using the facilities of the Venus site, Goldstone. Because of the narrow predetection bandwidth and the long integration time, considerable time was required to perform a frequency search when the received frequency was not at the nominal or expected value.

Analysis of the results of the five monthly tracks from November to March during which spectrograms were taken revealed a nominal performance of Mariner 4. One additional track was performed at DSS 13; during this period, a DC–17 command was transmitted to update the cone angle of the spacecraft's Canopus sensor.

Solar occultation

This period lasted from March 18 through April 12, 1966. Mariner 4 passed within 2° of the Sun near the end of March 1966. Because the Mars site was completed during March 1966, the DSN was capable of utilizing two-way doppler measurements to determine the electron-density profile of the solar corona. This was accomplished by measuring the additional frequency shift in the Mariner-received signal, induced by the presence of the electrons in the solar corona.

This frequency shift was in addition to the normal doppler shift caused by the radial motion of the spacecraft, relative to the tracking station.

The configuration used consisted of two sites at Goldstone: Venus (DSS 13) acted as the transmitting station (100 kW) and Mars (DSS 14) acted as the receiving station. Both operated at the state of the art with respect to system capabilities. The experiment depended upon the availability of the 210-ft antenna at DSS 14.

Solar occultation occurred while the 210-ft antenna was under construction. However, with the cooperation of the contractor, it was possible to perform the experiment in spite of this difficulty. The observations were interleaved with completion of the work that remained on the main azimuth bearing. Consequently, less than half of each view period was available for gathering data. Sometimes this was the first half, while work was being done on west sections of the bearing. When east sections needed attention, Mariner 4 was observed during the lowering part of the pass. Sometimes this interleaving was not possible and data were lost. Altogether, data were obtained over a 15-day period.

The various angles used to describe the passage of the spacecraft, almost behind the Sun as seen from Earth, are defined in figure 5–18. Because the angular diameter of the Sun, as viewed from Earth, is about 0.25°, it should be noted that the Sun-Earth-probe (SEP) angle must be less than 0.25° for the spacecraft to pass precisely behind the Sun. Figure 5–19, which contains a plot of the three angles defined in figure 5–18, reveals that the SEP angle reached a minimum of 0.8° on March 26, 1966. This means that the spacecraft passed behind the Sun no closer than one solar diameter, as observed from Earth.

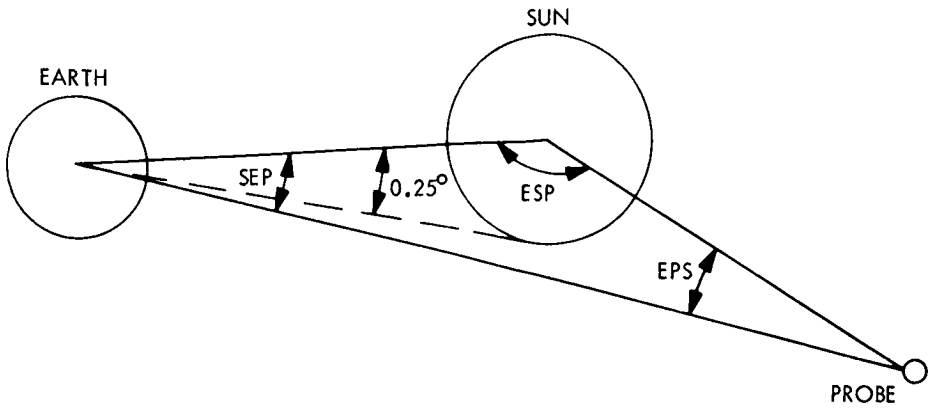

FIGURE 5–18.—Earth-Sun-probe geometry for Mariner 5.

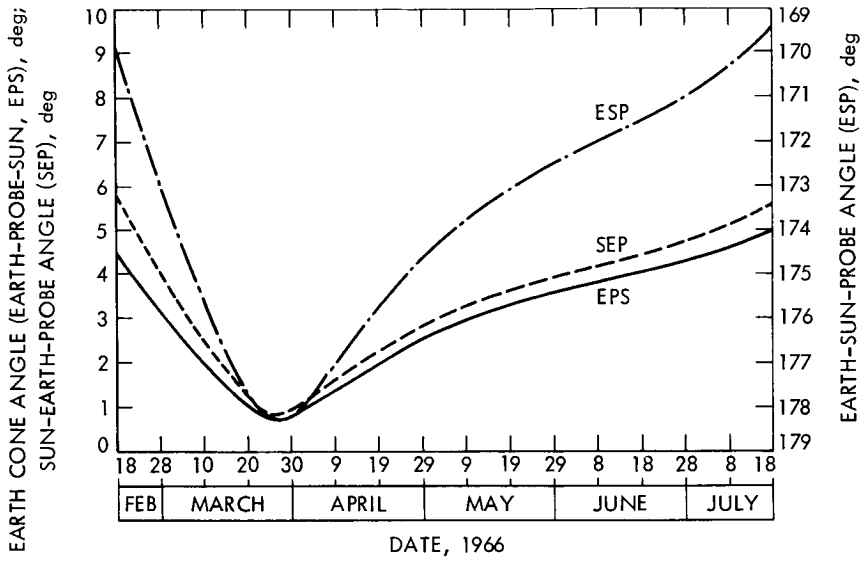

FIGURE 5–19.—Plot of angles shown in figure 5–18.

Two separate experiments were performed each day, time and construction work permitting. The first mode was one-way operation. That is, the ground transmitter was switched off and Mariner 4 transmitted from its free-running crystal oscillator. This signal passed through the solar corona once; the resulting spectrogram showed the amount of spectral broadening induced upon the signal by the corona. For 11 days, starting on the day of closest angular approach to the Sun, one-way spectrograms were obtained.

Data showed that the spacecraft oscillator was subject to an unpredictable component of frequency drift. Any such drift, during the integration time, is effective in broadening the spectrum of the signal. To determine the extent of this effect, six spectrograms were taken on May 3, when the Mariner 4 transmission path was far from the solar corona. (See fig. 5–20 for a sample one-way spectrogram.) These spectrograms were taken under essentially the same conditions as the first set of spectrograms and helped to calibrate the effect of oscillator drift on the spectral widths of the signals.

In the two-way mode of operation, the spacecraft transmitter was phase locked to the ground transmitter. To achieve this uplink lock, the ground transmitter was tuned slowly past the calculated frequency of the spacecraft receiver. The slow tuning, plus the 30-min flight time, used much of the precious time available; thus, to use the time efficiently, one-way spectral measurements were made during the tuning process.

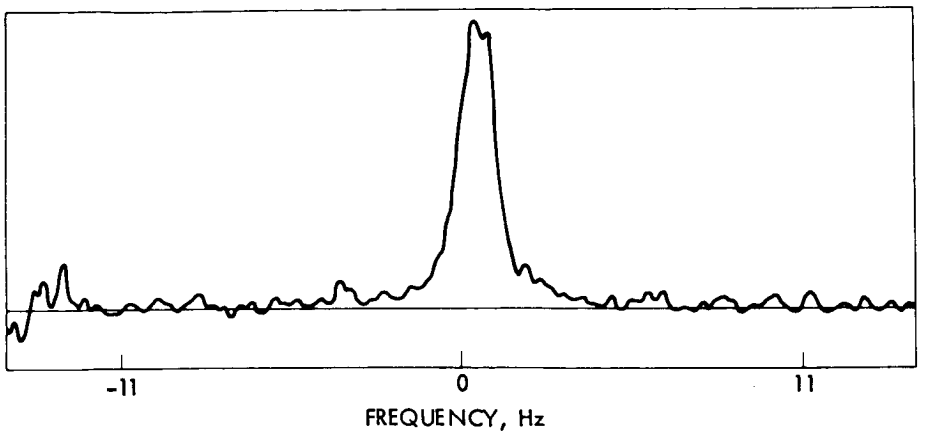

FIGURE 5–20.—Typical one-way spectrogram.

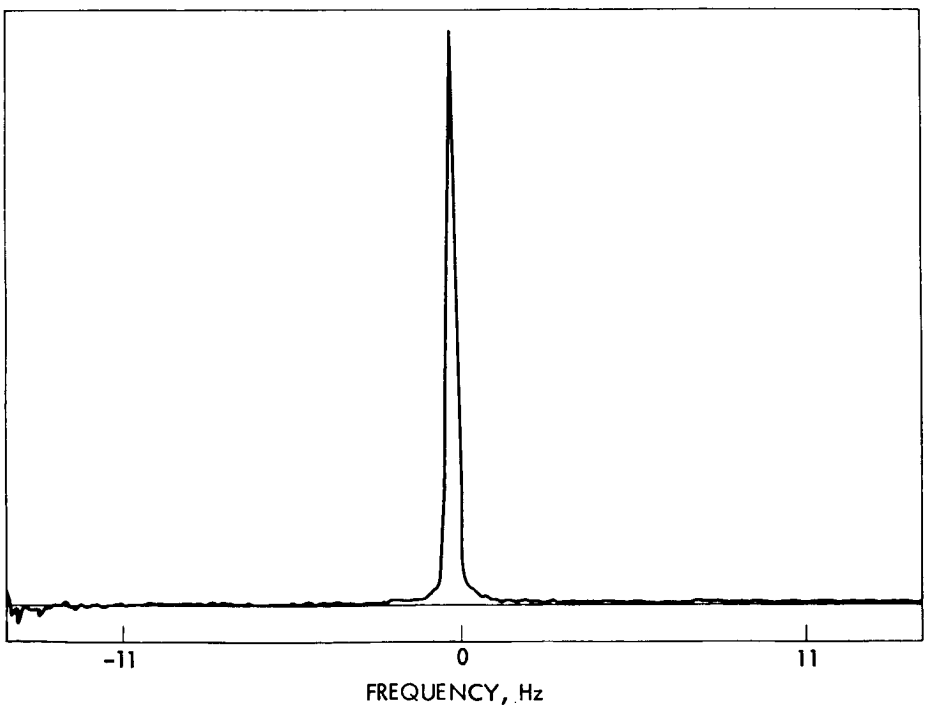

FIGURE 5–21.—Typical two-way spectrogram.

Two-way operation removed the troublesome drift in the spacecraft transmitter, but substituted another form of uncertainty. The signal received by the spacecraft had passed through the solar corona, and consequently was spectrally broadened. The spacecraft could track any phase variations of the signal, but none of the amplitude variations. The "mix" of amplitude and phase fluctuations, generated by the corona, is unknown. The reradiated signals passed through the corona a second time and were recorded as spectrograms. In all, 17 spectrograms were taken. The observed spectral broadening is attributed not only to two trips through the solar corona, but also to one trip through the spacecraft. Additional spectral broadening is also caused by any inaccuracies of ephemeris tuning and instabilities of the oscillators of the system.

Another test was made on June 5, when the Mariner 4 link was far from the influence of the Sun. On that day, a two-way spectrogram was made under essentially the same conditions as before. Figure 5–21 shows a combined spectral broadening, caused by the entire system, of only 0.32 Hz, including ephemeris tuning and spacecraft interaction. Thus, essentially all of the broadening of the one-way and the two-way spectra can be attributed to the effects of the solar corona and Mariner 4.

Mariner 5: Near-Earth Phase

Metric subsystem performance

Tables 5–VII and 5–VIII and figures 5–22 through 5–24 show the expected and actual coverages.

Telemetry subsystem performance

Launch-vehicle telemetry

Tables 5–IX and 5–X and figures 5–25 through 5–27 show the expected and actual coverages for the near-Earth-phase launch-vehicle telemetry subsystem. A list of mark events is presented in table 5–XI.

Spacecraft telemetry

Table 5–XII and figures 5–28 through 5–31 show the class I requirements, the expected coverages, and actual coverages.

Mariners 5 and 4: Deep-Space Phase

DSIF coverage

Table 5–XIII shows that the ultimate desired support was provided on 60.3 percent of the days that tracking was required or provided, and that class I requirements were not met on only 2 percent of the days. Two of the 3 days

Table 5–VII.—Launch-vehicle tracking coverage intervals (C-band radar) [a]

Station	Intervals of coverage, s	
	Expected[b]	Actual
Cape Kennedy (1.16)		10 to 265
KSC (19.18)	18 to 317	12 to 365
PAFB (0.18)	20 to 317	15 to 480
GBI (3.18)	104 to 428	98 to 450
(3.16)	100 to 400	69 to 467
GTK (7.18)	220 to 590	199 to 610
Bermuda (FPQ-6)	290 to 562	282 to 642
Antigua (91.18)	389 to 734	368 to 768
Ascension (12.18)	1243 to 1470	1232 to 1515
(12.16)	1243 to 1462	1245 to 1474
RIS: Twin Falls (FPS-16)	1421 to 1688	1414 to 1912
Pretoria (13.16)	1660 to 2240	1667 to 3046
		3078 to 4967
Carnarvon (FPQ-6)	2390 to 5130	2342 to 5178

[a] Required intervals of class I coverage based on nominal mark times: continuous coverage from L to $L+604$ s, any continuous 60 s between $L+1415$ and $L+1875$ s, and any continuous 60 s after $L+1882$ s.

[b] Based on 101° launch azimuth.

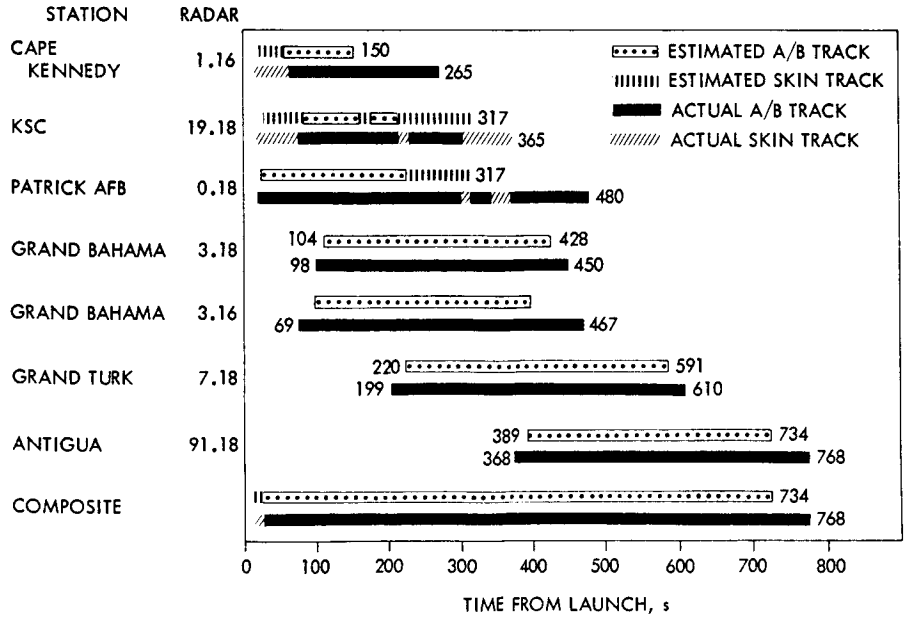

FIGURE 5–22.—Mariner 5 AFETR uprange radar coverage.

Table 5–VIII.—Radar coverage

Station	Radar	Acquisition of signal		Loss of signal		Total track, s
		Predicted GMT	Actual GMT	Predicted GMT	Actual GMT	
BDA	FPQ-6	06:05:50	06:05:42	06:10:22	06:11:42	360
BDA	FPS-16	Backup only				
CRO	FPQ-6	06:41:36	06:41:42	07:19:00	07:28:18	2568

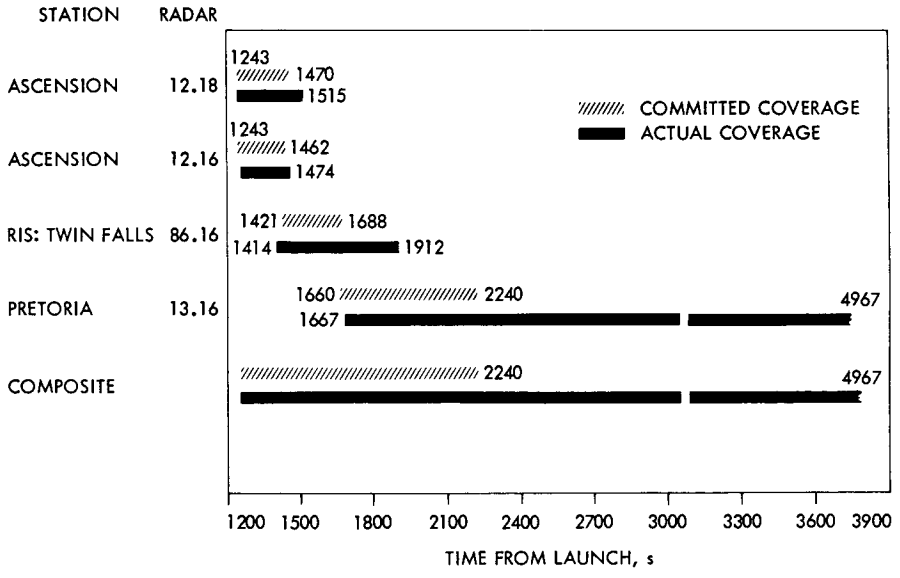

FIGURE 5–23.—Mariner 5 AFETR downrange radar coverage.

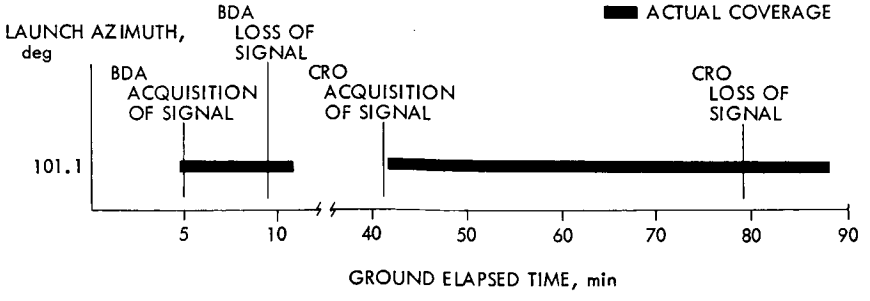

FIGURE 5–24.—Mariner 5 radar coverage: predicted and actual.

Table 5–IX.—Launch-vehicle telemetry coverage intervals [a] (Agena link, very high frequency)

Station	Intervals of coverage, s	
	Expected[b]	Actual
Tel 2	−420 to 416	0 to 483
Tel 4	−420 to 415	0 to 483
GBI	77 to 460	18 to 525
Bermuda	228 to 590	237 to 633
Antigua	379 to 706	330 to 773
Ascension	1236 to 1475	1158 to 1640
AFETR RIS: Coastal Crusader	1168 to 1376	1119 to 1430
AFETR RIS: Twin Falls	1398 to 2100	1341 to 2065
Pretoria	1631 to 3770	1615 to 5040
Tananarive	1760 to 2930	1756 to 3036
Carnarvon	2370 to 2820	2375 to 3990
Aircraft:		
Audit 1 TAA–4		945 to 1497
Audit 2 TAA–4		994 to 1591

[a] Required intervals of class I coverage based on nominal mark times: continuous coverage from $L-420$ to $L+544$ s, continuous coverage from $L+1300$ to $L+1435$ s, continuous coverage from $L+1565$ to $L+1597$ s, continuous coverage from $L+1865$ to $L+1895$ s.

[b] Based on 101 launch azimuth.

Table 5–X.—Telemetry coverage

Station	Frequency, MHz	Actual acquisition of signal and loss of signal		Predicted acquisition of signal and loss of signal		Total track, s
		Decommutator lock, GMT	Decommutator unlock, GMT	Decommutator lock, GMT	Decommutator unlock, GMT	
BDA	249.9	06:04:57	06:11:33	06:05:30	06:10:40	396
BDA	244.3	06:04:57	06:11:33	06:05:30	06:10:40	396
TAN	244.3	06:30:16	06:51:36	06:30:00	06:38:30	1280
CRO	244.3	06:40:35	07:07:30			1620

Table 5–XI.—Telemetry mark events

Station	Mark event	Time
BDA	4	06:05:56
BDA	8	06:06:20
BDA	9	06:07:22
BDA	10	06:09:44
TAN	11	06:32:13

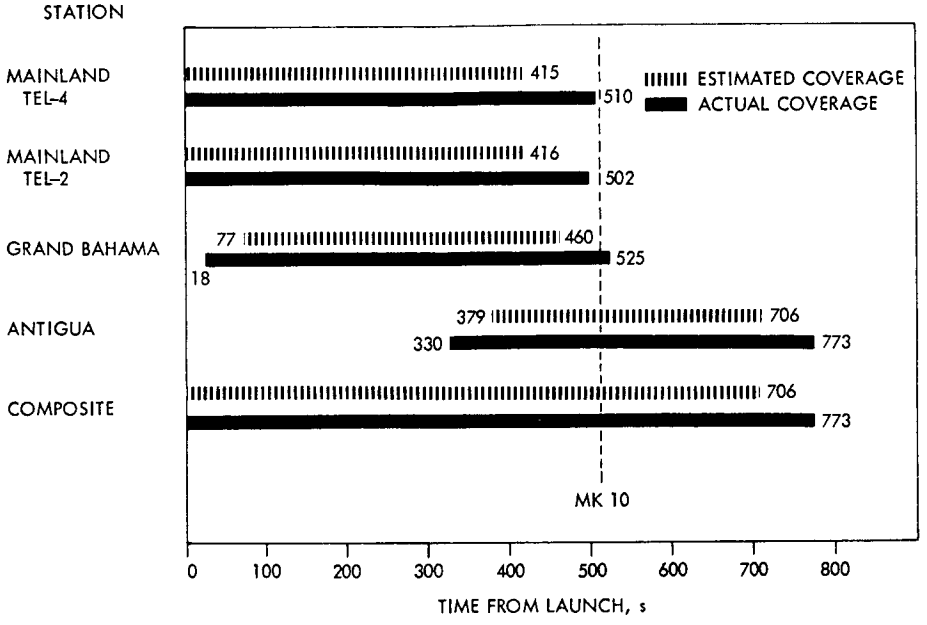

FIGURE 5–25.—AFETR station uprange very-high-frequency (244.3 MHz) telemetry coverage for Mariner 5.

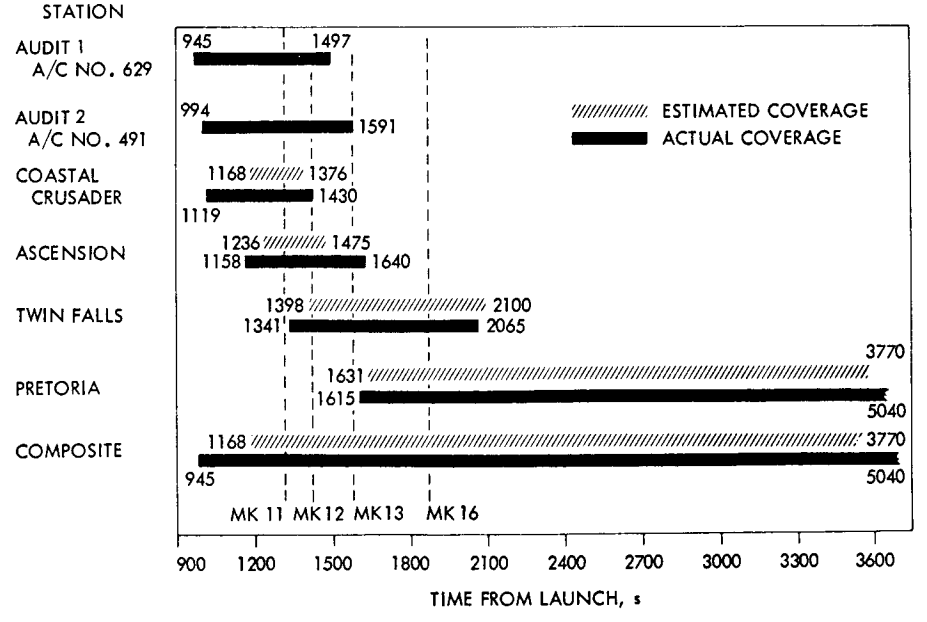

FIGURE 5–26.—AFETR station downrange very-high-frequency (244.3 MHz) telemetry coverage for Mariner 5.

Table 5–XII.—Spacecraft telemetry coverage intervals (*S*-band) [a]

Station	Intervals of coverage, s	
	Expected [b]	Actual [c]
DSS 71	0 to 50 and 80 to 180	0 to 428
Tel 4	0 to 50	0 to 364
GBI	106 to 216 and 350 to 375	None
Bermuda	Not committed	None
Antigua	462 to 633	340 to 715 (phase locked)
Ascension USB	1240 to 1510	1184 to 1629
Ascension	1266 to 1416	1183 to 1480, 1575 to 1593, and 1625 to 1643
DSS 72	1280 to 1590	1308 to 1500 and 1560 to 1620
AFETR RIS: Coastal Crusader	1260 to 1320	1119 to 1427
Pretoria	1661 to 2155	1633 to 5040
DSS 51	1640 to [d]	1718 to [d] (*S*-band-type antenna; auto-track at —95 dBm) 3720 to [d] (2-way doppler)
AFETR RIS: Twin Falls	1420 to 1664, 1720 to 1900, and 2070 to 2130	1361 to 2065
DSS 41	2680 to [d]	2940 to [d]
DSS 42	2880 to [d]	3120 to [d] 8940 to [d] (2-way doppler)

[a] Required intervals of class I coverage based on nominal mark times: continuous coverage from L to $L+544$ s, continuous coverage from $L+1575$ to $L+1875$ s, and continuous coverage from $L+3060$ to $L+3540$ s.

[b] Based on 101° launch azimuth.

[c] Based on phase-lock coverage.

[d] End time amounted to several hours because of the distance of the spacecraft from Earth.

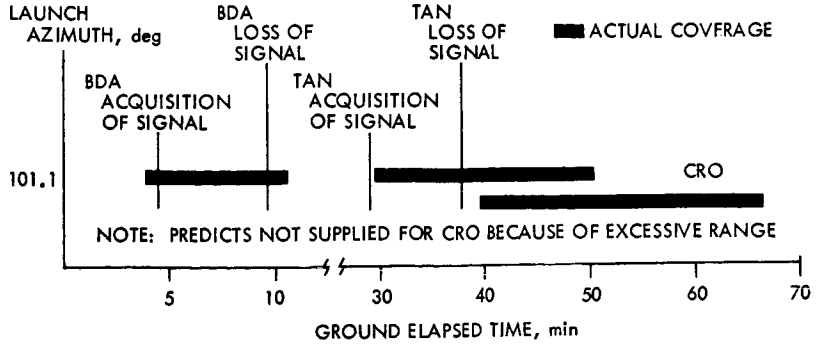

FIGURE 5–27.—Telemetry coverage: predicted and actual.

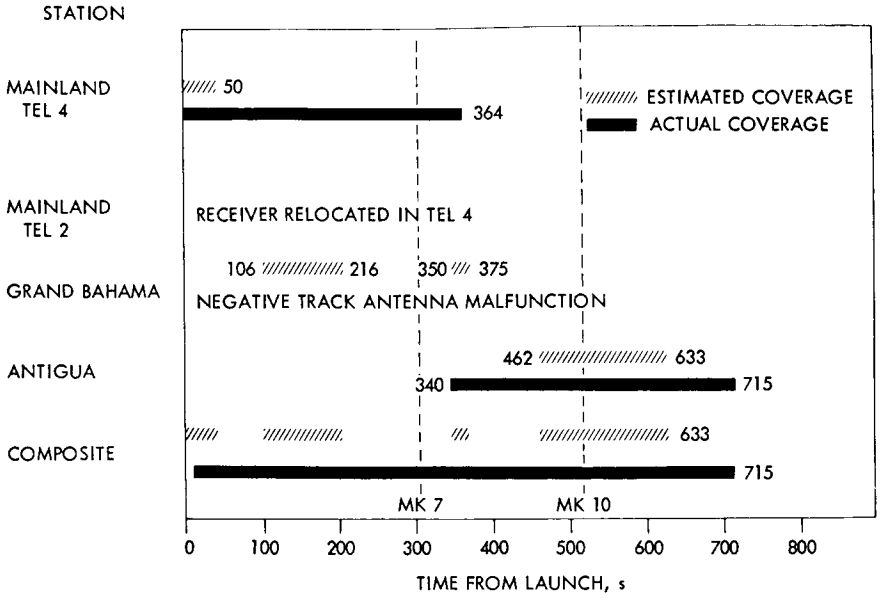

FIGURE 5–28.—AFETR station uprange telemetry coverage (*S*-band) for Mariner 5.

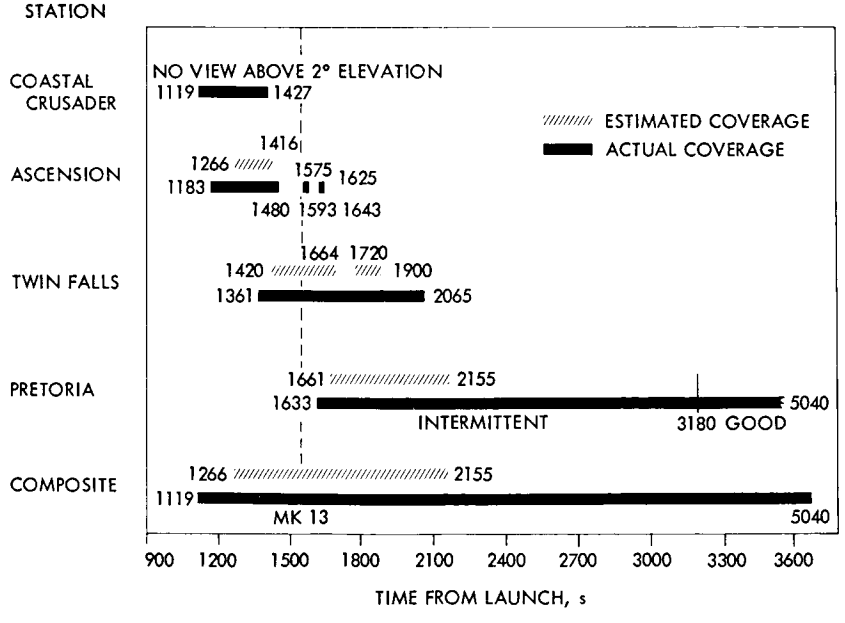

FIGURE 5–29.—AFETR station downrange telemetry coverage (*S*-band) for Mariner 5.

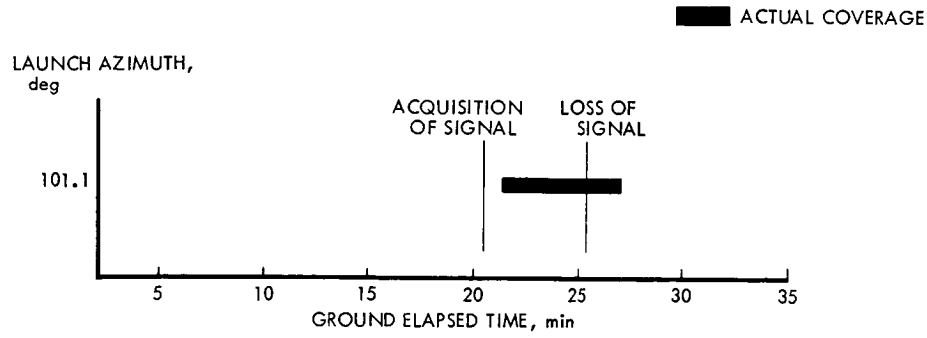

FIGURE 5–30.—USB site telemetry coverage: predicted and actual.

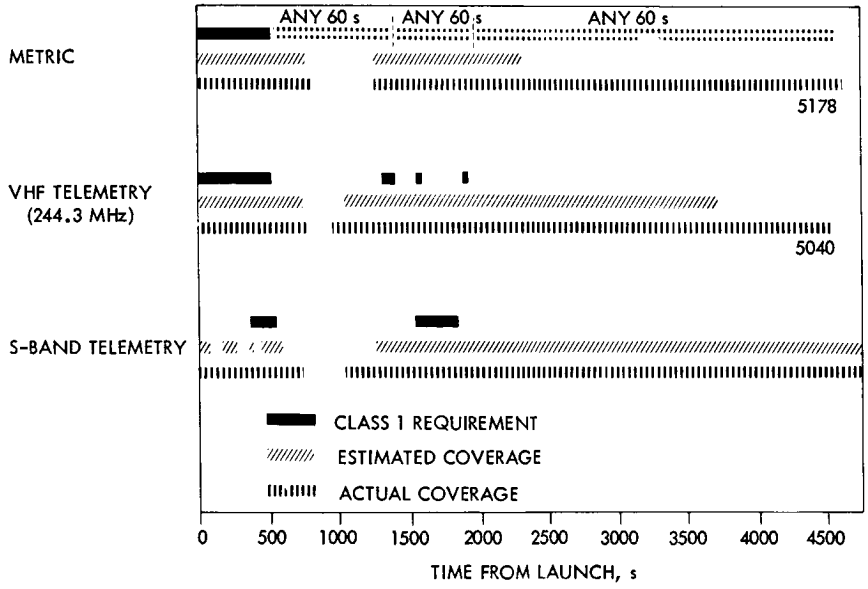

FIGURE 5–31.—DSIF telemetry coverage (*S*-band) for Mariner 5: near-Earth phase.

Table 5–XIII.—Mariner 5 support summary

Tracking support provided	Number of days	Percent of total
Less than class I	3	2
Class I, but less than class II	23	14.7
Class II, but less than class III	36	23
Class III	70	44.9
Greater than class III	24	15.4

that the class I requirements were not met occurred during the planned second playback of encounter data, which was neither required (because all data were recovered by the DSN from the first playback) nor performed. Most of the tracking in excess of class III resulted either from last-minute project requests for extra tracking or from backup tracking, provided at DSIF initiative, during encounter.

Tracking requirements and actual support provided to Mariner 4 are presented graphically in figure 5–32. Table 5–XIV shows that the minimum track-

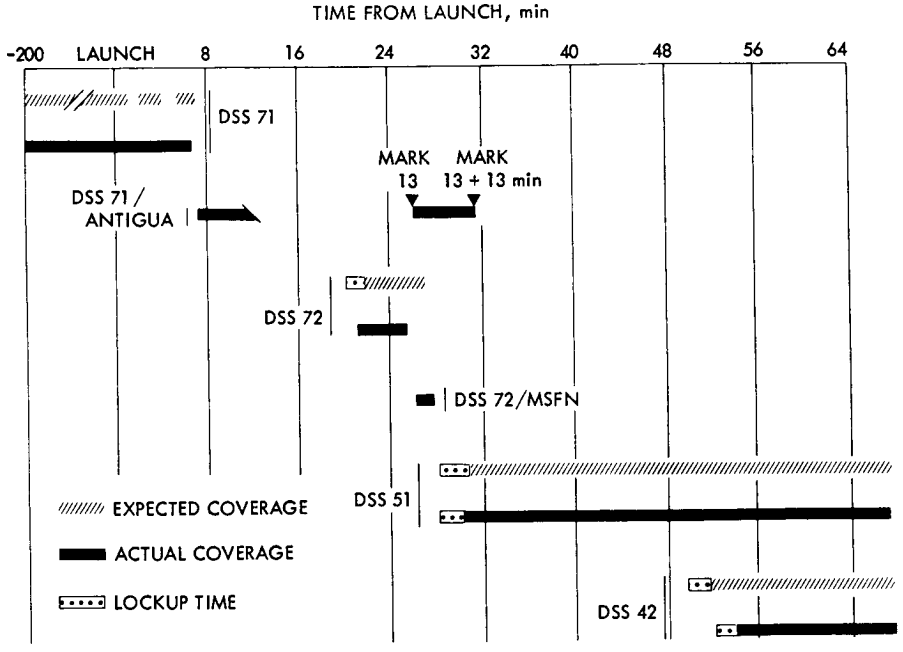

FIGURE 5–32.—Tracking requirements and support provided for Mariner 4.

Table 5–XIV.—Mariner 4 support summary

Tracking support provided	Number of days	Percent of total
Less than class I	62	35.2
Class I, but less than class II	61	34.6
Class II, but less than class III	23	13.1
Class III	23	13.1
Greater than class III	7	4.0

ing requirements were not met 35.2 percent of the days that tracking was required.

GCF coverage

Project requirements generally called for three Teletype circuits, one voice net, and one HSDL for each tracking pass. One Teletype circuit also was required to be operational whenever the spacecraft was in view of Stanford. On several occasions, the project voided the requirement because low received signal strength eliminated the possibility of any useful telemetry data decommutated by DSIF.

On four occasions during the Mariner 5 and Mariner 4 missions, GCF was unable to provide the full complement of required lines because of high-activity periods of other projects such as Surveyor and Apollo. Each case occurred during a Mariner low-activity cruise period and resulted in a reduction of only one Teletype line. GCF provided almost 100 percent of the requested coverage.

SFOF coverage

SFOF provided an equipped Mariner mission support area and flightpath analysis and command area whenever required for Mariner 5 or Mariner 4 operations. Voice communications, Teletype distribution, and closed-circuit television were provided throughout the mission.

DEEP-SPACE NETWORK MILESTONES

Mark I Ranging

Mariner 5 was the first spacecraft to be ranged beyond lunar distances with the Mark IA pseudorandom code ranging subsystem. The Mark IA subsystem ranged the spacecraft from after launch until the 22d day of flight. The subsystem ranged the spacecraft to a distance of 10 million km from Earth, with an accuracy of about 45 m.

R&D Planetary Ranging Subsystem (Mark II)

The Mark II ranging subsystem was designed and developed to be used on Mariner 5, and extensive tests and calibrations were performed within the stations. The first ranging operation on Mariner 5 occurred on June 21; valid range numbers were obtained.

The Mark II ranging subsystem operation continued routinely until about mid-August, when range data and predicts were in disagreement. This prompted redesign of the range coders. Subsequently, it was discovered that the predicts were in error; however, the redesign resulted in a system that was less susceptible to noise. Because the code acquisition time (a function of signal level) exceeded

the pass length, ranging was not attempted on the Mariner spacecraft until after the spacecraft was switched to its high-gain antenna on October 1. To insure the operational status of the subsystem, ranging was performed with a Lunar Orbiter spacecraft during the interim period. On the October 4 pass, Mariner 5 was successfully ranged, and the subsystem was declared ready for its primary objective—to range in the vicinity of Venus, thus providing the data enabling further refinement of the astronomical unit. The encounter sequence of events originally showed that the ranging operation was to cease some 4 hr before encounter to allow the command loop to be locked. To obtain maximum value from the ranging data, a test was proposed to determine whether the station uplink could be modulated by command and ranging modulation signals simultaneously, and whether there was any interaction between the two. On October 6, DSS 14 locked the spacecraft command loop and ranged the spacecraft. No interaction was observed. Later analysis showed there was no significant difference between range data with and without command modulation. Based on the favorable test results, ranging on Mariner 5 was performed up to 1 hr before encounter, thereby greatly enhancing data value. However, no commands were transmitted with ranging modulation applied. On November 5, ranging was accomplished to a distance of 157 million km, with an accuracy within 10 m.

Digital Demodulation Technique

The DDT was operationally tested at DSS 11 on four occasions. Results of the tests were encouraging, and the DDT program was transferred to DSIF and was successfully used at DSS 12 and DSS 51 between September 15 and October 1. The DDT, limited to the spacecraft mode 2 at 8⅓ bps (the normal cruise mode), improved telemetry thresholds by about 5 dB. On October 1, the spacecraft switched its transmitter output to the high-gain antenna, resulting in sufficient signal level for DSIF to be restored to its normal GTS configuration.

Redesign of 7044 Computer

The Mariner-Venus 1967 project was the first to use the 7044 redesign. After the midcourse maneuver and throughout the mission, the 7044 redesigned computer successfully processed data simultaneously from two spacecraft: Mariner 4 and 5, or Surveyor and Mariner 5.

Communications Processor

Mariner-Venus 1967 was also the first DSN-supported project to use the NASCOM CP subsystem, which provided computer switching of all Teletype messages throughout the facilities of the DSN.

Encounter and Playback

Playback of data from the onboard recorder during Mariner 5 encounter began during the next DSS 62 pass and continued for three passes, ending over DSS 62. All data transmitted by the spacecraft were recovered by the DSN; a second playback of the data was not necessary.

CHAPTER 6

Mission Operations System and Space-Flight Operations

The mission operations system (MOS) is composed of a combination of the Earth-based, mission-independent facilities and personnel provided by the TDS and the mission-oriented equipment, personnel, and procedures required to evaluate and direct space-flight operations for a given mission.

Premission activities include the required functional design and capabilities, mission-related hardware and software development, development tests and personnel training, and the preparation of a flight operations plan. Postlaunch operations include the analysis, decisionmaking, and control processes necessary to execute the required operations.

Basic concepts of the MOS for the Mariner-Venus 1967 project were extensions of those for the Mariner-Mars 1964 project. Differences were reflected in changes in the supporting facilities (i.e., DSN) as well as the change in missions.

Basic design guidelines were—

(1) Use Mariner 4 mission-related hardware and software wherever possible.

(2) Use new developments in the supporting facilities of the DSN, such as CP's and redesigned SFOF computers.

(3) Use onsite tracking station computers as a supplement and backup for SFOF computers.

(4) Use the multimission-support areas in DSIF to provide flexibility in obtaining tracking support.

(5) Obtain test experience and analysis-personnel training in conjunction with support of spacecraft checkout.

(6) Establish a single system for concurrent operation of Mariners 4 and 5.

A design team was established to formulate and develop the MOS design and to provide the plans, procedures, and tests required. The activities of the team were coordinated by the space-flight operations director (SFOD). The team consisted of (1) SFOD, (2) spacecraft analysis and command (SPAC) director, (3) flightpath analysis and command (FPAC) director, (4) space science analysis

and command (SSAC) director, (5) data processing operations director, (6) mission-related hardware (MRH) engineer, (7) DSN project engineer, and (8) other personnel as required.

Primary functions performed by the design team were to—

(1) Establish and monitor development and testing schedules.
(2) Prepare the NASA support instrumentation requirements document (SIRD) and supply inputs to the AFETR program requirements document.
(3) Prepare the space-flight operations plan and space-flight operations test plan.
(4) Assist in the preparation and review of appropriate intersystem interface documents.
(5) Coordinate and review requests for, and changes to, hardware and computer programs.

Basic configuration control and monitoring were accomplished by using established change control and failure reporting techniques. MRH rework and refurbishment were handled under the spacecraft system engineering change requirement procedure controlled by the spacecraft system engineer. A slight modification of this procedure was necessary when the MRH was transferred to the TDS for operations and maintenance.

A procedure almost identical to the DSN programing change requirements was used in computer program development. A three-phase freeze policy was adopted: (1) freeze of the requirements (functional design), (2) freeze of the detailed design, and (3) freeze of the entire program. The procedure was controlled by the SFOD and was carried over after integration of the programs into the DSN.

Changes to DSN capabilities or configurations were handled by standard DSN change control procedures. These procedures were available for hardware and software in all DSN systems.

Spacecraft problem failure report (PFR) procedure was used for MRH development and checkout. After transfer of the hardware to the DSN, the appropriate DSN failure reporting procedure was used (SFOF or DSIF).

The DSN/SFOF discrepancy reporting procedure was used for computer program checkout and general operations testing. After transfer of the onsite (DSIF) program to the DSN, the DSN/DSIF procedure was used for that particular program.

Basic guidelines regarding ground commands and their control were—

(1) Any command or commands considered necessary for corrective action or for achieving standard space-flight operation had to be approved by the SFOD. Upon concurrence of the project manager, the command or commands would be transmitted to the appropriate tracking station for execution.
(2) Command requests would be made only by the technical and operations teams within the SFOF, using approved command-decision procedures.
(3) Two trajectory-correction maneuvers would be available to achieve a nominal space-flight operation; the second maneuver would be used only if the first maneuver did not supply an adequate trajectory correction.
(4) Approved procedures would be used to transmit command instructions from the SFOF to the tracking stations.

General guidelines regarding the approval and transmission of commands to Mariner 5 were—

(1) No command would be sent that could be determined to have a potential failure mode catastrophic to the mission.
(2) No command would be sent that would substantially degrade the probability of achieving the primary mission objective.
(3) All sequences would be tested first by the model spacecraft in the spacecraft assembly facility (SAF).
(4) Confidence in the spacecraft capability should not be construed as a license to exercise all modes of operation without regarding their value to primary mission objective.
(5) No command would be approved that had not undergone a thorough analysis as to need and consequences.
(6) Command operations in support of failure analysis would be discouraged unless the analysis was necessary to meet the primary objective.

The three critical periods for the Mariner-Venus 1967 project were launch, midcourse maneuver, and encounter. Each of these periods was followed by a cruise phase, or noncritical period.

For the critical periods of flight, special procedures were established in areas of command, data processing, and operations. A nominal sequence of events was established for each phase of operation. A spacecraft flow diagram was developed to provide a direction for corrective action if certain nonstandard conditions should exist.

The operations team, the analysis teams (FPAC, SPAC, and SSAC), project office, DSN, DSIF, and other supporting agencies were staffed to permit personnel

changes when activity extended over long periods. Special personnel were required to maintain communications facilities and access control to areas involved in analysis and control and to operate dual-computer systems. Special personnel also were required in the complementary analysis team (CAT) areas for real-time backup.

CAT's provided a means for using the talents of personnel not directly assigned to flight operations, but who had detailed spacecraft or mission design knowledge. The teams functioned as advisers to subsystem cognizant engineers in the SPAC area.

The primary role of the teams was to provide knowledgeable support on specific problem areas, with no specific operational function to perform. Secondary roles were to—

(1) Provide a focal point for sustained interest and information on the part of the design, development, and management personnel during the flight operations phase.
(2) Provide some orientation and training for design and development personnel on the problems encountered in flight.
(3) Provide potential replacements for operations personnel in the SPAC area.

Because the primary function of the teams was to support individual analysts, and not to be a direct part of operations, an organization based on technology and line-organization discipline was dictated. For this reason, the teams were associated with the line-organization structure. Each manager of a technical division appointed a CAT coordinator who was responsible for all planning activities and for directing the teams during the flight. The CAT coordinator also provided liaison between the CAT and the SPAC analysts.

Data handling and voice communications equipment similar to the SPAC equipment were provided to the CAT area of each technical division (fig. 6–1). This equipment included 100-word/min computer-driven Teletypes, 60-word/min standard Teletypes, appropriate voice networks (listen only), television displays, and an HSDL.

The Teletypes were slaved to the subsystem (or divisional subsystem group) machines in the SPAC. The television displays provided mission time and ground communications status. The HSDL fed a digital-to-analog converter for stripchart display in the CAT area for the guidance and control division.

MISSION-RELATED HARDWARE DEVELOPMENT

The MRH for the Mariner-Mars 1964 project was returned to Goldstone

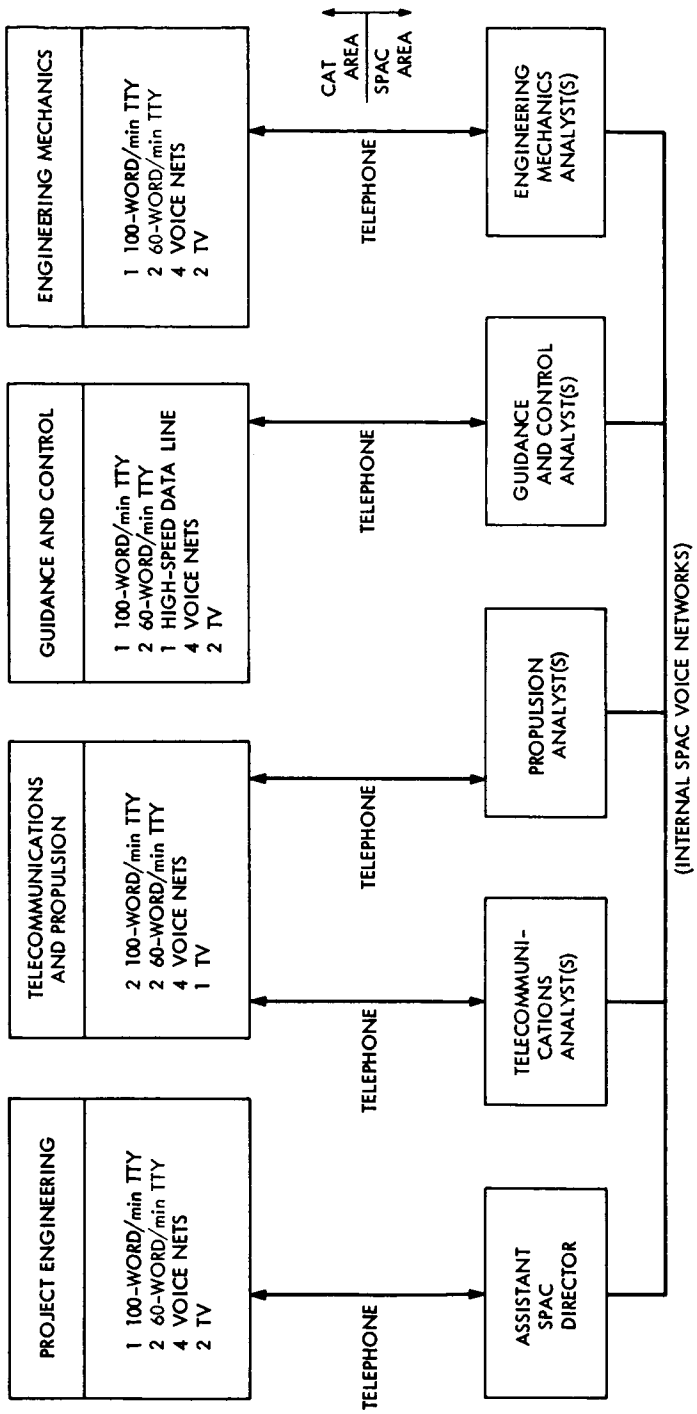

FIGURE 6–1.—CAT equipment provision.

by the various deep-space stations for refurbishments and modifications necessary to support the Mariner-Venus 1967 project. Equipment conditions and modifications for the various subsystems are described below.

Ground Command Subsystem

Equipment condition

Physical condition

The physical condition is the condition of the units after they have been received from the various locations. These statements may not apply to all units specifically but, as generalizations, are applicable to the read-write-verify (RWV) refurbishing effort.

In general, the commercial equipment within the consoles was in operating condition, although all units required calibration. After completion of an initial inventory, it became apparent that parts had been removed from the RWV's to supply equipment for other station requirements. Without considering spares, equipment shortages were as follows:

Equipment:	*Quantity*
Time display	5
Monitor receiver	9
Counter	3
Oscilloscope	3

Operational condition

During detailed checks of the operational condition, the RWV modulator and detector were realined and the machine was exercised through all of its operating modes. Some wiring errors and some component failures were located and repaired as a result of these checks.

After completion of the testing, all commercial equipment was removed from the RWV's and sent to Goldstone for preventive maintenance, calibration, and cleaning.

Refurbishment

Refurbishment of the RWV's began with a detailed test of all units. This test had two primary objectives: (1) to verify that the modifications installed in the units for the Mariner 4 mission were installed correctly and (2) to verify that the modified RWV was operating normally.

Modifications

Operation of the RWV and station reports indicated the areas in which the RWV was deficient and required modification. All modifications except one were made on the authority of engineering change reports (ECR's). The non-ECR

modification involved a change in the frequency coverage of the RWV monitor receiver.

Tests

Completion of the modification of the RWV's consisted of the installation of any mission commercial equipment and performance of two tests on each unit. These tests included a flight-acceptance test and an rf check. The flight-acceptance tests were witnessed in all cases by a DSN representative. Radiofrequency checks were performed to prove that the phase of the RWV output was of the correct sign so that the flight system would lock to the received command modulation. If this signal were inverted, the command subsystem would fail to lock and no commands would be transmitted to the spacecraft. These tests were performed using a command modulation checker (verified in the SAF at JPL) to simulate the spacecraft command detector. All units passed this test.

Ground Telemetry Subsystem

Equipment condition

Physical condition

The three GTS configurations were (1) eight DSN/GTS's, which consisted of a two-bay rack of equipment used at the deep-space stations to process the receiver output; (2) two system test complex (STC)/GTS's which consisted of five bays of equipment (two two-bay racks and a one-bay rack) used on the spacecraft test complex to check the spacecraft before launch; and (3) an SFOF/GTS, which consisted of a one-bay rack of equipment used in the SFOF to process data from the high-speed data lines as a backup for the 7044 computer.

Six of the eight DSN/GTS's performed the basic functions of demodulating the composite signal and, in turn, decommutating the demodulator output and printing it out on the printer. One GTS had been damaged while in transit, and another had a data programer problem. Four amplifiers and mounts were missing from one of the STC/GTS units.

Operational condition

During checks of the operational condition of each GTS, the missing amplifiers and mounts were replaced on the STC/GTS, the wiring of each single-bay rack was reinstalled, and a binary-coded decimal time input was added to the SFOF/GTS to make it compatible with the digital-to-analog-converter interface.

Refurbishment

Refurbishment of each GTS began with detailed testing of the unit. The equipment was disassembled, cleaned, recalibrated, modified, and reassembled.

Electrical checks were made, and the equipment was flight-acceptance-tested in the presence of a DSN representative.

All commercial equipment was calibrated, and all digital printers were checked.

Modifications

All modifications to the DSN/GTS's and STC/GTS's were made on the authority of ECR's.

Tests

After completion of the modifications, each GTS was reassembled and checked electrically. After the GTS was operating correctly, a final detailed inspection was made. Discrepancies found by the inspection were corrected, and the GTS was given a final flight-acceptance test.

Spares

Equipment condition

Physical condition

Inspection, after arrival of the spares, disclosed that the heavy equipment had torn loose within the shipping boxes, damaging both the equipment and the boxes. In some boxes with drawers, vibration had loosened screws holding the drawer sliders, causing the drawers to tilt, jam, and spill their contents. Some equipment was damaged.

Operational condition

Most of the effort regarding the spares centered on the spare printed circuit cards. Of the 2700 received, 965 were tested electrically to determine their operational condition. Power supplies, transformers, amplifiers, etc., were also inspected and tested.

Refurbishment

The printed circuit cards were inventoried as they arrived and were placed systematically on holding racks. This arrangement made all cards easily accessible and also protected them from further damage. A card file was generated to facilitate bookkeeping on each type of printed circuit card. This card file contained the printed circuit card assembly number, a list of MRH equipment in which the card was to be used, the quantity of cards required for spares, an inventory of cards received, the quantity of cards that had been electrically tested and determined "good," and the quantity of cards that had been electrically tested and determined "bad."

About 2700 cards were received and inspected as they were placed on the racks. Each printed circuit card was stamped "OK" if accepted, and an inspection report was generated for any discrepancy. All discrepancies were corrected before the card was stamped and accepted for use in the spares program.

There were 175 different types of printed circuit cards produced by six different manufacturers. Although 2700 cards were inventoried, only 965 cards were electrically tested and shipped to the oversea stations. Another set of spares was also generated for use in SAF.

Two additional kits of spares were sent to Goldstone. These two kits were tested by the DSN personnel at the Goldstone repair depot, and one set of spares was shipped to DSS 51. The second set of spares remained at the Goldstone repair depot as backup spares.

Another category of spares included small items such as connectors, crimping tools, inductors, small transformers, lamp bulbs, fans, etc. Because some of these items were not returned by the stations, it was necessary to purchase new parts as replacements. Most of the purchased parts were received before the initial shipment of spares to the deep-space stations. Other parts arrived after the initial shipment and were shipped to the stations for addition to the kits of spares.

Resistors, small capacitors, transistors, diodes, etc., were not distributed. Stocks of piece parts were considered adequate for emergency repairs at the oversea stations. Normal repair procedure was to return failed units to Goldstone where equipment and personnel were available to make complete repairs.

An effective equipment maintenance program requires not only spares but also an arrangement that permits the desired ones to be located and removed easily as the need arises. To allow the stations to organize the spares upon receipt, each part was identified by item number, part number, and the part nomenclature or description.

The test fixture was composed of a chassis with an appropriate card connector mounted on it. Each terminal of the connector was accessible by banana jacks. Any signal could be placed on any pin with the use of commercially available test equipment. A separate test fixture was built to accommodate each type of card connection. About 90 percent of the MRH spare cards were tested in this way; a few of the analog-type cards, which could not be conveniently tested by this method, were tested in the actual equipment by RWV and GTS equipment operators.

Digital-to-Analog Converter

Real-time analog display of guidance and control spacecraft functions were

required in the SPAC and guidance and control analysis team (GCAT) areas during launch, Sun acquisition, star acquisition and identification, trajectory-correction maneuvers, etc. Most of these engineering displays were required in real time to verify normal operation and to apply corrective action to the spacecraft if necessary. It was essential that these spacecraft critical measurements be available with minimum delay and with the highest probability of occurrence. For these reasons, the digital-to-analog converter (D/AC) and recorder were supplied to SPAC and GCAT for support during the Mariner 5 flight. The D/AC and recorder interfaced directly with the HSDL from each deep-space station.

A D/AC was designed, as part of the Mariner 4 CC&S, to display certain engineering telemetry data channels on an eight-channel analog recorder. This analog display was implemented for the purpose of real-time, quick-look, spacecraft engineering status, particularly with regard to the AC subsystem during acquisition and midcourse maneuver phases of the flight. Because this display proved valuable during the Mariner 4 flight, it was incorporated into the Mariner-Venus 1967 project.

A major change in the spacecraft data handling by the DSN caused the D/AC for Mariner 4 to be redesigned for Mariner 5. (See fig. 6–2.) This redesign was so extensive that a decision was made to build completely new equipment rather than to modify the existing unit. Also, because SPAC and GCAT would be located in different buildings, an additional D/AC was required.

The D/AC was designed to provide analog recorded display of the engineering telemetry channels associated with—

(1) Three subcommutated channels
(2) Pitch, yaw, and roll gyroscope outputs
(3) Pitch, yaw, and roll position sensor outputs
(4) Canopus intensity
(5) Earth sensor output
(6) Power switching and logic voltage

It also provided digital recorded display of time when operating from the HSDL; a recorded display of deck synchronizations and channel markers; Nixie display of event register status and time; compatibility with both Mariner 4 and 5 telemetry data; word synchronization, bit synchronization, and information associated with the 7 bits of spacecraft data to be used by external decommutating equipment, e.g., GTS and science; and HSDL station AGC as an analog output for remote recording.

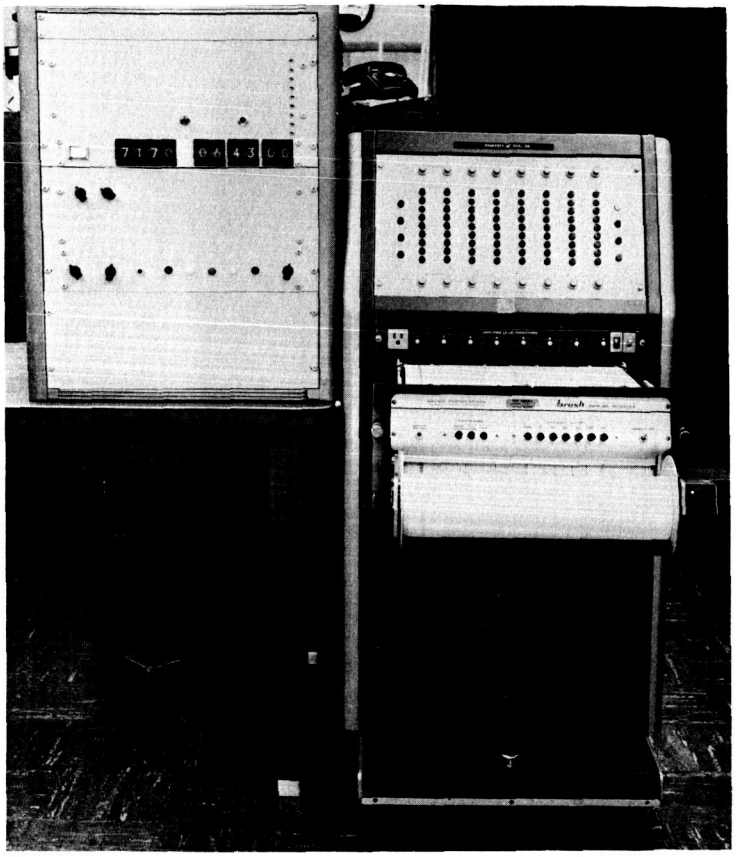

FIGURE 6–2.—Closeup of digital-to-analog converter.

High-speed data line logic

The primary mode of operation for the D/AC is associated with obtaining telemetry data from the HSDL. The D/AC used in SPAC has the additional capability of operating from the Teletype data if HSD are not available.

One HSDL data block is associated with each channel of spacecraft data. Each data block consists of 14 words of 5 bits, preceded by a 110-synchronization pattern. The first two words in this data block are all "ones" and are used as the data-block synchronization, whereas the 110-synchronization pattern is used as the individual word synchronization. The HSDL has two outputs: digital information and a 1200-Hz square-wave synchronization signal.

After the first two words have been received as the data-block synchronization, and the 110 pattern is recognized for each succeeding word, the 1200-Hz synchronization signal is used to count down a divide-by-5 bit counter. Each state of this bit counter corresponds to one of the 5 information bits associated

with each word. Each time the bit counter cycles through 5 bits, it steps a divide-by-12 word counter. Each state of this word counter corresponds to one of the 12 data-block words following the data-block synchronization. By selecting the appropriate word and bit time from these counters, each bit of data within the data block can be extracted and processed as desired.

Word 3, bit 1, identifies the data block as either a spacecraft telemetry channel or as a station AGC measurement. If this particular bit is a "one," the AGC flip-flop is set; if it is a "zero," the spacecraft word flip-flop is set. Word 3, bit 2, is not processed by the D/AC. Bits 3 and 4 contain the binary-coded decimal (BCD) data for tens of hours. Bit 5 in each word is a parity bit that is adjusted for an even number of "ones" in each word (except the first two data-block synchronization words).

Words 4 through 9 are associated with BCD data for hours, tens of minutes, minutes, tens of seconds, seconds, and tenths of seconds, respectively. Tenths of seconds are not displayed by the D/AC.

Words 10 and 11 contain the 7 bits of spacecraft data. These bits are routed to a temporary storage register. If they are all "ones" (binary 127) corresponding to an engineering frame synchronization, the engineering flip-flop is set. The divide-by-20 channel counter is now enabled and steps once for each succeeding data block. Each state of this counter corresponds to one of the spacecraft telemetry channels. During normal operation (telemetry mode 1 or 2), after this counter divides by 20, it resets itself and the engineering flip-flop and waits until another engineering frame synchronization or a science frame synchronization (binary 07) is received. If a science frame synchronization is received, the science flip-flop is set, the channel counter enabled, and the reset delayed until two cycles (frames) through the counter have occurred (40 spacecraft channels). In data mode 3, the reset is delayed until three cycles have occurred (60 channels), and in data mode 4, the reset is delayed for eight cycles (160 channels).

Connected to the temporary storage register is each of the storage registers associated with each channel on the analog recorder and its associated D/AC amplifier. The data are not transferred to any of the D/AC storage registers until a strobe, or transfer, signal for each register is generated. These strobe signals are obtained from the channel counter when the engineering flip-flop is set (engineering data). Preselected spacecraft engineering data are thus stored, converted to a convenient analog voltage, and displayed on the analog recorder.

Similarly, the data bits are associated with time and AGC, and are routed to their respective storage registers for Nixie display or recording.

The only remaining information bit processed by the D/AC is word 13,

bit 4, which is associated with the DSIF data synchronization condition. If this bit is a "one," the station-out-of-synchronization flip-flop is set. Each of the main control flip-flops is monitored by a light on the front panel for ease in determining the current data condition.

When operating from the HSDL, additional functions are available to aid in the display and readout of the data. A computer-processing capability is available for displaying the data in the normal mode when the data on the HSDL are the complement of the actual spacecraft data. A derived synchronization function is available to automatically generate deck synchronizations if the spacecraft data bit error rate is high.

Teletype logic

The Teletype data line is entirely different from the HSDL. (See fig. 6–3.) It consists of 6 bits of non-return-to-zero, single-line data (information only). A synchronization signal for processing the data must be generated internally. The signal level between words is always a "one," and the first bit of each word is always a "zero." Therefore, a transition from a "one" to a "zero" always occurs at the beginning of each word. This transition is used to generate the required synchronization signal. A gated synchronization generator is started at this transition and generates six synchronization pulses and stops until the next transition is sensed. These synchronization pulses are spaced in time coincident with the 6 information bits in the Teletype data.

The Teletype input buffer senses the transition from a "zero" to a "one" as well as the transition from a "one" to a "zero." A flip-flop is set or reset by the output of this buffer and, therefore, follows the data on the Teletype line. The output of this "information" flip-flop and the internally generated synchronization are used to load the last 5 Teletype information bits into a temporary storage register.

The 5 bits of data stored are binary-coded Baudot for operation with the Teletype machines. It is, therefore, necessary to convert the data from Baudot to 7-bit binary. Two Teletype words are required for each spacecraft telemetry word. These Teletype words are designated digit 1 and digit 2. A flip-flop is used to keep track of the correct digit for each telemetry word. This flip-flop is initialized (digit 1) whenever a 0, 1, or 2 (which are unique to the first digit) is sensed in the data. It is also initialized whenever a character other than a number is sensed (e.g., space, carriage return, line feed, etc.).

After the 5 bits of Teletype information are stored, a 2.5-kHz clock is started to process these data further. This clock generates 24-bit times for each Teletype word. (See fig. 6–4.)

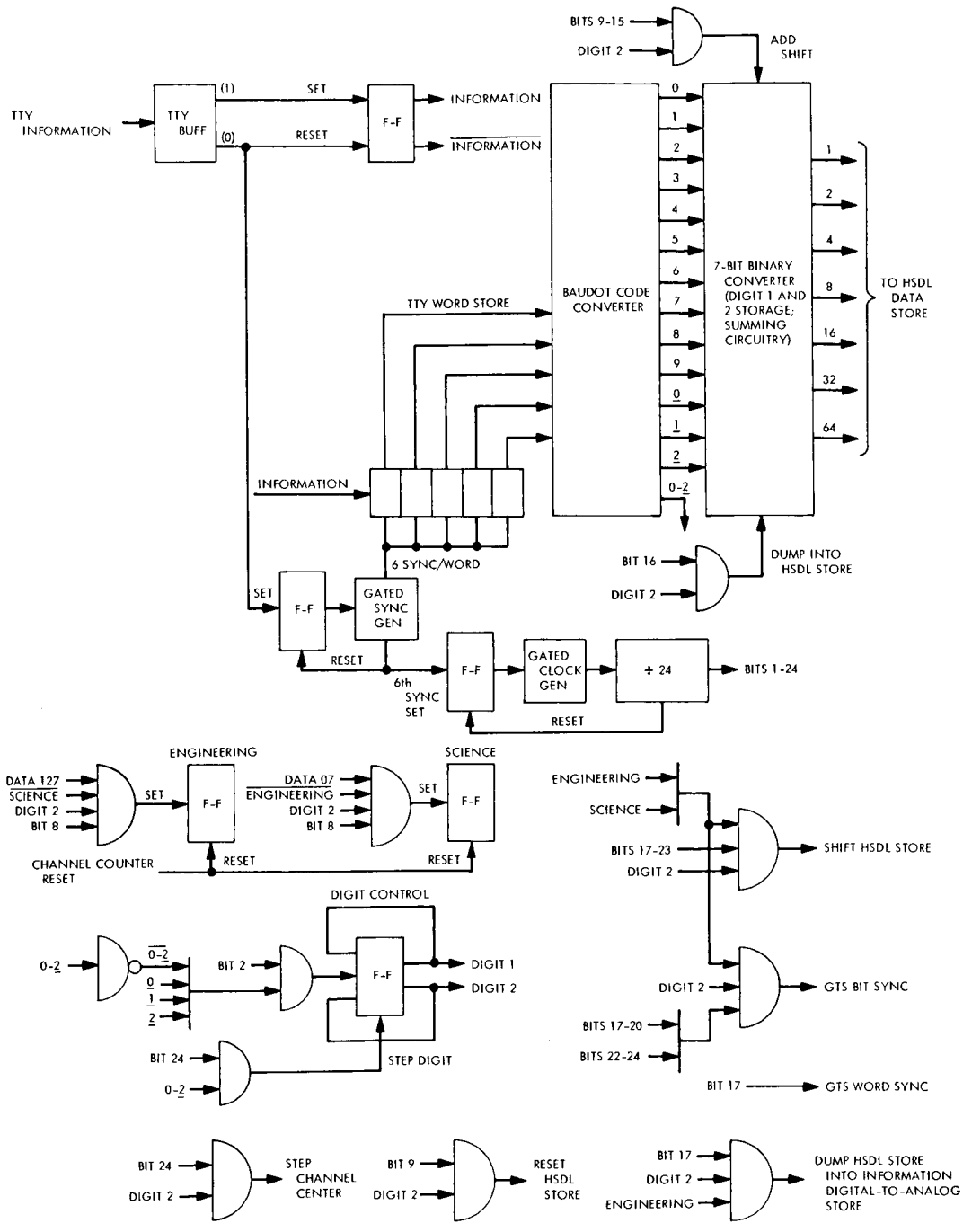

FIGURE 6–3.—Teletype logic block diagram.

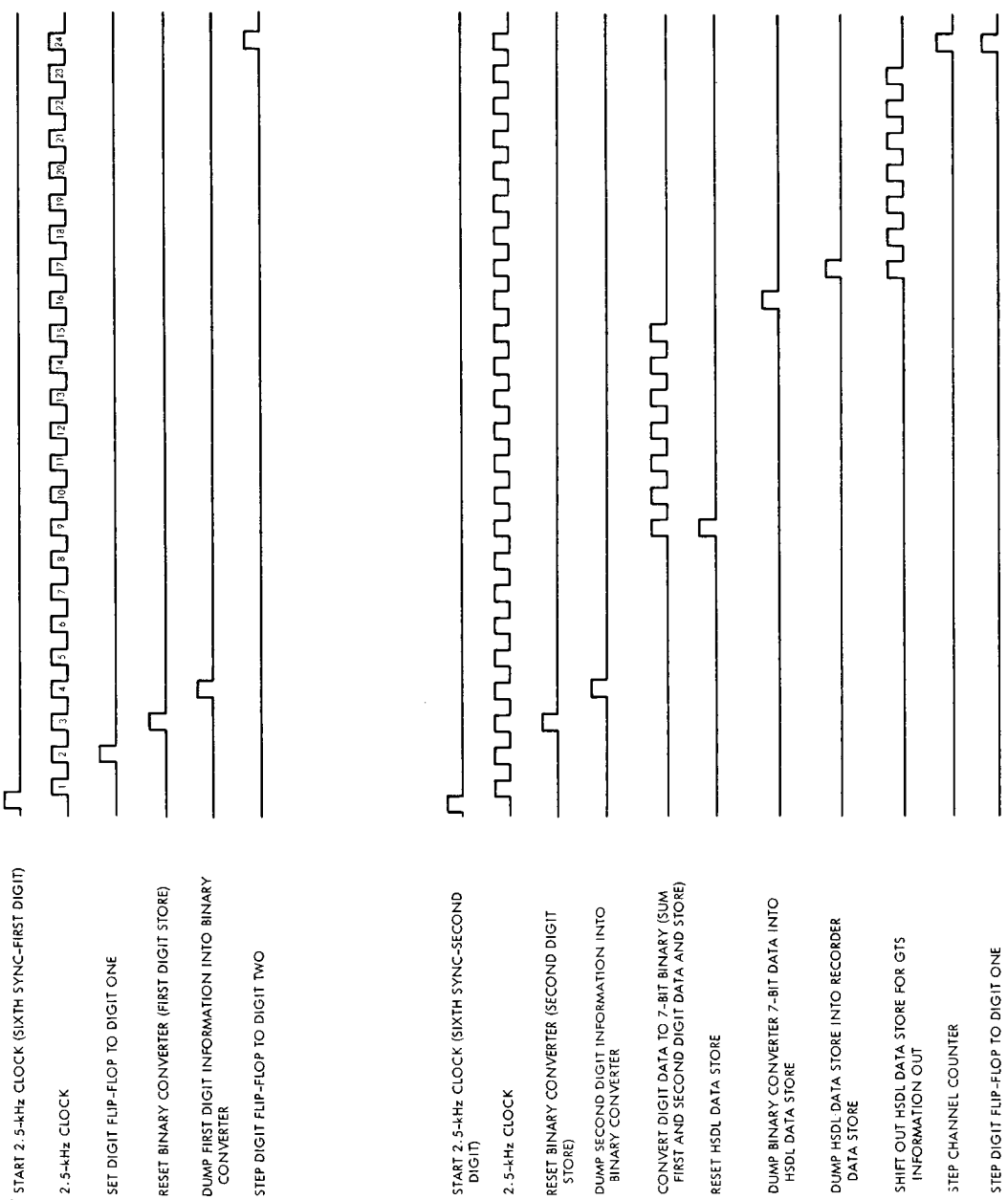

FIGURE 6–4.—Teletype conversion control timing diagram showing how each bit is used to process the Teletype word.

The 2.5-kHz clock is started by the last (sixth) synchronization pulse generated as the Teletype word is sensed. If the Teletype word is decoded as a nonfigure, 0, 1, or 2, the digit flip-flop is set to digit 1 at bit time 2. At bit 3, the storage register within the binary converter used to store the digit 1 data is reset. At bit 4, the digit 1 data are dumped from the Baudot decoder into this digit 1 store. Bit 24 steps the digit flip-flop to digit 2 if digit 1 is a number. It remains in the digit 1 position if the Teletype word is a space or some other nonnumber.

When the next Teletype word is sensed, the last synchronization starts the 2.5-kHz clock again. If the Teletype word is decoded as a number between 0 and 9, the digit flip-flop remains at digit 2. Bit 3 resets the digit 2 storage register within the binary converter. Bit 4 then dumps the digit 2 data into the digit 2 storage register. At bit 8 time, the contents of the digit storage registers within the binary converter are strobed for the presence of an engineering or science frame synchronization. If the two-digit word stored is a frame synchronization, the appropriate engineering or science flip-flop is set and the channel counter enabled. Bits 9 through 15 remove the digit data from each register. Then these bits are added together, and the result stored in the 7-bit digit 1 register. Bit 16 dumps these 7 bits of information (corresponding to the binary DN of one spacecraft telemetry channel) into the HSDL temporary storage register. Bit 17 then dumps these data from the HSDL temporary store into the appropriate D/AC storage register, as discussed previously. Bits 17 through 23 remove the data from the HSDL temporary store for use as the information output to the GTS equipment. Bit 24 steps the HSDL channel counter to the next channel and the digit flip-flop to digit 1. The process is then repeated for the next two Teletype words that correspond to a spacecraft telemetry data channel.

Event register status (telemetry channels 115 and 116) are Nixie tubes displayed on the front panel for both HSDL and Teletype operation. An audible alarm is also provided to signal when any of the event registers change by an odd number.

Recorder control

Eight analog channels, two event pens, and a remote speed control are provided by the analog recorder and are used in displaying telemetry data.

The analog channels are used to display the telemetry data output from the D/AC amplifiers. These D/AC amplifiers consist of a weighting network and an integrated-circuit operational amplifier (fig. 6–5). The analog output sensitivity from these amplifiers is 25 mV/DN. Switches are provided on the front panel of the D/AC to increase this sensitivity to 50 mV/DN. At this increased sensitivity, however, the D/AC amplifier will saturate at about 100 DN. The

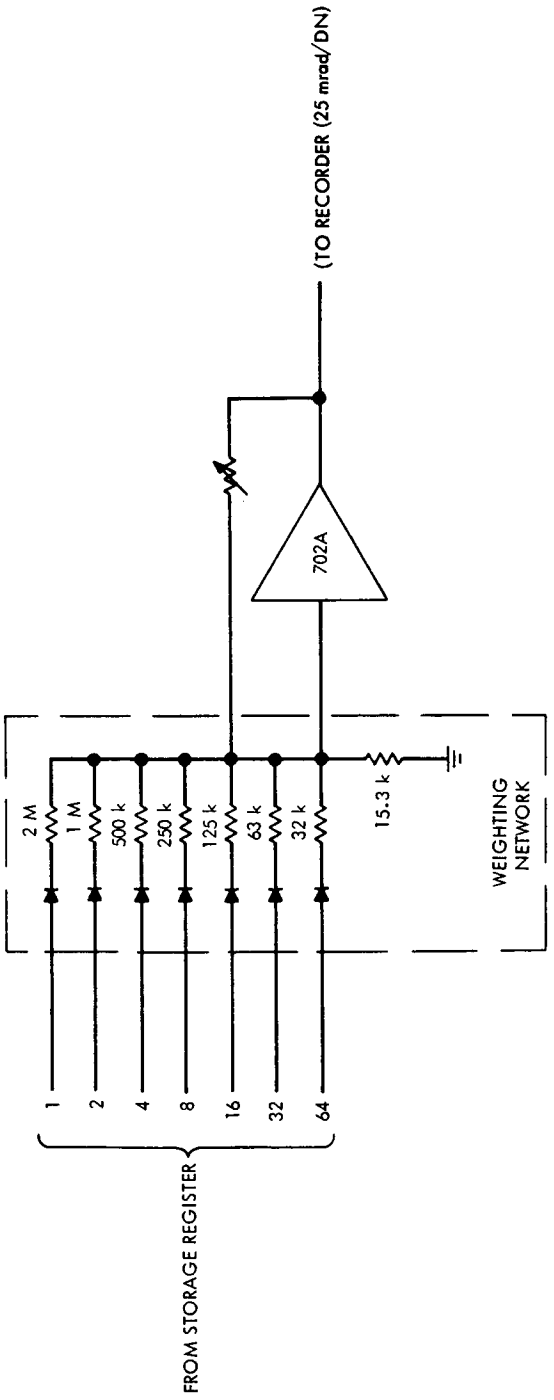

FIGURE 6–5.—D/A amplifier schematic.

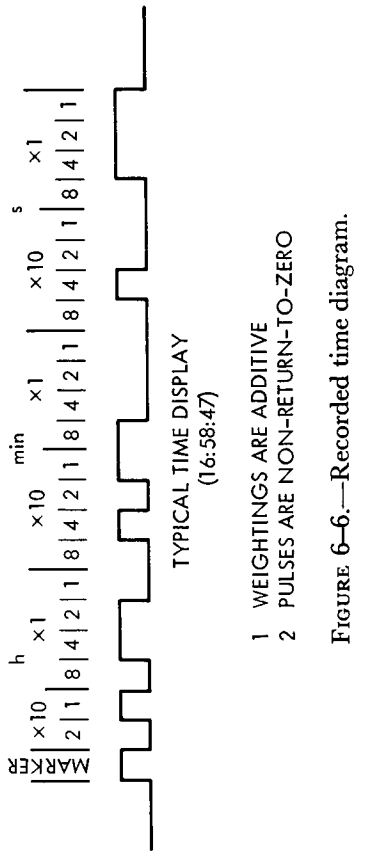

FIGURE 6–6.—Recorded time diagram.

recorder input attentuator can be adjusted to give the recorded scale factor desired. Normally, the data are recorded with a scale factor of 4 DN per small division on the record paper.

The left-event pen on the recorder is used for recording time when operating from the HSDL. (Time is not displayed or recorded when operating from Teletype.) This display consists of a marker pulse followed by appropriate pulses in BCD for hours, minutes, and seconds. (See fig. 6–6.) The right-event pen changes position when a station-out-of-synchronization indication occurs.

Remote recorder speed control is used to adjust the recording speed for optimum display and to conserve paper when nothing is being recorded. Three different speeds are used during normal data recording: (1) adjustable speed for recording time, (2) adjustable speed for recording telemetry data, and (3) fixed speed (slow) for nonrecording (e.g., science or no data). Speed switching is automatically controlled by the electronics within the D/AC. The actual speeds used for time and data recording can be selected from switches on the back of the D/AC.

All logic within the D/AC is implemented by diode transistor logic integrated circuits (14 lead flat packs) mounted four to a board. Of these devices, 344 are used in the D/AC containing both HSDL and Teletype logic, and 244 in the D/AC containing only HSDL logic.

The D/AC amplifiers utilize discrete components as well as an integrated-circuit operational amplifier. All buffer amplifiers required for input/output interfacing, other than with the analog recorder, utilize only discrete components.

All electronics are incorporated into two 48-cm panels installed in a semi-portable, 91-cm cabinet. A third panel area is provided for HSDL station selection equipment.

COMPUTER PROGRAM DEVELOPMENT, SOFTWARE

Figure 6–7 shows the hardware and software subsystems used to support the Mariner-Venus 1967 project. The software subsystem is divided into three major areas: DSIF, GCS, and SFOF. The software efforts discussed here are depicted by the blocks indicated by dashed lines (fig. 6–7).

Telemetry and Command Subsystem

The onsite subsystem includes the GTS and the TCP, which consists of an SDS 920 computer and a communications buffer. The communications buffer is essentially the external, or output, interface. The primary function of the TCP is to process Mariner spacecraft telemetry data by frame detection, engineering decommutation, science decommutation, Teletype output, HSD output, and data logging.

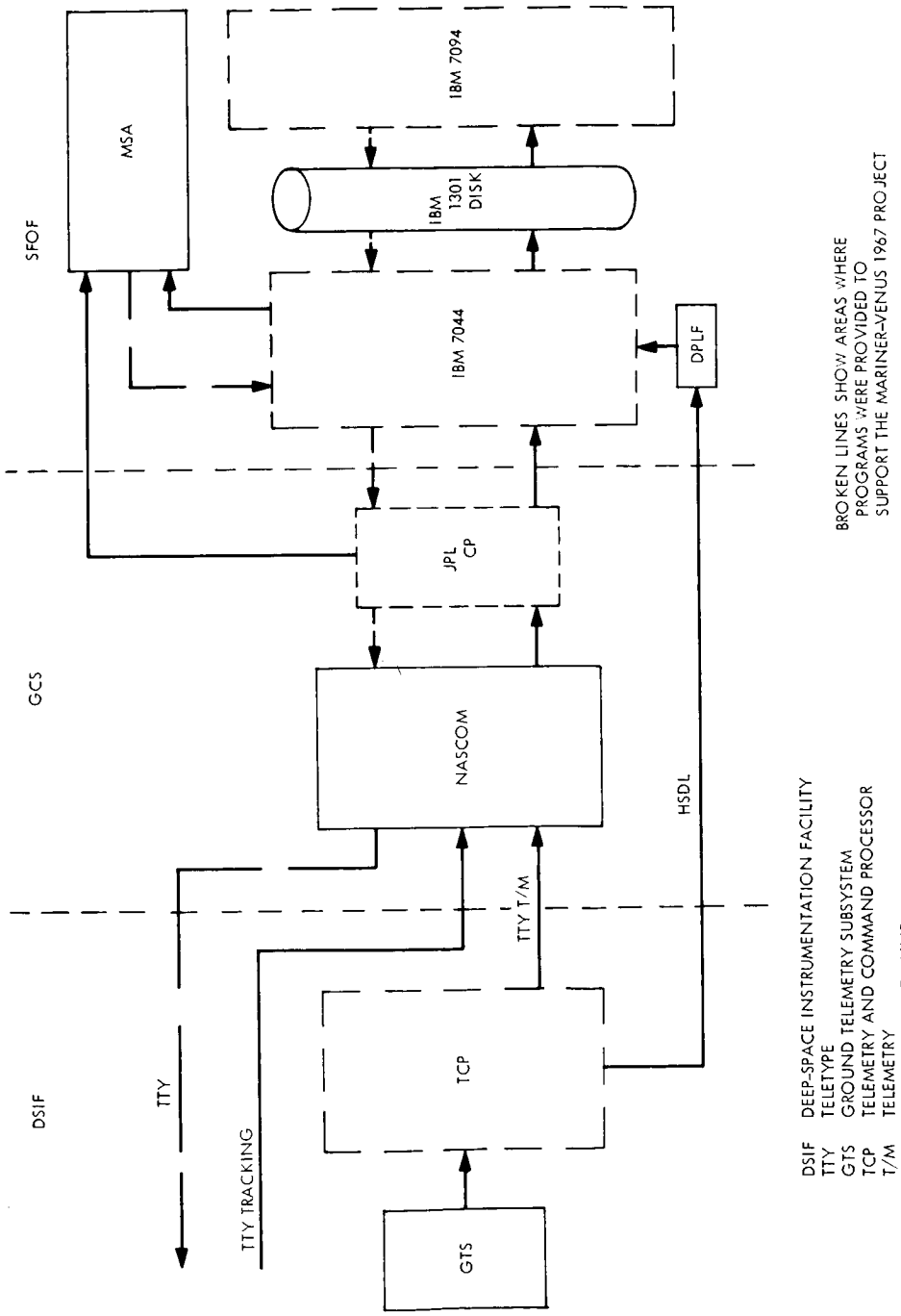

FIGURE 6–7.—Data processing subsystem for support of the Mariner-Venus 1967 project.

Data from the GTS are received in the form of digital telemetry data, word synchronization, bit synchronization, ground receiver AGC data, and receiver in-lock and out-of-lock status. The station-time input also is used in time tagging the data. The TCP online typewriter provides control inputs to the program.

Output data are formatted for transmission through the communications buffer on various Teletype lines and HSDL's for visual display of the spacecraft AGC and static phase error (SPE) at the deep-space stations. All data received by the TCP, except AGC data, are formatted and stored on a log tape.

Communications Processor

Transmission of Teletype data for the Mariner-Venus 1967 project was made via NASCOM. The software task in this area was primarily to define and operate a working interface between JPL and NASCOM.

Message switching was the basic transmission scheme used. In this procedure, messages originating at the deep-space stations are routed through CP's to desired terminal points in SFOF by means of routing data contained in headers affixed to the body of the message. The JPL CP's are also used for routing data originating within SFOF. Terminal points include teleprinters in the Mariner support area, TV printers, and the data processing subsystem. Messages are also routed from SFOF to the tracking stations.

7044 Redesign

Teletype data inputs to the SFOF data processing subsystem from the deep-space stations enter the SFOF CP, which transmits the data to the 7044 redesign subsystem via input/output programs and the 7288 multiplexer. The 7044 computer receives these inputs and stores the data in buffers. The CP input processor extracts the data from input buffers and sorts them into other buffers according to spacecraft number, data type, station identification number, and control inputs by operations personnel.

The 7044 computer operates the mission-dependent processors, as well as the tracking residual programs when an appropriate number of inputs have been received or when an appropriate time has elapsed after the inputs have been received. The mission-dependent processors process the data by performing decommutation, identification, scaling, and alarm checking. The information is stored into buffers to be formatted and sent to SC 3070 printers, Milgo plotters, and teleprinters. Data sent from 7044 computer to the SC 3070 printers and Milgo plotters are sent directly by the 7288 multiplexer. However, all Teletype data are sent to the CP, which drives the teleprinters in SFOF. No teleprinters are driven directly by the 7044 computers.

Data also are received from the telemetry-processing stations through the 7288 multiplexer and are stored in buffers. The appropriate processors are operated, and the data are extracted from the buffers. Inputs from the CP's and the telemetry-processing stations are stored on the 7044 log tape at the time they are received by the 7044 computer. If the computer is in mode 2, all inputs are stored on the disk for later processing by the 7094. When the data are stored on the disk raw file in mode 2, the 7094 is informed that the data are available by means of the direct data connection. The 7094 CP editor extracts the raw data from the disk at its leisure, processes it, and stores it in the master data tables, making it available to user programs.

Operations personnel at the user input/output stations request various 7094 user programs to operate. These programs extract the data from the master data tables, process the data, and generate outputs for the SC 3070 printers, the Milgo plotters, and the Teletype. These outputs are put on the disk, and the 7044 is informed that they are on the disk and available. The 7044 informs the operations personnel by means of an administrative printer that the information is available. At the request of operations personnel, the 7044 extracts the data from the disk and sends it to the 3070 printers and the Milgo plotters, as requested. The Teletype data on the disk requested for output are sent through the CP to the various teleprinters and deep-space stations, as required.

7094 Redesign

The user program environment is shown in figure 6–8. A 7044, 1301 disk, and a 7094 operate together and communicate with one another. Control inputs, usually from punched cards or switches, can be entered at the user areas, received by the 7044, and sent to the 7094 by way of the direct data channel.

Flightpath analysis and command user programs

As raw tracking data are received, they are placed on the disk by the 7044 computer. The raw data on the disk are then accessible to the 7094 user programs.

There are four tracking data-handling programs, but only one program operates within the 7094 computer at one time. The mission-independent editor acquires the raw Teletype data from the disk, which contains mixed tracking and telemetry data, and separates them by extracting the tracking data and storing them on the disk in the raw tracking data file.

The tracking data processor (TDP) program retrieves these data, edits and formats them, and then places them back on the disk in the master tracking data file.

The orbit data generator (ODG) program uses this file to prepare a block

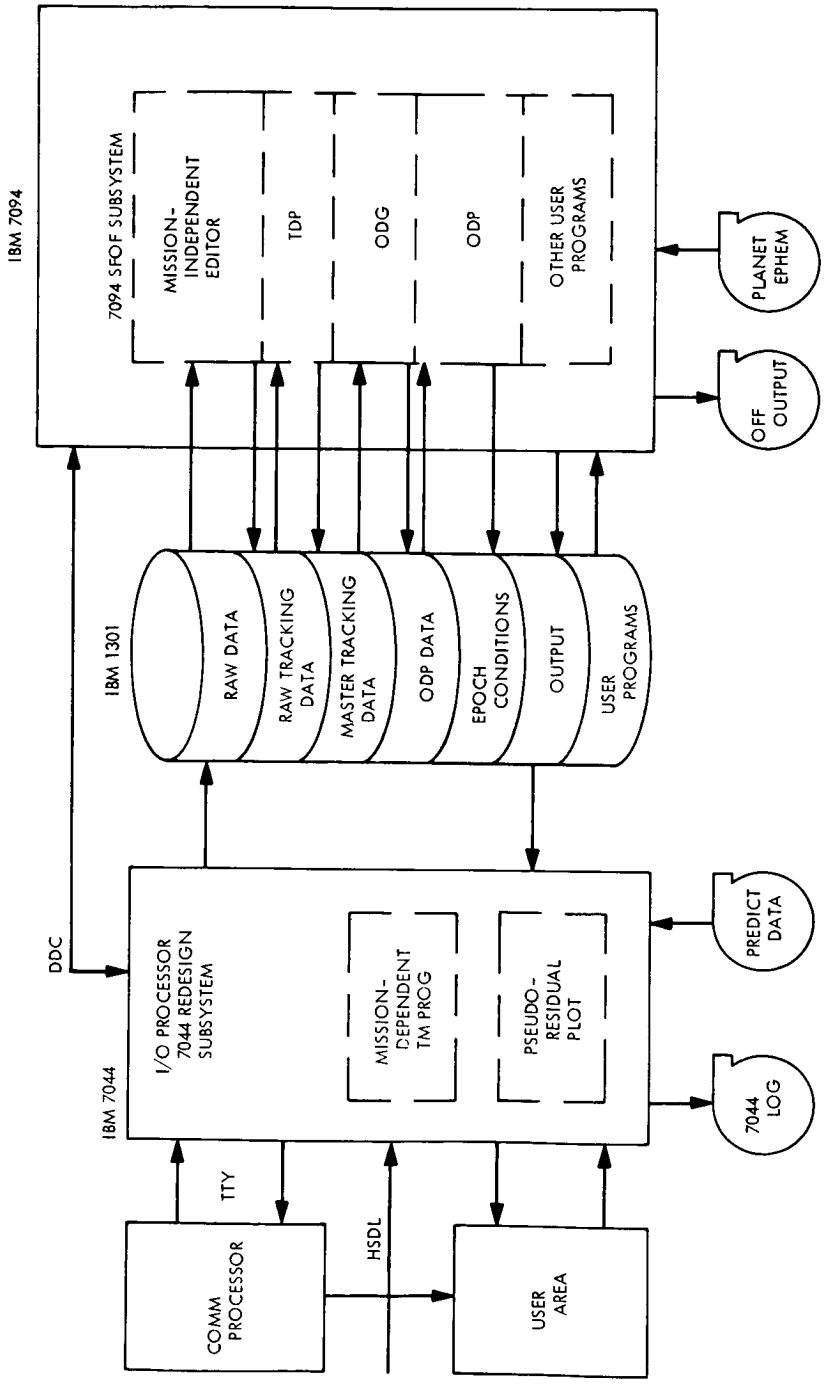

FIGURE 6–8.—7094 user program environment.

of data for the orbit determination program (ODP). Essentially, the ODG program extracts a subset from the master tracking data file and formats it by using control inputs that have been provided in the program. The ODP retrieves the data compiled by the ODG program and, employing a least-squares curve fit and using an iterative technique, determines the orbit of the spacecraft. The injection, or epoch, conditions are placed on the disk and are available to other programs. The area on the disk labeled "user programs" contains the actual programs called by the subsystem and brought into the 7094 for operation.

Trajectory computations are performed by the programs TJ1M and POWM. The injection conditions and the planetary ephemeris are used by TJ1M to compute the spacecraft ephemeris and generate a trajectory SAVE tape that consists of tabulated information computed at specified points along the trajectory.

These values include Earth-Sun-probe angles, clock angles, and velocities. Essentially, POWM is a trajectory program, except that it generates, during the burn, tracking predictions that are used for early acquisition and are based on predicted or actual liftoff time. DSIF acquisition predictions are computed by the program PRDX. It also predicts viewing periods of the stations and voltage-controlled oscillator frequencies of the transmitter. This information is formatted for Teletype and later transmitted to the tracking stations for aid in spacecraft acquisition.

PRDX also produces a predict data tape, which is used as an input to the 7044 for computation of pseudoresidual plots. PRDX uses the injection conditions and the planetary ephemeris as inputs.

The midcourse maneuver (MC1M) program provides the necessary information for selecting a midcourse maneuver that satisfies all trajectory constraints. In addition, it generates capability ellipse plots and formats the maneuver commands for transmission to the spacecraft. The inputs are the injection conditions and planetary ephemeris.

Spacecraft analysis and command user programs

The SPAC user programs are the star identification program (SIPM), the communication prediction program (CPPM), the attitude reference program (ATTREF), and AGC calibration program (AGCM).

SPAC programs receive telemetry data information from the user area. (The mission-independent editor has the system capability of extracting the telemetry data and storing them on the disk, as with the tracking data. However, this capability was not used by Mariner.) Another input for three of the SPAC programs (SIPM, CPPM, and ATTREF) is the trajectory SAVE tape, necessary

because these programs require an exact knowledge of the spacecraft's location in space to accomplish their tasks.

The results of all 7094 user programs are available to the user area by means of the 7044 and the output area of the disk. Selected results are recorded on magnetic tape for later off-line processing.

Non-SFOF Programs

Master data library (MDL) programs (see fig. 6–9) for the Mariner-Venus 1967 project were identical to those used for the Mariner-Mars 1964 project, except for two additional input processors and the MDL interface user program. The MDL programs do not operate in the SFOF software subsystem, but in the standard International Business Machines System (IBMSYS).

The purpose of the MDL programs is to generate, in non-real time, a tape containing the most accurate stream of telemetry data possible. This tape then becomes the basis for analysis by experimenters and spacecraft engineers. This processing of various input source tapes into a final tape is performed by the three basic software programs of the MDL chain: EDIT, REEDIT, and MERGE.

Data are recorded in various places and in various formats in the total data processing subsystem. The tapes containing these data are the inputs to the MDL programs. The telemetry-processing station and Teletype paper tape inputs were used for the Mariner-Mars 1964 project. For the Mariner-Venus 1967 project, they were replaced by two new sources: the TCP log tape, which was recorded at the TCP, and the 44 log tape, recorded at the 7044 computer.

Each tape input had an associated input processor, specifically designed to handle a particular format. The input processors performed a translation function from the varied input tape formats to a standard format recognizable by EDIT. This program performed frame detection and evaluated the quality of each frame.

Included in the telemetry data stream is status information regarding the processing, recording, and receiving equipment such as receiver in- and out-of-lock and demodulator in- and out-of-synchronization. EDIT program recognizes this information and uses it in evaluating the data quality during the frame-detection process.

In addition to the standard MDL tape, a bad data listing is recorded on magnetic tape. This listing is essentially an evaluation tool for determining the additional processing required to improve the MDL tape.

REEDIT provides a means to correct the MDL tape by supplying appropriate control cards whose information is based on the investigation of the bad data

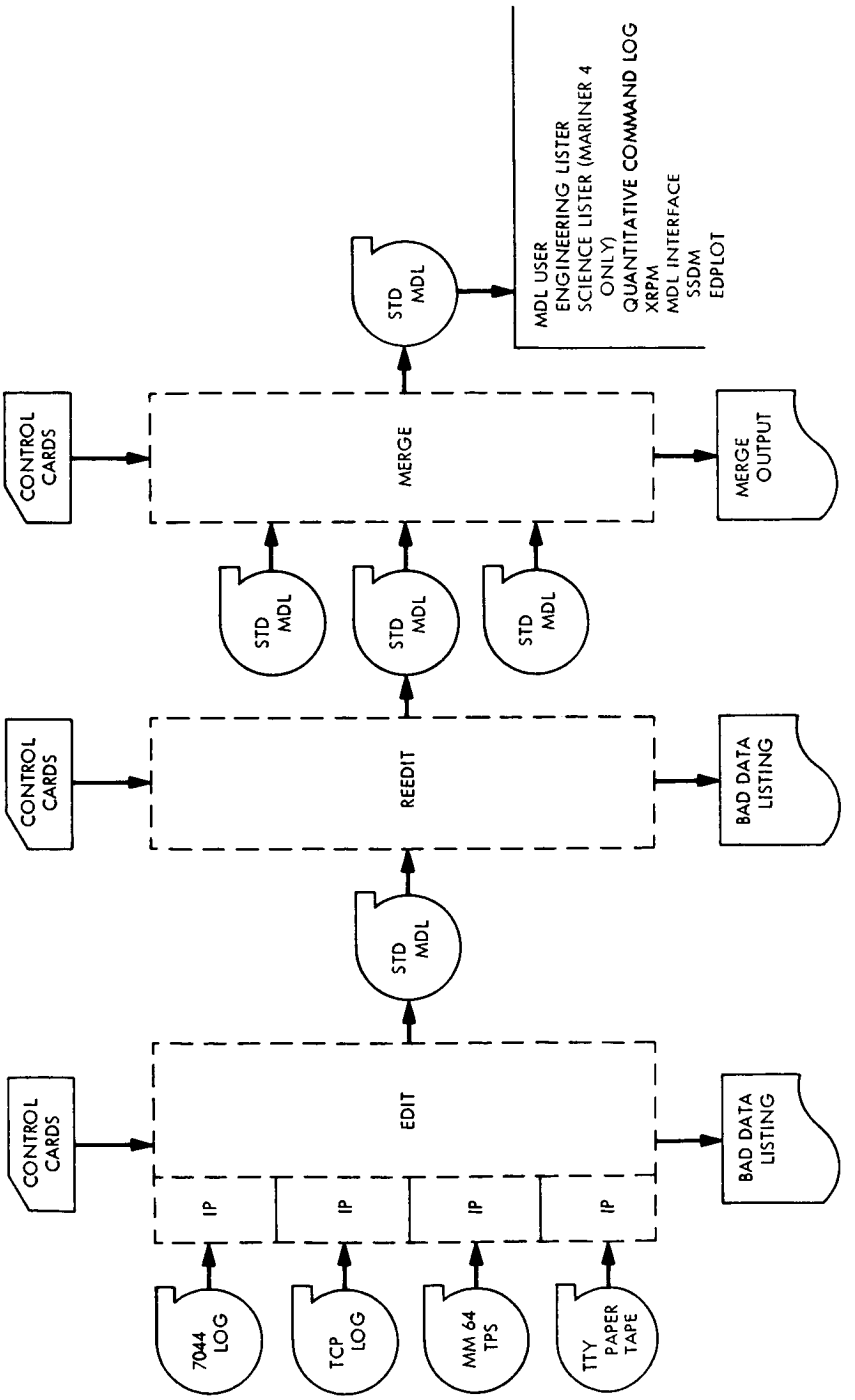

MM 64 MARINER-MARS 1964 PROJECT
TPS TELEMETRY PROCESSING STATION
TCP TELEMETRY AND COMMAND PROCESSOR
TTY TELETYPE
STD STANDARD
MDL MASTER DATA LIBRARY
IP INPUT PROCESSOR

FIGURE 6–9.—MDL programs.

listing. REEDIT also produces a bad data listing which, if the correction process has been performed properly, will be appreciably shorter than that produced by EDIT.

MERGE processes a number of tapes (up to six) from various sources covering the same period of transmission and merges them into one best possible standard MDL tape. The tapes processed by EDIT and REEDIT were from a variety of sources. Consequently, many tapes contained telemetry data for identical tracking periods. This occurred during station overlaps (i.e., when more than one station was tracking the spacecraft at one time) and also during in-station overlaps, when a switch was made from one tape to another during a pass (i.e., when the second recorder was started before the first had finished).

Master data library user programs

The MDL user programs are used as tools in the evaluation process of the standard MDL tapes generated at any stage (i.e., EDIT, REEDIT, or MERGE). Standard MDL tapes, regardless of the stage of processing, are in an identical format. As REEDIT and MERGE refine the data stream without altering this format, any of the MDL user programs can use any MDL tape as an input.

The engineering lister extracted all engineering data from an MDL tape and organized them into a quick-look format. The science lister did essentially the same thing with science data, but for Mariner 4 only. XRPM is a selective extract program. For example, a magnetometer experimenter, by providing certain control inputs to XRPM, can extract all magnetometer data from a given MDL tape.

The MDL interface program acted as a common boundary between the MDL tape and two programs carried over from the Mariner-Mars 1964 project. In the discussion of SPAC user programs, it was pointed out that telemetry data were not stored on the 1301 disk as were tracking data. Mariner 4, however, did store telemetry data on the disk; two very useful programs (SSDM and EDPLOT) utilized this feature. The MDL interface program allowed these programs to operate from the standard MDL tapes. EDPLOT provides a plot of the engineering values recorded. SSDM is a suppressed data printout; that is, only values which violate certain constraints are printed out and repetitive values are ignored.

Control over changes to the software was put into effect almost as soon as development started. The software control underwent successive stages: (1) control over basic program design, (2) control over detail design, and (3) control over program code. A change control form approved by the data processing project engineer (DPPE), SFOD, and MOS managers was required for changes to any program under one of the three levels of change control.

Software testing

A set of tests was performed on each of the four basic software subsystems: 7094 user programs, 7044 redesign, CP, and TCP. The following list is an example of the tests performed on the 7094 user programs. The same types of tests were used on other software subsystems.

(1) *Integration tests.* These tests demonstrated that each set of user programs (source deck) operated correctly in mode 4 using the 7094 redesign SFOF monitor and the mission-independent editor.
(2) *Compatibility tests, 1.* These tests demonstrated that the user programs operated correctly in mode 2 using the 7044 computer.
(3) *Compatibility tests, 2.* These tests demonstrated compatibility between the user programs, the 7044 computer, the CP, and the DSIF. Only those user programs that bound the CP or DSIF were tested.
(4) *Demonstration tests.* These tests were used to demonstrate to the DSN and the Mariner project personnel that the entire MOS was ready to support Mariner 5 simulations. A sequence of events, in which all phases of the mission were covered, approximated the sequence to be used in the simulations.

Data processing subsystem

In general, the performance of the data processing subsystem on Mariner 5 from launch to midcourse was excellent. The subsystem was in SFOF mode 2 on two computer strings for 36 hr during launch, as well as for several 8-hr periods before midcourse. All user programs worked well; no problems occurred in the sequence of events.

MISSION OPERATIONS TESTING AND TRAINING

Operational readiness was accomplished by a four-phase test program:

(1) Development tests for MRH and computer programs
(2) Compatibility testing and integration of hardware and software into TDS facilities
(3) Spacecraft/MOS compatibility
(4) Operational training and procedural tests

Development Tests

Development tests were conducted as part of the MRH and computer program development. Successful completion of the tests and demonstration of the element (command equipment package, telemetry equipment package, or computer program) indicated its readiness to be integrated into the final configuration.

The hardware and software transferred for maintenance were accompanied by test, change control, and failure report logs.

Mission Operation System/Tracking Data System Integration and Compatibility Tests

By mutual agreement between the MOS and the TDS, the compatibility testing and integration of hardware and software into TDS facilities were accomplished under TDS auspices.

Spacecraft/Mission Operation System Compatibility Tests

Objectives of these tests were to train the space-flight operations teams, to train the SPAC team in evaluating spacecraft-flight sequence and data mode changes as a result of commanding the spacecraft, and to exercise the MOS hardware and software with live spacecraft data.

The tests were conducted using the telemetry data source from the spacecraft at the SAF and at Building AO (AFETR). The composite signal was sent through the MRH and the TCP. The formatted Teletype output of the TCP was received at SFOF and distributed in the mission-support area on 60-word/min Teletype machines. HSD were received at SFOF, sent to the 7044, processed, and sent to the CP, the 30 by 30 plotters, and the 3070 printers. The communications processor output was distributed to the 100-word/min Teletype machines.

Operational Training and Readiness

The primary objective of these tests was to train SPAC and SSAC personnel in evaluating live spacecraft data in real time while in their space-flight operation environment. Live spacecraft data were made available by combining the training tests with selected ongoing spacecraft testing. Spacecraft testing was conducted under the direction of the spacecraft test operations manager.

Spacecraft analysis and command and space science analysis and command training tests

SPAC and SSAC groups monitored the live spacecraft data on a noninterference basis. The tests included the following training tests:

(1) *Parameter variation tests:* specific parameters varied to maximum/minimum tolerance.
(2) *Space simulator tests:* tests conducted in the space simulator to create the expected flight temperatures and vacuum environment.
(3) *Systems tests:* tests conducted to insure that all spacecraft subsystems performed according to design specifications.

(4) *Simulated launch:* prelaunch final full-scale checkout of all launch and operation systems.
(5) *Failure-mode tests:* an exception in that the SPAC and SSAC groups, under the direction of the SPAC director, were allowed to generate and carry out, with live spacecraft, command sequences that were designed to overcome anomalous conditions induced by the spacecraft test operations team. By appropriate reactions of the spacecraft test operations team to the commanded sequences, the resulting spacecraft performance simulated realistic spacecraft failure and recovery situations.

Flightpath analysis and command tests

Several FPAC tests were conducted with the objective of training FPAC personnel to accomplish those flightpath functions necessary for space-flight operations.

Simulated tracking data sources were used to exercise the FPAC team in orbit determination, trajectory analysis, maneuver command generation, and predict generation through all critical phases of the mission. This included launch, maneuver, and encounter phases. Nonstandard as well as standard simulated flight sequences were used for these three critical mission phases.

Combined operational tests

A series of combined operational tests that did not involve the flight spacecraft was conducted before launch. The data source for these tests was composed of a combination of simulated data and spacecraft test tapes recorded during spacecraft tests in the SAF.

The primary purpose of these tests was to insure that all the elements of the MOS, including technical and operational personnel of the DSN, were prepared to support the spacecraft after launch. The tests indoctrinated and exercised the MOS operational and technical personnel in the system and in the procedures to be used for the mission. The first combined operational test was supported by the following facilities:

(1) SFOF (mission-support area; data processing subsystem, mode 2; telemetry-processing station; communications center; simulated data conversion center; and the track area).
(2) DSS 11, 14, and 61, forming an encounter configuration.

The test was conducted over a period of 2 days, with the first day covering midcourse (MC) -3 hr to MC$+90$ min and 3.5 hr of cruise data. The second day covered the periods from $E-3$ hr to $E+2$ hr (about 45 min of spacecraft

mode 2) and $E+14$ hr to $E+16$ hr (2 hr of mode 4). Simulated data packages transmitted to the participating deep-space stations before the test were processed by the onsite computers and transmitted to SFOF. There they were analyzed in real time by the analysis teams in the mission support area and flightpath analysis area 2.

The second combined operational test was supported by the same SFOF areas and DSS 11, 14, and 42. The first day of the test covered the periods from $L-30$ min to $L+6.5$ hr and 3 hr of dual-mission cruise (Mariner 4 and simulated data from the deep-space stations). The second day of the test covered the periods from $E-6$ hr to $E+2$ hr (about 45 min of spacecraft mode 2) and $E+14$ hr to $E+16$ hr (2 hr of tape playback).

The third combined operational test also was supported by the AFETR, and DSS 42 and 51. The first day of the test covered the period from $L-30$ min to $L+90$ min, $L+16$ hr to $L+18$ hr, and MC -3 hr to MC$+90$ min. The second day covered MC -3 hr to MC$+2$ hr and 2 hr of cruise.

Operational readiness tests

Two operational readiness tests were prepared for the Mariner 5 launch. The first test was conducted over a 2-day period and lasted for 23 hr. The second and final test was conducted over a 3-day period and lasted 32 hr. The spacecraft tracking and telemetry data for the operational readiness tests were used to simulate the mission, in the same manner as in the combined operations test, by activating and exercising the equipment and subsystems of the deep-space stations to the greatest extent possible.

Participation of the AFETR in the test included the following tasks:

(1) Simulating and providing Atlas/Agena booster launch countdown and boost-phase flight events through injection
(2) Simulating and providing AFETR tracking data
(3) Calculating the parking orbit, transfer orbit, orbital elements, injection criteria, and DSIF look angles
(4) Transmitting all these data to SFOF by way of the communications subsystem

Deep-space stations at Goldstone, Woomera, Tidbinbilla, Madrid, Johannesburg, Cape Kennedy, and Ascension participated in the tests by processing the simulated tracking and telemetry data through the station equipment. They then transmitted the data to SFOF in keeping with established procedures and

sequence of events. The stations also received and acknowledged receipt of commands and tracking predictions. The deep-space stations executed the commands and verified the execution times in accordance with established procedures. Tracking and telemetry data received at SFOF were responded to in real time. AFETR tracking data were processed, and spacecraft tracking look angles and prediction data were transmitted to the appropriate deep-space stations. Tracking data from the deep-space stations were processed to establish the orbit of the spacecraft, and additional prediction data were transmitted to the appropriate stations. The tracking data were used to determine the orbit of the spacecraft, as well as the requirements for the maneuver corrections. Maneuver commands were transmitted to the appropriate stations for simulated transmission to the spacecraft.

Five tests were conducted in preparation for the Mariner 5 encounter of Venus. These tests were designed primarily to familiarize and train personnel in the analysis and response required for real-time operations during encounter. For each test, the model spacecraft in the SAF provided real-time spacecraft telemetry data to analysis teams in the Mariner mission-support area. Known spacecraft anomalies were introduced by the spacecraft test team.

Tracking data for all tests were provided by the ASI–6050 and/or the 7094 computer and were controlled from the simulated data conversion center located in the SFOF. Operational readiness tests were supplemented by real-time tracking data (simulated) transmitted over the HSDL from DSS 14. Tracking data transmitted over HSDL consisted of 1-s samples containing doppler and resolver information.

SPAC and SSAC teams participated in all tests involving analyses of spacecraft telemetry data. Spacecraft anomalies, introduced by the test team in the SAF, were recognized and corrective measures were recommended. Spacecraft telemetry data were processed by the 7044 real-time processor, located in the SFOF, for display to the analysis teams in the Mariner mission-support area.

The FPAC team computed orbital, trajectory, residual, and prediction data with the 7094 computer, using the incoming simulated data as their source. The FPAC team operated from the flightpath analysis area.

The first three tests used a 7044/7094 combination for rapid data movement within the facility. The last two tests used two such combinations (7044/7094 X and 7044/7094 W) to exercise personnel in operations required during critical mission phases. This configuration provided additional assurance that one computer subsystem (7044/7094) would be available during critical periods. The testing achieved the desired results.

EARLY MISSION PERFORMANCE

Flightpath Analysis and Command

Tracking data coverage

During the nonpowered transfer flight period between June 14 at 06:29 GMT and June 19 at 23:07 GMT, essentially continuous tracking coverage was obtained by DSS 11 (Goldstone, Pioneer), DSS 41 (Woomera), DSS 42 (Tidbinbilla), DSS 51 (Johannesburg), and DSS 61 (Madrid). DSS 41 and DSS 51 participated only briefly in the early phase of this period. The following types of data were used in determining the orbit of the spacecraft:

(1) HA, DEC (hour angle, declination): the pointing angle of the tracking antenna, in degrees, used only in early orbits.

(2) CC3 (*S*-band phase-coherent counted doppler): a measure of the topocentric radial velocity of the spacecraft and the primary type of orbit data (1 m/s≃15.3 Hz).

Only angle data were obtained until 07:03:57 GMT, about 40 min after injection into transfer orbit. The angles from DSS 51 were biased until this time, when it was discovered that the antenna had been tracking on a side lobe.

Premaneuver orbit determination results

The ODP uses a weighted least-squares technique for estimating up to 20 parameters and forming up to a 20 by 20 covariance matrix. The first 12 premaneuver orbits, through 19:38 GMT, on June 15, estimated only geocentric equatorial position and velocity of the probe, with a corresponding 6 by 6 covariance matrix.

Midcourse maneuver analysis based on orbit information

Orbit determination after spacecraft injection showed that a midcourse maneuver would be required. Accordingly, pitch and roll turns were planned, followed by a nominal 17.66-s motor burn.

The premaneuver pitch and roll commands were successfully executed by the spacecraft preparatory to motor ignition. (See figs. 6–10 and 6–11.) The amplitude of the observed doppler residuals depended upon the antenna offset from the center of gravity at the spacecraft and the time period over which the turns were executed.

Trajectory analysis

During the Atlas sustainer and vernier stages, commands in vehicle attitude and engine cutoff times were given to adjust the altitude and velocity at Atlas vernier-engine cutoff. After Atlas/Agena separation, a short coast period pre-

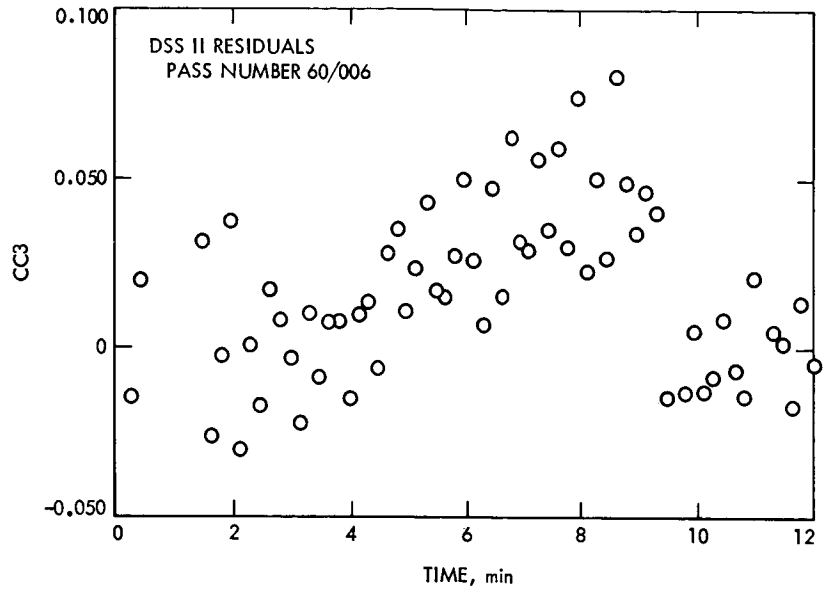

FIGURE 6–10.—Doppler tracking residuals from DSS 11 during premaneuver pitch turn.

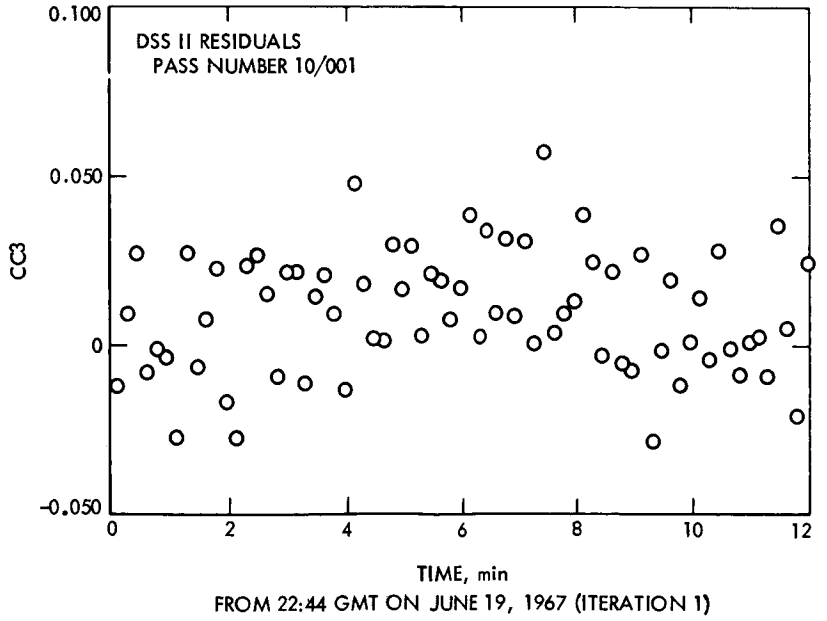

FIGURE 6–11.—Doppler tracking residuals from DSS 11 during premaneuver roll turn.

ceded the first Agena ignition. At a preset value of velocity increment, the Agena engine was shut off; at that time both the Agena and the attached spacecraft were moving in a circular parking orbit at a distance of about 185 km above the Earth and were traveling at a speed of 7.8 km/s, space fixed. After a coasting time of 13.3 min in the parking orbit, the second Agena ignition was initiated.

At the end of Agena final cutoff (23 min 19 s after liftoff), Agena, with the spacecraft, was traveling at a speed of 11.4 km/s, space fixed. The latitude and longitude of injection (Agena cutoff) into the geocentric hyperbolic orbit were $-4.7°$ and $+351.5°$, respectively, over the South Atlantic Ocean.

Within the hour after injection, the spacecraft receded from the Earth with decreasing speed in an almost radial direction. This reduced the geocentric angular rate of the spacecraft in inertial coordinates until the rotational rate of the Earth exceeded the geocentric angular rate of the spacecraft. The direction of the Earth track of the spacecraft then reversed from increasing to decreasing longitude over the surface of the Earth.

Five days after launch, at 23:08:28 GMT on June 19, 1967, the midcourse maneuver was executed. The spacecraft was then 1.58×10^6 km from the Earth and still moving under the influence of the Earth in an Earth-centered hyperbolic orbit. The velocity of the spacecraft was 2.99 km/s with respect to the Earth and 27.02 km/s with respect to the Sun. Postmidcourse computations showed that the closest approach to Venus would occur at 17:34 on October 19, 1967.

Spacecraft Analysis and Command

Radio subsystem

The radio subsystem performed normally during the launch-through-midcourse phase of the mission. The cavity amplifier supplied spacecraft transmission power, and the spacecraft's low-gain antenna was used for transmitting and receiving. Spacecraft radio power-up occurred normally at spacecraft separation. Radio subsystem data were consistent with preflight predictions. Items of specific interest are discussed in the following paragraphs.

Radio power-up

Shortly after radio power-up, channel 213 (cavity power output to the low-gain antenna) began to decrease from an initial DN of 75. After the radio subsystem temperatures stabilized, channel 214 stabilized at a DN of 70 to 71. Data obtained from the space simulator tests indicated that the cavity amplifier responded normally. The observed change was attributed to a decreasing temperature in bay VI and to the time required for the cavity power output to stabilize. Channel 300 (cavity cathode current) also responded normally.

Frequency predictions for first DSIF acquisition

Predictions of DSIF acquisition frequencies for both uplink and downlink were based upon predicted spacecraft temperatures and on curves of spacecraft transmitter and receiver frequencies versus temperature. Observed frequencies agreed with predictions.

During the midcourse maneuver, the radio subsystem temperatures increased by 4.4 K (within the predicted range). Spacecraft power switched from the solar panels to the battery during the pitch turn. While battery power was used, channels 214 (transmitter power output) and 300 (cavity cathode current) decreased by 1 DN. This decrease was the result of a slight drop of the cavity power supply voltage because of a lower primary input voltage from the spacecraft battery. After Sun acquisition, channels 214 and 300 returned to their normal DN readings.

A command was transmitted to the spacecraft to turn on the ranging receiver. The following channels had changes in DN values to indicate that ranging was on:

(1) Channel 424 (spacecraft receiver voltage-controlled oscillator temperature) increased by 1 to 2 DN. This change is attributed to the increased power (0.7 W) dissipated in the ranging phase detector module when ranging is on.

(2) Channels 203, 205, 225, and 227 (spacecraft power subsystem current monitors) increased by 1 DN. An increase in these channels reflects the additional 0.7 W of power drawn when ranging is on.

Command subsystem

Telemetry data of the subsystem to which commands were sent showed that all commands were detected and decoded correctly.

Tape-recorder subsystem

Nineteen tape passes were accumulated during the launch phase. The tape recorder was turned off about $5\frac{1}{3}$ s after Agena/spacecraft separation.

Data encoder subsystem

One deck skip, which was a normal skip, was observed at the time of the Agena/spacecraft separation.

Attitude-control subsystem

The operation of the AC subsystem was normal.

Gas subsystem

The spacecraft was launched with 2.35 kg of gas in the AC subsystem (1.17 kg in the $+x/-y$ tank, and 1.18 kg in the $-x+y$ tank). Gas consumption during the phase from launch through midcourse was normal.

Inertial sensors

Performance of the gyros was normal. The launch caused saturation of all three axes. While the separation rates cannot be easily measured, they were no smaller than +7.0 mrad/s (0.4°/s clockwise) in pitch, −15 mrad/sec (0.86°/s counterclockwise) in yaw, and −2.65 mrad/s (0.15°/s counterclockwise) in roll. The decrease in angular velocity as the solar panels deployed was clearly visible at the time of the separation-initiated timer (SIT) event. The panels were deployed in less than 12.6 s; the angular velocity decreased by 1.4 mrad/s in pitch, 1.5 mrad/s in yaw, and 0.3 mrad/s in roll. Although the conservation of angular momentum predicts an increase in angular velocity in pitch and yaw at solar-panel deployment, the increase of the moment arm of the gas jets (about 0.3 to 2.4 m) more than offsets the corresponding increase in angular velocity by causing a decrease in the acquisition rates. The magnetometer calibrate spin rate was 78 DN or −3.72 mrad/s. The Canopus search rate was 73 DN or −2.13 mrad/s, based upon telemetry before acquisition. After acquisition of the Earth, the spin rate was again 73 DN. After acquisition and subsequent deacquisition of the Moon, however, the spin rate dropped to 71 DN or −1.86 mrad/s until Canopus acquisition.

The first gyro telemetry data showed readings of 63 DN in pitch, 65 DN in yaw, and 64 DN in roll. Because the pitch, yaw, and roll DN readings did not change when the gyros were turned on, it was concluded that the turn-on transient was minimal. Pitch and roll turn rates for the midcourse maneuver were in accord with those predicted. The CC&S was programed for a 304-s pitch turn (desired magnitude, 55.3503°; commanded turn, 55.2672°, or 0.0831° short) and a 380-s roll turn (desired magnitude 71.0248°; commanded turn, 70.946°, or 0.0788° short). Data received showed that the turns were accurate and that they were performed according to the specified polarity and duration. The pitch turn was 55.18°±0.2°; the roll turn was 70.93°±0.04°.

Celestial sensors

After the spacecraft emerged from the shadow of the Earth, all indications were that the Earth sensor looked at the Sun until the start of Sun acquisition. Earth sensor outputs were obtained during the magnetometer calibration phase. An Earth sensor output was obtained during the roll search, verifying the search rate and aiding identification of the objects acquired by the Canopus sensor.

The Sun sensor showed saturated outputs. To acquire the Sun, the spacecraft was driven clockwise in pitch and counterclockwise in yaw. However, light from the Earth, which illuminated the secondary Sun sensors, biased the electrical null about 78 mrad (4.5°) off the probe-Sun line. The AC subsystem had acquired the false null in yaw and was in nonperiodic oscillation (limit cycling) about the

false null; however, the null also had to be acquired in pitch to trigger the Sun gate because the Sun-gate field of view is about 5.1°. The location of the false null was such that all points of a normal limit cycle within the deadband placed the Sun in the Sun-gate field of view so that the Sun-gate event, when removing the power to the secondary Sun sensors, also removed the false null.

The Canopus sensor was turned on. The expected acquisition of the Earth was achieved. The maximum brightness of 30 DN noted corresponds to about 2.5 times that of Canopus; a brightness of about 0.75 times that of Canopus had been predicted. After Earth acquisition, two commands were transmitted to the spacecraft to override Earth acquisition. The first command was sent to the spacecraft to override acquisition on the first stable null of the Earth. The second command was timed to arrive at the spacecraft shortly after the second stable null of the Earth was reached and before the gyros were turned off. The second command caused the spacecraft to roll off the Earth and, shortly afterward, to acquire the Moon. (A limit cycle was not established because the Moon apparently did not have a stable null.) The sensor moved off the Moon in the search (counterclockwise) direction, indicating a low-gate dropout of between 48 and 49 DN (0.22 to 0.19 times that of Canopus). The maximum observed brightness of the Moon was 34 DN, about 1.6 times that of Canopus.

Roll search continued until Canopus acquisition. The initial Canopus brightness reading of 37 DN remained for about 6 hr and then dropped to 38 DN, accompanied by a decrease in sensor temperature from 75 to 73 DN (about 1.8 K). The present and most stable value of one times that of Canopus seems to be 38 DN or 0.89 V and agrees closely with the calibration of 0.886 V made before delivery to the SAF.

Canopus, Sun, and Earth sensors performed normally during the cruise and maneuver periods. After the midcourse maneuver, during the roll searches, the Canopus sensor made a star map that correlated with the map produced by the Mariner star identification program. Several celestial objects were observed and identified in real time. The Earth sensor viewed the Earth during these roll searches and during the initial Canopus reacquisition.

Position deadbands

Position deadbands of the attitude-control subsystem were:

Pitch: 34 to 35 DN = 7.77 to 7.46 mrad;
95 to 94 DN = −7.97 to −7.67 mrad
Yaw: 34 to 35 DN = 8.42 to 8.09 mrad; 95 DN = −8.69 mrad
Roll: 53 to 54 DN = 6.87 to 6.42 mrad; 75 DN = −3.21 mrad

Because of a 1.7-mrad null offset in the Canopus sensor, the roll limit cycle was asymmetrical in position. Minimum-rate increments have not been calculated, but some disturbance torques have been; the maximum torque observed thus far is about 100 μN m and some are as low as 10 μN m. The role of derived rate in the initial Sun acquisition is evident in that the rates were significantly reduced during the acquisition process.

During the motor burn, the autopilot maintained the thrust vector orientation of the spacecraft; the results were inferred from the postmidcourse analysis of the pitch and roll turns.

Central command and sequences subsystem

CC&S operation was completely normal. All events (deploy solar panels, turn on attitude control, and turn on Canopus sensor) occurred at their nominal times (within the resolution of the telemetry).

All maneuver events (gyros on and data mode 1, pitch turn start and polarity, pitch turn stop, roll turn start and polarity, roll turn stop, motor burn start, motor burn stop, reacquire start, and maneuver counter overflow) occurred at their nominal times (within the resolution of the telemetry). The CC&S timing of events in telemetry channel 220 gave the correct number of overflows and the expected final readings for each of the turns and for the motor burn. The resolution of this channel is twice the word synchronization time ($\pm$0.42 s).

Power subsystem

Operation of the power subsystem was nominal during the launch and the magnetometer-calibration roll; all operating voltages and currents were within expected ranges. A total of 4.3 A h was removed from the battery during launch; 50.7 A h were available at Sun acquisition, indicating that an assumed nominal of 55.0 A h was available at $L-7$ hr. By 21:00 GMT on June 18, 1967, 4.1 A h had been returned to the battery.

A calculated total of 55.5 A h was available before the midcourse maneuver. During midcourse maneuver, a total of 2.33 A h was removed from the battery; 53.17 A h were available at Sun acquisition. The battery supplied more power during the maneuver than was originally estimated, but was within tolerance.

Shading of the solar panels by the spacecraft bus occurred as expected during the maneuver. After the pitch turn, solar panel 4A7 was sufficiently shaded by the deployed Sun shade to preclude obtaining an output from that panel. This caused battery sharing to occur at a rate higher than expected. When the roll turn began, the shading moved from solar panel 4A7 to 4A5, which was only partially shaded at the end of the 70.93° turn.

Temperature-control subsystem

Very little change was observed in the spacecraft temperatures during ascent and parking orbit. Temperatures at Sun acquisition were within expected tolerances. Cooling of external items occurred during boost because of the gas expansion under the shroud; further cooling occurred while the spacecraft was in the shadow of the Earth. It can be inferred, from the near-normal temperatures, that the Sun shade was correctly deployed.

When the spacecraft entered the near-Earth cruise configuration, temperatures remained within design limits. The average spacecraft temperature was 1.1 K above the predicted level during pre-Canopus-acquisition cruise and 0.6 K above the predicted level after Canopus acquisition. There were no bus temperatures that departed more than 2.2 K from prediction during the pre-Canopus-acquisition period nor more than 1.1 K from prediction after Canopus acquisition. Equipment temperatures outside the bus showed larger deviations than predicted.

After the postmidcourse Sun acquisition, an apparent anomaly in the $-y$ pitch jet temperature (channel 425) was observed. A temperature of 244 K was observed 2 min before the completion of Sun acquisition. At 41 min after Sun acquisition, a 1-DN decrease in temperature to 243 K was observed. Because of solar heating and a conduction heat input to the assembly 40 min before the anomalous reading, such a decrease in temperature was completely unexpected. The results of analysis suggested two possible explanations:

(1) Pitch jets continued to release a considerable amount of N_2 at the time of the anomaly, which caused cooling of the assembly because of gas expansion.

(2) At the time of Sun acquisition, the gas valves were subcooled approximately 5.6 K below the manifold temperature because of gas expansion during acquisition.

If the first explanation were a valid assumption, the average temperature of the assembly would have increased because of increased solar heating, while the measured temperature would have decreased because of heat losses to the cooler valves. The second theory is more plausible; both the test data and the flight data, however, are insufficient to permit a positive conclusion.

Structural and mechanical devices

Nominal spacecraft performance indicated that the spacecraft structure performed adequately through the critical launch and boost environments. The pyro arming switch actuated normally, and the SIT squib-firing current event occurred normally, allowing for a maximum of 7-s deployment time for solar

panels. The corresponding SIT actuation time was 170 to 175 s (which corresponds to a SIT temperature of 296±2.2 K). As this temperature is close to the predicted value of 300 K, it can be concluded that the SIT operation was normal. The spacecraft performance was evidence that the spacecraft structure performed normally during the midcourse maneuver and the cruise.

Temperature-control reference

Temperature-control reference (TCR) data were obtained approximately ½ hr after Sun acquisition; all values were within predicted tolerances. A subsequent decrease in DN value of channels 413 and 432 over the next 3 hr indicated a decreasing thermal input from the Earth early in the mission. (There was a similar effect on the solar panels.) The lower equilibrium temperatures, apparently beyond Earth influence, were still within tolerance.

The changes on the white TCR's (412 and 432) permitted a resolution of change in solar absorptance (change only, not absolute value) of white coatings to an order of magnitude better than that possible in the laboratory. (The results of TCR performance were recorded to a much finer degree than can be achieved in a laboratory.) The results recorded during the second week of flight indicated that the temperature-control coatings on the TCR's were different in space than in laboratory tests, and further support the results of the first week of flight. White S–13M continued to darken at a faster rate than expected; black continued to bleach faster than expected; and white S–13M degraded faster than predicted.

Channel 412, S–13M White. The S–13M white coating was expected to degrade and be on scale within 10 to 15 hr after launch. This did not occur until $L+30$ hr, indicating either a lower initial solar absorptance or a slower initial degradation rate.

Channel 432, S–13M White. Initial results were within predicted tolerances, but the increase in absorptance was greater than expected. The first increase (0.5 percent) was evident within 5 hr after launch.

Channel 413, Black. The black TCR temperature decreased following Sun acquisition (apparently as the Earth influence decreased) and appeared to have reached equilibrium at 7 DN (333 K), 3 hr after launch. At $L+20$ hr, the DN changed to 6 (333 K). This change could be explained by assuming that the previous value of 7 DN was just above the switch point. However, the change to 5 DN at $L+83$ hr and continuous readings of 5 DN after $L+83$ hr indicate that a bleaching of the black reference was in process. A 1-DN reading change corresponds to less than 1 percent in the product $S\alpha/\varepsilon$, where S is solar intensity, α is solar absorptance, and ε is infrared emittance.

Postinjection propulsion subsystem

Telemetry data confirmed that the propulsion subsystem maintained a normal condition during launch. Thrust-chamber pressure dropped to zero while the shroud-cavity pressure dropped, as expected, during the boost phase. After injection, the propulsion subsystem ΔV capability was about 92 m/s.

Following injection, propulsion subsystem temperatures decreased to within 1.1 K of the predicted values. As the temperatures decreased, the pressures decreased according to predictions. During this dynamic period from launch through injection the propulsion subsystem remained leaktight.

Data analysis showed that thermal equilibrium of the postinjection propulsion subsystem occurred during cruise by June 18, 1967. The temperature and pressure parameters are shown in table 6–I. All parameters agreed with the tolerances of prelaunch predictions.

Table 6–I.—Temperature and pressure parameters of Mariner-Venus 1967 project

Parameter	Post-launch	Cruise equilibrium
Thrust-chamber pressure, MN/m^2	0	0
Fuel tank pressure, MN/m^2	2.020	1.910
Fuel tank temperature, K	295	286
Nitrogen tank pressure, MN/m^2	20.416	19.789
Oxidizer pressure, MN/m^2	2.744	2.689
Terminator sensor excitation	Off	Off
Nitrogen tank temperature, K	293	284
ΔV capability, m/s	92.1	91.9

Propulsion subsystem performance during the motor burn of the midcourse maneuver was normal in all respects. There were deviations of 2 or 3 DN from the predicted chamber pressure.

After the midcourse motor burn, temperatures during soakback were not excessive. When cruise conditions were established following the maneuver, temperatures returned to within 0.6 K of premaneuver values. There were no indications of any leaks during or after midcourse maneuver. Telemetered propulsion parameters during and immediately following the motor burn are shown in table 6–II.

Postmaneuver tracking data established that the velocity increment imparted to the spacecraft during the maneuver was about 4.5 percent less than that planned.

Table 6–II.—Telemetered propulsion parameters from Mariner-Venus 1967 project

Parameter	Data no.	Engineering unit
Thrust-chamber pressure (during steady state), MN/m^2	79 to 80	1.276 to 1.289
Propellant tank pressure (during steady state), MN/m^2	79	2.110
Propellant tank temperature, K	37	0.288
Nitrogen tank pressure (at end of motor burn), MN/m^2	79	16.810
Oxidizer pressure (at end of motor burn), MN/m^2	93	2.496
Nitrogen tank temperature, K	47	0.294

An extensive investigation was initiated in an attempt to determine whether the cause of the deviation from the predicted trajectory was in the velocity increment provided by the motor burn or in some other area.

Pyrotechnic subsystem

All pyrotechnic subsystem parameters remained normal during and after launch. Pyro was armed by the pyro arming switch at separation, and the event was recorded in register 3. Solar-panel pinpullers were fired by the SIT at 06:30:19 GMT, and events were recorded in registers 1 and 3. No additional events were recorded when solar-panel deployment occurred. The terminator sensor excitation remained off, as expected.

During the midcourse maneuver, pyrotechnic events were recorded in registers 1 and 3 for motor-burn start and motor-burn stop. It can be concluded from the telemetry data that both pyro units discharged and that all squibs fired when commanded. The terminator sensor excitation remained off, as expected.

Science subsystem

All science instruments maintained their normal condition during launch. After Agena/spacecraft separation, the plasma probe high-voltage inhibit was removed; the magnetometer was saturated on all axes; and the magnetometer ignition backup, ultraviolet calibration and drift check, trapped-radiation detector, DFR calibration, and DAS functions were normal. The magnetometer roll calibration was normal.

The Stanford University antenna began to send signals to the DFR on the spacecraft shortly after Mariner 5 first rose over the Stanford horizon; the DFR responded correctly.

After midcourse maneuver, two anomalies were observed in the ultraviolet photometer data. The ultraviolet photometer calibration and drift-check se-

quence changed during the telemetry mode 1 period. The ultraviolet photometer channel C readings also decreased from about 20 DN before midcourse to about 6 DN after midcourse maneuver and Canopus acquisition. (See SSAC mission performance next.)

Space Science Analysis and Command

Ultraviolet photometer

After Canopus acquisition (01:09:13 GMT on June 15), the channel C rest state was about 20 DN, as compared with a predicted value of less than 10 DN. It was thought, initially, that the 20-DN reading indicated hydrogen in the ecliptic. As a result of the 20-DN reading, the spacecraft was rolled, after the midcourse correction, to provide further evaluations.

After the midcourse maneuver and return to telemetry mode 2, all channels showed an increase in readings; the readings decreased to normal for channels A and B, but to about 6 DN for channel C. Throughout the postmidcourse rolls, all channels responded to the Milky Way and several stars. However, the channel C response was lower than expected. After final Canopus reacquisition, the channel C rest state was about 6 DN rather than 20 DN as before the maneuver. Thus far, this apparent drop in sensitivity is unexplained.

Following the switch to mode 2, another anomaly was observed. Before midcourse, the ultraviolet photometer calibrations occurred on frames divisible by 16, and drift checks occurred on frames divisible by 8. After the midcourse maneuver, the calibrations occurred on frames divisible by 16 with a remainder of 7, and the drift checks occurred on frames divisible by 8 with a remainder of 7. All other science instruments were unchanged. The counters inside the ultraviolet photometer were altered during the telemetry mode 1 part of the maneuver.

Solar-plasma probe

The period from launch through midcourse was successfully completed with no anomalous behavior. As expected, no plasma was detected until the spacecraft left the magnetosphere. At this transition, the instrument showed the proper readings for the plasma shock wave.

No abnormal collector currents were measured at the steps corresponding to the highest modulator grid voltage.

Helium magnetometer

The period from launch through midcourse was successfully completed with no anomalous behavior. The magnetometer assisted in the spacecraft roll and acquisition phases as planned.

Trapped-radiation detector

After launch, the trapped-radiation detector observed the Van Allen belts near Earth, variations in proton and electron activity, and changes in the solar X-ray activity. The overall performance through midcourse maneuver was normal.

Dual-frequency receiver

Flight performance through midcourse was normal. Stanford reported that both carrier levels were within 1 dB of calculated values.

MISSION-INDEPENDENT SUPPORT

Facilities and Support

Deep-space information facility

The DSIF telemetry configuration for the Mariner-Venus 1967 project consisted of an 85-ft parabolic antenna that provided a receiving gain of about 53 dB. The 210-ft parabolic antenna at DSS 14 provided a gain of about 61 dB. Two receivers at each station provided backup capability. A predemodulation/postdemodulation analog recording and a digital recording of the TCP output were provided by DSS 14.

The TCP digital output tape was used as the prime data source for constructing the MDL. When the TCP digital tape did not meet MDL requirements, the analog tape was requested and used as the data source. The analog tape was used exclusively when the telemetry threshold was exceeded.

During the encounter phase, which occurred during the Goldstone pass, DSS 11, 12, 13, and 14 provided primary and backup coverage. (See fig. 6–12.)

Communications

The communications configuration consisted of the Teletype, voice, and HSDL's required for data acquisition at SFOF, and for voice communications with all of the tracking stations. This configuration covered both the cruise and encounter periods of the mission. Special microwave coverage, communications engineering support, and communications prediction information were available for encounter.

With the exception of test activity and command operations, the Venus operations controllers coordinated the operations effort for the project during the cruise phase on a 24-hr/day basis during periods when the spacecraft was continually tracked. All voice communications from supporting agencies, including telephone communications between Stanford and the SFOF, were channeled through the Venus operations controller.

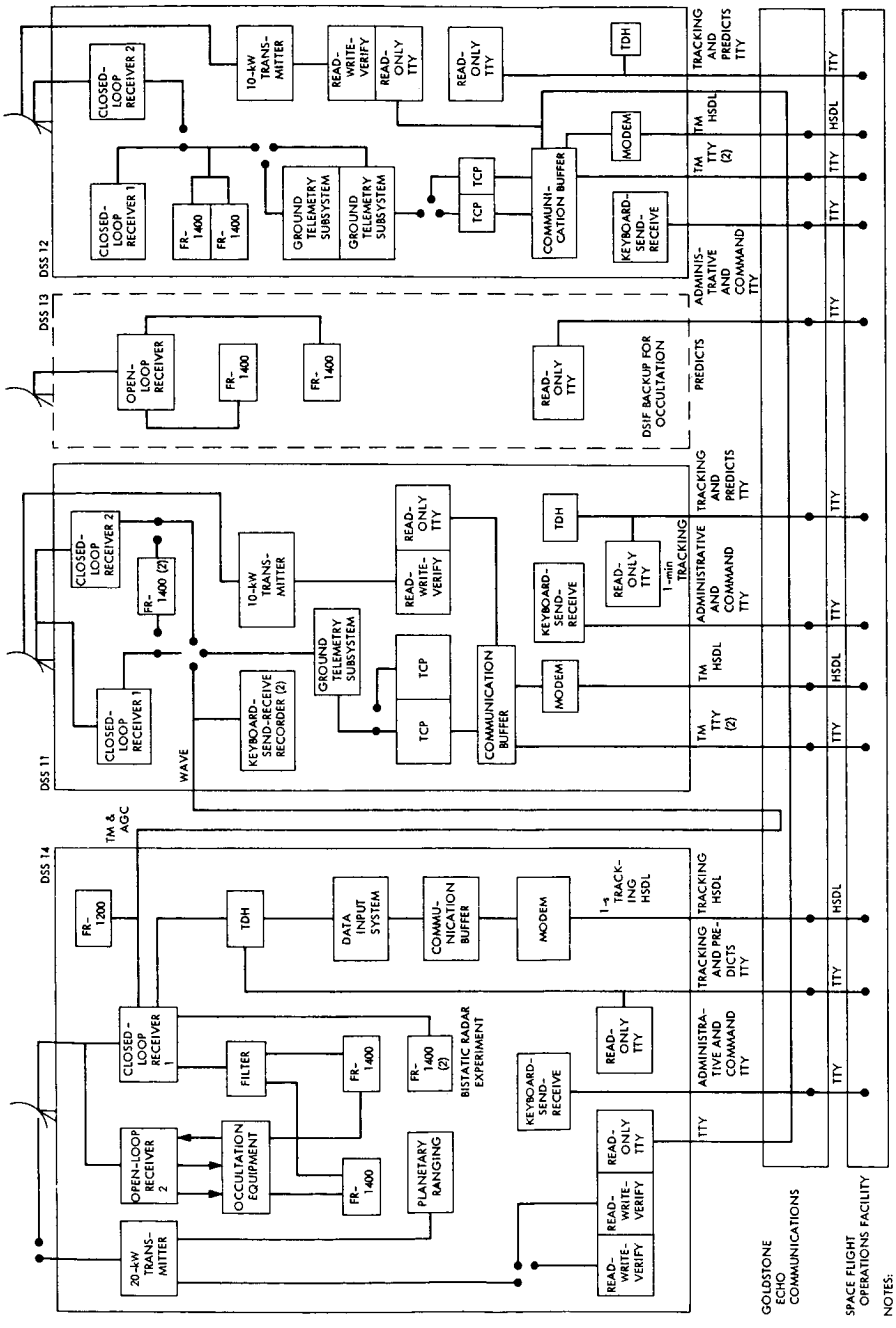

FIGURE 6–12.—DSIF/GCS configuration for Mariner 5 encounter.

Mission control network (MI–CON) was used by the project manager, the SFOD, and the area directors for discussing mission direction. Positions assigned to this network are shown in figure 6–13.

Operations control network (VAL–PRIME) was controlled by an assistant SFOD (ACE–5 position). The ACE–5 position was responsible for conducting the sequence of events, requesting reports, and obtaining reports from all area directors on the network. Positions assigned to this network are shown in figure 6–14.

Facilities operations control network (FAC–PRIME) was controlled by an assistant SFOD (PRIME–5 position) and used in conjunction with the VAL–PRIME network for conducting the sequence of events. The PRIME–5 position requested and obtained reports from the DSN on matters relating to the sequence of events. This network was also used by the Venus operations controllers for cruise-phase coordination. Network positions are shown in figure 6–15.

FPAC analysis control network (FPAC–3) was controlled by the FPAC director. All internal FPAC coordination was conducted over this network. Stations assigned to this network are shown in figure 6–16.

SPAC analysis control network (BUSS) was controlled by the SPAC director. This analysis network was used for conference discussions, moderated by the SPAC director or his authorized representative, and for periodic reporting on spacecraft subsystem status to the SPAC director. Stations assigned to this network are shown in figure 6–17.

SSAC analysis control network (SPACE) was controlled by the SSAC director. This analysis network was used for conference discussions and reporting on the status of the science instruments. Stations assigned to this network are shown in figure 6–18.

Command network (MAR–COMMAND) was used and controlled by the SFOD for conducting all command activities. Access to this network was limited to the SFOD, the SPAC director, and the track chief. Command execution and verification by the DSIF were reported here. Positions assigned to this network are shown in figure 6–19.

Data-coordination network (DA–COR) was under control of the data processing operations director and was used as a coordination network between him and computer-support personnel. This network was also used for data processing coordination by the Venus operations controllers during the cruise phase. Positions assigned to this network are shown in figure 6–20.

A special network was established during the encounter phase for coordination between the occultation personnel at Goldstone and those at SFOF.

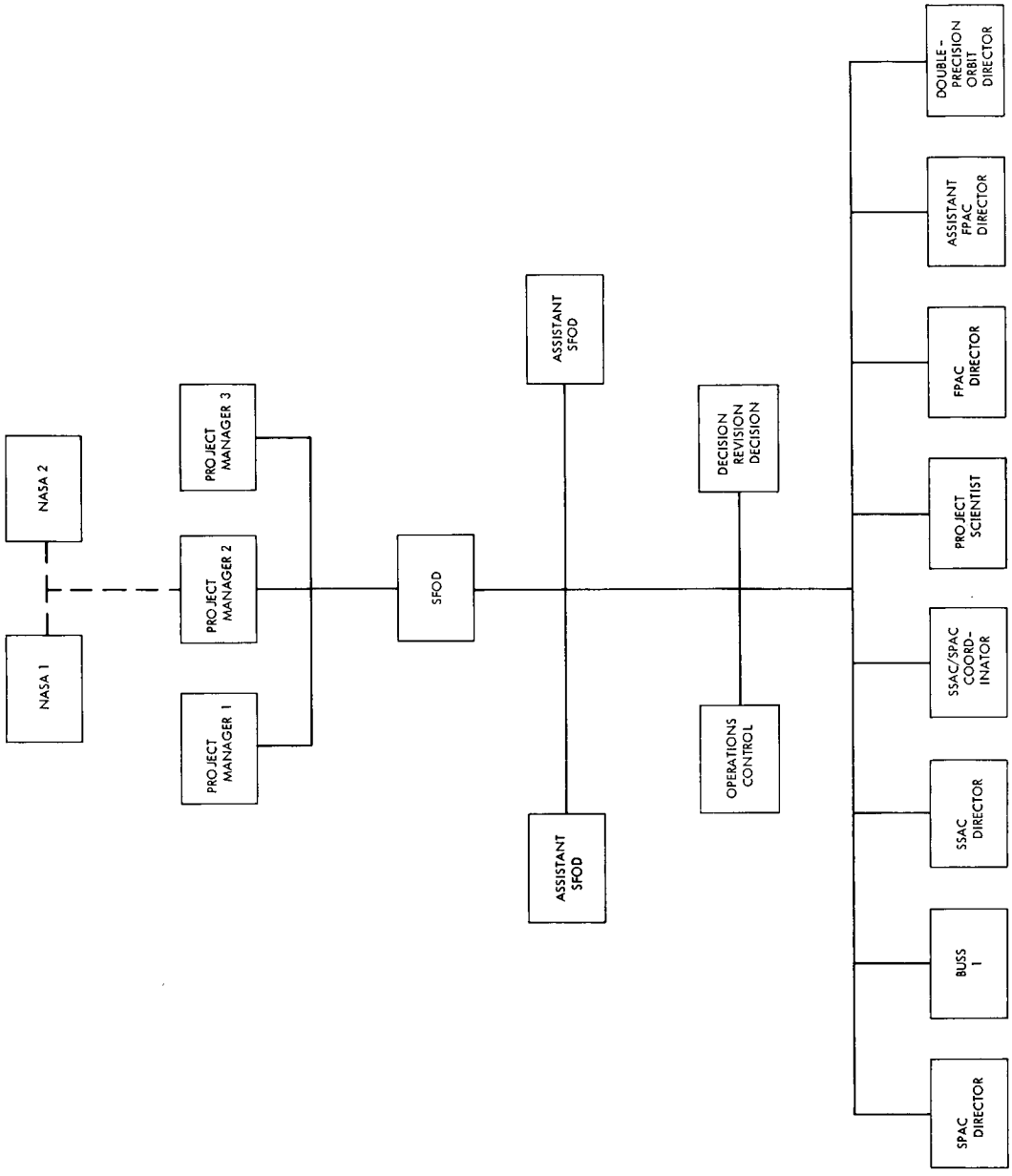

FIGURE 6–13.—Mission control network (MI–CON).

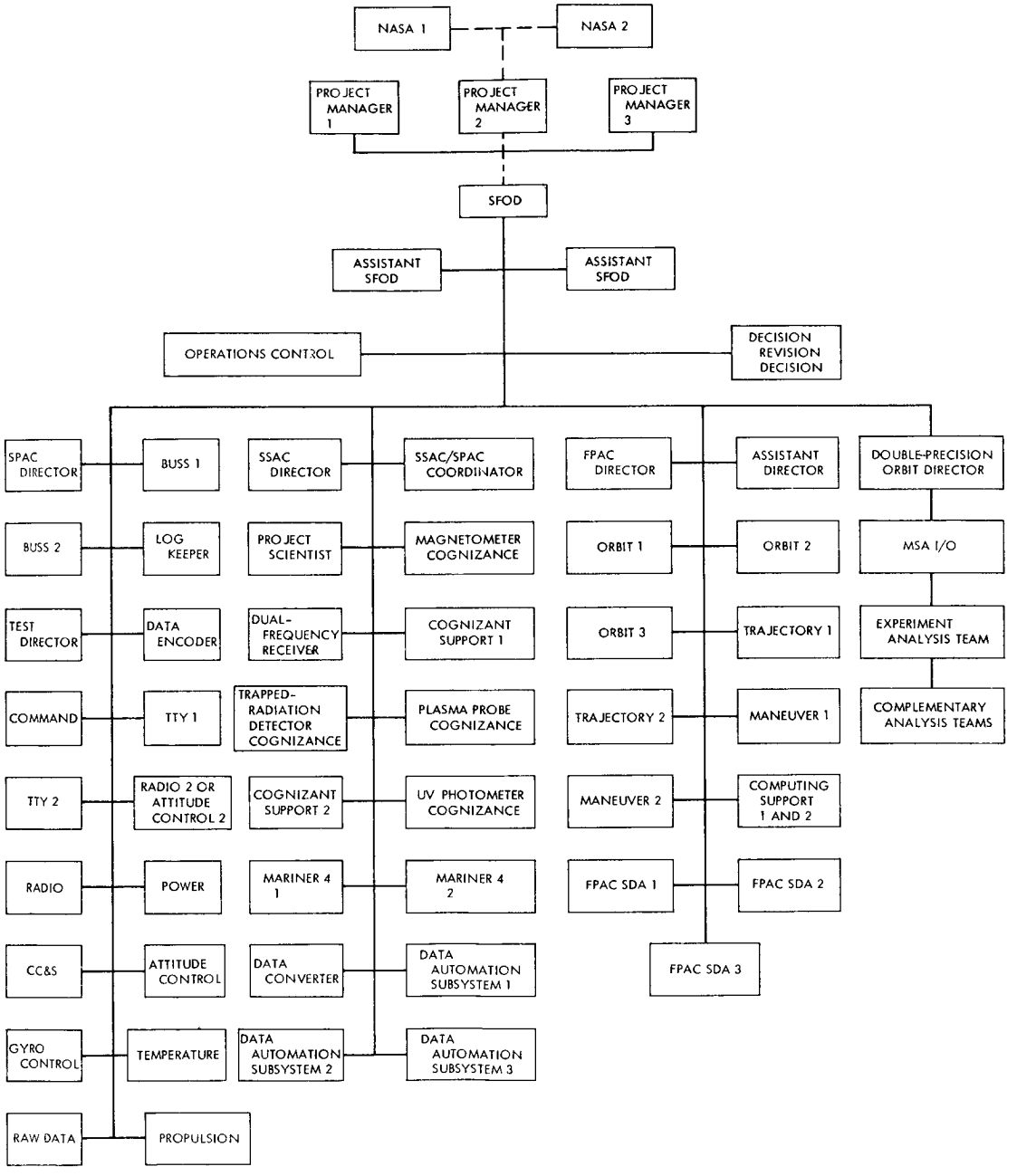

FIGURE 6–14.—Operations control network (VAL–PRIME).

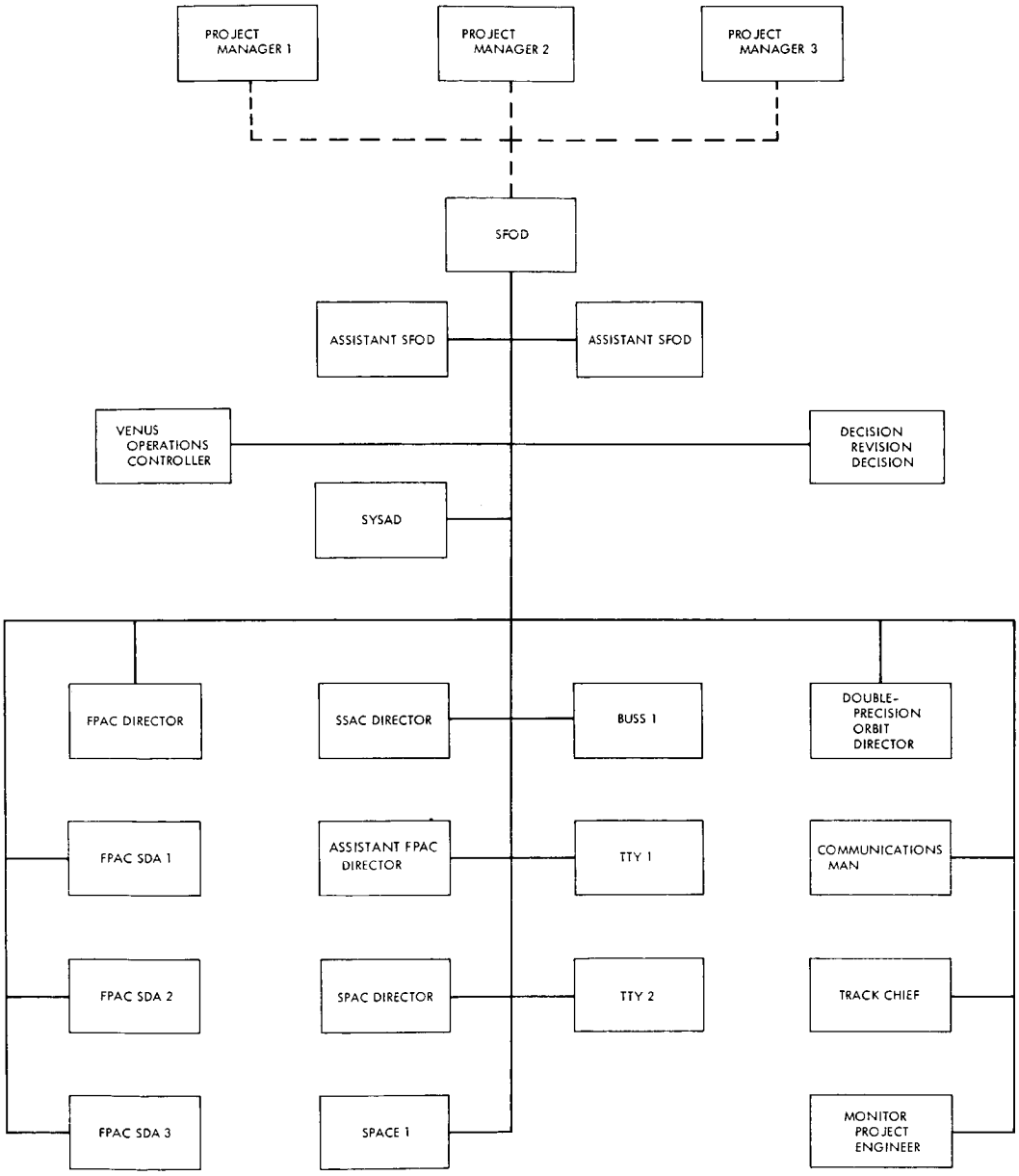

FIGURE 6–15.—Facilities operations control network (FAC–PRIME).

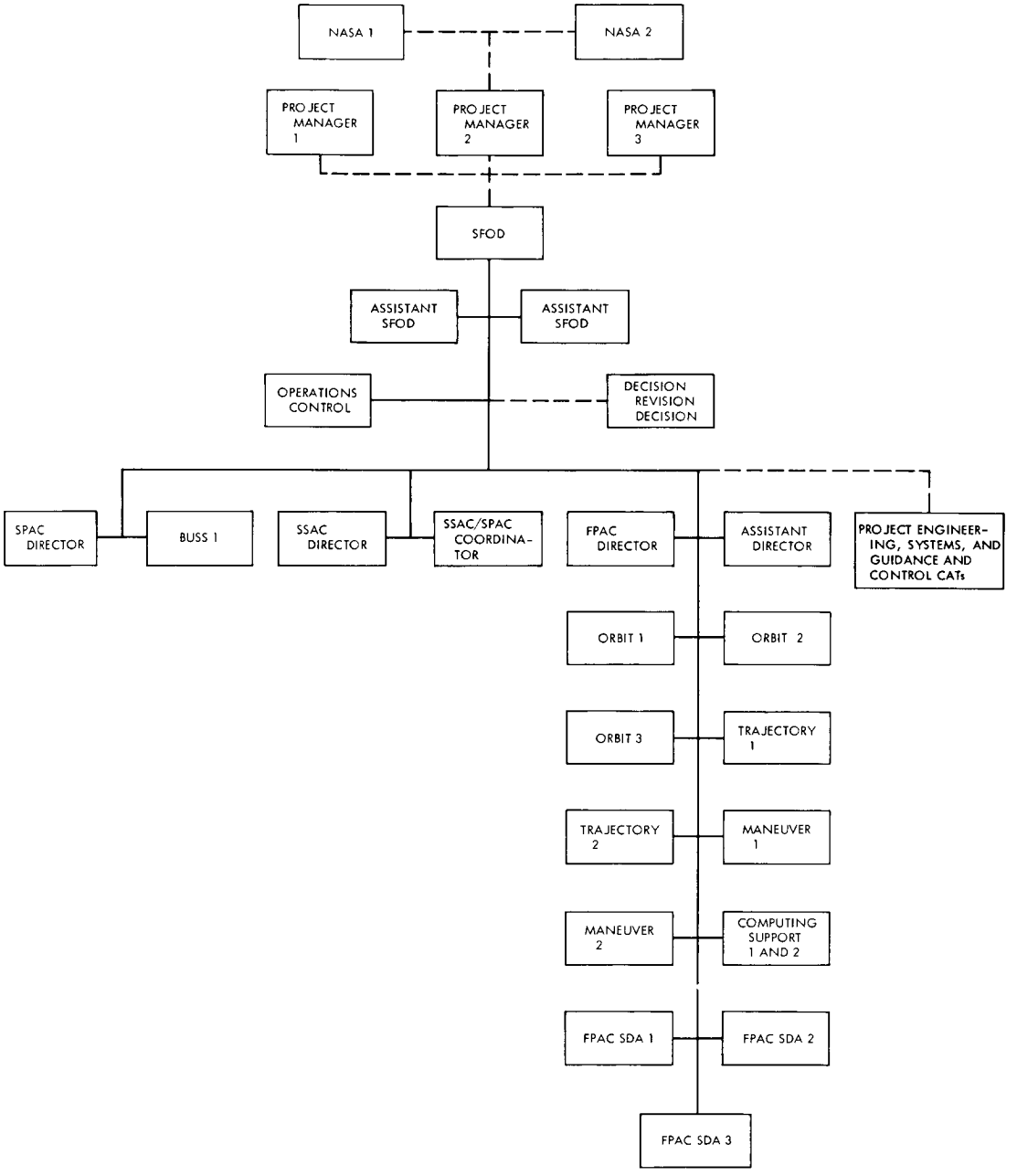

FIGURE 6–16.—FPAC analysis control network (FPAC–3).

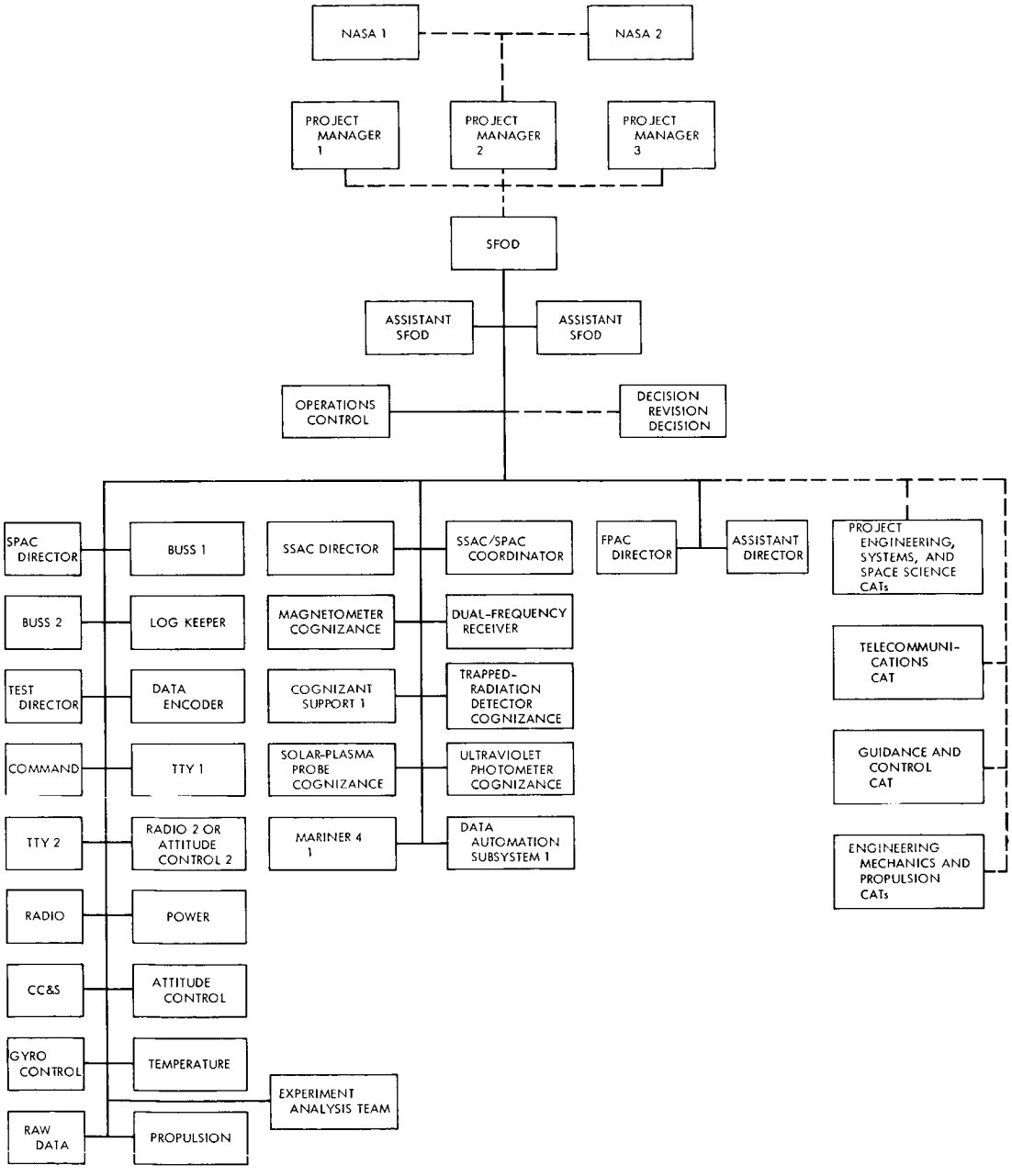

FIGURE 6–17.—SPAC analysis control network (BUSS).

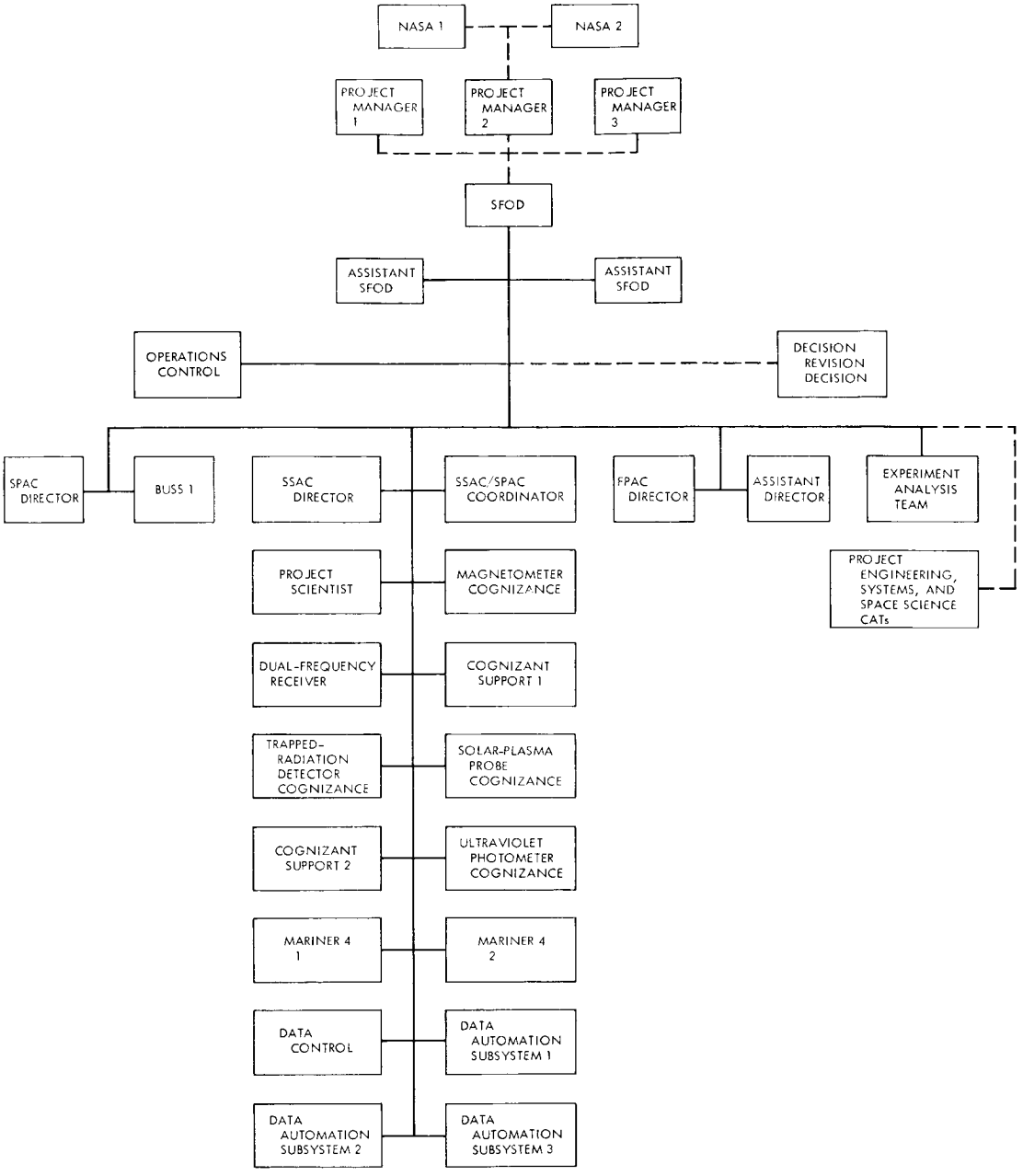

FIGURE 6–18.—SSAC analysis control network (SPACE).

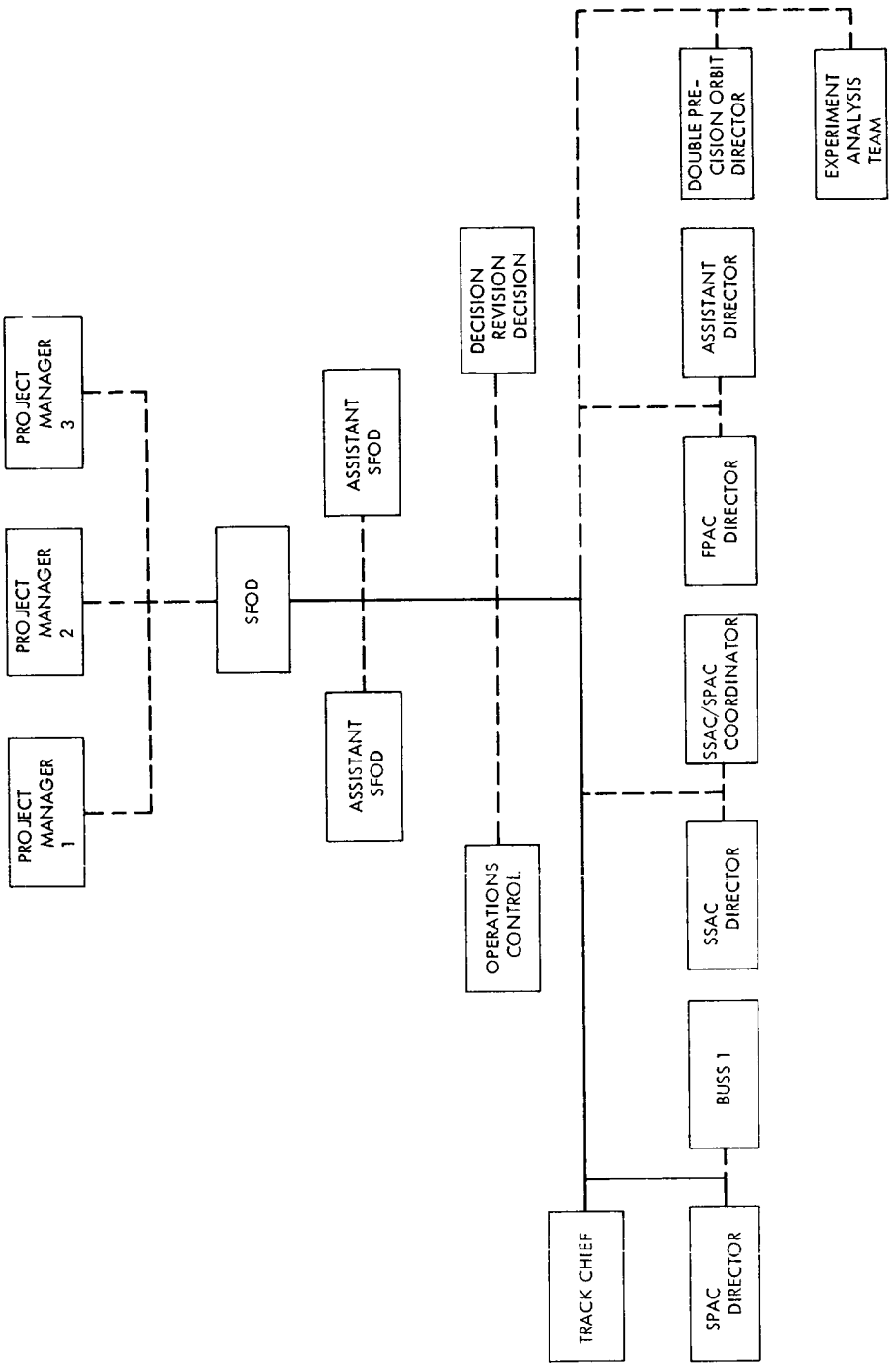

FIGURE 6–19.–Command network (MAR–COMMAND).

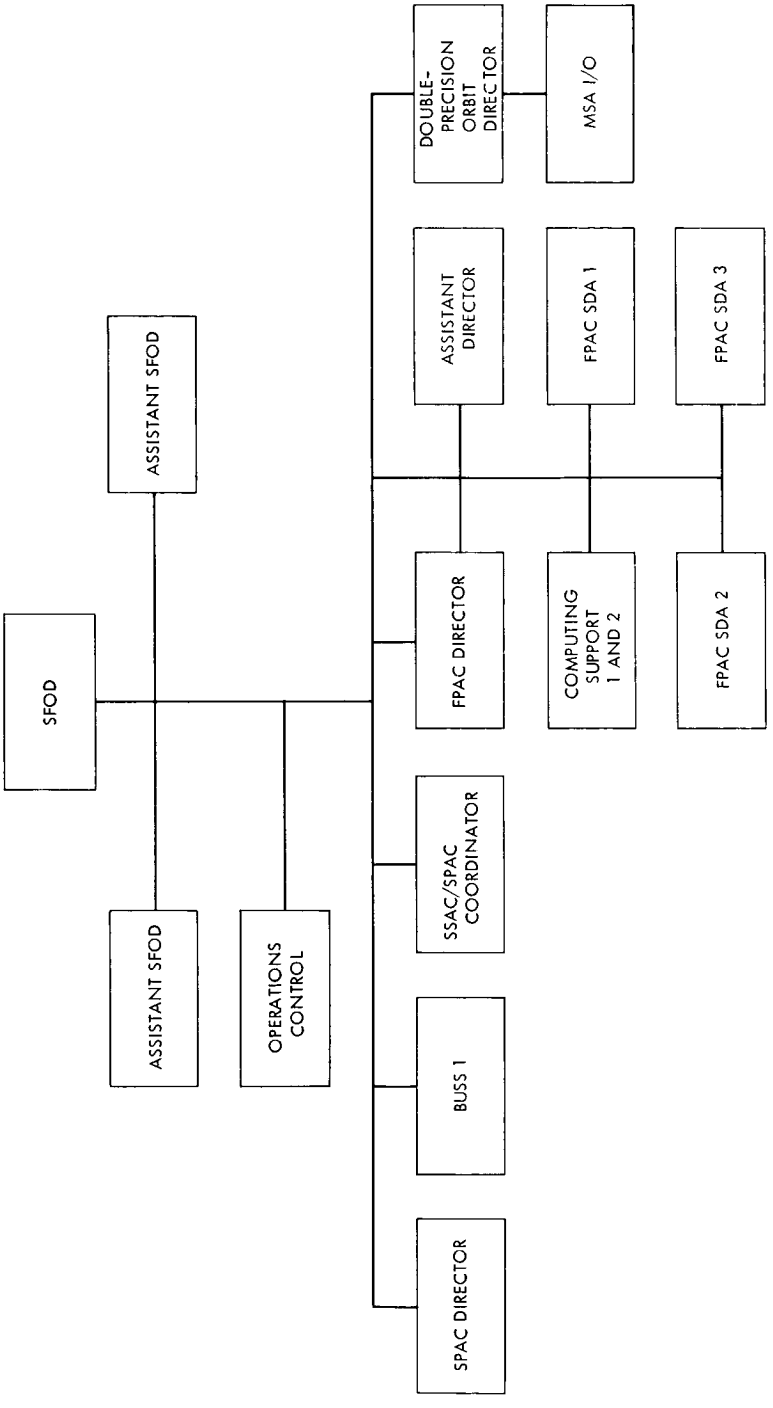

FIGURE 6–20.—Data-coordination network (DA–COR).

Schedule and Control of Interfaces

Scheduling for encounter and preencounter testing was conducted exactly as it was during the mission. Users of DSN facilities submitted requirements to three types of DSN scheduling techniques: (1) the 16-month loading schedule, which was an attempt to predict DSN loading 16 months in the future; (2) the DSN 12-week schedule, which allocated DSN resources to project requirements on an hours per week basis; and (3) the DSN 7-day operations schedule, which defined project requirements and was used to conduct DSN activities on a day-by-day, hour-by-hour basis. Changes to the DSN 7-day schedule were conducted through the DSN operations control group. The DSN scheduling requirements for the Mariner-Venus 1967 project followed prescribed routes, whether the time was for testing or flight support. All interfacing with respect to scheduling was conducted through the DSN project engineer whose responsibility it was to collect and review all inputs to eliminate all possible internal project conflicts and redundancy in requests for DSN resources. His approval was required on all inputs to the DSN scheduling systems.

Mark I and Mark II Ranging Subsystems

Mark I ranging

Mariner-Venus 1967 was the first project to use the JPL-developed Mark IA pseudorandom code-ranging subsystem (fig. 6–21) to range a spacecraft beyond lunar distances.

The first TURN RANGING ON command was transmitted by DSS 11 at 02:39:00 GMT on June 20, 1967; the Mark IA ranging system first became active on that day during the DSS 61 pass. Ranging modulation was applied at 11:32:58 GMT, and the ranging receiver was in lock at 11:33:34 GMT. The first range code was acquired at 12:11:00 GMT.

The Mark IA ranging system was used through $L+22$ days. At $L+23$ days, an unsuccessful attempt to range on the spacecraft occurred. On July 10, 1967 ($L+25$ days), a decision was made to attempt no more ranging with the Mark IA subsystem. All ranging accomplished after this date employed the Mark II R&D planetary ranging subsystem. The Mark IA subsystem ranged to a distance of 6×10^6 km from Earth to an accuracy of about 45 m.

Mark II ranging

The Mark II ranging subsystem (fig. 6–22) was designed and developed as one of the experiments on Mariner 5. The purpose of this experiment was to range in the vicinity of Venus and, thus, to refine the astronomical unit. The

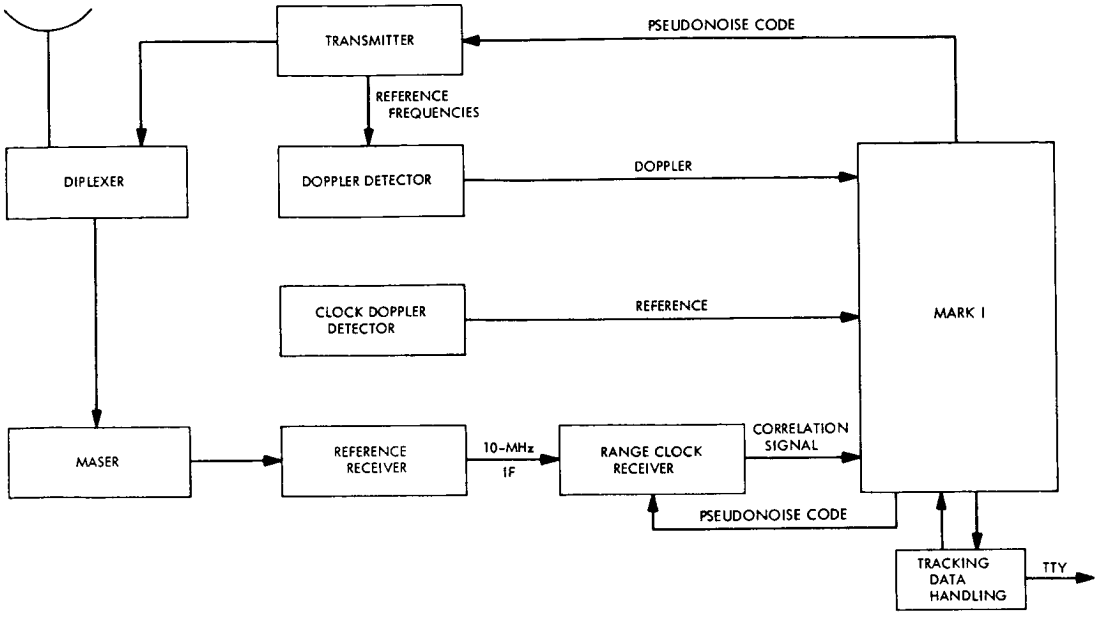

FIGURE 6–21.—Configuration of Mark I ranging subsystem.

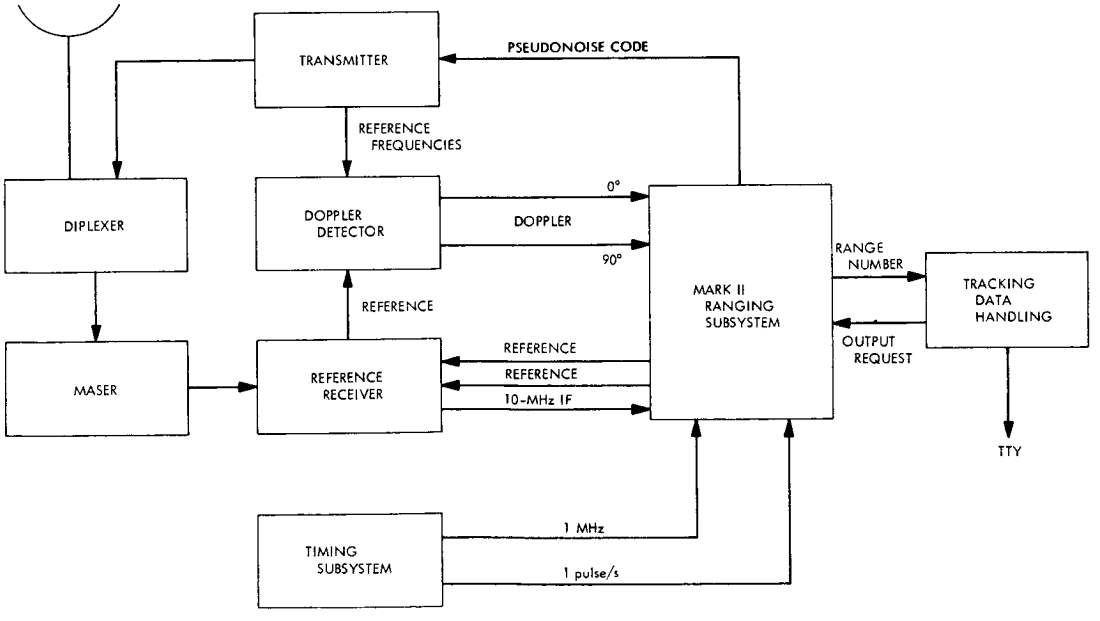

FIGURE 6–22.—Configuration of Mark II ranging subsystem.

R&D ranging subsystem was installed at DSS 14 in May 1967. One of the major interfaces between Mark II ranging and the GSDS receiver was to replace the 20-MHz free-running oscillator in the receiver with a 10-MHz signal and the required multipliers, which were coherently related to the station rubidium standard and developed in the Mark II ranging subsystem. This coherent reference signal was also required and used for the occultation experiment.

The first ranging operation on the Mariner 5 spacecraft took place on June 21, 1967. Valid range numbers were observed, except for a 3-μs difference between engineering predicts and range numbers. This was attributed to two factors: (1) predicts did not include spacecraft delay (933 ns) and (2) the station delay was unknown. R&D ranging operations continued routinely until about mid-August, when range data and predicts were in gross disagreement, prompting redesign of the subsystem range coders. It was subsequently discovered that the predicts were in error; however, the redesign resulted in a system that was less susceptible to noise. Because of code-acquisition time (a function of signal level), ranging was not attempted on Mariner 5 until after the spacecraft had switched to its high-gain antenna. Ranging on the Mariner 5 spacecraft was next accomplished on October 4, 1967.

The value of the Mark II ranging data was greatly enhanced as the spacecraft approached Venus. The encounter sequence was initially planned to stop ranging about 4 hr before encounter to allow the command loop to be locked. To obtain maximum value from the ranging data, a test was made to determine whether the station uplink could be modulated by command and ranging modulation signals simultaneously and whether there was any interaction between the two. On October 6, 1967, DSS 14 locked up the spacecraft command loop and ranged the spacecraft. No interaction was observed. Later analysis showed that there was no significant difference between range data with and without command modulation. During the mission, no commands were transmitted with ranging modulation applied. Ranging on the Mariner 5 spacecraft was performed up to 1 hr before encounter. Ranging on the spacecraft was accomplished to a distance of 98 million km, with an accuracy of about 10 m.

Although the third mode is normally used for Mariner operations, three modes of recording the telemetry data are available for selection:

(1) Non-return-to-zero display of all channels
(2) Return-to-zero display of all channels
(3) Return-to-zero display of all channels except return-to-64 display for gyroscope and position sensor channels

The recorder channel assignments for Mariners 4 and 5 are as follows:

Recorder channel 1: deck synchronization; channel marker; station out of synchronization (HSDL only).
Recorder channel 2: spacecraft telemetry channel 101.
Recorder channel 3: spacecraft telemetry channel 102.
Recorder channel 4: spacecraft telemetry channel 110.
Recorder channel 5: spacecraft telemetry channel 109 or station AGC.
Recorder channel 6: spacecraft telemetry channels 103, 104, and 107 (Mariner 5); 105, 106, and 107 (Mariner 4).
Recorder channel 7: spacecraft telemetry channels 112, 113, and 114.
Recorder channel 8: spacecraft telemetry channels 108 and 118 (Mariner 5); 108 only (Mariner 4).
Recorder left-event pen: time in BCD (HSDL only).
Recorder right-event pen: station out of synchronization (HSDL only).

CHAPTER 7

Spacecraft Performance

From Mariner 5 launch on June 14 until the nominal end of the mission on November 21, performance of the spacecraft was excellent. Useful scientific and engineering data were acquired during the interplanetary cruise and during planetary encounter.

On November 21 the combination of high-gain-antenna pointing and Earth-spacecraft range exceeded the limits required for obtaining useful telemetry data. As a result, the spacecraft transmitter was commanded to switch from the high-gain to the low-gain antenna. This command was designed to enable the reacquisition of telemetry data if the spacecraft was still operating. Analysis of spacecraft performance indicated that data from the spacecraft would continue to be received in the last quarter of 1968.

The nominal flight sequence of events for Mariner 5 was designed to be totally automatic, requiring no action from the ground for a normal flight (except for the trajectory-correction maneuver and activation of the ranging receiver). Provided that the CC&S operated correctly, such a design relieved the mission from any dependence upon the ground-to-spacecraft communication link (uplink). The ground-command function was necessary to the success of the mission only if the CC&S failed.

The nominal flight sequence adopted for Mariner 5 before launch is presented in table 7–I (p. 266). Table 7–II (p. 273) is a chronological sequence of events for the Mariner 5 mission, starting with liftoff and ending with the transfer of the spacecraft transmitter to the low-gain antenna on November 21, 1967.

Major deviations from nominal flight sequence are as follows:

(1) Spacecraft was rolled three times after the midcourse maneuver to allow the ultraviolet photometer to scan for atomic hydrogen in the extended atmosphere of the Earth and to calibrate the instrument.
(2) Lunar ranging was turned on after midcourse manuever to obtain an independent data source for orbit redetermination.
(3) Battery charger was turned off when the battery was fully charged.
(4) Planetary encounter sequence was modified by ground command to provide maximum in backup capability for all critical functions.

(5) Planetary ranging was obtained as close to the planet before encounter as possible for celestial mechanics and orbit determination.
(6) Bit-rate change exercise was performed for ultraviolet photometer calibration and signal-level change monitoring.
(7) Spacecraft was rolled three times to allow the ultraviolet photometer a calibration at 8⅓ bps when the spacecraft had completed 180° of a revolution, in the heliocentric orbit (from (1), above). The dual-frequency radio propagation experiment also wanted these data for comparison with the Earth-based measurements of antenna patterns.
(8) Encounter exercise and midcourse pointing exercise were combined to allow a calibration of the ultraviolet photometer by repointing the sensor at the point in celestial space it had been observing at the time of the CC&S MT–6 event.
(9) Spacecraft was conditioned for the long-term cruise.

Although spacecraft performance was excellent, the mission was not without incident. Several spacecraft problems were evident:

(1) Ultraviolet photometer channel C reading had a step function decrease in average reading following midcourse maneuver.
(2) Ultraviolet photometer calibrations and drift checks changed frame count on which they occurred after midcourse maneuver.
(3) Midcourse maneuver change in velocity was smaller than predicted.
(4) Ultraviolet photometer channel C reading increased significantly more than expected at the switch in data-encoder bit rate (CC&S MT–6) to 8⅓ bps.
(5) CC&S produced two event-register indications when master-timer events and cyclic events occurred concurrently.
(6) Station automatic gain control and data-subcarrier signal-to-noise ratio increased at switch in data-encoder bit rate from 33⅓ to 8⅓ bps.

In addition, minor anomalies were encountered in the mission:

(1) Data-encoder deck skip observed upon arming of pyrotechnic subsystem.
(2) Sun sensors acquired Earth-straylight false null.
(3) Canopus sensor acquired Earth straylight during Canopus search.
(4) Open-circuit voltage of standard solar cell was higher than predicted.
(5) Ranging receiver turn-on was observable by small current and temperature increases.
(6) Many small roll transients were observed.
(7) Battery-charger off produced a data-encoder deck skip and a DAS status-bit change in step.

(8) Ultraviolet photometer temperature increased above predicted value after switch to 8⅓ bps.
(9) White TCR's degraded (darkened) faster than predicted; black degraded (bleached) faster than predicted.
(10) Ultraviolet photometer had a slight error in pointing angle.
(11) PIPS propellant decomposition caused slight increase in pressure.
(12) Transmission of DC–V9 caused command subsystem to drop lock.
(13) Earth sensor observed Venus straylight, which had not been predicted.
(14) Tape-recorder subsystem dropped a few bits during playback.
(15) Solar panels degraded because of radiation damage.
(16) Ultraviolet photometer channel C data were higher than predicted when spacecraft was pitched and rolled to point in celestial sphere where CC&S MT–6 had occurred.
(17) Planet sensor observed first and second limb of Venus.
(18) APAC squib shorted combustion products that produced an event at APAC backup.

The problems and performance characteristics primarily involved individual subsystems and are described in this chapter. The following paragraphs are intended to provide some insight into the Mariner 5 mission from an overall systems point of view.

LAUNCH TO CANOPUS ACQUISITION

Launch was accomplished on June 14, 1967, at 06:01:00, after one hold was called in the countdown to allow better downrange telemetry coverage than the nominal opening of the window. Both the Atlas and the Agena stages of the launch vehicle performed well, injecting the spacecraft on a trajectory well within launch tolerances. An expanded plot of gyro telemetry received upon Agena/spacecraft separation is shown in figure 7–1.

DSS 71 (Cape Kennedy) tracked the spacecraft until $L+7$ min. At the nominal time, the received carrier power from the spacecraft increased, indicating shroud ejection. After DSS 71 set, the Agena channel F (98-kHz) spacecraft telemetry was sent from Antigua by a submarine cable to DSS 71 and was processed in real time until $L+12$ min. DSS 72 (Ascension Island) transmitted data in real time to the SFOF from $L+22$ min, 14 s, until $L+26$ min. During that period, spacecraft telemetry confirmed that the solar panels were reacting to sunlight. At $L+28$ min, 45 s, DSS 51 (Johannesburg) acquired demodulator lock, and data were available after that time.

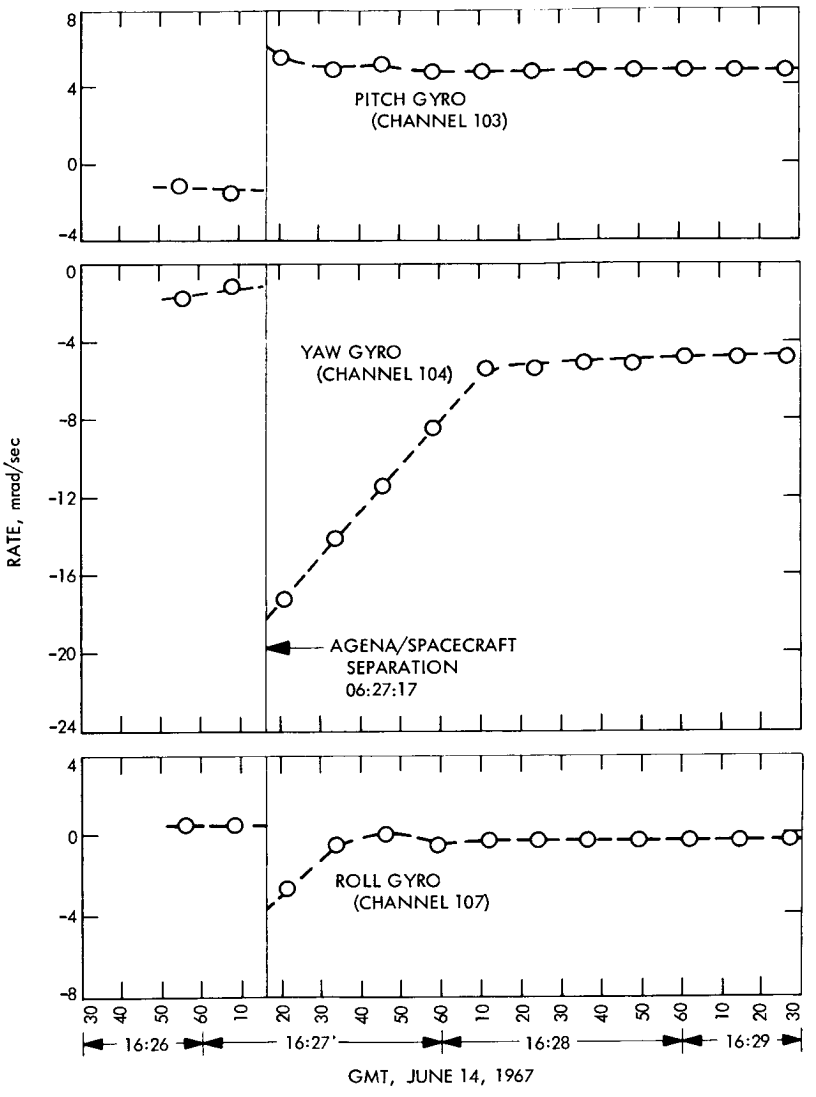

FIGURE 7–1.—Agena/spacecraft separation (June 14, 1967).

When DSS 51 acquired the spacecraft, the data-encoder event channels changed from a reading of 0614 to 2735 (octal), indicating that all separation functions had occurred normally; i.e., pyrotechnics were armed, pyrotechnic current flowed in A and B channels, and all four solar panels were deployed. Other telemetry measurements indicated that the Sun shade was deployed,

science was on, radio power was switched to the high-power mode, the tape-recorder launch motor was off, the CC&S relay hold was off, and the spacecraft was starting to acquire the Sun. A data-encoder deck skip occurred (probably associated with the arming of pyrotechnics upon spacecraft separation). Deck skips with this event had been experienced during the systems testing; therefore, this one was considered normal.

The Sun sensors, activated by the PAS upon spacecraft separation, initially had saturated outputs. The spacecraft was driven clockwise in pitch and counterclockwise in yaw to acquire the Sun. Earthlight on the secondary Sun sensors biased the electrical null at least 78 mrad (4.5°) off the spacecraft/Sun line. The AC subsystem acquired the false null in yaw at 06:33:50 GMT and began to limit cycle about it. The Sun-gate field of view was a cone of about 5.1°. The location of the false null was such that points of its limit cycle placed the Sun in the Sun-gate field of view.

The AC subsystem acquired the Sun-gate event at 06:44:23 GMT, indicating that the pitch axis was also less than 5.1°. The Sun-gate event terminated the power to the secondary Sun sensors, which removed the false null and allowed the Sun to be acquired. This placed the spacecraft into a programed roll at 12.4°/min to furnish calibration data for the magnetometer.

At 06:53:56 GMT, telemetry showed an event in register 2, indicating that the CC&S L–1 event had occurred on time. The solar panels had been deployed by the SIT, so there were no other changes at that time. No events occurred in registers 1 and 3, which indicated that no short circuits existed in the combustion products from the SIT solar-panel pinpuller squib firings. The CC&S LT–2 event occurred normally at 06:57:56 GMT, backing up the already completed PAS function of turning on the AC Sun sensors and acquisition logic.

The roll for the magnetometer calibration was a spin of –3.6 mrad/s, which was within the resolution of the telemetry and the roll-rate deadband and about the nominal spin rate of –3.5 mrad/s. There were 33 complete rolls during the calibration period. The magnetometer, trapped-radiation detector, and plasma probe observed the magnetopause and shock wave of the Earth, and gave the expected indications.

Mariner 4 had an Earth detector that shared a telemetry channel with the roll gyro. When the gyros were on, however, only the roll-gyro output was available. It was recognized that, for the Mariner 5 mission, the Earth sensor could be used as a backup for the Canopus sensor to perform the trajectory-correction maneuver. This backup capability required that the Earth sensor

have its own high-rate telemetry channel so that its output could be read while the gyros were on. This channel also provided the capability for the Earth sensor to view the Earth during each roll of the magnetometer calibration. Data provided on the apparent motion of the Earth and its size allowed an accurate prediction of the spacecraft spin rate. This rate was extrapolated to the CC&S L–3 event to determine the celestial sphere area in which the Canopus sensor would be pointing at turn-on and thus to allow prediction of the objects that could be acquired by the Canopus sensor.

On June 14 at 22:38:00 GMT, the CC&S L–3 event was observed in the data. Canopus-sensor telemetry confirmed that it was powered, and the spacecraft went into a normal roll search. Before launch, it was recognized that the Canopus sensor could acquire straylight from the Earth. Modeling of the terrestrial straylight was very difficult, and was felt to be an order-of-magnitude indication only; the cone angle of the Earth at acquisition was 111°, or 30° outside the Canopus-sensor field of view; the effective Canopus ratio of Earth was about 2.5×10^6 times Canopus. As predicted, straylight from the Earth entered the sensor field of view and permitted acquisition of Earth straylight at 22:49:01 GMT. The predicted Earth brightness was 0.75 times that of Canopus, and the maximum detected straylight brightness was 2.5 times that of Canopus.

It was decided to proceed with Canopus acquisition by ground command from DSS 11. The first roll-override command (DC–V21) was transmitted to the spacecraft and verified in the telemetry at 00:31:07 GMT on June 15. The gyros were turned on, and the spacecraft went into a normal roll search off the first stable null of the Earth. In an effort to prevent the gyros from turning off if a reacquisition were accomplished on the second stable null of the Earth, a second DC–V21 was sent 4 min after the first command. The second DC–V21 caused the spacecraft to roll off the terrestrial straylight second stable null, and to search until acquisition of lunar straylight was achieved. On the basis of the brightness of the terrestrial straylight, the acquisition of the lunar straylight was predicted. The lunar straylight apparently did not have a stable null, and a limit cycle was not established. The sensor moved off of the lunar straylight in the counterclockwise search direction, indicating a low gate dropout of about 0.20 times that of Canopus. The maximum observed lunar straylight was 1.6 times that of Canopus. The spacecraft acquired Canopus at 01:09:02 GMT, which established the logic for gyro turnoff some 200 s later. This completely standard sequence was the initiation of the premaneuver cruise phase of the mission.

CRUISE BEFORE TRAJECTORY CORRECTION

This part of the early flight was generally without incident, except that the TCR did not follow preflight predictions. The white samples showed an increase in absorptance (darkening) that was larger than anticipated, and the black sample began to bleach at a faster rate than expected. These changes had no effect upon the mission, but supplied information useful in the temperature control of future spacecraft. All spacecraft temperatures were within 1.1 K of their predictions; all external equipment showed larger deviations, but were well within tolerances.

TRAJECTORY-CORRECTION MANEUVER

The trajectory-correction maneuver was performed on June 19 at 23:08:28 GMT (time of motor burn), and was successfully completed. Canopus acquisition was maintained until the inertial-control mode was established at MC+1 hr. Telemetry during the maneuver sequence verified that all turns were correct, and that the PIPS motor burn seemed normal.

The CC&S was programed for the following maneuvers:

(1) A 304-s pitch turn that had a 55.267° magnitude. The pitch turn accomplished was a positive 55.18° turn from trajectory information (0.2σ turn in terms of standard deviations).
(2) A 380-s roll turn that had a 70.946° magnitude. The roll turn accomplished was a positive 70.93° turn from trajectory information (0.04σ turn in terms of standard deviations).
(3) A 17.651-s burn time, which is equivalent to 16.127 m/s in spacecraft velocity. Thrust-chamber pressure telemetry was 1 or 2 DN (1.5 percent) below the burning-time calculation predictions, but well within tolerance.

The autopilot maintained the thrust-vector orientation of the spacecraft during the motor burn, as inferred by the postmidcourse analysis of the pitch-and-roll turns. Analysis of the AC subsystem indicated large deflections of the jet vanes during the motor burn. Trajectory analysis indicated that a 15.392-m/s change in velocity occurred as a result of the motor burn, which was 4.5 percent (about 6σ) less than the desired motor burn. This moved the aiming point from $\mathbf{B} \cdot \mathbf{T}$ of 81 483 to 24 278 km; $\mathbf{B} \cdot \mathbf{R}$ of 65 340 to $-14\,855$ km; and time of arrival from 03:53 to 17:34 GMT on October 19, 1967.

Battery Sharing

The magnitude of the pitch turn (55.18°) was great enough to cause the

deployed Sun shade to shade the first few solar cells on the end of solar panel 4A7. This effectively cut off the current flow in each of the solar cells shaded. The solar cells were in three sections on each panel, arranged in series-parallel combinations to produce the desired current and voltage. When the current flow from solar panel 4A7 was inhibited, the spacecraft went into a battery-share mode. When the spacecraft performed the 70.93° roll turn, solar panel 4A7 again became sunlit; and current began to flow. Because the end of solar panel 4A5 became partially shaded, some sections did not produce current. The maneuver required a total of 2.33 A h to be drained from the battery, which exceeded the predicted amount for unshaded, conducting solar panels.

Geometry of the Sun shade in the deployed position, the solar-panel celled surface, and the pitch turn was such that the end of the panel was certain to be shaded. It was thought that the cells would not conduct when shaded and thus would perform as if they were open circuited, necessitating additional battery drain. This was not a problem, as 53.17 A h of the battery remained.

Bay II Primary Sun-Sensor Temperature

During the trajectory-correction maneuver, the bay II primary Sun sensor reached a maximum temperature of about 310 K, 6.7 K lower than predicted. These data were significant because the primary Sun sensors represented a key factor in determining the pitch constraint of a possible second midcourse maneuver near Venus encounter. The difference between the predicted and actual ΔT was attributed almost entirely to a less severe soakback from the motor burn than was expected. Most of the increase in temperature was due to solar heating, which agreed well with predictions. The thermal analysis that constrained the pitch angle for near-Sun maneuvers considered only that heat factor; consequently, the constraints generated before launch seemed realistic.

Ultraviolet Photometer Three-Roll Exercise

Start of Sun reacquisition after the maneuver (June 19, 23:14:11 GMT) also switched the data encoder back to data mode 2. During the maneuver, science was on, but not read out, to allow more engineering data. Sun reacquisition was completed at 23:21:24 GMT after a normal sequence of slightly more than 7 min. Canopus was reacquired at 23:32:19 GMT after a completely normal roll-search sequence. This reacquisition process also allowed the ultraviolet photometer to view an additional segment of the celestial sphere.

The ultraviolet photometer observed the Earth and its upper atmosphere after spacecraft separation, as predicted. The instrument also observed atomic

hydrogen in the extended upper atmosphere and a lesser amount in the anti-Earth direction during the magnetometer calibration. These facts, plus the channel C rest state of about 20 DN, which was higher than predicted, caused the experimenter to request that the spacecraft be rolled after midcourse maneuver.

The spacecraft was rolled three times after the completion of midcourse maneuver. This decision was based upon the potential scientific value to be gained and the fact that no spacecraft function was required that had not been successfully performed in this flight. The roll sequence was as follows: As soon as Canopus was acquired, command DC–V21 was sent to override Canopus acquisition and to put the spacecraft into the normal counterclockwise roll search. The first DC–V21 command was observed in the data at 23:34:07 GMT. Each roll override was accomplished before the gyros turned off to reduce the power transients induced into the spacecraft. Each of the three rolls in the roll-search mode was completely normal, and Canopus was reacquired for the last time before Venus encounter at 02:06:15 GMT on June 20. The gyros turned off about 200 s later, preparatory to the cruise state after the trajectory-correction maneuver. These rolls allowed the ultraviolet photometer to see, during each roll, some stars that were of ultraviolet radiation.

INTERPLANETARY CRUISE

After the reestablishment of postmaneuver cruise-mode operations, the spacecraft entered the interplanetary-cruise phase of the mission. This phase continued until the start of the planetary-encounter phase on October 19. Included in the cruise phase were the following flight-operation sequences, which modified the cruise configuration to some extent:

(1) Insertion of the maneuver minimum-turn and burn-duration commands as protection against a failure-induced, inadvertent trajectory-correction maneuver while the spacecraft was not being monitored
(2) Turning on and off of the spacecraft ranging receiver
(3) Switching of the spacecraft transmitter from the triode-cavity power amplifier to the TWT power amplifier to maximize the probability of mission success
(4) Turning off of the battery charger when the battery was fully charged
(5) DC–V15 roll-control mode command to lessen the possibility of loss of the roll reference

Minimum-Maneuver Commands

Minimum-maneuver commands were transmitted to the spacecraft following

the CC&S maneuver-counter-overflow event (the first time that new values could be stored in the CC&S after the start of the trajectory-correction maneuver). The minimum-pitch-turn command (the first to be sent) was observed in the data at 02:20:13 GMT on June 20. The three commands were transmitted on 5-min centers; all produced the expected results.

Ranging

On June 20 Mariner 5 first used the turnaround ranging capability. At 02:39:00 GMT, a DC–V9 command was transmitted to activate the spacecraft ranging receiver to provide an additional independent data source for orbit redetermination after the maneuver. Ranging and doppler data were used to determine the need for a second trajectory-correction maneuver. A second midcourse maneuver was not required.

Ranging-receiver performance was excellent throughout the mission. Ranging was used whenever the signal was above threshold, ranging time was available at the stations, and the need existed for orbit determination or celestial mechanics data.

The Mark I (lunar) ranging system did not reach threshold until July 7, 1967. At that time, the geocentric range was in excess of 6×10^6 km. This was an uplink, received signal level of about -120 dBm, which was much better than originally predicted.

Roll Transient

At 21:08:20 GMT on June 23, 1967, a roll transient was observed. The Canopus sensor observed a bright object and tracked it for several seconds. Optical control of the roll axis was not lost, and it took 11.5 min for the roll limit cycle to return to normal. Many roll transients were observed by Mariner 4 during its flight to Mars, necessitating an in-flight operational mode change. A Mariner 5 design change was made to remove the roll override associated with Canopus intensity, which was too high. More than 20 roll transients were observed in the Mariner 5 data, and none caused a loss of roll control.

Power Amplifier Switching by Command

Early in the Mariner 5 flight, a recommendation was made to switch the radio to the TWT amplifier via ground-command action. This action represented the implementation of a radio flight plan formulated before launch. Command action (DC–V7) was initiated on June 27, 1967, at 00:28:00 GMT; and the transfer from the cavity amplifier to the TWT amplifier was successfully completed.

Battery-Charger Turn-Off

At 00:58:00 GMT, the battery charger was turned off. The battery charger had returned 5.64 A h to the battery since the maneuver, and it was fully charged with a capacity of 58.8 A h. In an effort to demonstrate long-term battery storage in space, it was decided to keep the Mariner 5 battery fully charged during the flight and not to trickle-charge it. Battery performance data from Mariner 5 then could be compared with data from Mariner 4 to determine the better storage technique.

Central Computer and Sequencer Master-Timer Events

Six CC&S master-timer (MT) events occurred during the interplanetary-cruise phase of the mission. All commands used by the CC&S were correctly transferred to the appropriate spacecraft subsystems.

The first MT command issued was the bit-rate switch event (MT–6), which occurred on July 24, 1967, at 19:19:21 GMT. The data encoder responded normally, switching from a rate of 33⅓ to 8⅓ bps.

On August 24, at 08:41:33 GMT (ground-receipt time), the first Canopus-sensor cone-angle update (MT–1) was issued by the CC&S. The event was normal in every respect as far as the data were concerned, and telemetry subsequently verified that the cone angle had changed from the preset position of 79.68° to the MT–1 position of 85.125°. (CC&S CY–1 No. 26 occurred simultaneously and produced the other expected event.)

The second Canopus-sensor cone-angle update (MT–2) was observed in the telemetry data on September 10 at 00:41:52 GMT. (CC&S CY–1 No. 32 occurred simultaneously, and produced the other expected event.) The event was normal, and telemetry subsequently verified that the cone angle had changed to 90.25°.

The third Canopus-sensor cone-angle update (MT–3) was received in the data on September 26 at 16:42:43 GMT. (CC&S CY–1 No. 38 occurred simultaneously and produced the other expected event.) All data indicated a normal cone-angle update to 95.37°.

The fifth CC&S MT command issued was the transmitter switch to the high-gain antenna (MT–5), which occurred on October 1 at 16:43:33 GMT. Station AGC changed from a reading of −165.4 to −156.8 dBm after MT–5, well within the predicted signal-level change for the antenna-Earth cone and clock angles. All expected changes were verified in the data. Removal of all rf losses from the low-gain antenna mast caused the antenna to drop 10.6 K in

temperature. The temperature of the magnetometer sensor also decreased significantly (7.8 K), indicating good conductive coupling between the sensor and mast.

The fourth Canopus-sensor cone-angle update from 95.19° to 100.5° by a CC&S command (MT–4) occurred at 14:04:14 GMT on October 10. The event was normal. (CC&S CY–1 No. 43 occurred simultaneously and produced the expected event.)

Temperature-Control References

The TCR performance proved that independence from net absorbed solar thermal energy must be used for planetary spacecraft thermal design.

The S–13M white TCR went off scale on July 23, 1967, 39 days after launch. The apparent solar absorptance had changed from 0.20 to 0.326 in a period that had been predicted to be from 60 to 100 days. The 0.12 change in absorptance in 900 hr compares with two separate laboratory tests of 1200 and 1500 hr, in which the results were 0.06 and 0.02, respectively. This rapid degradation occurred on a treated white paint formulated to improve stability for use in spacecraft design.

The S–13 white TCR went off scale on August 1, 32 days earlier than predicted from laboratory tests. The white paint on the TCR (the type used on the spacecraft for thermal control) was used even though degradation was known to be relatively high because it was the best characterized white paint available. (S–13M was flown to AFETR for the S–12M TCR.) Degradation rate was rapid for the first 4 days, after which the rate approached that of the S–13M sample. Solar absorptance of S–13 became an almost constant 0.07 higher than the S–13M sample. (On July 20, S–13 was 0.388, compared to 0.319 for S–13M.)

Thermal shades and shields were used on Mariner 5 for protection against direct-sunlight degradation of the white paint. The black TCR used Cat-A-Lac black paint, and went off scale on October 27, 1967, 22 days after the nominal expected time. Bleaching of approximately 4 percent of the black TCR had occurred by the time it went off scale. This black paint was used predominantly on the spacecraft areas in which high absorptivity was required.

Thermal Deviations

Thermal predictions were within tolerances for all measurements where the material properties did not change from those predicted. The lower thermal-shield temperature increased faster than expected because of degradation (darken-

ing) of the Teflon outer layer; the effect upon the bus temperatures was negligible. The increased temperature did not represent a threat to the shield materials, which have a failure limit of 422 K compared with a predicted perihelion temperature of 394 K.

PLANETARY ENCOUNTER

Planetary Acquisition and Record Sequence

The encounter sequence was initiated with the transmission of a DC–V25 command from DSS 41 at 02:49:00 GMT on October 19, 1967; the command was observed in the data at 02:58:25 GMT. Spacecraft response was normal; the tape-recorder subsystem 2.4-kHz power was turned on, and the terminator sensor was energized. Power levels and temperature increased, as predicted.

The CC&S MT–7 event was observed in the telemetry at 04:45:06 GMT; inasmuch as it had been preempted by DC–V25, however, it had no effect upon spacecraft performance.

Command modulation was applied, and command in-lock was established at 06:30:07 GMT to prepare for the DC–V9 command to turn on the ranging receiver. The spacecraft was operating normally, and DC–V9 was transmitted at 08:50:00 GMT. The ground receiver dropped lock at 08:59:28 and reacquired it at 08:59:30 GMT, with about 1-dBm decrease in signal level. The spacecraft command subsystem was out of lock until 09:01:49 GMT, when the spacecraft returned to normal with ranging on. Each of these events was normal.

The command to start the DAS encounter mode (DC–V24) was transmitted at 10:50:00 GMT. The switch to data mode 3 occurred at 10:57:29 GMT, along with the DAS status bits indicating that DAS clock B was enabled; the plasma probe had gone to mode 3, and the planet-sensor excitation was on. The DC–V24 command was sent before the CC&S MT–8 event to set up the DAS logic so that only one DC–V24 would be required to inhibit DAS clock B if it malfunctioned. By sending DC–V24 before MT–8, evidence was provided that the command was received and acted upon.

CC&S MT–8 occurred at 11:25:03 GMT as a change in DAS status bit 16. Since DC–V24 had preempted MT–8, this was the only change. The solar-plasma probe completed a cycle before it actually switched to the new mode. Consequently, the DC–V24 command set up the plasma-probe mode 3 logic, but the instrument did not go to mode 3 operation untll 11:28:00 GMT.

Spacecraft operation and performance were completely normal up to this point; therefore, command modulation was removed at 11:31:00 GMT to allow two-way rf transfer from DSS 62 to DSS 14. The two-way transfer was com-

pleted at 11:47:00 GMT, and command was in lock at 12:30:10 GMT. The time for acquiring command in-lock is a variable; for planning purposes, 12 min had been used. In this case, about 4 min were required; therefore, the application of ranging modulation was moved up from 12:44:00 GMT to maximize ranging time. Planetary-ranging modulation was applied at 12:35:00 and was in lock at 12:48:35 GMT. Ranging modulation was turned off at 12:20:00 GMT in preparation for the transmission of the DC–V16 timed command (start encounter backup clock). Two criteria were used for selecting the transmission time:

(1) It was desired to select a time based upon the latest available trajectory data ($E-4$ hr) so that DAS clock A would provide APAC backup at the center of occultation. This was an attempt to obtain the most data possible for any atmosphere.
(2) It was desired to obtain a DFR modulation-phase measurement (DAS word 21) in an even-numbered DAS frame, as close as possible to (but no later than) 195 s before closest approach. This was the most useful single item of DFR data that could be obtained in real time.

Transmission time for DC–V16 was selected as 14:31:43 GMT, which would provide the DFR measurement in frame 208. The RWV was set up in the automatically timed start mode, which was the mode used for all previous commands. Initiation of the automatic mode at 14:31:00 started as expected; however, at 14:31:03 GMT (40 s early), the RWV tape reader began to read the tape. It took 27 s before the RWV began to transmit the command; therefore, no command bits were sent because the command modulation was removed before the command left the RWV. The onboard spacecraft subsystem continued to operate well, which meant that the primary function would complete encounter in a nominal manner.

Planet-sensor output was provided at 16:34:22 GMT. This inhibited ultraviolet photometer calibrations, caused the DAS to issue "start tape" commands each 50.4 s, and caused the track 1 data record to start. The far limb of Venus passed out of the planet-sensor field of view at 16:38:24 GMT. This behavior was normal in function and in time of occurrence. The planet sensor started DAS clock B, which in turn started the tape-recorder record mode.

The DC–V9 command to turn off the spacecraft ranging receiver was transmitted at 16:40:00 GMT. This command increased the spacecraft received signal strength by 0.7 dBm, providing the capability to go slightly deeper into the atmosphere during occultation. The spacecraft was performing in a nominal manner, so command modulation was removed at 16:41:30 GMT, and the

ground transmitter was turned off 30 s later. This prepared the spacecraft for the desired one-way rf mode to enter occultation.

The tape recorder started to record data on tape track 2 at 16:46:46 GMT. The normal onboard command to start this record sequence came from DAS clock B. At 16:50:52 GMT, the auxiliary oscillator began warmup for the occultation experiment.

Occultation

The spacecraft *S*-band rf signal was lost on the closed-loop receiver at DSS 14 (Mars site, 210-ft antenna, Goldstone) at 17:39:08 GMT on October 19, 1967, as Mariner 5 entered the Earth-occultation region of Venus. Four Goldstone *S*-band stations tracked the spacecraft during the occultation experiment: DSS 14 was prime because of the extra capability afforded by the 210-ft antenna; DSS 13 was the primary backup because of its lower system-noise temperature; and DSS 11 and 12 provided additional backup. All stations were able to acquire usable data. The open-loop receiver at DSS 14 was able to maintain lock until 17:42:05 GMT, providing additional data.

The terminator sensor provided its output, which caused APAC to occur in the data, at 17:46:51 GMT. These data were actually the recorded data, as determined during the playback. The 17.6° APAC for the *S*-band high-gain antenna produced a decrease of 2 to 3 dBm in ground-received signal strength.

Closest approach to Venus occurred at 17:34:56 GMT (at the spacecraft). The altitude above the Venusian surface was 4094 km, using a Venus radius of 6056 km. On Earth, this event took place during the occultation, and was derived from the FPAC trajectory data. The orbit was almost as predicted.

The spacecraft *S*-band radiofrequency began exit occultation, which allowed the DSS 14 receiver to acquire lock at 17:59:59 GMT. Received signal strength was 3 dBm lower than before occultation, giving an early indication of a successful APAC. Predicted time for exit occultation, based upon the entire occultation time, was accurate to about 1 min. The DAS real-time data confirmed the APAC event after the demodulator acquired lock. All spacecraft data indicated a normal encounter.

The DSS 12 transmitter had been turned on at 17:52:00 GMT, with a transmitter frequency for closest approach plus 1370 s at the spacecraft (17:57:45 GMT). This frequency was chosen to acquire all denser atmospheric data in one-way lock and the ionospheric data in two-way lock. This would prevent the possibility of acquiring two-way lock and losing it before a solid two-way lock could be established.

The DFR had been receiving a signal from the Stanford transmitter since station rise. The Stanford ground antenna used was a 150-ft parabolic steerable antenna using transmitter powers of 350 kW at the lower frequency and 30 kW at the higher frequency. The signal from the 49.8-MHz antenna was acquired at 11:05:42 (ground-receipt time); the signal from the 423.3-MHz antenna was acquired at 11:09:04 GMT. (See fig. 7–2.) The 49.8-MHz signal dropped lock because of Earth occultation at 17:38:10; the 423.3-MHz signal lost lock at 17:39:00 GMT. At exit occultation, the 423.3-MHz signal was reacquired at 18:00:31; the 49.8-MHz signal acquired solid lock at 18:03:13 GMT. There was also a short period, from 18:00:51 to 18:01:11 GMT, when the 49.8-MHz signal was obtained. The DFR performed as predicted for occultation.

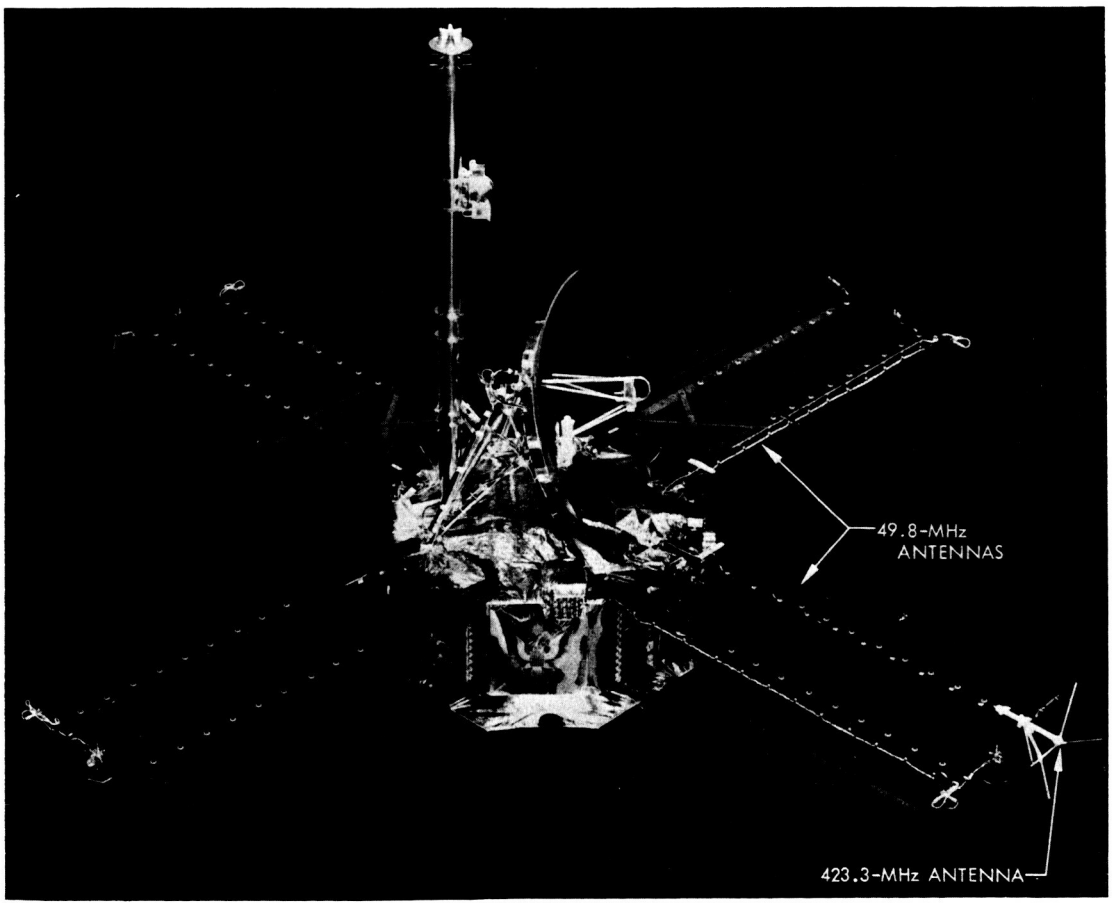

FIGURE 7–2.—Locations of DFR antennas.

Completion of Record Sequence

DSS 14 was used for two reasons: (1) DSS 14 was the only station that had the capability of planetary ranging, and (2) the extra uplink capability of this station could be used for commanding the spacecraft even if it lost roll control. To obtain two-way doppler data, which were needed for orbit determination (for flight use as well as for the celestial mechanics experiment), it was important to acquire two-way lock early after occultation. The DSS 14 transmitter was turned on at 18:17:00 GMT. Two-way lock was reestablished at 18:19:00 GMT.

The APAC backup command was given by DAS clock A at 18:10:10 GMT, as expected. The terminator sensor performed the APAC function during occultation, so only the DAS status bit changed at that time. After the data encoder switched back to data mode 2, an extra event was found, which indicated that a path to ground existed through the squib-combustion products. This type of event first occurred on Mariner 2.

Commands to end track 2 data and to stop sensing "start tape" commands were given by DAS clock B at 18:34:18 GMT. The tape recorder turned the record motor off at 18:41:51 GMT, when the EOT foil passed over the record heads. Clock B also stopped the record sequence at 18:47:45 GMT, removed plasma-probe mode 3, and switched the data encoder to data mode 2. Each of these events occurred on schedule, and the spacecraft continued to perform in an excellent manner.

The command subsystem was in lock at 18:51:03 GMT, allowing DC–V9 (ranging receiver on) to be transmitted at 19:00:00 GMT (10 min earlier than scheduled). The DC–V9 command was observed in the data at 19:25:17 GMT. The ranging code was locked up within the next 40 min, and remained in lock until after ranging modulation was removed at 21:48:00 GMT because of DSS 14 set.

Preplayback Cruise After Encounter

The Earth sensor was receiving straylight from Venus when the switch to data mode 2 took place. The Venus clock and cone angles were such that the straylight continued to be observed by the Earth sensor until data mode 4 started again at 20:09:32 GMT on October 21, 1967, during the second playback.

Temperature effects of the encounter with Venus were evident when the spacecraft switched back to data mode 2. The high-gain antenna registered an increase in temperature of 18.9 K from −171 K; the temperature later decreased to −183 K. The difference between the latter value and the peak was attributed to the thermal input from Venus. This behavior was as predicted. The APAC

event reduced the radiative coupling between the high-gain antenna and the upper thermal shield and increased the coupling between the high-gain antenna and the solar panels. Thus, a temperature decrease of 6.7 K resulted for the upper thermal shield; and an increase of 11.7 K, for the high-gain antenna. The magnetometer was 7.8 K warmer (265 K), and the low-gain antenna was 12.8 K warmer (222 K) at the time of the first postencounter data. The magnetometer temperature returned to preencounter levels, and the low-gain antenna temperature increased 2.2 K because of the effects described. The spacecraft bus performed as expected; temperatures increased 0.6 to 1.1 K because of effects from the planet.

The DSS 14 transmitter was turned off on time. This produced an out-of-lock condition at 21:59:03 GMT because the spacecraft switched from the voltage-controlled oscillator to the auxiliary oscillator (rf one-way mode). The stability of the auxiliary oscillator remained normal, and produced the expected warmup curve. This was a postcalibration test for the *S*-band occultation experiment. The auxiliary oscillator test ended at 23:00:41 GMT, when two-way rf lock was reestablished with DSS 41. The Stanford station was set at 23:10:00 GMT, completing the real-time, near-Venus DFR data.

The second roll transient in the near-Venus environment was observed in the attitude-control data at 00:40:28 GMT on October 20. This roll transient showed that the roll-position readout approached the clockwise limit-cycle edge at about 3 μrad/s, and suddenly went to the counterclockwise limit-cycle edge at about 170 μrad/s. (A normal limit-cycle reversal is 14 μrad/s for both valves firing once.) The roll motion was back to normal within 10 min. Two other roll transients in the near-Venus environment (at 20:20:12 GMT on October 19 and 08:04:50 GMT on October 20) were less dynamic.

Two-way rf handover from DSS 41 to DSS 62 occurred smoothly at 04:19:00 GMT on October 20. Command modulation was applied, and command was in lock at 06:16:21 GMT for any malfunction that could occur at the beginning of the Venus-recorded data playback. The spacecraft performed as planned throughout the entire encounter sequence.

PLAYBACK

Tape-recorder playback was initiated by the CC&S MT–9 event at 07:25:23 GMT on October 20, as observed in the data. The switch to data mode 4/track 1 (4/1) was confirmed by about 50 s of mode 4 data—the last Venus data recorded on track 1. The track 1 recording continued until the EOT foil stopped the

tape-recorder motor; the track 2 recording was commanded off about 7 min before end of tape, so no data were acquired near the EOT foil on track 2. Mode 1 data (engineering) that started at 07:26:12 GMT indicated that all subsystems were performing correctly. The CC&S MT–9 event was registered, and turn-on of the tape-recorder playback motor was observed in the power readings.

The 4/1 test pattern began at 07:44:33 GMT, exactly as the readout of these data occurred in the prelaunch tests. This demonstrated the tape-recorder playback capability and the correct functioning of the tape-recorder/data-encoder interface. The track 1 test pattern ended at 08:00:36 GMT and switched the data-encoder 4/1 logic back to data mode 1. Engineering data were normal, so command modulation was removed; command went out of lock at 08:15:04 GMT.

Switch to data mode 4 at 08:15:38 GMT started the playback of some old test data. The tape did not always stop in the same place at the end of the launch because of temperature effects on the launch motor, bearings, and tape. The launch mode ended on the tape where the record runup began. This was as expected, and the Venus-data playback started at 08:17:52 GMT. All recorded data seemed normal. Each eighth bit was an encounter, real-time bit. These were compared with data received on Earth in real time during the record sequence.

Track 1 Venus-data playback ended at 01:13:01 GMT on October 21, when the EOT foil switched the playback heads to track 2. Command modulation was applied just before EOT in case the switch to track 2 did not take place. Mode 1 data at the beginning of the tape ended when the track 2 test pattern began at 01:32:59 GMT. The test pattern was unchanged from prelaunch test readouts. The test pattern ended, and the 4/1 logic switched back to data mode 1 at 01:49:03 GMT. Because all subsystems were performing normally, command modulation was removed.

First playback of the track 2 Venus data started at 03:58:08 GMT, and proceeded smoothly until 16:44:58 GMT, when CC&S CY–1 No. 47 turned off the spacecraft ranging receiver. This produced a small receiver anomaly at DSS 12; data were obtained by using the predemodulator tapes at both DSS 12 and 11. Track 2 playback ended at 18:18:30 GMT when the switch to data mode 1 took place.

Command modulation was applied so that a DC–V9 command could be sent to turn on the ranging receiver, and also in case the switch to track 1 did not occur after EOT. The DC–V9 was observed in the data at 18:54:44 GMT.

All indications were normal for the ranging-receiver-on mode. End of tape occurred at 19:18:17 GMT; the tape was switched back to track 1 and a normal second playback. This second playback was necessary to insure the recovery of any data missing from the first transmission, and to provide duplication of the remainder of the data for comparison purposes.

A DC–V2 command was transmitted at 07:55:00 GMT on October 23, and was observed at 08:04:54 GMT. Data mode 2 indicated that all scientific instruments were functioning correctly. The 2.4-kHz power to the tape-recorder electronics was turned off to protect the spacecraft from any possible failure in the tape-recorder subsystem while its energizing was not required. The DC–V28 command, which turned off the tape-recorder 2.4-kHz electronics and turned the battery charger on or off, was transmitted at 08:25:00 GMT. It was observed in the data at 08:35:27 GMT. Telemetry verified that the tape-recorder 2.4-kHz power was turned off and that the battery charger was turned on. The battery charger was operating at a 15-mA rate, and was left on to charge the battery completely. This was an effort to put the battery in the mode (fully charged) that was least likely to degrade during the warm period around perihelion. All science instruments and engineering subsystems were now back to a cruise condition, thus ending the playback sequence.

POSTENCOUNTER CRUISE

The spacecraft continued to perform well throughout the final month of the Mariner-Venus 1967 project. This phase consisted primarily of operations to obtain additional calibration data for the ultraviolet photometer, communication subsystem performance tests, and conditioning for long-term heliocentric cruise.

Postencounter Cruise Conditioning

The AC subsystem had been commanded to the DC–V15 mode before encounter. At this time, the tracking stations could no longer be committed to 24-hr coverage of Mariner 5. This necessitated returning the spacecraft to the normal mode so that, if roll control were lost, the spacecraft would automatically search for Canopus. This command would also provide a gyro-on event that would be stored and that would provide data for the nontracked periods. The DC–V19 command to restore the normal AC mode was observed in the data at 21:05:56 GMT on October 26.

After about 84 hr of charging, the battery was fully charged with 60 A h capacity, which was an increase of 1.2 A h during the charging period. The

DC–V28 command to turn off the battery charger was observed on Earth at 21:23:51 GMT. A data-encoder deck skip of the low and low-low decks took place as a result of the battery-charger-off transient. Deck skips associated with this function were common during the test phase and were considered normal.

Three Spacecraft Rolls

The spacecraft was rolled three times on November 7, 1967. At this time, the spacecraft had completed 180° of a revolution in the heliocentric orbit from the point at which the three rolls had been performed after midcourse maneuver. A roll at that point would expose the ultraviolet photometer to the same space and stars, but in the opposite order from the earlier rolls. This roll was performed with the data encoder at 8⅓ bps, compared with 33⅓ bps previously. This provided an additional calibration of the ultraviolet photometer to be used for evaluation of the 33⅓ bps data.

Ultraviolet photometer data thus obtained indicated that the channel C background level was approximately 20 DN at the start of the roll, and increased 8 DN in a cyclic manner. Data from the three rolls were in close agreement, and indicated that the northern galactic hemisphere contains more hydrogen than does the southern. This result was observed at 33⅓ bps, but the change was only 2 DN with a 6-DN background level because of the different scale factor.

The DFR data obtained from the playback enabled the antenna pattern to be compared with Earth-based measurements. The antenna pattern at 423.3 MHz was the same; the 49.8-MHz pattern was similar, but had slight deviations caused by fluctuations in the ionosphere of the Earth and the propagation path. The cone angle at which the roll was performed was not the encounter cone angle, but it provided a calibration of the Earth-based measurements.

Solar-Panel Radiation Degradation

The solar panels degraded about 12.5 percent by the end of the mission. This degradation was approximately linear during the mission because there were no large solar flares to cause degradation as there had been during the Mariner 4 mission; the basis for the degradation was the standard cell readings, which were assumed to an accurate indication of the panels. The short-circuit current of the short-circuit-current/open-circuit-voltage transducer cell had decreased 8 percent from the predicted value; the open-circuit voltage had decreased 5.5 percent. Maximum power was then calculated by drawing the new current-versus-voltage curve. The open-circuit voltage changed about 1 percent for each 2°K temperature difference; therefore, an error in prediction of temperature could

affect the results significantly. This amount of degradation would not affect spacecraft performance because the spacecraft would always be inside the Venus orbit, where the solar-panel capability greatly exceeds the requirement. (The solar panels were sized for the near-Earth condition.)

Conditioning for Long-Term Cruise

Only two commands were required to set up the long-term cruise, but it was decided to obtain a small amount of additional data by sending three other commands.

At 15:51:00 GMT on November 21, 1967, DSS 14 sent a DC–V9 command (turn ranging receiver on), which was observed in the data 14 min and 20 s later. Ranging modulation was turned on to obtain a range fix on the spacecraft before the long-term cruise began. Three separate attempts of 30 min each were made to lock up the range code. They were all unsuccessful because the ranging threshold had been slightly exceeded. This was caused by the pointing geometry of the antenna and by the range exceeding 118×10^6 km.

One of the commands required to establish the long-term cruise mode was the DC–V15, which was sent to keep the gyros off when Canopus acquisition was lost. The Canopus-gate-inhibit override was observed in the data at 18:49:09 GMT. If the command had not been sent, there would have been days when no stars of the required brightness fell within the Canopus-sensor acquisition level; therefore, the roll search would have continued until a star satisfied the logic. The gyros would have been on for rather long periods, increasing the internal bus temperature. This temperature increase, plus the switching transients associated with turning the gyros on and off, was not desirable when the acquisition of a definite object was not required.

It was accepted that Canopus acquisition would be lost in late December 1967, when the star moved out of the MT–4 Canopus-sensor field of view. The heliocentric orbit would be quite fast later (less than 200 days), which would require Canopus cone-angle updates frequently. (Even one was impossible after this time because the Mariner 5 antennas pointed away from Earth until late July 1968.)

The spacecraft was next commanded to transmit on the high-gain antenna and receive on the low-gain antenna. This configuration provided a few data samples for interferometer pattern mapping. The ranging receiver was commanded off, leaving only one command required to set up the long-term cruise.

The DC–V12 command to transmit and receive on the low-gain antenna was observed in the data at 19:31:59 GMT, when the ground-receiver AGC

dropped from −149.2 to −159.0 dBm. This established the long-term cruise mode by setting up the spacecraft to transmit data to Earth so that they could be received in late July 1968. The spacecraft was capable of receiving an uplink signal earlier.

A record-only pass was performed with DSS 14 on December 4 between 16:02:00 and 20:00:00 GMT at a signal level of −170.0 dBm. This indicated that the spacecraft was still functioning as designed. At that time, Mariner 5 had been in space for 14 hr more than 173 days. The spacecraft had transmitted more than 210 million bits of data to Earth and had responded successfully to 96 ground commands.

Table 7–1.—Flight sequence adopted before launch

Event	Time	Source	Destination	Comments
1. Verify number of encounter update pulses to be inserted at L—7 min (event 3).	L—15 min	Launch complex equipment (LCE).	CC&S	Number of pulses inserted determines time from launch to CC&S MT-7, which varies with trajectory flight time.
2. Switch to internal power	L—7 min	LCE	Power	
3. Clear counters and insert encounter update pulses.	L—7 min	LCE	CC&S	
4. Release LCE relay hold	L—5 min	LCE	CC&S	
5. Tape recorder to launch mode	L—4 min	LCE	Tape recorder	Monitor DE channel 221; maneuver booster regulator (B/R) output current to determine whether tape recorder is in launch mode.
6. Release CC&S real-time inhibit.	L—3 min	LCE	CC&S	
7. Clear relay release	Event 6+119 s	CC&S	LCE	
8. Liftoff	$L=0$			Provided event 7 occurs within tolerance relative to event 6.
9. Shroud separation	L+317 s (approx)	Agena timer	Agena pyrotechnics	S-band signal level increases.
10. Spacecraft injection	I (L+19.1 to L+35.2 min)	Agena D		Injection is completion of Agena second burn.
11. Spacecraft separation (S)	$S=1$ +2.6 min	Agena D timer	Agena pyrotechnics	Spacecraft V-band released.
a. Radio frequency power-up and turn on science.		Separation connector	Power	Backup to rf power-up is gyros-off; backup to science on is DC-V2.
b. Remove relay hold and enable CC&S.		Separation connector	CC&S	
c. End tape-recorder launch mode.	$S=0$ to S+114 s	Separation connector	Tape recorder	This signal is "NANDed" with first EOT signal after separation and switches tape-recorder launch motor off; gyro power off at spacecraft acquisition is a backup to tape-recorder launch motor off.
d. Remove plasma probe 10-kV inhibit.		Separation connector	Plasma probe	This allows plasma probe to supply 10 kV to its sensor.
e. Arm pyrotechnics		Pyrotechnics arming switch (PAS).	Pyrotechnics	This switch is wired in parallel with SIT for redundancy.

f. Agena isolation amplifier turned off	.....	PAS.....	DE.....	Event in DE register 3.
g. Turn on AC subsystem.	.....	PAS.....	Pyrotechnics, DE.....	
(1) Arm pyrotechnics.	$S+30\pm20$ s.....	SIT.....	Pyrotechnics.....	Backup to event 11*e*.
(2) Pyrotechnics-armed indication.	$S+180\pm80$s.....	SIT.....	DE.....	Event in DE register 3, if event in step 11*f* has not occurred.
(3) Deploy solar panels and Sun shade.	$S+190\pm80$ s.....	SIT.....	Pyrotechnics.....	
12. Deploy solar panels and Sun shade.	$L+53$ min.....	CC&S L-1.....	Pyrotechnics.....	Backup to event 11*g*(3).
13. Turn on AC subsystem.....	$L+57$ min.....	CC&S L-2.....	AC.....	Backup to event 11*g* (backup: DC-V13).
14. Sun acquisition complete; begin to calibrate magnetometer roll rate.	Event 11*g* or 13+0 to 20 min.	Sun gate.....	AC.....	If DC-V13 is used to turn on AC, Canopus acquisition will begin at event 14.
15. Start magnetometer calibration.	$L+4$ hr.....	.....	.....	Begin calibration after spacecraft has passed 8 Earth radii.
16. Turn on Canopus sensor and initiate roll search about spacecraft z axis.	$L+997$ min.....	CC&S L-3.....	AC.....	Backup: DC-V13. Inhibit magnetometer-calibration roll signal.
17. Canopus acquisition complete..	Event 16+0 to 16+60 min.	.....	.....	This is at 0.1°/s.
18. Begin trajectory-correction maneuver.	$L+2$ to $L+10$ days....	.....	.....	
a. Load pitch-turn duration and polarity.	.....	Command QC-V1-1	CC&S.....	
b. Load roll-turn duration and polarity.	.....	Command QC-V1-2	CC&S.....	
c. Load motor-burn duration.	.....	Command QC-V1-3	CC&S.....	
d. Arm first propulsion maneuver.	MC—10 min.....	Command DC-V29....	Pyrotechnics.....	This will insure that propulsion transfer relays are in correct state for first maneuver.
e. Remove propulsion inhibit.	MC—5 min.....	Command DC-V14....	Pyrotechnics.....	This will insure that pyrotechnic relays are not inhibited.
f. Initiate maneuver sequence.	MC.....	Command DC-V27....	CC&S.....	

Table 7–1.—Continued

Event	Time	Source	Destination	Comments
18. Begin trajectory = correction maneuver – Con.				
g. Maneuver sequence start.	MC=0			
(1) Turn on gyros for warmup		CC&S M-1	AC	
(2) Switch to data mode 1		AC	DE	Backup: DC-V1.
h. Begin maneuver	MC+59 to MC+60 min.			
(1) Spacecraft to inertial control (all axes); autopilot on; Canopus sensor off.		CC&S M-2	AC	
(2) Set turn polarity.		CC&S M-3 or M-3	AC	M-3 positive turns, M-3 negative turns.
(3) Start pitch turn		CC&S M-4	AC	Magnitude inserted by QC-V1-1 before maneuver start (1000 s=180° turn).
i. Stop pitch turn	Event 18*h*+1 to 1319s (1-s resolution).	CC&S M-4	AC	
Reset turn polarity		CC&S M-3	AC	
j. Start roll turn	Event 18*h*+22 min	CC&S M-5	AC	
Set turn polarity		CC&S M-3 or M-3	AC	See comments on event 18*h*(2).
k. Stop roll turn	Event 18*j*+1 to 13 19 s (1-s resolution).	CC&S M-5	AC	Magnitude inserted by QC-V1-2 prior to maneuver start (1000 s= 180° turn).
Reset turn polarity		CC&S M-3	AC	
l. Ignite midcourse motor	Event 18*h*+44 min	CC&S M-6	Pyrotechnics	Relay pulsed.
m. Stop midcourse motor	Event 18*l*+0.060 to 102.34 s (0.040- to 0.080-s resolution).	CC&S M-7	Pyrotechnics	Relay pulsed; magnitude inserted by QC-V1-3 before maneuver start.
19. Begin automatic reacquisition of references.	Event 18*h*+50 min	CC&S M-1 and M-2	AC	If L-3 has failed to operate in event 16, Canopus sensor will be turned off by this signal; this condition can be corrected by sending DC-V13.
Switch to data mode 2		AC	DE	Backup: DC-V2.

20. Sun acquisition complete	Event 19+0 to 20 min			
21. Canopus acquisition complete	Event 20+0 to 60 min			
22. Turn off maneuver counter	Event 18*f*+199 min	CC&S	CC&S	Internal function to CC&S that permits subsequent maneuver to be executed.
23. Maneuver sequence inhibit	Event 22+10 min			Loading minimum turns and motor-burn times into CC&S maneuver clock prevents possibility of maximum-duration maneuver events occurring, if CC&S maneuver clock is actuated as a result of certain possible component failures.
a. Load minimum pitch-turn duration.		Command QC-V1-1	CC&S	
b. Load minimum roll-turn duration.		Command QC-V1-2	CC&S	
c. Load minimum motor-burn duration.		Command QC-V1-3	CC&S	
24. Transfer to traveling-wave tube (TWT) amplifier.	*L*+10 days (nominal)	Command DC-V7	Radio	This transfers radio power amplifier from low-power cavity amplifier used during launch to higher power TWT amplifier.
25. Second maneuver sequence. Repeat steps 18–23 if a second maneuver is required.				
26. Switch bit rate to 8⅓ bps	*E*—87.0 days	CC&S MT-6	DE	Backup: DC-V5.
27. Set Canopus sensor cone angle 1.	*E*—56.4 days	CC&S MT-1	AC	Backup: DC-V17.
28. Set Canopus sensor cone angle 2.	*E*—39.7 days	CC&S MT-2	AC	Backup: DC-V17.
29. Set Canopus sensor cone angle 3.	*E*—23.0 days	CC&S MT-3	AC	Backup: DC-V17.
30. Transmit via high-gain antenna; receive via low-gain antenna.	*E*—18.5 days	CC&S MT-5	Radio	Backup: DC-V10.
31. Set Canopus sensor cone angle 4.	*E*—9.2 days	CC&S MT-4	AC	Backup: DC-V17.
32. Turn off ranging	*E*—19⅓ hr	CC&S CY-1	Radio	CC&S CY-1 turns ranging receiver off; *S*-band occultation constraints preclude ranging turn-on during occultation period. Backup: DC-V9.
33. Begin encounter sequence	*E*—12⅔ hr (nominal)	CC&S MT-7	Power	Backup: DC-V25.
a. Tape-recorder power on.		MT-7	Power	Tape recorder receives power; however, recording sequence is inhibited.
b. Energize terminator sensor.		MT-7	Pyrotechnics	
c. Battery charger to boost mode.		MT-7	Power	

Table 7-1.—Continued

Event	Time	Source	Destination	Comments
34. Begin DAS encounter mode	*E*—6 hr (nominal)	CC&S MT-8	DAS	Backup: DC-V24.
a. Switch to data mode 3		DAS	DE	With data mode 3, a faster sample rate for science data is established for real-time transmission by eliminating engineering frame from data format; no data are stored at this time.
b. Planet-sensor power on		DAS	Planet sensor	
c. Switch plasma probe to encounter format.		DAS	Plasma probe	
d. Remove inhibit from timer B.		DAS	Timer B	
35. Initiate DAS timer A	*E*—3 hr 8 min (approx).	Command DC-V16	DAS	DC-V16 is transmitted at a time so that outputs from timer A occur to serve as backups to critical encounter events.
36. Acquisition of planet sensor output (PSO).	*E*—60±12 min	Planet sensor	DAS	
a. Start timer B		Planet sensor	DAS	MT-8 or DC-V24 must have occurred.
b. Start tape recorder	*E*—59 min 10 s	DAS	Tape recorder	Tape recorder requires about 0.25 s to reach record speed.
c. Begin track 1 recording	*E*—59 min 10 s	DAS	Tape recorder	Data to track 1 preceded by 80 zeros.
d. Begin ultraviolet photometer high data rate.		DAS	DAS	
e. Inhibit ultraviolet photometer calibrate signal.		DAS	Ultraviolet photometer.	Inhibit removed by timer A or B.
f. Issue backup	Receipt of DC-V16 +121 min (approx).	Timer A	DAS	Backup for PSO event.
37. Begin track 2 recording	Event 36 (PSO)+ 13.45 min.	DAS (timer B)	Tape recorder	Begins high-data-rate sampling and storage of DFR data; 80 zeros precede data.
Issue backup	Receipt of DC-V16 +2 hr 13 min (approx).	DAS (timer A)	Tape recorder	
38. Enter occultation	*E*—5 min. (nominal estimate)	Trajectory		During period preceding occultation, rf signal transmitted from Earth-based transmitters will be refracted through atmosphere of planet.
39. Closest approach	*E*=0			
40. Antenna pointing angle change.	*E*+8 min (approx)	Terminator sensor	Pyrotechnics	Pyrotechnics activates a pinpuller that allows antenna to change position for optimizing *S*-band occultation experiment; for command backup, see event 45.

Issue backup	Receipt of DC-V16 +3 hr 8 min (approx), E+15 min (approx).	DAS (timer A)	Pyrotechnics	Timer output serves as backup to terminator sensor.
41. Exit occultation	E+21 min (nominal estimate).	Trajectory		Spacecraft rf signal emerges from behind planet.
42. Stop recording on track 2	Event 37+107.5 min	DAS (timer B)	Tape recorder	Terminate storage of dual-frequency radio propagation data.
Issue backup	Receipt of DC-V16 +4 hr 2 min (approx).	DAS (timer A)	Tape recorder	An output of timer A serves as a backup for this event from timer B.
43. EOT in tape recorder	E+1 hr 10± 3 min	Tape recorder (EOT foil).	Tape recorder DAS	This stops record motor and thereby terminates data-storage sequence.
44. Switch to data mode 2	E+1 hr 14 min	DAS (timer B)	DE	Backup: DC-V2.
a. Start sending "stop tape" commands.		DAS (timer B)	Tape recorder	Backup to event 43; "stop tape" commands issued every 50.4 s from this point.
b. Planet sensor off		DAS (timer B)	Planet sensor	
c. Release ultraviolet photometer calibrate inhibit.		DAS (timer B)	Ultraviolet photometer.	
d. Switch plasma probe to cruise format.		DAS	Plasma probe	
e. Issue backup	Receipt of DC-V16 +4 hr 15 min (approx).	Timer A	DAS	Timer A serves as backup for event 44.
f. Inhibit encounter outputs of timers A and B.		DAS	Timers A and B	
45. Transmit DC-V22	As soon as possible after exit occultation (if necessary).	Command	Pyrotechnics	Because of high doppler rates that exist during encounter, successful command transmission could not be assumed until some time after encounter.
46. Transmit DC-V9	As soon as possible after two-way lock is established.	Command	Radio	Turns on ranging receiver.
47. Switch to data mode 4	E+14 hr	CC&S MT-9	DE	Backup: DC-V4.
Begin stored data playback		DE	Tape recorder	
48. Switch tape-recorder data tracks.	E+32.2 hr	EOT foil	Tape recorder	Backup: DC-V3.
49. Turn off ranging	E+1 day (23.33 hr)	CC&S CY-1	Radio	Backup: DC-V9.

Table 7–I.—Concluded

Event	Time	Source	Destination	Comments
50. End of first data playback	$E+2$ days (2.4 hr)	Tape recorder		Data playback consists of about 1 hr of real-time engineering data followed by 17 hr of science data on track 1, and about 2 hr of real-time engineering data followed by 14 hr of science data, followed by 1 hr of real-time engineering data on track 2 (no assurance existed as to which track the tape recorder would select to begin playback).
51. Start of second data playback	$E+2$ days (2.4 hr)	EOT foil	Tape recorder	Second playback is an optional operation.
52. Transmit DC–V9	$E+2$ days (2.9 hr)	Command	Radio	Turn on ranging receiver assuming no second data playback.
53. Switch tape-recorder data tracks.	$E+2$ days (20.6 hr)	EOT foil	Tape recorder	Backup: DC–V3.
54. End of second data playback	$E+3$ days (14.8 hr)	Tape recorder		
55. Switch to data mode 2	$E+3$ days (14.8 hr) (approx).	Command DC–V2	DE	If only one playback of stored data is performed, this command will be transmitted after first playback sequence is terminated.
56. Transmit DC–V9 commands	At appropriate Goldstone rise times.	Command	Radio	Exercise ranging subsystem as long as capability lasts.

Table 7–II.—Mariner 5 sequence of events

Date, 1967	GMT	Event
June 14	06:01:00	Liftoff.
	06:27:17	Radiofrequency power up, science on, plasma-probe high voltage on, CC&S relay-hold off, Agena channel F telemetry off, pyrotechnics armed, SIT started, AC on, and tape-recorder launch mode off.
	06:30:19	Solar panels and Sun shade deployed.
	06:43:25	Sun acquisition completed; beginning of magnetometer-calibrate roll.
	06:53:57	CC&S L–1 event (deploy solar panels and deployable Sun shade); no action (preempted by SIT).
	06:57:56	CC&S L–2 event (turn on AC); no action (preempted by PAS).
	22:38:00	CC&S L–3 event (turn on Canopus sensor); spacecraft into roll search.
June 15	01:12:26	Gyroscopes off; spacecraft had acquired Canopus after two roll-override commands (DC–V21).
June 19	21:23:57	Trajectory-correction maneuver initiated (DC–V27).
	23:08:28	End of motor burn.
	23:32:19	Sun and Canopus reacquired after midcourse maneuver.
June 20	02:09:49	Gyroscopes off upon completion of 3 rolls for ultraviolet photometer.
	02:30:18	Last of minimum turn and motor-burn-duration commands observed.
	02:39:00	Ranging receiver on (DC–V9 No. 1).
June 27	00:28:00	DC–V7 (switch power amplifiers) transmitted; TWT into 90-s warmup, then standard mode at 40.2-dBm output.
	00:59:05	Battery charger off; boost mode enabled.
July 24	19:19:21	CC&S MT–6 (switch bit rates) transferred telemetry to 8⅓ bps.
Aug. 24	08:41:33	CC&S MT–1 (Canopus-sensor cone-angle update) switched sensor cone angle from 79.7° to 84.5°.
Sept. 10	00:41:52	CC&S MT–2 (Canopus-sensor cone-angle update) switched sensor cone angle from 84.5° to 90.0°.
Sept. 26	16:42:43	CC&S MT–3 (Canopus-sensor cone-angle update) switched sensor cone angle from 90.0° to 95.2°.
Oct. 1	16:43:34	CC&S MT–5 (transfer spacecraft transmitter to high-gain antenna).
Oct. 10	14:04:14	CC&S MT–4 (Canopus-sensor cone-angle update) switched sensor cone angle from 95.2° to 100.3°.
	14:25:00	DC–V15 (Canopus-gate-inhibit override) transmitted.
Oct. 19	02:49:00	DC–V25 (begin encounter sequence; tape recorder on) transmitted; tape recordre on, terminator-sensor excitation on, and science-overload-inhibit override on.
	04:45:06	CC&S MT–7 (begin encounter sequence; tape recorder on); no action (preempted by DC–V25).
	08:50:00	DC–V9 (turn on ranging receiver 16) transmitted.
	10:50:00	DC–V24 (begin DAS encounter mode) transmitted; DE switched to data mode 3, DAS clock B enabled, planet-sensor excitation on, and plasma probe to data mode 3.
	11:25:04	CC&S MT–8 (begin DAS encounter mode); no action (preempted by DC–V24).
	15:01:43	DC–V16 (start encounter backup clock) transmitted; DAS clock A enabled, and science frame count reset to zero.
	16:33:57	Planet-sensor output; start DAS timer B, start tape-recorder record motor, begin track 1 recording, and inhibit ultraviolet photometer calibration signal.
	16:40:00	DC–V9 (turn off ranging receiver 2) transmitted.
	17:46:51	Terminator sensor output and APAC.
	18:41:51	Tape-recorder EOT and tape-recorder record motor off.
	19:00:00	DC–V9 (turn on ranging receiver 17) transmitted.

Table 7—II.—Concluded

Date, 1967	GMT	Event
Oct. 20	07:25:23	CC&S MT-9, start of Venus recorded data playback; data encoder transferred to data mode 4.
Oct. 21	18:45:00	DC-V9 (turn on ranging receiver 18) transmitted (CC&S CY-1 No. 47 had turned it off).
Oct. 23	07:55:00	DC-V2 (data encoder transferred to data mode 2, tape recorder to standby mode) transmitted; a later DC-V28 turned on battery charger.
Oct. 25	20:35:00	DC-V5 (switch back to 8⅓ bps transmitted; earlier DC-V5 switched to 33⅓ bps.
Oct. 26	20:55:00	DC-V19 (return AC to normal mode) transmitted; DC-V28 turned off battery charger.
Nov. 7	09:15:00	DC-V26 (turn science off) transmitted; subsequent commands turned science on, data mode 3, tape recorder on, started DAS clock A counting, switched to data mode 2, started record sequence, rolled spacecraft; acquired Canopus, rolled spacecraft, switched to transmit low-gain antenna, acquired Canopus, rolled spacecraft; EOT stopped record sequence, acquired Canopus, switched to transmit high-gain antenna (this ended recording of 3-roll ultraviolet photometer calibration data).
Nov. 8	21:00:00	DC-V4 (mode 4, begin data playback) transmitted; subsequent commands switched tape recorder to standby mode and restarted playback.
Nov. 10	18:58:10	DC-V2 (transfer data encoder to data mode 2, and tape recorder to standby mode) transmitted; subsequent commands turned tape recorder off, battery charger on, and battery charger off.
Nov. 19	13:00:00	QC-V1-1 (−17.18° pitch) transmitted; subsequent commands to point ultraviolet photometer at CC&S MT-6 point in celestial space set roll magnitude, removed maneuver inhibit, turned science off, turned science on, data mode 3, tape recorder on, started DAS clock A counting, switched to data mode 2, armed first burn, initiated midcourse-maneuver sequence, gyros on, data mode 1; switched to data mode 2; switched to transmit low-gain antenna; started record sequence, pitched, rolled, reacquired Sun, acquired Canopus, EOT stopped record sequence; switched to transmit high-gain antenna.
	18:40:00	DC-V13 (maneuver command inhibit) transmitted; subsequent commands removed science on/overload-inhibit override, turned science off, turned science on, minimum pitch, minimum roll, minimum burn duration, transmit and receive on high-gain antenna.
	22:00:00	DC-V4 (start tape playback) transmitted.
Nov. 20	16:58:10	DC-V2 (transfer data encoder to data mode 2, tape recorder to standby mode) transmitted; subsequent commands turned tape recorder off, battery charger on, battery charger off, started DAS clock A counting to restore plasma-probe mode 2 format.
Nov. 21	19:18:05	DC-V12 (switch receiver and transmitter to low-gain antenna) transmitted; previous commands turned on ranging for 21st time, established Canopus-gate-inhibit override mode, turned off ranging for 3d time by command, switched receiver to low-gain antenna.

CHAPTER 8

Mariner-Venus 1967 Extension Project

The primary objectives of the Mariner-Venus 1967 extension project were to—

(1) Map uncharted regions of the celestial sphere at very short wavelengths
(2) Acquire data on the interplanetary environment close to the Sun during a period of high solar activity
(3) Continue refinement of celestial mechanics constants

A secondary objective was to obtain additional engineering knowledge about the effects of close perihelion passage on spacecraft equipment.

Overall NASA Headquarters responsibility for the Mariner-Venus 1967 extension project was assigned to the Office of Space Science and Applications (OSSA). Responsibility for management of the project, the MOS, and the TDS was assigned to the Jet Propulsion Laboratory. Other management functions were under the direct cognizance of the project manager at JPL. The project organization is shown in figure 8–1.

Mariner 5 was conditioned for the long-term cruise mode on November 21, 33 days after the successful flyby of Venus. No equipment failures had been discovered. No evidence of degradation was found in the telemetry to indicate that a component was failing. It was believed that the spacecraft was performing as designed and would survive the maximum temperature conditions at perihelion.

On November 21, Mariner 5 was 97.9×10^6 km from the Sun and 118.5×10^6 km from the Earth. The Sun-probe-Earth angle was 85.6°. The ecliptic latitude was −0.06°; ecliptic longitude was 111.7°. The predicted date for perihelion was January 4, 1968.

The last contact with Mariner 5 was on December 4, 1967. On that date DSS 14 (Mars site) was able to detect and lock up the ground receiver on the spacecraft downlink carrier frequency. However, the signal level (−170 dBm) was below the ground demodulator threshold of the GTS, and real-time telemetry was not available. An analog record of the ground receiver output (predemodulation tape) was obtained during the receiver-in-lock period from 16:02:00 to 20:00:00 GMT, at which time the pass ended as scheduled.

The analog predemodulation tape for this pass was processed at the Jet

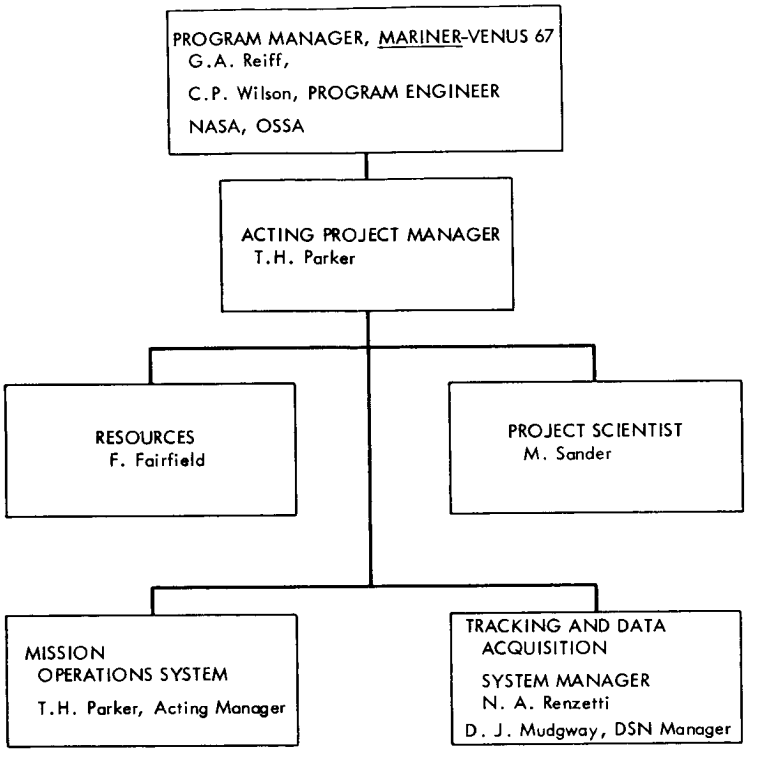

FIGURE 8–1.—Organization of Mariner-Venus 1967 extension project.

Propulsion Laboratory, using the digital demodulation technique. This program extended the capability for extracting telemetry from signals below the threshold of the normal onsite tracking station hardware. Telemetry frame synchronization was established for two short intervals of the 4-hr pass. Recognizable data periods were from 17:01:31 to 17:23:21 GMT and from 19:15:55 to 19:35:14 GMT, giving a total of 42 min of usable data.

Spacecraft conditions, as determined from the data available, were as follows:

(1) The attitude was stable, with limit cycling occurring about each of the three primary axes.
(2) The Canopus sensor was locked on Canopus.
(3) All power subsystem voltages and currents were normal, indicating that the overall spacecraft power demands had not changed.
(4) The radio transmitter seemed to be operating as designed, based on the frequency, frequency stability, and level of the detected downlink signal.

(5) The propulsion and AC subsystem pressures were normal.
(6) All event counters were registering the correct number of counts; the counter 2 register had correctly advanced four counts since November 21, as a result of the CC&S cyclic (CY–1) command issued each 66⅔ hr.
(7) The few temperature readings that were available agreed with their predicted values. Most of the temperature channels were low-deck readings and were not available for analysis; therefore, the complete temperature profile of the spacecraft could not be determined.

Information related to the spacecraft celestial position on December 4, 1967, is given in table 8–I. The same parameters are included for January 4, 1968. On December 4, 1967, the solar intensity had reached 2.67 times the mean Earth value, and the spacecraft had progressed through 85 percent of the total excursion in solar intensity. It appeared that Mariner 5 was operating normally at a point closer to the Sun than had been reached previously by any manmade object.

REACQUISITION ATTEMPTS FOR NOMINAL SPACECRAFT

The first five attempts to reacquire the Mariner 5 spacecraft (see table 8–II) were conducted by the DSN (see fig. 8–2), using one basic configuration. These frequency searches involved the long-time integration technique discussed later in this chapter. Using this integration technique, a limited band of frequencies could be searched for a signal of very low level.

These searches were conducted with the assumption that the radio subsystem was operating normally in the TWT power amplifier/exciter B mode, and that it was transmitting via the low-gain antenna. This was the spacecraft radio subsystem configuration when last observed.

Table 8–I.—Mariner 5 trajectory comparison

Parameter	Dec. 4, 1967[a]	Jan. 4, 1968[b]
Distance from Sun, km	93.1×10^6	86.75×10^6
Distance from Earth, km	137.5×10^6	187.2×10^6
Sun-probe-Earth angle, deg	76.8	49.9
Ecliptic latitude, deg	0.54	1.39
Ecliptic longitude, deg	137.0	206.7

[a] Last telemetry.
[b] Perihelion.

Table 8–II.—Summary of reacquisition attempts for a nominal spacecraft

Attempt	Date, 1968	Predicted signal level,[a] dBm	DSS	Activity
1	Apr. 26	−190 to −200	13/14	Frequency search using integration technique and special equipment.
2	May 3	−190 to −200	13/14	
3	May 23	−190 to −200	13/14	
4	May 31	−180 to −190	13/14	
5	June 18	−178 to −188	13/14	

[a] Signal levels noted are nominal for TWT/exciter combinations.

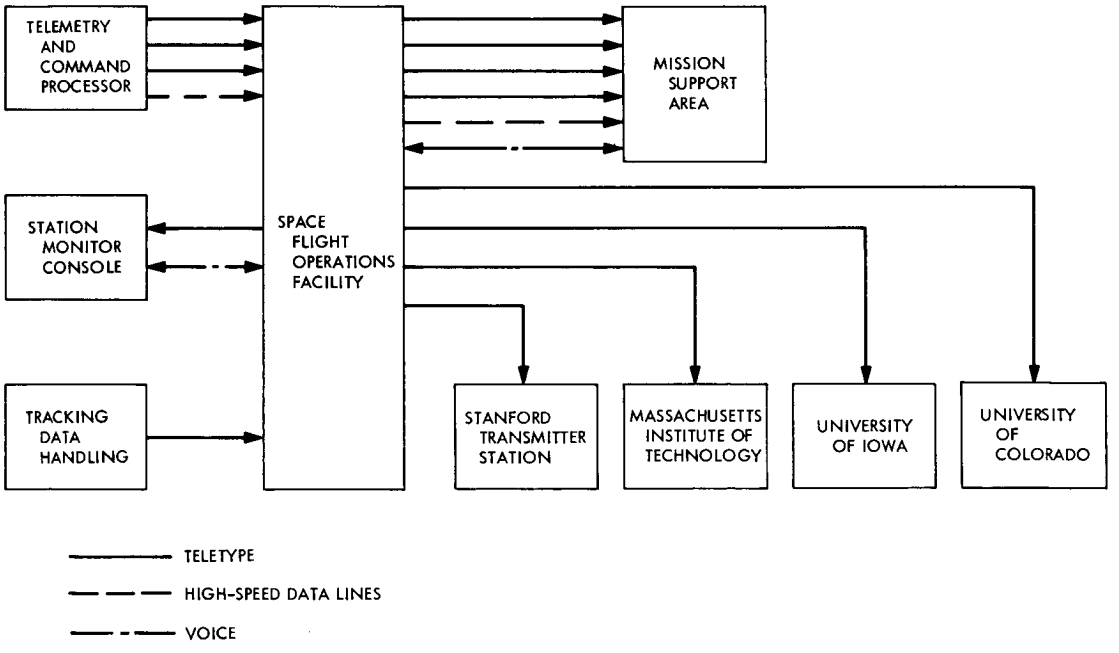

FIGURE 8–2.—Communications configuration for reacquisition of Mariner 5.

First Attempt

The first reacquisition attempt was conducted on April 26, 1968, using DSS 14 and special equipment and integration techniques at DSS 13. The predicted downlink signal level was between −190 and −200 dBm.

A 5-hr frequency search was made ±1300 Hz around the predicted TWT/

exciter B frequency at 360-Hz intervals, integrating for a period of 15 min at each point. No evidence of a Mariner 5 signal was detected.

Second Attempt

The second attempt to reacquire Mariner 5 was conducted on May 3. The predicted downlink signal level on that date was between −190 and −200 dBm.

A frequency search was conducted ±1300 Hz around the predicted TWT/exciter B frequency at 360-Hz intervals, integrating for a period of 15 min at each point. The search, conducted over a 5-hr interval using DSS 14 and the special integration techniques at DSS 13, resulted in no evidence of a spacecraft signal.

Third Attempt

The third attempt to reacquire Mariner 5 was conducted on May 23. The predicted signal level at that time was between −190 and −200 dBm.

A frequency search was conducted ±1300 Hz around the predicted TWT/exciter B frequency at 360-Hz intervals, integrating over a 15-min period at each point. At the conclusion of the frequency search, which involved DSS 14 and the special integration techniques at DSS 13, no Mariner 5 signal was observed. It was concluded that the tolerance on the predicted nominal value remained a contributing factor in keeping the signal level below the detectable threshold.

Fourth Attempt

The fourth attempt at reacquisition occurred on May 31. The predicted signal level at that time was between −180 and −190 dBm.

A frequency search was conducted ±1300 Hz around the predicted TWT/exciter B frequency at 360-Hz intervals, integrating over a 15-min period at each point. At the conclusion of the frequency search, which involved DSS 14 and the special integration techniques at DSS 13, no signal was observed.

The plan at this time was to conduct another search on June 18, using the same procedure. If no spacecraft signal were observed, it would be concluded that the spacecraft frequency had changed, and a new search plan covering a wider frequency range would be employed.

Fifth Attempt

The fifth reacquisition attempt was conducted on June 18. The predicted downlink signal level at that time was between −178 and −188 dBm.

A frequency search was conducted ±1300 Hz around the predicted TWT/exciter B frequency at 360-Hz intervals, integrating over a 15-min period at

each point. The result of the frequency search was negative. It was concluded that the spacecraft could be on any one of the four radio configurations: TWT/exciter A, TWT/exciter B, cavity/exciter A, or cavity/exciter B. All remaining searches, therefore, were based on this assumption.

NONCATASTROPHIC FAILURE MODE ANALYSES

After these five reacquisition attempts brought no results, a detailed study was undertaken by the SPAC team to formulate anomalous spacecraft conditions that would explain the inability to acquire a downlink signal for Mariner 5. The major emphasis of this study was first directed toward noncatastrophic spacecraft failure modes; i.e., abnormal or anomalous spacecraft conditions that could be overcome by modifying the nominal DSIF tracking plan (look for different frequency, search two-way, etc.) or by commanding the spacecraft to an acceptable mode. A discussion of the postulated noncatastrophic spacecraft failure modes is presented in the following paragraphs.

Telecommunications Analyses

There are many possible conditions on the spacecraft (such as small variations in temperature, power transients, etc.) that may cause variations in the spacecraft-transmitted signal. Most of these variations would be observed as frequency or power-level differences from those predicted. The spacecraft signal could still be acquired with this class of anomalies without requiring command action. A wider search in frequency and received power level would be required to cover the possible signal variations.

There is a class of possible failure modes in which the spacecraft-transmitted signal, when using the auxiliary oscillator (one-way mode), may not be acquired. An example of this class of failures is a failure in the receiver AGC circuit, so that an in-lock indication is present when the receiver is out of lock. This failure would cause a transfer of the downlink frequency to the spacecraft receiver voltage-controlled oscillator when the only input to this oscillator is noise. The DSIF receivers probably would not acquire the resulting carrier at low ground-received signal levels, but the spectrum should be observable with the R&D receiver and using the integration technique. If it is assumed that no other failures occurred, the solution to this problem is to acquire two-way lock with the uplink and have the ground receivers search out the two-way frequency.

The radio subsystem switching logic was such that a single failure in an exciter or power amplifier would result in automatically switching to a backup unit at the next cyclic command (CY–1) from the CC&S. This would result

in a change in the carrier frequency, and possibly in the power level, that would be searched for in the one-way mode. The spacecraft was in the TWT/exciter B mode when last observed in December 1967.

Another possibility, although quite unlikely, is that a power transient of some sort on the spacecraft caused the control unit to switch the transmitter to the high-gain antenna. This switching would result in the spacecraft's transmitting, but with no downlink signal received except when the spacecraft-to-Earth vector was within the beamwidth of the high-gain antenna.

Noncatastrophic telecommunication subsystem failure modes and the associated corrective action are listed in table 8–III.

Guidance and Control Analyses

Open gas jet

If one of the N_2 gas jets of the AC subsystem failed to close after firing, all N_2 gas in that half-gas system would be depleted through the open jet, and a translational and rotational force would be imparted to the spacecraft.

The AC subsystem can null the rotational force, in maintaining AC, by firing the two gas valves opposing the applied moment. A good approximation to the amount of gas expended during this operation is that two-thirds of the gas in one half-gas system is expended through the open valve, the remaining one-third expended through the valve opposing rotation, and an equal amount expended

Table 8–III.—Radio problems affecting Mariner 5 reacquisition

Problem	Corrective action
TWT failure (output less than 35.5±1 dBm)	Search one way for cavity/exciter B mode (about 2.8 kHz at *S*-band above nominal TWT/exciter B frequency).
Exciter B failure (output less than 24±1 dBm)	Search one way for cavity/exciter A mode (about 2.4 kHz at *S*-band below nominal TWT/exciter B frequency).
	Search one way for TWT/exciter A mode (about 7.0 kHz at *S*-band below nominal TWT/exciter B frequency).
TWT failure, and cavity degradation below cyclic threshold.	Search for cavity during both odd- and even-cyclic (CY–1) periods.
Transmitting via high-gain antenna	Send DC–V12 to insure spacecraft transmission via low-gain antenna.
Failure in auxiliary oscillator and voltage-controlled-oscillator switching logic.	Search for spacecraft in two-way mode.
TWT failure; CY–1 logic was inoperable (double failure).	Send DC–V7 to switch to cavity.
Exciter B failure; CY–1 logic was inoperable (double failure).	Send DC–V8 to switch to exciter A.

from the other half-gas system through the other valve opposing rotation. The gas left after the half-gas system is emptied is two-thirds of the gas in the other half-gas system.

If such a failure had occurred on December 5, 1967, then the following conditions would have been noted on August 19, 1968:

(1) *Remaining N_2 weight.* Two-thirds of one tank plus normal gas usage for 259 days at about 1.13 g/day is 430 g, enough for about 380 days more.
(2) *Spacecraft position.* Incremental velocity ΔV, added because of translational force, would be weight of gas expelled multiplied by the specific impulse I_{sp} for N_2 divided by spacecraft mass; thus, ΔV would be about 2 m/s. After 259 days, the translation would be about 22 400 km. At a distance of 1 AU, the 0.14° beamwidth of the 210-ft antenna covers a circle of 18 000-km radius; thus, the spacecraft would still be within the pattern of the 210-ft antenna.

Open or shorted cruise Sun sensor

The most probable failure mode for a cruise Sun sensor is for the CdS photocell or the connecting lead to open. Because of the construction of the cell, the possibility is small that a short would occur.

If the cell did open, the other cell in the matched pair would provide an error voltage to the switching amplifier, driving the spacecraft in a direction that would shadow the good cell. The cell is completely shadowed when it is less than 2° off the sunline, and its resistance rises exponentially with the decrease in light intensity. Eventually, its resistance would become large enough to limit the current input to the switching amplifier below the 5 μA required at the input, and the switching amplifier would shut off.

Either of two possibilities could occur:

(1) If solar torques of sufficient magnitude were present, to stop or reverse the spacecraft residual rate, the process would be repeated as soon as sufficient light fell on the cell to enable switching amplifier operation.
(2) If the solar torques did not remove the residual rate, the spacecraft would continue to move until the Sun disappeared from the Sun-gate field of view. When this happens, the acquisition sensors are turned on, and their output drives the spacecraft back to the sunline until the Sun gate reacquires the Sun, reinitiating the entire cycle. With a DC–V15 command in effect, the gyros will not come on when the Sun gate is violated; the Canopus sensor would turn off at loss of Sun gate,

however, and turn back on at Sun reacquisition. The resulting limit cycle would be one sided; the maximum deviation from the sunline would be about 6°.

Temperature-Control Analyses

During much of the attempted reacquisition period, the solar intensity at the spacecraft was higher than that previously experienced in test or in flight. For this reason, there is a possibility that some unexpected degradation of the temperature-control hardware occurred. For a near-Sun approach, the vital elements in the temperature-control subsystem were the lower thermal shield, the deployable Sun shade, and the six louver assemblies. The operation of these elements is described in the following section, together with an assessment of the probability and effects of any malfunction.

Lower thermal shield

This shield was constructed of multiple layers of 13-μm Mylar, aluminized on both sides. Alternate sheets of this material were spacers that had been corrugated by the Dimplar process. The resulting flexible blanket was about 16 mm thick, and was faced with 25-μm aluminized Teflon, with the Teflon side out. The lower blanket had a total of 19 layers.

The upper temperature limits were 439 K for the Mylar and 503 K for the Teflon. The darkening of the sunlit Teflon layer in flight had a negligible effect on bus temperatures. An extrapolation of this degradation to perihelion yielded shield temperatures well below the failure limit for Mylar and Teflon. No likely reason for shield damage at perihelion has been found, but the effect of any mechanical or thermal damage would be to raise bus temperatures, thus lowering the auxiliary oscillator frequencies.

Deployable Sun shade

The deployable Sun shade was fabricated from a single sheet of 25-μm Teflon, aluminized on the side away from the Sun. When deployed, the shade formed an octagonal awning approximately 254 mm wide around the periphery of the spacecraft, with a total area of about 1.2 m^2.

Space simulator test data indicated that, for a fully failed (undeployed) Sun shade, the bus-temperature average was increased 18.3 K at Venus solar intensity. The corresponding increase at perihelion would be possibly twice this value. Mechanical shade damage or disappearance of the aluminizing could cause part of this temperature effect, depending on the nature and extent of the damage. Again, no plausible reason for such damage has been found.

Louvers

Variable emittance louver assemblies were mounted on six of the seven electronic bays. The effective emittance varied from 0.15 to 0.7 over a 16.7 K actuation range. Eleven pairs of louver blades per assembly were individually controlled by means of a spiral bimetallic element.

The failure mechanism would be the sticking of the louver blades in some position, thereby eliminating the emittance control capability. Assuming that all 66 actuators failed, the temperature change in the bus between aphelion and perihelion (normally 5.0 K) would be increased by about a factor of 3, a noncatastrophic event that would affect auxiliary oscillator frequencies. On the basis of past experience with louvers, including the Mariner 4 flight, such a common mode failure is considered unlikely.

Propulsion and Pyrotechnics Analyses

Propulsion subsystem

The propulsion subsystem, by nature of its design, was a simple pressure-fed, constant-thrust device. The number of single-component failure modes is limited. The most deleterious noncatastrophic failure would be a nitrogen gas leak from the high-pressure circuit or a propellant leak to free space. The effect of this condition would be a small random velocity increment ΔV imparted to the spacecraft.

Pyrotechnic subsystem

There is no single-component failure mode that would produce the right conditions for loss of spacecraft signal.

Science Subsystem Analyses

Individual science subsystem units aboard Mariner 5 were, with one exception, fused. The fuses were located in the primary winding side of the 2.4-kHz power transformers used to isolate the users from the spacecraft power subsystem. The single exception to the fusing was the mission-critical DAS.

The design of the power converter in the DAS included protection against overloading the spacecraft 2.4-kHz bus. This protection was accomplished by the installation of a current limiter in the primary side of the main power transformer. The current limiter was isolated from spacecraft ground and from the load side of the power converter. Test data on the power converter indicated that a dead short condition on the 4-V logic power supply would result in an average 4-W load, with a 40-W peak pulse on the spacecraft 2.4-kHz bus (the normal load is 11.1 W).

Review of the power-converter circuits indicates that no single failure would cause an overload on the spacecraft power subsystem. A short on the 4-V logic supply and a simultaneous failure of the current limiter would increase the load to a maximum of 40 W. This condition could be removed by turning science power off by ground command (DC–V26), assuming that command capability existed.

One failure mode exists whereby noise could be introduced into the spacecraft system from one of the units of the science subsystem. Some filters were introduced into the interfaces between specific instruments and the spacecraft to eliminate known sources of noise, but a failure in an unfiltered instrument or in an existing filter could introduce transients. The most probable effects of such an event would be deck skipping by the data encoder, frequent issuing of science gates, and garbling of the data. Such an event would not induce a failure of the radio subsystem to the extent that no rf carrier would be generated.

Tracking and Data System Analyses

When it became apparent that the acquisition attempt would be nonstandard, the character of DSN support was changed. New resources were used, including angle searches, uplink searches, and the special long-time integration technique. Other resources used in a different manner from the premission plans included wide frequency searches using the standard receivers at DSS 14 and command activity using the full DSN, from SFOF to DSIF. The equipment and procedures for the search periods are discussed briefly.

Long-time integration configuration

The functional sequence used for the long-time integration technique is shown in figure 8–3. The signal enters the antenna, which is fitted with a low-noise "ultra cone," and is amplified by the low-noise maser. This low-noise input has a system noise temperature of about 19° with the antenna pointing at zenith. The output of the maser is sent through a power splitter to the R&D receiver (for the integration technique) and the DSS 14 receivers.

The R&D receiver, which houses the first stages of the long-time integration equipment, is located in the Alidade room at DSS 14. The *S*-band signal entering the receiver first encounters a frequency conversion to 50 MHz by mixing with a signal from a programed local oscillator. This local oscillator is guided by an SDS 920 computer so that the effects of doppler shift resulting from spacecraft orbital motion are canceled, leaving a stable 50-MHz signal. The SDS 920 computer uses as its input a set of polynomial prediction cards generated in SFOF from the latest orbit computations.

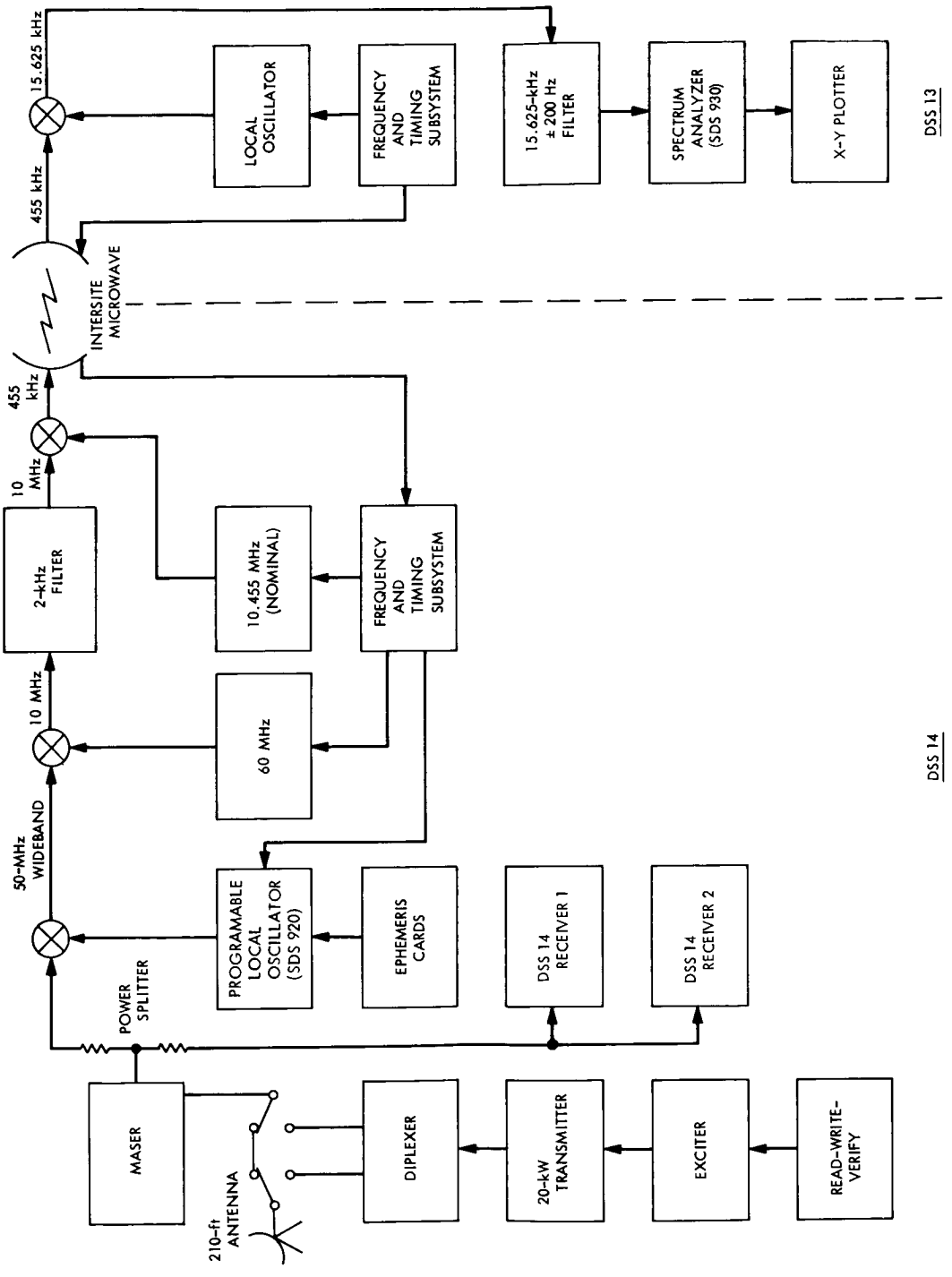

FIGURE 8-3.—Functional sequence used for long-time integration technique: DSS 14/DSS 13 configuration.

The 50-MHz signal is mixed with a fixed 60-MHz local oscillator signal, producing a 10-MHz output that is restricted in bandwidth by a 2-kHz-wide bandpass filter. A final stage of conversion mixes a variable signal (nominally 10.455 MHz) with the 10-MHz signal, resulting in a 455-kHz signal that can be transmitted several miles via microwave to DSS 13 where the spectrum analyzer is located.

At DSS 13, a conversion is made to 15.625 kHz, the center frequency of a 400-Hz-wide passband filter. It is this band-limited signal that is observed by the spectrum analyzer, which is a combination of a special-purpose hardware computer and a general-purpose SDS 930 computer. Within this equipment, the functions of sampling, autocorrelation, Fourier transformation, and plotting take place. The output is a computer-generated graph (hardcopy), which is scrutinized visually for any trace of a signal.

Because of the end effects on the 15.625-kHz bandpass filter, only the center 360 Hz is fully usable. Therefore, the integration method is limited to looking at a slice of spectrum, 360 Hz wide. To look at adjacent slices of spectrum, the 10.455-MHz local oscillator at DSS 14 is detuned by multiples of 360 Hz. This procedure can be used only to cover a band of about 2 kHz because of the 2-kHz-wide bandpass filter in the 10-MHz intermediate frequency. Additional excursions in frequency are possible only by entering a new set of polynomial predict cards into the programable local oscillator (SDS 920). Typically, up to 10 sets of predict cards have been used during a single-day track.

The entire system is synchronized to the frequency and timing subsystem at DSS 13. A reference frequency is sent from DSS 13 to DSS 14 via the intersite microwave, and the frequency and timing subsystem at DSS 14 is locked to this reference frequency.

Calibration and thresholds

At the beginning of a track, noise is sent through the system and an integration is made. The resulting spectrum is a plot of the response of the 15.625-kHz filter to pure noise in the absence of a signal. The noise spectrum is stored in the spectrum analyzer and subtracted from all future integration runs, thus providing a flat baseline on the spectral plots.

A calibration of the system sensitivity was made by pointing the DSS 14 antenna at a Pioneer spacecraft and then biasing the antenna off the spacecraft to cut down the signal to a specified (known) level. Integration runs on Pioneer showed that 20-min integrations revealed a signal of −187 dBm, and integration times as short as 7 min revealed a −183-dBm signal.

DSS 14 configuration

DSS 14 conducted a number of searches using the standard DSIF receivers. Sometimes, these searches were conducted by DSS 14 alone; at other times, they were conducted simultaneously with the long-time integration searches.

As shown in figure 8–3, the output from the maser is sent to the R&D receiver and to the DSS 14 receivers. The DSS 14 receivers have several loop bandwidths available; the pertinent bandwidths are 12, 8, and 3 Hz. The signal levels were predicted to be near the threshold of the 12-Hz loop; therefore, primarily the 8- and 3-Hz loops were used.

Numerous tests with various receiver operators showed that, in a frequency-uncertainty band of ±2.5 kHz, an *S*-band carrier of −173 dBm could be reliably acquired in 20 min, and a signal of −170 dBm could be acquired in less than 5 min. If the signal was as high as −165 dBm, it could be found within an entire channel 21 uncertainty in 10 min. All numbers were based on the following assumptions:

(1) Spacecraft elevation greater than 20°
(2) DSS 14 system noise temperature of 17°
(3) Carrier phase jitter of the extension project comparable to Pioneers 6 and 7

Angle search

To cover the possibility of an error in orbital parameters or in the generation of predicts, an angle search was conducted. A search pattern was developed in a rectangular array of pointing angles spaced about 70 percent of the 3-dB beamwidth of the ground station antenna.

In operation, the antenna was biased from a set of predicts to obtain each pointing angle within the array (and still compensate for the motion of the Earth). The antenna was held on that point in space long enough for the receiver operators to sweep the band of interest.

Uplink searches and commanding

To transmit to the spacecraft, the diplexer must be inserted between the maser and the ultra cone. This diplexer usage causes the system noise temperature to increase to about 28°.

Uplink searches were conducted by using a mechanical tuner (called the "pencil sharpener") to smoothly and slowly sweep the uplink frequency, as directed by the project. When the transmitter was turned off, the diplexer could be bypassed in less than 1 min, again affording an opportunity to search at a low-noise temperature for the remainder of the round-trip light time.

Commanding was attempted using the RWV unit, which had already been fully integrated and checked. Command procedures were those developed during the early stages of DSN/project planning.

OPERATIONS BASED ON FAILURE MODE ANALYSIS

Starting with the sixth reacquisition attempt to completion of Mariner 5 activity, all operations were conducted under the control of the Mariner-Venus

Table 8–IV.—Summary of reacquisition attempts

Attempt	Date, 1968	DSS	Predicted signal level,[a] dBm	Activity
6	June 28	13/14	—175 to —186	Frequency search using integration technique and special receiver at DSS 13, and both standard receivers at DSS 14.
7	July 12	14	—173 to —179	Frequency search using both standard receivers at DSS 14.
8	July 22	13/14	—170 to —175	Angle search.
9	July 23	13/14	—170 to —175	Frequency search using integration technique and special receiver at DSS 13, and both standard receivers at DSS 14.
10	July 25	13/14	—168 to —172	Frequency search using integration technique and special receiver at DSS 13, and both standard receivers at DSS 14.
11	Aug. 1	13/14	—168 to —172	Frequency search using integration technique and special receiver at DSS 13, and both standard receivers at DSS 14.
12	Aug. 8	13/14	—166 to —169	Frequency search using integration technique and special receiver at DSS 13, and both standard receivers at DSS 14.
13	Aug. 12	14	—165 to —168	Commands: switched to transmit low/receive low.
14	Aug. 15	14	—164 to —167	Commands: switched to transmit low/receive low, and switched backup rf subsystems.
15	Aug. 16	14	—164 to —167	Commands: changed Canopus cone angle so that it would acquire Earth; rolled spacecraft to point high-gain antenna toward Earth.
16	Aug. 19	14		Commands: switched to high-gain antenna; rolled spacecraft to point high-gain antenna toward Earth.
17	Sept. 9	14	—160 to —167	Frequency search using both standard receivers at DSS 14.
18	Sept. 16	14	—157 to —162	Frequency search using both standard receivers at DSS 14.
19	Sept. 17	14	—156 to —161	Frequency search using both standard receivers at DSS 14.
20	Sept. 30	14	—152 to —157	Frequency search using both standard receivers at DSS 14.
21	Oct. 11	14	—149 to —154	Frequency search using both standard receivers at DSS 14; search terminated because of low film height.
22	Oct. 14	61	—148 to —153	Angle search.

[a] The signal levels noted are nominal for TWT/exciter radio mode configurations.

1967 extension project, with operations controlled from the Mariner 5 mission support area. The spacecraft at this time was considered to be in a nonstandard mode. A summary of Mariner 5 operations, from the sixth reacquisition attempt, is presented in table 8–IV.

Sixth Attempt

The sixth reacquisition attempt was conducted on June 28, 1968. The operation involved both DSS 13 and DSS 14. (See fig. 8–3.)

Because no spacecraft signal was observed during the five previous frequency search operations, a new search procedure was established, using the long-time integration technique with special equipment and the two standard receivers at DSS 14.

The search of these frequencies occurred during an odd-cyclic period. Because a cyclic can switch the radio configuration, a search of these frequencies also was conducted during an even-cyclic period. The search revealed no spacecraft signal.

During the early part of the pass, an attempt was made to establish the uplink frequency from DSS 14 in an effort to gain control of the downlink frequency. Uplink searches were performed by using a mechanical tuner to accomplish a smooth and controlled (3 Hz/min) sweep of the uplink frequency.

The transmitter was turned off to bypass the diplexer so that a search at a low-noise temperature could be conducted. This search was accomplished by both standard receivers and by the long-time integration technique. This operation yielded negative results.

Seventh Attempt

A frequency search was conducted on July 12, 1968, using DSS 14 and the standard receivers during the period that DSS 14 was operating in support of the operational readiness test. The search was made over a 14-kHz frequency band that included the four radio configurations. During this 4-hr search, no Mariner 5 spacecraft signal was observed.

Eighth Attempt

To cover the possibility of a pointing error, an angle search was conducted on July 22, 1968. Offsets of 0.1° increments were selected for this operation. As the hour angle is more likely than the declination angle to be in error, a larger hour-angle search was made.

The 0.1° increments were selected because the 210-ft antenna at DSS 14 had a half-power beamwidth of 0.14°. The use of 1-beamwidth offsets created

gaps in the angle-search pattern, where less than half-power points were observed (see the shaded area in fig. 8–4). Therefore, offsets of 0.707-beamwidth increments ($0.707 \times 1.414° = 0.1°$) were used to eliminate these gaps (fig. 8–5).

A 30-min frequency search was conducted around each of the offsets shown

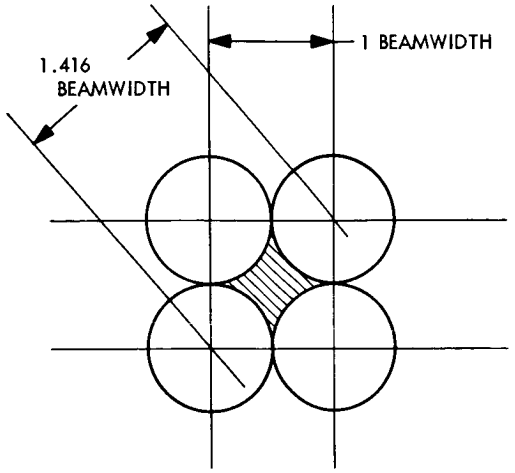

FIGURE 8–4.—Angle search pattern with a gap.

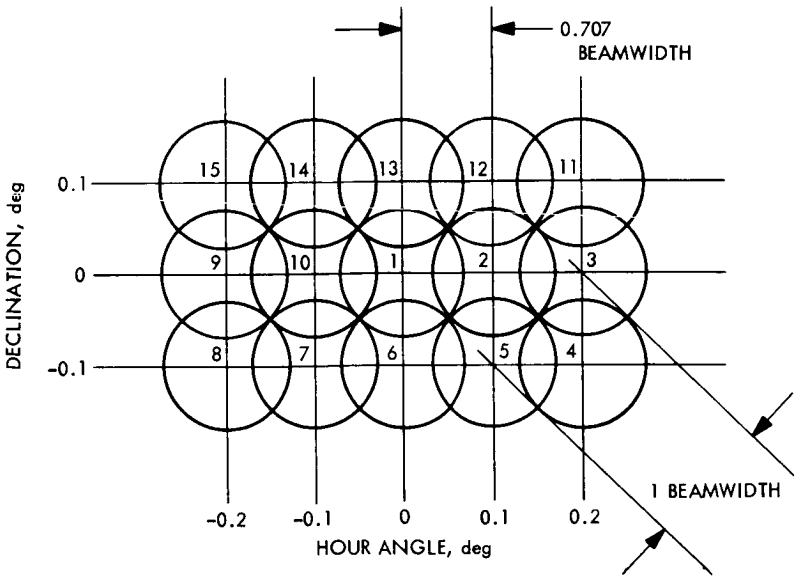

FIGURE 8–5.—Angle search pattern on July 22, 1968.

Table 8–V.—Angle search sequence on July 22, 1968

Sequence	GMT of starting	Offsets, deg	
		Hour angle	Declination
1	20:00:00	0.0	0.0
2	20:30:00	.1	.0
3	21:00:00	.2	.0
4	21:30:00	.2	—.1
5	22:00:00	.1	—.1
6	22:30:00	.0	—.1
7	23:00:00	—.1	—.1
8	23:30:00	—.1	—.1
9	00:00:00	—.2	.0
10	00:30:00	—.1	.0
11	01:00:00	—.2	.1
12	01:30:00	—.1	.1
13	02:00:00	.0	.1
14	02:30:00	.1	.1
15	03:00:00	.2	.1

in table 8–V. Receiver 1 searched ±2 kHz and receiver 2 searched ±270 kHz around the predicted declination. This operation covered a timespan of 7 hr. No Mariner 5 spacecraft signal was observed.

Ninth Attempt

A frequency search was conducted on July 23, 1968, using both the standard receivers at DSS 14 and the special equipment and integration techniques involving DSS 13. This operation was conducted during an even-cyclic period.

At one point in the operation, an error was thought to exist in the predicts; therefore, an offset of 0.16° was made in hour angle. It was later determined that the predicts were correct, thus voiding all operations after the offset. This resulted in the valid coverage of only those frequencies around the cavity/exciter A radio configuration.

The standard receivers at DSS 14 also covered a 14-kHz band that included all possible radio configurations. No Mariner 5 spacecraft signal was observed during the 8-hr operation period.

Tenth Attempt

A frequency search was conducted on July 25, 1968. The two standard receivers at DSS 14 covered a 14-kHz band that included the four radio configurations.

The long-time integration technique and special equipment involving DSS 13 were used in the frequency search operation. Hardware and software problems at DSS 13 voided all integration searches with the exception of the radio coverage of the TWT/exciter B and cavity/exciter A configurations. The last part of the operation was used to perform a frequency sweep in an attempt to lock the uplink frequency. No Mariner 5 signal was detected during the operation.

Eleventh Attempt

A frequency search was conducted on August 1, 1968. The first part of the operation was used to perform a frequency sweep in an effort to lock the uplink frequency. The results were negative.

Special equipment and integration techniques at DSS 13 were used in the frequency search; the standard receivers at DSS 14 swept the entire 14-kHz band. The integration technique and special equipment operation at DSS 13 produced several spikes; however, upon investigation, which included pointing the antenna 2° off predicts, it was concluded that the spikes were caused by noise in the ground subsystem.

The operation was conducted during an odd-cyclic period, and only the cavity/exciter A area was covered by the integration technique. No Mariner 5 signal was observed.

Twelfth Attempt

A frequency search was conducted on August 8, 1968, during an even-cyclic period. Special equipment and integration techniques involving DSS 13 were used.

The standard receivers at DSS 14 searched a frequency band of about 43 kHz, which covered all possible radio configurations and allowed for a 22.2 K greater temperature than that predicted. No Mariner 5 signal was observed.

Thirteenth Attempt

The 13th reacquisition attempt was conducted on August 12, 1968, and was the first in a series of command operations. The first commands were sent to increase the probability that the spacecraft was transmitting via the low-gain antenna.

A system glitch or power transient (recognized by the radio switching logic as a DC–V10 or DC–V11) would have switched Mariner 5 transmission to the high-gain antenna; in this mode, it was highly unlikely that the spacecraft would be illuminating Earth. Therefore, a series of DC–V12 commands (transmit low/receive low) was transmitted. No Mariner 5 signal was observed.

Fourteenth Attempt

The 14th reacquisition attempt was conducted on August 15, 1968, for the purpose of switching redundant radio elements.

During the initial phase of the operation, three DC–V12 commands were transmitted on August 12 and were sent on an even-cyclic period. Because cyclics switch the receive capability when the spacecraft is in any mode other than transmit low/receive low, it also was necessary to transmit the DC–V12 command during an odd-cyclic period.

After the DC–V12 commands, the redundant radio elements were commanded on line in the event that a double failure had occurred (a failure of one of the radio subsystems and the inability of the cyclic logic to switch). During the exercise, all possible combinations of the radio modes were commanded. No Mariner 5 signal was observed.

Fifteenth Attempt

The 15th reacquisition attempt was conducted on August 16, 1968, for the purpose of placing the spacecraft in roll to sweep the high-gain antenna past Earth. This would illuminate the deep-space stations for approximately 1 min per complete roll (360°), thus providing information on spacecraft position.

Before rolling the spacecraft, the Canopus cone angle was placed in the MT–2 position by a series of DC–V17 commands. This made Earth the only object that could be acquired by the Canopus sensor. No Mariner 5 signal was observed.

Sixteenth Attempt

The 16th reacquisition attempt was conducted on August 19, 1968, for the purpose of rolling the spacecraft in defined and controlled increments until the high-gain antenna pointed toward Earth.

Before the start of the inertial roll control sequence, a series of DC–V10 commands was transmitted to the spacecraft to insure that the spacecraft was transmitting via the high-gain antenna. No Mariner 5 signal was observed.

Seventeenth Attempt

A frequency search was conducted on September 9, 1968, using DSS 14. The search covered a span of 3.5 hr. No Mariner 5 signal was observed.

Eighteenth Attempt

A frequency search was conducted on September 16, 1968, using DSS 14. The antenna at DSS 14 was on point at 19:00:00 GMT. A complete search of

channel 21 was conducted during the first 30-min portion of the pass. The predicted downlink signal strength was between −157 and −162 dBm. No Mariner 5 signal was observed.

Nineteenth Attempt

A frequency search was conducted on September 17, 1968, using DSS 14. The antenna at DSS 14 was on point at 19:00:00 GMT. The search ranged from −65 to +67.5 kHz about the predicted downlink frequency. The expected signal strength was between −156 and −161 dBm. No signal was observed.

Twentieth Attempt

A frequency search was conducted on September 30, 1968, using DSS 14. The antenna at DSS 14 was on point at 17:55:00 GMT. The search ranged from −67.5 to +67.5 kHz about the predicted downlink frequency. The expected signal strength was between −152 and −157 dBm. No Mariner 5 signal was observed.

Twenty-first Attempt

A frequency search was conducted on October 11, 1968, using DSS 14. The antenna at DSS 14 was on point at 16:16:39 GMT. The search ranged from −22.4 to +22.5 kHz about the predicted downlink frequency. The expected signal strength was between −149 and −154 dBm. The search was terminated prematurely because of a low film height on the antenna support bearing. No Mariner 5 signal was observed.

Twenty-second Attempt

An angle search was conducted on October 14, 1968, at DSS 61. The antenna was on point at 09:00:00 GMT. The search ranged from −0.24° to +0.24° in declination and −0.48 to +0.48° in hour angle. The expected signal strength was between −148 and −153 dBm. No Mariner 5 signal was observed.

REACQUISITION OPERATIONS

Telecommunications

Attempts to reacquire Mariner 5 during June, July, and early August of 1968 yielded no spacecraft signal. During this period, the R&D receiver at DSS 14 was used in conjunction with the spectral analysis program of DSS 13. The frequency range searched was about ±7.5 kHz at *S*-band from the nominal frequency for the TWT amplifier/exciter B configuration (the last observed pacecraft condition). This range covered all other possible exciter and power

amplifier combinations with at least a 2-kHz tolerance, the outside boundary of the frequency range in which it was expected that the spacecraft would be found. Searching this range for the low signal level case with the R&D receiver required approximately one station pass to complete; thus, wider searches were not made at this time. As the predicted signal level at the ground increased, the DSS 14 phase-lock receiver was used to search a wider frequency range. Through September and early October, the 12- and 48-cycle standard DSIF receivers were used as the predicted ground-received signal level increased. Before October 14, searches with phase-lock receivers covered about ±70 kHz from nominal predicted frequency with 12- and 48-cycle loops.

One-way acquisition

On October 14, the receiver operator at DSS 14 obtained a lock on the Mariner 5 signal with a 152-cycle loop and a center frequency about 30 kHz below the nominal frequency predicts. The signal was exhibiting wild (greater than 1 kHz at *S*-band) frequency variations, and the 152-cycle receiver could maintain only a marginal lock. A 200-cycle MSFN receiver was tried; using this receiver, it was possible to maintain a reasonable lock (where the receiver would track the signal even though frequent out-of-lock glitches occurred) during the remainder of the pass. The signal level at this time was about −157 dBm maximum, with minimum excursions to below threshold for the 200-cycle loop.

Since the initial acquisition, the spacecraft was tracked 13 times; the characteristics of the signal observed during each track are listed in table 8–VI. As the spacecraft approached aphelion (October 22), the quality of the signal improved until it was good enough to be acquired and tracked by a 12-cycle loop, almost as easily as a normally operating spacecraft.

It is not possible to evaluate the behavior of the signal before October 14 with any degree of certainty. Searches were conducted using phase-lock receivers at the frequency of the signal found before October 14, with negative results. On October 14, the signal was of poor quality, and acquisition and tracking were marginal.

Two-way acquisition

On Sunday, October 20, DSS 14 succeeded in obtaining uplink lock with the spacecraft receiver. The ground transmitter frequency at that time was about 35 kHz higher than expected.

Both ground receivers dropped lock at the one-way frequency and subsequently relocked at the two-way frequency, thus verifying that the spacecraft receiver was in lock and that the spacecraft exciter had switched from auxiliary

Table 8–VI.—Spacecraft characteristics observed

Date, 1968	Ground receiver carrier power,[a] dBm	Nominal receiver carrier power range,[a] dBm	One-way frequency offset from predicts (*S*-band), kHz	Short-term variation in downlink frequency (*S*-band), Hz	Uplink frequency offset from predicts (*S*-band), kHz	Receiver 2 BL_o used for best signal reception, Hz
Oct. 14	—157	—153 to —148	30	>1000		200
Oct. 15	—157	—153 to —148	35	<1000		152
Oct. 16	—155	—153 to —148	40	500		48
Oct. 18	—155	—153 to —148	46	500		48
Oct. 20	—155	—152 to —147	53	400	35	152
Oct. 22	—155	—152 to —147	62	100	37	12
Oct. 24	—155	—151 to —146	65	10	40	12
Oct. 26	—155	—151 to —146	67	10	43	12
Oct. 28	—155	—151 to —146	68	10	41	12
Oct. 29	—155	—151 to —146	69	10	44	12
Oct. 30	—155	—151 to —146	70	>10	44	12
Nov. 2	—155	—151 to —146	72	<100	41	12
Nov. 5	—155	—152 to —147	73	100	41	12

[a] Based on DSS 14 210-ft antenna.

oscillator to the receiver voltage-controlled oscillator for its frequency reference. The quality of the ground-received signal was unchanged between the one-way lock and the two-way lock, indicating that the problem probably was not in the exciter auxiliary oscillator. Observations made while in two-way lock are presented in table 8–VI.

Telemetry

Attempts were made to lock the demodulator to the data subcarrier at both 8⅓ and 33⅓ bps.

Initially, it was thought that the wide frequency variations of the carrier had not been completely tracked by the rf loop, and that the resulting jitter on the subcarrier was too much for the demodulator to handle. Subsequent analysis indicated that a data subcarrier probably was not present on the downlink signal.

Tracking and Command Operations

The first successful reacquisition was accomplished by DSS 14 at 16:35 GMT on October 14, 1968. The first two-way acquisition was made by DSS 14 at 19:30 GMT on October 20, 1968. No telemetry was detected in the downlink signal in either the one-way or the two-way mode. Many commands were transmitted to the spacecraft; however, no effect was noted.

ANALYSES AND CONCLUSIONS

Initially, plans were made to terminate reacquisition activities on October 31, 1968, when it became evident that no spacecraft signal would be detected within a reasonable length of time. With this in mind, project personnel initiated a series of analyses in which known spacecraft failures were discussed.

Parts of the radio subsystem were still operating normally, but the inability to detect any telemetry or response to ground commands indicated that some failures had occurred within the spacecraft. Accordingly, each subsystem was reviewed again, taking into account the observed tracking data.

Tests conducted by varying the input power to the rf subsystem could not duplicate the observed downlink signal behavior. It is hypothesized that disturbances of the input power to the exciter could have resulted in a spectral breakup of some type, leading to the observed carrier variations. If part of the carrier were spread over a wide bandwidth because of spectral breakup, it could result in a lower-than-predicted signal level.

The lower-than-predicted signal level also could be due to the spacecraft's orientation off the Sun, resulting in the spacecraft-to-Earth vector being lower on the antenna pattern. It is not believed that the rf power amplifier created the observed problem.

No available information indicates that the spacecraft reacted to any ground commands. Commands that should have resulted in a noticeable change in the downlink signal were transmitted with no response, possibly because the rf receiver distorted the command signal so badly that the command detector could not recognize it. Another possibility is that the command subsystem voltage-controlled oscillator stopped oscillating.

Efforts to explain the behavior of the spacecraft have resulted only in an indication from doppler residuals that the spacecraft rolled about its center of gravity at a rate of about 4 rpm. The total absence of telemetry, especially that pertaining to engineering data, effectively prevented any meaningful analysis.

Operations were terminated at the end of the track from DSS 61 at 07:46 GMT on November 5, 1968. Although Mariner 5 will continue to orbit the Sun and, periodically, to approach Earth within tracking range, no plans have been made for future reacquisition attempts or data analyses.

APPENDIX

Acronyms

AC	attitude control
AFETR	Air Force Eastern Test Range
AGC	automatic gain control
AGCM	automatic gain control calibration program
APAC	antenna-pointing-angle change
ATTREF	attitude reference program
BCD	binary-coded decimal
B/R	booster regulator
CAT	complementary analysis team
CC&S	central computer and sequencer
CP	communications processor
CPPM	communication prediction program
DAS	data automation subsystem
DDT	digital demodulation technique
DE	direct encounter
DFR	dual-frequency receiver
DIC	data insertion converted
DIS	data input subsystem
DN	data number
DPPE	data processing project engineer
DSIF	Deep-Space Information Facility
DSN	deep-space network
DSS	deep-space station
ECR	engineering change reports
EOT	end of tape
FPAC	flightpath analysis and command
GCAT	guidance and control analysis team
GCF	Ground Communications Facility
GM	Geiger-Mueller
GMT	Greenwich mean time
GSDS	Goldstone duplicate standard

GSFC	Goddard Space Flight Center
GTS	ground telemetry subsystem
HA, DEC	hour angle, declination
HSD	high-speed data
HSDL	high-speed data line
IRV	interrange vector
JPL	Jet Propulsion Laboratory
KSC	Kennedy Space Center
LCE	launch complex equipment
LeRC	Lewis Research Center
LMC	large Magellanic cloud
MDL	master data library
MOS	mission operation system
MRH	mission-related hardware
MSFN	Manned Space Flight Network
MT	master timer
NASCOM	NASA communications network
NTP	normal temperature and pressure
ODG	orbit data generator
ODP	orbit determination program
PAS	pyrotechnics arming switch
PCA	pyrotechnic control assembly
PFR	problem failure report
PIPS	postinjection propulsion subsystem
PSO	planet-sensor output
RIS	range instrumentation ship
RTCS	real-time computer subsystem
RWV	read-write-verify
SAF	Spacecraft Assembly Facility
SFOD	Space Flight Operations Director
SFOF	Space Flight Operations Facility
SIPM	star identification program
SIRD	support instrumentation requirements document
SIT	separation-initiated timer event
SOPM	standard orbital parameter message
SPAC	spacecraft analysis and command
SPE	static phase error
SSAC	space science analysis and command

STC	System Test Complex
TCP	telemetry and command processor
TCR	temperature-control reference
TDH	tracking data handling
TDP	tracking data processor
TDS	tracking and data system
TWT	traveling-wave tube
ULO	Unmanned Launch Operations
USB	unified *S*-band
VCO	voltage-controlled oscillator
VSWR	voltage standing wave ratio

☆ U. S. GOVERNMENT PRINTING OFFICE : 1972 O - 429-110